

**Ethylene Response and Phytohormone-Mediated Regulation of Gene Expression in
Komagataeibacter xylinus ATCC 53582**

by

Richard Vincent Augimeri

A Thesis Submitted in Partial Fulfillment
of the Requirements for the Degree of

Masters of Science

In

The Faculty of Science

Applied Bioscience

University of Ontario Institute of Technology

April 2016

© Richard Vincent Augimeri, 2016

ABSTRACT

Komagataeibacter xylinus ATCC 53582 is a fruit-associated, cellulose-producing bacterium that responds to and synthesizes phytohormones. This thesis elaborates on the ecophysiology of *K. xylinus*. Responses to indole-3-acetic acid (IAA), abscisic acid (ABA) and ethylene, produced *in situ* from ethephon, were of particular focus. The effect of these phytohormones on *K. xylinus* cellulose production and expression of cellulose biosynthesis-related genes (*bcsA*, *bcsB*, *bcsC*, *bcsD*, *cmcAx*, *ccpAx* and *bglAx*) were determined using pellicle assays and reverse transcription quantitative polymerase chain reaction (RT-qPCR), respectively. Ethylene enhanced cellulose yield by upregulating *bcsA* and *bcsB* expression, while IAA decreased cellulose yield by downregulating *bcsA*. Differential gene expression within the bacterial cellulose synthesis (*bcs*) operon is reported and a phytohormone-regulated CRP/FNR transcription factor was identified that may influence *K. xylinus* cellulose biosynthesis. Based on evidence provided in this thesis, the classification of *K. xylinus* as a saprophyte and its potential to accelerate fruit ripening in nature is proposed.

Keywords

Komagataeibacter xylinus ATCC 53582

Bacterial cellulose

bcs operon

Ethylene

Ethephon

Indole-3-acetic acid

Abscisic acid

CRP/FNR

Plant-microbe interaction

Fruit-bacteria interaction

Fruit ripening

Saprophyte

Ecophysiology

Biofilm

Pellicle

RT-qPCR

ACKNOWLEDGEMENTS

I am profoundly indebted to my supervisor and mentor, Dr. Janice Strap, for her ample amounts of time spent assisting me with experiments and for her continuous support and guidance throughout this research project. Without her constant motivation, understanding and wise words, this work would not have been possible. I would also like to thank my advisory committee for their constructive comments, suggestions and motivation. In particular, I would like to extend my gratitude to Dr. Dario Bonetta for teaching me the ways of a plant scientist, providing *Arabidopsis thaliana* seeds, assisting me with gas chromatography and for helpful discussions. Many thanks go out to all of my lab mates over the past few years, but especially to Andrew Varley for enlightening conversations and for collaborating with me on our review paper. I also want to thank Dr. Liliana Trevani and Dr. Jean-Paul Desaulniers for letting me use their UV-visible spectrophotometers, Dr. Julia Green-Johnson for providing centrifuges, microscopes and the qPCR thermocycler, and Dr. Franco Gaspari and Simone Quaranta for providing and teaching me how to use the FT-IR spectrometer. A big thank you goes out to my girlfriend for her ongoing love, encouragement and motivation. Lastly, I would like to thank my parents for their unconditional love and support throughout my years as a university student. I am forever grateful for my experience in the Molecular Microbial Biochemistry Laboratory and look forward to sharing the knowledge I have obtained during my studies in my future endeavors.

TABLE OF CONTENTS

1	INTRODUCTION	1
1.1	Cellulose: Structure and uses	1
1.2	Cellulose biosynthesis: Plants vs. bacteria	2
1.2.1	Cellulose synthesis complexes	2
1.2.2	Bacterial cellulose synthesis complex subunits	6
1.2.3	Cellulose biosynthesis	10
1.2.4	Cellulose crystallization.....	11
1.2.5	Plant vs. bacterial cellulose.....	12
1.3	Microbial biofilm formation	13
1.4	Environmental diversity of BC producers	17
1.4.1	Insect-bacteria interactions of BC-producing acetic acid bacteria.....	18
1.4.2	Plant-bacteria interactions of BC producers	20
1.4.2.1	Persistence of pathogenic <i>Enterobacteriaceae</i> on fresh produce	20
1.4.2.2	Fruit-bacteria interactions of <i>Komagataeibacter xylinus</i>	22
1.4.2.2.1	Phytohormone-mediated fruit-microbe interactions of <i>K. xylinus</i>	25
1.5	Ethylene: Response and biosynthesis in plants and bacteria	33
1.6	Purpose, hypotheses, and rationale of thesis research.....	37
2	METHODOLOGY	39
2.1	Chemicals and growth medium	39
2.2	Bacteria and starter culture growth conditions	39
2.3	Periplasmic protein isolation and analysis.....	40
2.4	Prediction of disordered protein domains.....	41
2.5	Triple response assay.....	42
2.6	Gas chromatography (GC).....	43
2.7	Time-course pH analysis of ethephon-exposed cultures.....	44
2.8	Minimum inhibitory concentration (MIC) assay	47
2.9	Growth kinetics	47
2.10	Pellicle assays and analysis	48
2.11	Colony morphology.....	50
2.12	Reverse-transcription quantitative polymerase chain reaction (RT-qPCR)	50
2.12.1	Growth conditions	50

2.12.2	RNA purification, quality control and first-strand cDNA synthesis	51
2.12.3	Bioinformatic identification of <i>crp/fnr_{Kx}</i>	52
2.12.4	Primer Design.....	53
2.12.5	RT-qPCR	56
2.12.6	Analysis and selection of reference genes	57
2.12.7	RT-qPCR quality control, data analysis and statistics.....	60
3	RESULTS	61
3.1	IAA and ABA influence the periplasmic protein profiles of <i>K. xylinus</i>	61
3.2	The MtfB protein from <i>K. xylinus</i> has predicted disordered regions	66
3.3	<i>K. xylinus</i> produces low levels of endogenous ethylene	66
3.4	<i>K. xylinus</i> has proteins similar to other ethylene-forming enzymes	67
3.5	Ethylene is produced from ethephon decomposition in SH medium (pH 7).....	67
3.6	<i>K. xylinus</i> culture pH allows for ethephon decomposition	71
3.7	<i>K. xylinus</i> cultures have an increased final pH in the presence of ethylene	71
3.8	Ethephon is relatively non-toxic to <i>K. xylinus</i>	74
3.9	Ethylene does not affect the growth of <i>K. xylinus</i> in agitated broth cultures	75
3.10	Ethylene increases BC yield and decreases <i>K. xylinus</i> pellicle hydration due to an increase in crystallinity	77
3.11	Ethylene increases <i>K. xylinus</i> BC production on solid medium	83
3.12	The genome of <i>K. xylinus</i> contains potential ethylene-receptor genes	85
3.13	RT-qPCR	86
3.13.1	Steady-state mRNA levels are affected by IAA and ABA in <i>K. xylinus</i>	86
3.13.1.1	IAA and ABA induce differential steady-state expression of <i>bcs</i> operon genes that depends on hormone concentration and bacterial growth phase	86
3.13.1.2	IAA and ABA affect the steady-state expression levels of <i>bglAx</i> , but do not affect expression of <i>cmcAx</i> and <i>ccpAx</i>	89
3.13.1.3	IAA and ABA upregulate the steady-state levels of <i>crp/fnr_{Kx}</i> during the exponential growth phase of <i>K. xylinus</i>	91
3.13.1.4	The steady-state expression levels of <i>oprB</i> are downregulated by IAA and upregulated by ABA during the early stages of <i>K. xylinus</i> growth.....	91
3.13.2	Phytohormones influence the active mRNA levels of <i>K. xylinus</i> genes	94
3.13.2.1	Ethylene and IAA cause differential expression of <i>bcs</i> operon genes	94
3.13.2.2	Ethylene and ABA affect the expression of genes flanking the <i>bcs</i> operon	95

	3.13.2.3	The CRP/FNR _{Kx} transcription factor gene is hormonally-regulated ...	96
4		DISCUSSION	97
5		CONCLUSIONS AND FUTURE DIRECTIONS	119
6		REFERENCES	121
7		APPENDIX	154

LIST OF TABLES

Table 1. Diversity of experimentally proven BC producers in the phylum <i>Proteobacteria</i>	5
Table 2. Environmental relationships between BC producers and various hosts.....	18
Table 3. GC conditions used for the detection of ethylene	44
Table 4. Function of proteins encoded by genes analyzed by RT-qPCR in this study.....	54
Table 5. Details of primer sets used in this study	55
Table 6. RT-qPCR assay optimization.....	59
Table 7. Proteins identified in the CS-36 protein band by LC-MS.	64
Table 8. Proteins identified in the CS-46 protein band by LC-MS.	65
Table 9. DELTA-Blast results comparing the <i>K. xylinus</i> E25 proteome to protein sequences of known ethylene receptors from <i>Arabidopsis thaliana</i>	85

LIST OF FIGURES

Figure 1. Chemical structure of cellulose	1
Figure 2. The number of publications regarding BC and <i>Komagataeibacter xylinus</i>	4
Figure 3. Structural and genetic organization of the BCSC and the <i>K. xylinus bcs</i> operon.	7
Figure 4. The turnover over of c-di-GMP is controlled by environmental conditions.	16
Figure 5. Genetic organization of the three cyclic diguanylate (<i>cdg</i>) operons in <i>K. xylinus</i>	17
Figure 6. Sugar-loving insects, such as the fruit fly <i>Drosophila melanogaster</i> , acquires and deposits acetic acid bacteria (AAB) onto fruit in nature	20
Figure 7. Chemical structures of phytohormones.....	26
Figure 8. Proposed model of the bi-directional transfer of phytohormones influences bacterial physiology and fruit development during <i>K. xylinus</i> fruit colonization	32
Figure 9. Schematic of the ethylene signaling pathway in <i>Arabidopsis thaliana</i>	34
Figure 10. Plate layout for the triple response assay with <i>K. xylinus</i>	45
Figure 11. Plate layout for the triple response assay with ethephon as an <i>in situ</i> source of ethylene	46
Figure 12. IAA and ABA influence the periplasmic protein profiles of <i>K. xylinus</i>	63
Figure 13. Disordered regions are predicted in the amino acid sequence of MtfB from <i>K.</i> <i>xylinus</i> E25	66
Figure 14. <i>K. xylinus</i> produces low-levels of endogenous ethylene.....	69
Figure 15. Ethylene is released by ethephon decomposition in SH medium (pH 7).....	70
Figure 16. The pH of <i>K. xylinus</i> cultures grown in SH medium (pH 7) stays above 3.5, allowing for efficient decomposition of ethephon into ethylene.....	72
Figure 17. Ethephon-derived ethylene causes an increase in the final pH of <i>K. xylinus</i> broth cultures.....	73
Figure 18. Ethephon is relatively non-toxic to <i>K. xylinus</i>	75
Figure 19. Ethephon does not affect the growth of <i>K. xylinus</i> when grown in SH broth with agitation.....	76
Figure 20. Ethephon-derived ethylene influences the properties and yield of <i>K. xylinus</i> BC pellicles	78
Figure 21. Ethephon-derived ethylene reduces pellicle hydration by causing an increase in pellicle crystallinity	79
Figure 22. FT-IR spectra of BC pellicles produced by <i>K. xylinus</i>	81
Figure 23. Ethephon enhances <i>K. xylinus</i> BC production when grown on solid medium.	84
Figure 24. IAA and ABA influence the steady-state expression levels of genes within the <i>bcs</i> operon	88
Figure 25. IAA and ABA influence the steady-state expression level of <i>bglAx</i>	90
Figure 26. IAA and ABA influence the steady-state expression levels of <i>crp/fnr_{Kx}</i> and <i>oprB</i>	93
Figure 27. <i>K. xylinus</i> genes are regulated by phytohormones.....	95

Figure 28. Proposed model illustrating the influence of IAA and ABA on *K. xylinus* growth and BC yield by altering the mRNA and protein expression of OprB 102

Figure 29. Updated model for the phytohormone-mediated fruit-bacteria interactions of *K. xylinus*..... 118

LIST OF APPENDICES

APPENDIX FIGURES

Appendix Figure A1. The drop in pH of <i>K. xylinus</i> cultures grown in SH medium (pH 5) may impair decomposition of ethephon into ethylene.....	154
Appendix Figure A2. Ethephon itself does not affect the properties of <i>K. xylinus</i> pellicles	155
Appendix Figure A3. All primer sets designed for RT-qPCR analysis produce the expected amplicons.....	156
Appendix Figure A4. Agarose gel electrophoresis results for time-course RNA	158
Appendix Figure A5. Pulse experiment RNA.....	159
Appendix Figure A6. RT-qPCR standard curves	161
Appendix Figure A7. RT-qPCR melt-curve analysis	162
Appendix Figure A8. Reference gene analysis for 3 day time-course RT-qPCR	167
Appendix Figure A9. Reference gene analysis for 4 day time-course RT-qPCR.....	168
Appendix Figure A10. Reference gene analysis for 5 day time-course RT-qPCR	169
Appendix Figure A11. Reference gene analysis for 6 day time-course RT-qPCR.....	170
Appendix Figure A12. Reference gene analysis for 7 day time-course RT-qPCR	171
Appendix Figure A13. Reference gene analysis for IAA pulse RT-qPCR.....	172
Appendix Figure A14. Reference gene analysis for ABA pulse RT-qPCR.....	173
Appendix Figure A15. Reference gene analysis for ethephon pulse RT-qPCR.....	174
Appendix Figure A16. <i>K. xylinus</i> growth in the presence of IAA and ABA.....	176
Appendix Figure A17. The expression of genes known to be involved in <i>K. xylinus</i> BC biosynthesis are not affected by phosphate and chloride.....	177

APPENDIX TABLES

Appendix Table A1. Average A_{260}/A_{280} values and RNA concentrations of time-course and pulse RNA samples	157
--	-----

LIST OF ABBREVIATIONS

A₂₆₀- Absorbance at 260 nm (UV-visible spectroscopy)
A₂₈₀- Absorbance at 280 nm (UV-visible spectroscopy)
A₈₉₅- Absorbance at 895 cm⁻¹ (FT-IR)
A₁₄₃₇- Absorbance at 1437 cm⁻¹ (FT-IR)
AAB- Acetic acid bacteria
ABA- Abscisic acid
ACC- 1-aminocyclopropane-1-carboxylic acid
ACO- ACC oxidase
ACS- ACC synthase
ALI- Air liquid interface
ANOVA- Analysis of variance
BC- Bacterial cellulose
BCSC- Bacterial cellulose synthesis complex
BLC- Bacterial lignocellulose
BSA- Bovine serum albumin
c-di-GMP- Bis-(3'→5')-cyclic diguanylate monophosphate
cDNA- Complimentary deoxyribonucleic acid
CESA- Plant cellulose synthase protein
CI- Crystallinity index
CI(IR)- Crystallinity index determined by FT-IR
CRP/FNR- Cyclic AMP receptor protein and fumarate-nitrate reductase
CS- Protein band extracted from Coomassie-stained protein gel
CSC- Cellulose synthase complex
C_t- Cycle threshold value
DEPC- Diethylpyrocarbonate
DGC- Diguanylate cyclase
DMSO- Dimethyl sulfoxide
DNA- Deoxyribonucleic acid
DP- Degree of polymerization (length of glucan chain)
E- Efficiency of PCR assay
EBD- Ethylene binding domain
eDNA- Extracellular deoxyribonucleic acid
EDTA- Ethylenediaminetetraacetic acid
EFE- Ethylene-forming enzyme
EPS- Extracellular polysaccharide
GA₃- Gibberellic acid
GAF- cGMP-specific phosphodiesterase, adenylyl cyclase and FhlA domain
GC- Gas chromatography
gDNA- Genomic deoxyribonucleic acid
HE-EPC- Hard to extract extracellular polysaccharide
FT-IR- Fourier transform infrared spectroscopy

GT-2- Family 2 glycosyltransferase
IAA- Indole-3-acetic acid
IDP- Intrinsically disordered protein
kDa- Kilodaltons
KMBA- 2-keto-4-methylthiobutyric acid
KPS- K-antigen polysaccharides
LC-MS- Liquid chromatography mass spectrometry
LCO- Lipo-chito-oligosaccharide
LDR- Linear dynamic range
LPS- Lipopolysaccharide
M- Reference gene stability value calculated by geNorm
MCP- Methyl-accepting chemotaxis protein
MIC- Minimum inhibitory concentration assay
MIQE- Minimum information for the publication of quantitative PCR experiments guidelines
mRNA- Messenger ribonucleic acid
MW- Molecular weight
NRT- No reverse transcriptase control
NTC- No template control
OD₆₀₀- Optical density (absorbance) at 600 nm
PB- Protein band of interest
PC- Plant cellulose
PCR- Polymerase chain reaction
PCWC- Plant cell wall component
PDE- Phosphodiesterase
PAS- Per Arnt Sim domain
PGA- poly- β -1,5-GlcNAc
PMSF- Phenylmethylsulfonyl fluoride
pSym- Symbiosis plasmid
RDML- Real-time PCR data markup language files
RLQ- Relative linear quantities
RNA- Ribonucleic acid
rRNA- Ribosomal ribonucleic acid
RT-qPCR- Reverse transcription quantitative PCR
SAM- S-adenosylmethionine
SD- Standard deviation
SDS-PAGE- Sodium dodecyl sulfate polyacrylamide gel electrophoresis
SH- Schramm and Hestrin medium
SP- Surface polysaccharide
SS- Protein band extracted from silver-stained protein gel
SSAB- Solid surface associated biofilm
SYP- Symbiosis polysaccharide
TAE- Tris-HCl, acetic acid and EDTA running buffer for agarose gel electrophoresis

T_{a, opt.}- Optimal annealing temperature for primer sets determined empirically
T-DNA- Transfer deoxyribonucleic acid
TE- Tris EDTA buffer
TEM- Transmission electron microscopy
TF- Transcription factor
Ti plasmid- Tumor-inducing plasmid
TM- Transmembrane
TRA- Triple response assay
tRNA- Transfer ribonucleic acid
UDP- Uridine diphosphate
UPP- Unipolar polysaccharide
UTR- Untranslated region
UV- Ultraviolet light
V- Pair-wise variation value of reference genes calculated by geNorm

LIST OF PUBLICATIONS

1. Augimeri, R.V., Varley, A.J., and Strap, J.L. (2016). Using ethephon (2-chloroethylphosphonic acid) as a tool to study ethylene response in bacteria. *JoVE*. Accepted.

A portion of the work presented in this thesis has been published in the following:

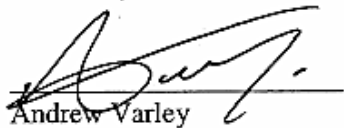
2. Augimeri, R.V. and Strap, J.L. (2015). The phytohormone ethylene enhances bacterial cellulose production, regulates CRP/FNR_{Kx} transcription and causes differential gene expression within the cellulose synthesis operon of *Komagataeibacter (Gluconacetobacter) xylinus* ATCC 53582. *Front. Microbiol.* 6: 1459. doi: 10.3389/fmicb.2015.01459.
3. Augimeri, R.V., Varley, A.J., and Strap, J.L. (2015). Establishing a role for bacterial cellulose in environmental interactions: Lessons learned from diverse biofilm-producing *Proteobacteria*. *Front. Microbiol.* 6. doi:10.3389/fmicb.2015.01282.

Note: Figures which have been previously published are used in accordance with the Creative Commons Attribution License employed by the journal, *Frontiers in Microbiology* and are cited.

01/29/2016

Richard Augimeri has my permission to include material from the following paper, of which I was a co-author, in his MSc thesis.

Augimeri, R.V., Varley, A.J., and Strap, J.L. (2015). Establishing a role for bacterial cellulose in environmental interactions: Lessons learned from diverse biofilm-producing *Proteobacteria*. *Front. Microbiol.* 6. doi:10.3389/fmicb.2015.01282.

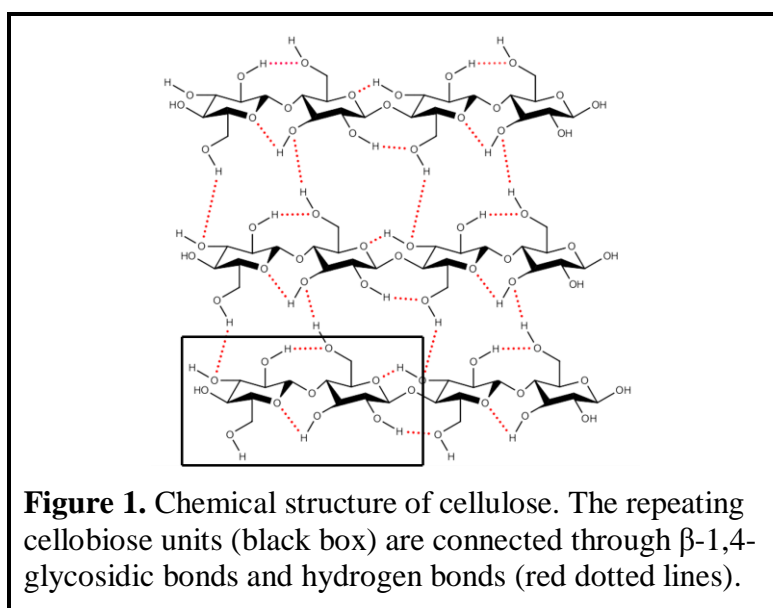


Andrew Varley

1 INTRODUCTION

1.1 Cellulose: Structure and uses

The production of the organic biomaterial cellulose is common to various eukaryotic and prokaryotic organisms, including vascular plants, green algae, oomycetes, hyphochytriomycetes, tunicates, and numerous bacterial species (Kimura and Itoh, 2007; Römling, 2002; Sarkar *et al.*, 2009; Stone, 2005). Structurally, cellulose is an unbranched biopolymer consisting of β -D-glucopyranose units connected through β -1,4-glycosidic linkages (**Figure 1**). Each of the glucopyranose residues is rotated 180° with respect to its neighbor (O'Sullivan, 1997), making cellobiose (**Figure 1**) the disaccharide unit of cellulose (Somerville, 2006). The two dominant cellulose allomorphs, cellulose I and cellulose II, differ in terms of their intra- and intermolecular hydrogen bonding patterns. Cellulose I contains the β -1,4-glucan chains oriented in parallel with the same polarity, resulting in a highly crystalline structure (**Figure 1**). In contrast, cellulose II contains less ordered parallel β -1,4-glucan chains, causing its structure to be more amorphous (Kudlicka and Brown, 1996). Specific allomorph content results in varied structural characteristics of the final cellulose product. For example, in the textiles industry, cellulose I is converted to cellulose II through the process of mercerization to make the material more amorphous and better able to absorb colored dyes (Heins, 1944; Okano and Sarko, 1985).



The most plentiful source of cellulose is plant cellulose (PC). It is the main constituent of the plant cell wall and is in complex with hemicellulose, pectins, lignin and glycoproteins. Along with providing plant cells with structural support, PC forms the apoplastic network (xylem) that facilitates the transport of water, carbon dioxide and other solutes throughout vascular plant tissues (Kudlicka and Brown, 1996). High concentrations of cellulose are found in cotton and wood, both of which are globally-traded commodities (Lejeune and Deprez, 2010). Cellulose can be hydrolyzed into its constituent sugars and used as a fermentable substrate for bioethanol production by yeast (Jørgensen *et al.*, 2007). As of 2014, numerous companies are producing biofuels from cellulosic feedstocks in the United States of America, highlighting the advancement of the cellulosic biofuel industry. However, in order for cellulosic biofuels to become economically sustainable and more valuable than fossil fuels, the process must be made more efficient in regards to cellulose purification and saccharification. Cellulose is believed to be the most abundant renewable carbon source on the planet, thus making it an important industrial resource with immense socioeconomic value.

1.2 Cellulose biosynthesis: Plants vs. bacteria

1.2.1 Cellulose synthesis complexes

The synthesis of cellulose can be attributed to plasma membrane-localized (Brown and Montezinos, 1976; Brown *et al.*, 1976) cellulose synthesis complexes (CSCs) that have diverse geometries in different cellulose-producing organisms. Plant CSCs consist of cellulose synthase (CESA) proteins arranged into hexagonal rosettes (Kimura *et al.*, 1999), while bacterial CSCs (BCSCs) form single or multiple linear arrays along the longitudinal axis of the cell (Iyer *et al.*, 2011; Kimura *et al.*, 2001; Sunagawa *et al.*, 2013; Tsekos, 1999). The genome of *Arabidopsis thaliana*, a model organism for cellulose biosynthesis in plants, contains 10 *cesa* genes (Richmond and Somerville, 2000) that are classified into two groups: those encoding proteins responsible for cellulose biosynthesis in the primary cell wall (Desprez *et al.*, 2007), and those encoding proteins responsible for cellulose production in the secondary cell wall (Li *et al.*, 2014; Taylor *et al.*, 2003). CESA proteins are classified as family 2 glycosyltransferases (GT-2; Richmond and Somerville, 2000)

that catalyze the formation of glycosidic bonds between β -D-glucopyranose monomers using UDP-glucose as the substrate (Lin *et al.*, 1990; Omadjela *et al.*, 2013; Saxena *et al.*, 1995; Somerville, 2006). GT-2 family enzymes include all cellulose, chitin and hyaluronan synthases (Kudlicka and Brown, 1996). The active site of glycosyltransferases contain the D,D,D,Q(Q/R)XRW motif that binds the substrate and facilitates catalysis (Omadjela *et al.*, 2013; Saxena *et al.*, 1990). Higher plant CESA proteins also contain a plant-conserved region (P-CR) between D₁ and D₂ of the D,D,D,Q(Q/R)XRW motif, and a class-specific region (CSR) between D₂ and D₃ (Sethaphong *et al.*, 2013). These additional regions have been proposed to be involved in rosette assembly and plant-specific regulation of cellulose biosynthesis (Sethaphong *et al.*, 2013).

Interestingly, plant CESA proteins have a bacterial origin, since the genes that encode them were obtained from cyanobacterial endosymbionts (Nobles and Brown, 2004; Nobles *et al.*, 2001). Research regarding bacterial cellulose (BC) biosynthesis spans 7 decades (Aschner and Hestrin, 1946; Hestrin *et al.*, 1947). The number of publications in the BC field, and in regards to its model organism, *Komagataeibacter* (formerly *Gluconacetobacter*) *xylinus*, have increased steadily in the last 15 years (**Figure 2**). This is likely due to the improvement of next-generation sequencing technologies, publication of genome sequences of numerous BC producers (Römling and Galperin, 2015), increased availability of genetic tools and the 1987 discovery of the primary activator of the BCSC, bis-(3'→5')-cyclic diguanylate monophosphate (c-di-GMP; **Figure 2**; Ross *et al.*, 1987).

Genera of BC producers include *Komagataeibacter*, *Gluconacetobacter* (formerly *Acetobacter*), *Enterobacter*, *Pseudomonas*, *Achromobacter*, *Alcaligenes*, *Aerobacter*, *Azotobacter*, *Agrobacterium*, *Burkholderia*, *Dickeya*, *Escherichia*, *Rhizobium*, *Salmonella*, and *Sarcina* (Römling and Galperin, 2015; Römling, 2002; Ross *et al.*, 1991). The most prominent phylum of BC producers are the *Proteobacteria* which inhabit diverse environmental habitats (**Table 1**; Augimeri *et al.*, 2015).

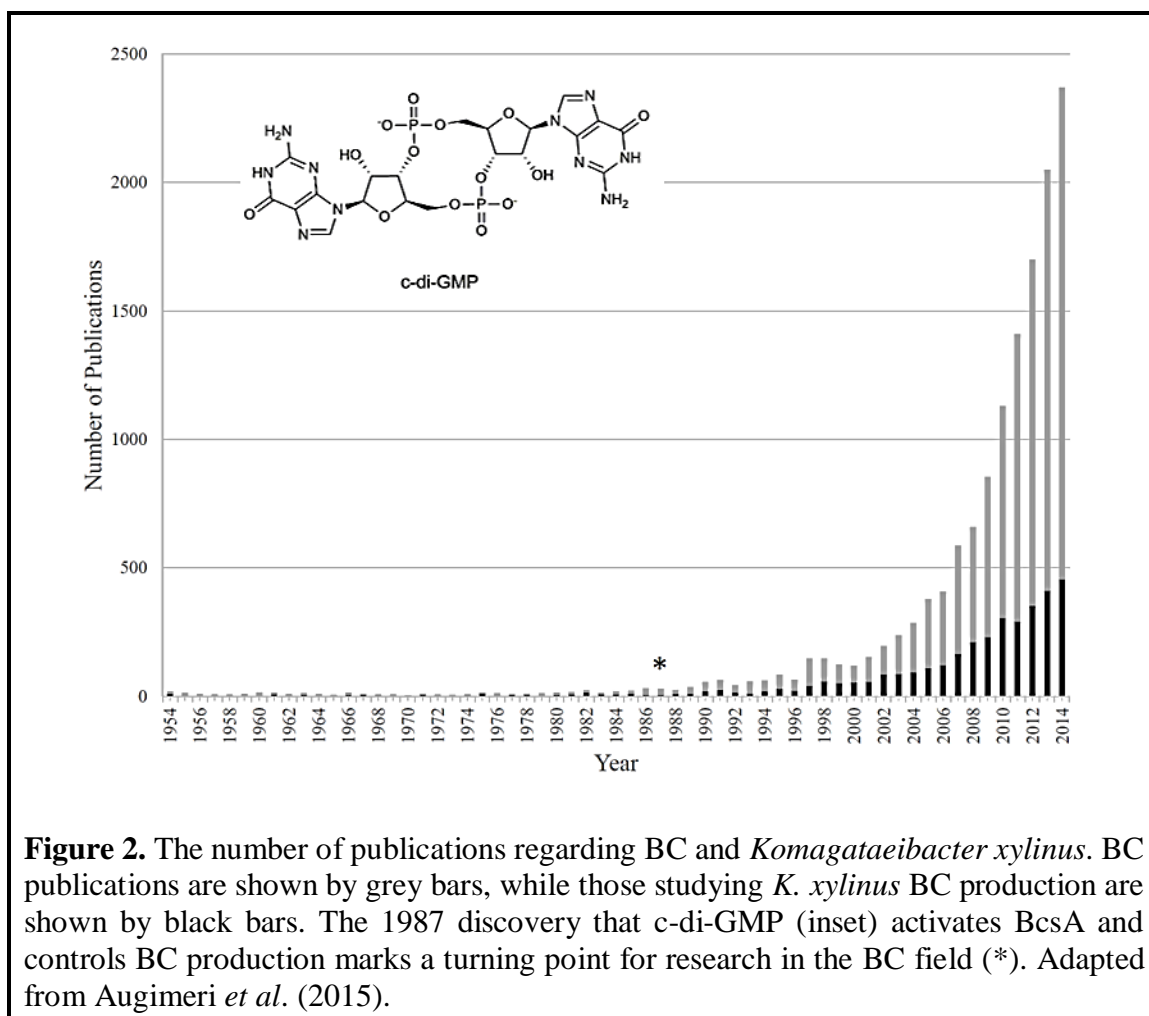


Figure 2. The number of publications regarding BC and *Komagataeibacter xylinus*. BC publications are shown by grey bars, while those studying *K. xylinus* BC production are shown by black bars. The 1987 discovery that c-di-GMP (inset) activates BcsA and controls BC production marks a turning point for research in the BC field (*). Adapted from Augimeri *et al.* (2015).

Four bacterial cellulose synthesis (*bcs*) genes (*bcsABCD*; **Figure 3B**) were initially identified and characterized in the acetic acid bacterium (AAB), *K. xylinus* (Saxena *et al.*, 1990, 1994; Wong *et al.*, 1990). Since then, genome sequences of numerous bacterial strains were shown to contain organizationally diverse *bcs* operons that encode varied BCSCs (Römling and Galperin, 2015; Römling, 2002). BC is synthesized on the cytoplasmic side of the inner membrane (Bureau and Brown, 1987) and is subsequently transported through the periplasmic space before it is released into the extracellular environment (**Figure 3A**; Morgan *et al.*, 2013).

Table 1. Diversity of experimentally determined BC producers in the phylum *Proteobacteria*. From Augimeri *et al.* (2015).

Class	Order	Family	Genus	Host	Reference ¹
<i>α-proteobacteria</i>	<i>Rhizobiales</i>	<i>Rhizobiaceae</i>	<i>Agrobacterium</i>	Plant	Matthysse <i>et al.</i> (1981)
			<i>Rhizobium</i>	Plant	Laus <i>et al.</i> (2005)
		<i>Acetobacteriaceae</i>	<i>Komagataeibacter</i>	Plant	Brown <i>et al.</i> (1976)
			<i>Asaia</i>	Animal	Kumagai <i>et al.</i> (2011)
<i>β-proteobacteria</i>	<i>Neisseriales</i>	<i>Chromobacteriaceae</i>	<i>Chromobacterium</i>	Animal	Recouvreux <i>et al.</i> (2008)
<i>γ-proteobacteria</i>	<i>Enterobacteriales</i>	<i>Enterobacteriaceae</i>	<i>Enterobacter</i>	Plant/Animal	Basavaraj <i>et al.</i> (2010)
			<i>Escherichia</i>	Plant/Animal	Ellermann <i>et al.</i> (2015)
			<i>Salmonella</i>	Plant/Animal	Römling and Lunsdorf (2004)
			<i>Dickeya</i>	Plant	Jahn <i>et al.</i> (2011)
	<i>Pseudomonadales</i>	<i>Pseudomonadaceae</i>	<i>Pseudomonas</i>	Plant/Animal	Spiers <i>et al.</i> (2003)
<i>Vibrionales</i>	<i>Vibrionaceae</i>	<i>Aliivibrio</i>	Animal	Bassis and Visick (2010)	

¹Select reports demonstrating BC production from the respective bacterial genus

BCSCs form a single linear row along the longitudinal axis of the rod-shaped *K. xylinus* cell (Brown *et al.*, 1976; Kimura *et al.*, 2001; Sunagawa *et al.*, 2013) and are responsible for the synthesis and export of BC. This arrangement allows adjacent glucan chains to be hydrogen bonded as they are being exported; coupling elongation, translocation and crystallization of BC (Morgan *et al.*, 2013).

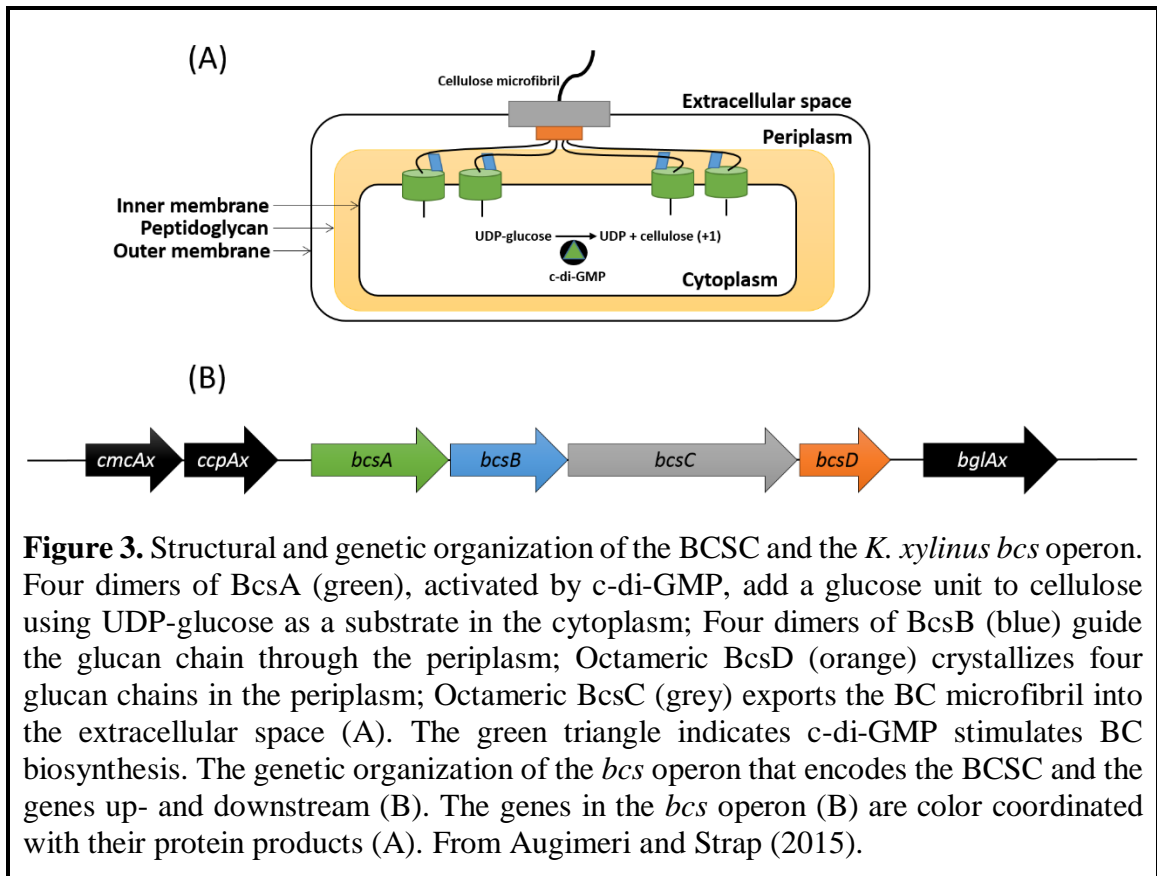
1.2.2 Bacterial cellulose synthesis complex subunits

The BC synthase protein, BcsA, is encoded in the *bcs* operon (*bcsA*) along with other genes that encode BCSC proteins (**Figure 3A**; Kawano *et al.*, 2002b; Römling and Galperin, 2015; Ross *et al.*, 1987). BcsA is an integral inner membrane protein with eight transmembrane (TM) domains in clusters of 4+4 (Kumar and Turner, 2014; Omadjela *et al.*, 2013). It contains a very small cytosolic N-terminal domain and a large central glycosyltransferase domain. It was first thought that the activator of BcsA, c-di-GMP, was binding to the 85 kDa BcsB subunit, suggesting that BcsB regulated the levels of free c-di-GMP that could activate the glycosyltransferase domain (Amikam and Benziman, 1989). However, subsequent studies revealed that c-di-GMP was actually binding to a 200 kDa membrane-bound protein complex that has not yet been further characterized (Weinhouse *et al.*, 1997) but has been hypothesized to represent either a dimer of the BcsA subunit or a BcsAB subunit. A bioinformatics study determined that BcsA contains a cytosolic C-terminal PilZ domain that binds and regulates levels of free c-di-GMP (Amikam and Galperin, 2006). The PilZ domain was found to be ubiquitous in bacteria and is believed to be the binding domain of c-di-GMP receptors. The C-terminal PilZ domain binds c-di-GMP and controls the catalytic domain through conformational changes (Amikam and Galperin, 2006; Morgan *et al.*, 2014; Römling *et al.*, 2013; Ryjenkov *et al.*, 2006).

BcsB is a periplasmic protein attached to BcsA by a single C-terminal TM helix and contains two carbohydrate binding domains (CBD1 and CBD2) that likely chaperone the synthesized glucan chain through the periplasm (**Figure 3A**; Morgan *et al.*, 2013). The functional BcsA subunit is stabilized by BcsB (Morgan *et al.*, 2013). BcsA and BcsB are the only two proteins that are essential for *in vitro* BC synthesis, but *in vitro*-formed BC is less crystalline than cell-produced BC (Omadjela *et al.*, 2013; Wong *et al.*, 1990).

Extrusion of BC from the periplasm to the extracellular environment is thought to be facilitated through the action of BcsC (**Figure 3A**) which, based on its structure, is predicted to form a pore in the outer membrane of *K. xylinus*. Consistent with the view that BcsC is an outer membrane porin, is the observation that BcsC is essential for *in vivo*, but

not *in vitro* BC biosynthesis (McManus *et al.*, 2016; Saxena *et al.*, 1994). The mechanisms of BC export by BcsC have not been studied to date, but BcsC contains two conserved domains; a COG3118 (thioredoxin containing protein responsible for post-translational modifications and protein turnover) domain, and a COG4783 (putative Zn-dependent protease containing TPR repeats) domain (Marchler-Bauer *et al.*, 2005). The TPR (tetratricopeptide repeat) motif is a 34 amino acid sequence that forms a molecular scaffold that facilitates protein-protein interactions, and is most often associated with large multi-protein complexes (Blatch and Lässle, 1999). There is little to no conformational change when TPR repeats bind to their respective ligand indicating TPR domains form an unchanging molecular structure that is folded to allow protein partners to associate (Cortajarena and Regan, 2006). This suggests that BcsC may interact with other subunits of the BCSC through the TPR motif however, there are no studies describing these interactions.



Crystallization of BC is achieved in part, through the action of BcsD, a cylindrical octameric periplasmic protein (Iyer *et al.*, 2011) that contains four spiral channels that facilitates hydrogen bonding of four glucan chains during export through BcsC (**Figure 3A**; Hu *et al.*, 2010). *K. xylinus* *bcsD* knock-out mutants still synthesize BC but the yield and crystallinity were much reduced compared to the wildtype (Saxena *et al.*, 1994; Sunagawa *et al.*, 2013) suggesting that *bcsD* is not essential for BC synthesis but is required for maximal production and crystallinity. BcsD is also required for optimal BC production *in vitro* (McManus *et al.*, 2016). It is possible that BcsD interacts with BcsC through the TPR motif to couple crystallization and export of BC. However, this has yet to be investigated. In *K. hansenii* ATCC 23769, *bcsD* is regulated independently of the other *bcs* genes (Deng *et al.*, 2013), as a 321 base pair untranslated region (UTR) separates *bcsC* and *bcsD*, leaving room for a functional promoter (Deng *et al.*, 2013). In contrast, the coding regions of *bcsC* and *bcsD* in *K. xylinus* have a 1 base pair overlap, suggesting that *bcsD* is regulated from the same promoter as the rest of the *bcs* genes in this strain.

Römling and Galperin (2015) proposed a model for the organization of the entire BCSC based on crystal structure data of the *Rhodobacter sphaeroides* BcsAB complex, the BcsC-like AlgK-AlgE protein complex of *Pseudomonas aeruginosa*, and the BcsD protein of *K. xylinus*. The model predicts a BCSC stoichiometry of [(A₂B₂)₄C₈D₈], in which four dimers of BcsA and BcsB associate with one octameric unit of BcsC and BcsD to facilitate the crystallization of four glucan chains as they are exported from one BCSC (**Figure 3A**).

Various ancillary genes are also involved in *K. xylinus* BC biosynthesis. Located upstream of the *bcs* operon, is *bcsZ* (formerly and for the rest of this thesis called *cmcAx*; **Figure 3B**), which encodes an endo-β-1,4-glucanase (CmcAx) that belongs to the glycoside hydrolase 8 family of enzymes (Yasutake *et al.*, 2006). CmcAx has cellulose-hydrolyzing activity *in vitro* on cellopentose or longer oligosaccharide substrates (Kawano *et al.*, 2002a) and is localized to the outer membrane (Yasutake *et al.*, 2006). KOR and CelC, homologous endoglucanases from *A. thaliana* and *Agrobacterium tumefaciens*, respectively, are also anchored to the plasma membrane (Matthysse *et al.*, 1995; Nicol *et*

et al., 1998). Antibodies that inhibit CmcAx (Koo *et al.*, 1998), and a *cmcAx* knock-out mutant (Nakai *et al.*, 2013) have shown that this enzyme is required for BC biosynthesis in *K. xylinus*. The *cmcAx* deletion mutant produced remarkably reduced amounts of BC compared to wildtype (Nakai *et al.*, 2013). BC fibrils were packed together irregularly in a tight and highly-twisted ribbon, suggesting that CmcAx is responsible for cleaving the twisting glucan chains as they are being exported from the BCSC. It is likely that the BcsD subunit causes the twisting of the glucan chains due to its four twisted cylindrical passageways (Hu *et al.*, 2010). The hyper-twisting of BC microfibrils likely clog the BCSC and reduce BC production by preventing export. In small amounts, exogenous CmcAx enhances BC production of *K. xylinus* (Kawano *et al.*, 2002a). Likewise, endogenous overexpression of *cmcAx* increases BC yield (Kawano *et al.*, 2002a); cellulose hydrolyzing activity of CmcAx may therefore exert a regulatory effect on BC biosynthesis.

In the same upstream operon as *cmcAx*, is *bcsH* (formerly and for the rest of this thesis called, *ccpAx*; **Figure 3B**), which encodes the cellulose-complementing protein (CcpAx). This protein is essential for *in vivo* BC biosynthesis (Deng *et al.*, 2013; Standal *et al.*, 1994), and is required for optimal BC production *in vitro* (McManus *et al.*, 2016). CcpAx interacts with BcsD on the extracellular side of the cell membrane, suggesting that CcpAx is a critical part of the BCSC (Sunagawa *et al.*, 2013). CcpAx is involved in BC crystallization, as *ccpAx* knock out mutants produce less cellulose I, and more cellulose II, compared to the wildtype (Nakai *et al.*, 2002). Disruption of *ccpAx* results in a significant reduction in the levels of BcsB and BcsC, but not BcsA in *K. hansenii* ATCC 23769 (Deng *et al.*, 2013; McManus *et al.*, 2016). The genes that encode all three proteins are located within the same operon, indicating CcpAx plays a post-transcriptional regulatory role in BC biosynthesis. Since this protein is of low molecular weight and has predicted secondary structures rich in α -helices, CcpAx may facilitate protein-protein interactions for the spatial assembly of BCSCs (Sunagawa *et al.*, 2013). Sequence analysis using the Protein Disorder Prediction System (PrDos) showed that the CcpAx sequence includes a C-terminal disordered region that could act as a scaffold to mediate protein-protein interactions between CcpAx and other BCSC subunits (Hsu *et al.*, 2012).

Downstream of the *bcs* operon is *bglX* (formerly and for the rest of this thesis called *bglAx*; **Figure 3B**), which encodes a β -glucosidase (BglAx; Tajima *et al.*, 2001) that belongs to the family 3 glycoside hydrolase enzyme group. This monomeric enzyme is secreted (Tahara *et al.*, 1998) and has the ability to hydrolyze oligosaccharides larger than three residues into single β -D-glucose units (Tahara *et al.*, 1998; Tajima *et al.*, 2001). BglAx exhibits slight activity towards cellobiose (Tahara *et al.*, 1998; Tajima *et al.*, 2001). It has been proposed that BglAx works with CmcAx to edit exported glucan chains or to relieve oligosaccharide-induced inhibition of CmcAx activity (Deng *et al.*, 2013). In addition to its cellulose hydrolyzing ability, BglAx produces gentiobiose through a condensation reaction, which positively regulates the expression of *cmcAx* (Kawano *et al.*, 2008). Furthermore, the expression of *bglAx* is transcriptionally-regulated by CRP/FNR_{Kh}, a cyclic-AMP receptor/fumarate nitrate reductase protein in *K. hansenii* ATCC 23769 (Deng *et al.*, 2013). Transposon insertion into *crp/fnr_{Kh}* (GXY_00863) completely abolished production of BC and BglAx, providing evidence that CRP/FNR_{Kh} controls BC biosynthesis at the transcriptional level. Since *bglAx* deletion results in reduced BC synthesis, but not the absence of BC production observed with *crp/fnr_{Kh}* deletion, it is probable that CRP/FNR_{Kh} controls the expression of additional genes that are essential for BC biosynthesis (Deng *et al.*, 2013). Therefore, research regarding the effect of CRP/FNR transcription factors on BC biosynthesis warrants further investigation.

1.2.3 Cellulose biosynthesis

In addition to their catalytic function, CESA and BcsA form a pore in the plasma membrane with their eight TM domains that facilitate translocation of glucan chains (Morgan *et al.*, 2013; Sethaphong *et al.*, 2013). Though the cytosolic domains of CESA and BcsA share low amino acid sequence similarity (Doblin *et al.*, 2002), the glycosyltransferase domains are generally conserved (Sethaphong *et al.*, 2013), supporting the notion that the D,D,D,Q(Q/R)XRW motif is responsible for cellulose polymerization. In contrast to BCSCs that are fixed in position with respect to the cell surface (Iyer *et al.*, 2011; Kimura *et al.*, 2001; Sunagawa *et al.*, 2013), plant CSCs are motile within the plasma membrane and associate with microtubules (Harris *et al.*, 2012; Paredez *et al.*, 2006). In

bacteria, crystallization of BC occurs immediately when glucan chains exit the cell (Haigler *et al.*, 1980), and due to the fixed nature of BCSCs, a consistent cell shape and distance between the enzyme complexes are required for maximum crystallinity. For example, pellicin, a chemical inhibitor of pellicle production in *K. xylinus* ATCC 53582, increases cell size, and as a result contributes to the reduction in BC crystallinity (Strap *et al.*, 2011). It is not known if pellicin, like the fluorescent dye Calcofluor-white (Haigler *et al.*, 1980), directly interferes with hydrogen bonding interactions between glucan chains. Furthermore, the peptidoglycan layer within the bacterial cell wall plays a role in BC crystallization. Deng *et al.* (2015) demonstrated that *K. hansenii* ATCC 23769 mutants defective in genes encoding for lysine decarboxylase and alanine racemase display a reduction in BC crystallinity. This study also showed that these mutations affect cell shape, suggesting that a highly structured peptidoglycan network is required for proper cell shape and consequently, the formation of crystalline BC.

1.2.4 Cellulose crystallization

Hydrogen bonding and van der Waals interactions work to crystallize individual glucan chains to form cellulose microfibrils. Generally, 3 nm elementary microfibrils aggregate into thicker microfibrils (5-10 nm wide), which then aggregate to form cellulose ribbons with widths of 30-50 nm (Zhang *et al.*, 2014). Precise microfibril widths depend on the organism that produced them. According to a computational molecular energy study by Cousins and Brown (1995), crystallization of cellulose I is achieved by: formation of mini-sheets produced by the interaction of individual glucan chains through van der Waals forces as they exit the enzyme active site; aggregation of mini-sheets through hydrogen bonding to form elementary microfibrils as glucan chains exit the CSC; and association of elementary microfibrils through hydrogen bonding to form a crystalline cellulose microfibril. The crystallization step limits cellulose polymerization in both plants and bacteria (Benziman *et al.*, 1980; Haigler *et al.*, 1980; Harris *et al.*, 2012).

1.2.5 Plant vs. bacterial cellulose

Structurally, BC is more pure than PC since it lacks hemicellulose, pectin, and lignin that are found in the plant cell wall. BC also exhibits a higher crystallinity index (CI) and degree of polymerization (DP) than PC (Czaja *et al.*, 2004; Sethaphong *et al.*, 2013; Strap *et al.*, 2011). Increased crystallinity of BC may be explained by the presence of the BcsD protein that is unique to the BCSC (Delmer, 1999; Römling and Galperin, 2015) and shown to be involved in crystallization (Saxena *et al.*, 1994; Sunagawa *et al.*, 2013). These structural characteristics, along with the ability to form BC-nanocomposites have made BC of great interest to numerous industries, particularly those involved in drug-delivery systems, medical devices, food products and acoustics (Abeer *et al.*, 2014; Iguchi *et al.*, 2000; Nwodo *et al.*, 2012; Siró and Plackett, 2010).

Ground-breaking research has begun that could revolutionize the cellulosic biofuel industry; the production of BC from genetically-altered photosynthetic cyanobacteria. Small quantities of BC are produced naturally from cyanobacteria (Nobles and Brown, 2004; Nobles *et al.*, 2001). However, cloning of the *bcsAB* genes from *K. xylinus* into a cyanobacterium (*Synechococcus leopoliensis* UTCC 100), resulted in the production of much larger quantities of BC using sugars obtained through photosynthesis (Nobles and Brown, 2008). This system was improved by Zhao *et al.* (2015), who overexpressed the entire *K. xylinus bcs* operon and its flanking genes (*cmcAx*, *ccpAx* and *bglAx*) in a cyanobacterium (*Synechococcus* sp. PCC 7002). BC produced by heterotrophic organisms like *K. xylinus* is not a suitable feedstock for biofuel production since these bacteria must be fed purified sugars. PC is not an ideal feedstock either since plant growth requires the use of limited arable land that should be used for food crops, and copious amounts of fresh water, while producing a cellulose product that contains contaminating components that are difficult and costly to remove. Furthermore, the need for petroleum-based fertilizers to grow current feedstock crops intrinsically ties biofuels to fossil fuels. Cyanobacteria can thrive on non-arable land and be nourished with salt water, providing a useful alternative to plants. Therefore, using BC produced by photosynthetic cyanobacteria could finally

sever the tie between biofuels and fossil fuels, preserve arable land and fresh water, and provide a truly carbon-neutral fuel source.

1.3 Microbial biofilm formation

In addition to some mechanistic and structural differences, PC and BC have different functions in the organisms that produce them. PC acts as a structural component of the plant cell wall and is essential to plant survival. In contrast, BC is not essential for bacterial survival, but does confer a survival advantage under certain conditions. When BC producers are grown statically in liquid, they often form a solid surface-associated biofilm (SSAB) at the bottom of the vessel. Biofilms are described as multicellular, surface-associated microbial communities embedded within an extracellular matrix comprised of extracellular polysaccharides (EPS), proteins and nucleic acids (Costerton *et al.*, 1995; Flemming and Wingender, 2010; Geesey *et al.*, 1978). Various polysaccharides are found in microbial biofilms, including BC, alginate and curdlan (Brown *et al.*, 1976; Hentzer *et al.*, 2001; Laus *et al.*, 2005; Matthysse *et al.*, 1981; Römling *et al.*, 2004; Saldaña *et al.*, 2009; Vu *et al.*, 2009; Williams and Cannon, 1989).

Aerobic bacteria often build a floating biofilm at the air-liquid interface (ALI), commonly referred to as a pellicle. The ALI is a favorable environment for aerobic bacteria as it provides high concentrations of oxygen from the air, while still allowing access to nutrients present in the soluble medium. Pellicle formation has been thoroughly studied in regards to the Gram-positive bacterium, *Bacillus subtilis* (Vlamakis *et al.*, 2013), but is less characterized in Gram-negative bacteria. However, current data suggests that planktonic cells aggregate, causing them to become buoyant and float to the ALI where high oxygen concentrations stimulate pellicle production (Armitano *et al.*, 2014).

Some BC producers make soluble hemicellulose-like EPS that contain glucose, mannose, rhamnose, galactose and glucuronic acid in variable molar ratios (Fang and Catchmark, 2014, 2015). Most of the EPS can be removed by solvent precipitation of culture supernatant, but some EPS cannot be removed. This “hard to extract” EPS (HE-

EPS) complexes with the BC matrix (Fang and Catchmark, 2014, 2015). By binding in between adjacent glucan chains, these HE-EPS impact cellulose ribbon assembly and crystallization by disrupting the highly ordered hydrogen bonding pattern of crystalline BC (Deng *et al.*, 2015; Fang and Catchmark, 2014).

Bacteria that form SSABs can switch between a motile, planktonic state, and a sessile, biofilm-forming state, depending on environmental signals (Flemming and Wingender, 2010). This adaptive mechanism allows motile bacterial species to search for a suitable growth environment. Once a nutrient-rich area is found, growth and biofilm production commences to initiate colonization of the substrate. This transition is controlled by the antagonistic action of diguanylate cyclases (DGCs) and phosphodiesterases (PDEs) that contain conserved GGDEF and EAL or HD-GYP domains, respectively (Galperin *et al.*, 2001; Simm *et al.*, 2004). These catalytic domains are responsible for the synthesis (GGDEF) and degradation (EAL and HD-GYP) of the ubiquitous bacterial second messenger and activator of BcsA, bis-(3'→5')-cyclic diguanylate (c-di-GMP; Amikam and Benziman, 1989; Ross *et al.*, 1987). Bifunctional GGDEF-EAL and GGDEF-HD-GYP enzymes also exist (Römling *et al.*, 2013). Many of these proteins contain upstream sensory domains that control the activity of the downstream catalytic domains in response to environmental cues. There are different types of sensory domains, such as the Per-Arnt-Sim (PAS) and GAF domains, the latter being named after the proteins in which it is found: cGMP-specific PDEs, adenylyl cyclases and FhlA (*E. coli*). These sensory domains contain prosthetic groups, such as heme, flavin mononucleotide, flavin adenine dinucleotide and various chromophores which allow proteins to sense a variety of signals, including O₂ (Chang *et al.*, 2001; Gilles-Gonzalez and Gonzalez, 2004), the redox status of the cell (Qi *et al.*, 2009) and light (Tarutina *et al.*, 2006). Binding of these ligands modulates the activity of the catalytic GGDEF, EAL and HD-GYP domains and couples environmental signals with the turnover of c-di-GMP. Typically, low-levels of c-di-GMP is a cellular signal for motility and virulence, while high levels of c-di-GMP initiates the transition to a biofilm-forming state by activating enzymes involved in biofilm formation (**Figure 4**).

In *K. xylinus*, three *cdg* (cyclic diguanylate) operons encode DGCs and PDEs that display hierarchical control of BC biosynthesis (**Figure 5**; Tal *et al.*, 1998). Disruption of each DGC results in reduced BC production *in vivo* (Tal *et al.*, 1998). The PDE, AxPDEA1, contains a heme-based PAS domain that binds oxygen and inactivates the c-di-GMP-cleaving EAL domain (Chang *et al.*, 2001). Oxygen binding leads to increased c-di-GMP and BC levels (Chang *et al.*, 2001). The *K. xylinus* DGC, AxDGC2, contains a flavin cofactor-binding PAS domain (Qi *et al.*, 2009). Non-covalent binding of FAD to AxDGC2 induced higher catalytic activity compared to FADH, demonstrating a role of cellular redox status in *K. xylinus* BC biosynthesis (Qi *et al.*, 2009). Regeneration of FAD primarily occurs at the electron transport chain which uses oxygen as a terminal electron acceptor in aerobic organism like *K. xylinus*. Oxygen is required for effective activation of AxDGC2 and inhibition of AxPDEA1, resulting in increased c-di-GMP and BC levels.

In addition to DGCs and PDEs, the *K. xylinus cdg1* operon also encodes two transcriptional regulators: CDG1A and CDG1D (**Figure 5**; Tal *et al.*, 1998). The *cdg1a* gene encodes a CRP/FNR transcription factor that has a positive effect on BC production (Tal *et al.*, 1998). Bacteria respond to environmental changes using CRP/FNR family transcription factors which regulate processes that are critical to bacterial growth and survival (Matsui *et al.*, 2013). Some of these processes include catabolite repression, aerobic growth, nitrogen fixation, oxidative stress responses, stationary phase survival, arginine catabolism and pathogenicity (Körner *et al.*, 2003). Binding of various ligands by CRP/FNR proteins alters their DNA binding specificity, and results in the activation or repression of target gene expression. The role of CDG1D in BC biosynthesis has not been demonstrated, but sequence analysis reveals that it belongs to the poorly characterized Rrf2 repressor family of transcriptional regulators. The *B. subtilis* CymR protein is the most studied Rrf2 regulator (Shepard *et al.*, 2011), and is responsible for the repression of many genes involved in cystine (cysteine dimer) uptake and cysteine biosynthesis (Even *et al.*, 2006). Therefore, CDG1D may repress genes involved in *K. xylinus* BC biosynthesis through a yet to be discovered mechanism. CDG1A and CDG1D are poorly understood

regulators in *K. xylinus*, and warrant further investigation due to their genetic loci within the *cdg1* operon that most strongly controls BC biosynthesis.

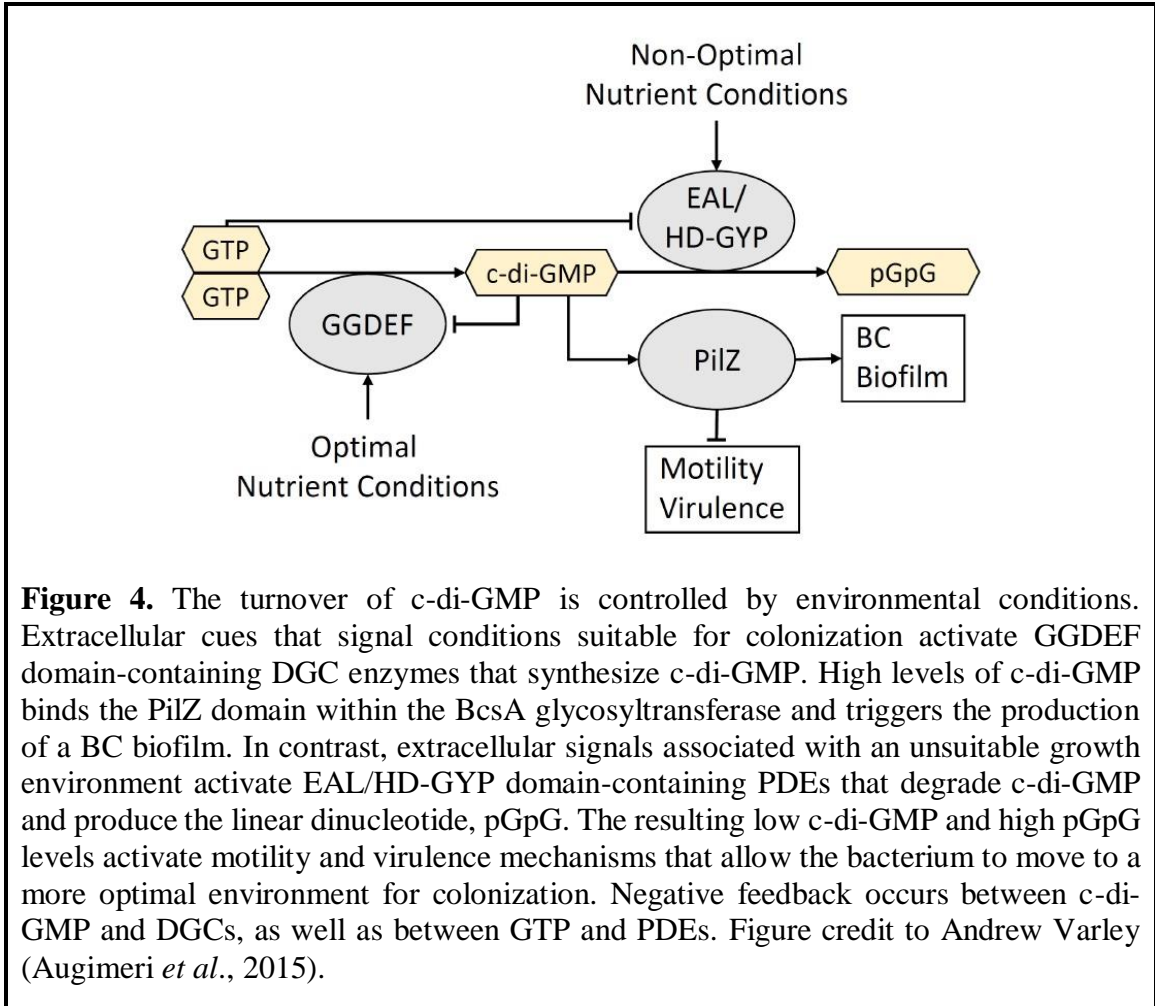
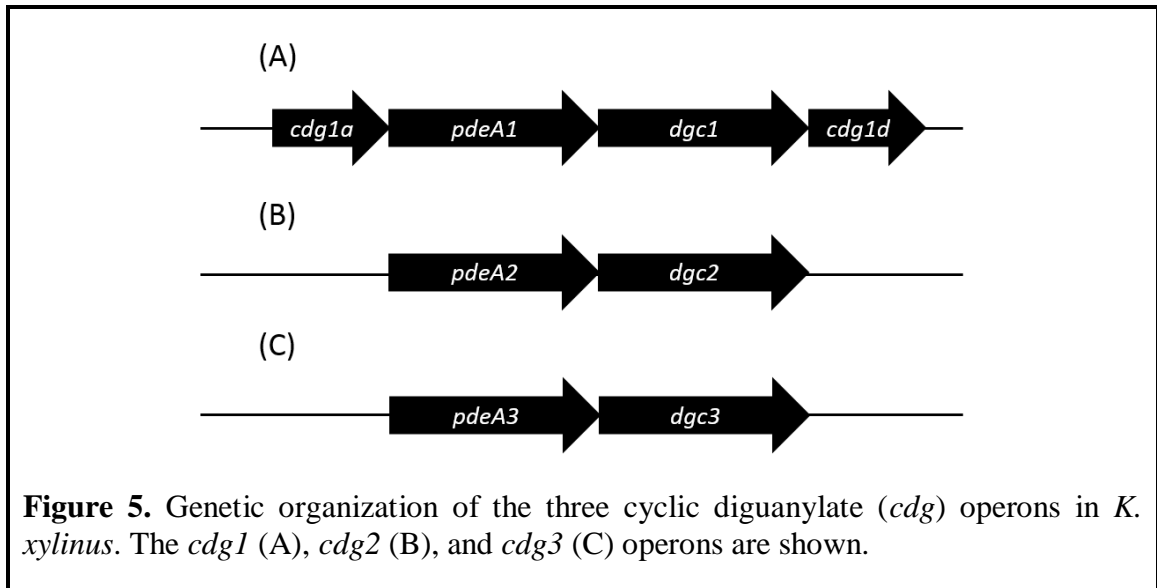


Figure 4. The turnover of c-di-GMP is controlled by environmental conditions. Extracellular cues that signal conditions suitable for colonization activate GGDEF domain-containing DGC enzymes that synthesize c-di-GMP. High levels of c-di-GMP binds the PilZ domain within the BcsA glycosyltransferase and triggers the production of a BC biofilm. In contrast, extracellular signals associated with an unsuitable growth environment activate EAL/HD-GYP domain-containing PDEs that degrade c-di-GMP and produce the linear dinucleotide, pGpG. The resulting low c-di-GMP and high pGpG levels activate motility and virulence mechanisms that allow the bacterium to move to a more optimal environment for colonization. Negative feedback occurs between c-di-GMP and DGCs, as well as between GTP and PDEs. Figure credit to Andrew Varley (Augimeri *et al.*, 2015).



1.4 Environmental diversity of BC producers

In the environment, SSABs serve to anchor bacteria to their host to establish close contact and facilitate symbiotic or pathogenic relationships. Bacteria take advantage of host-derived nutrients and use biofilm formation to colonize their preferred substrate. Numerous examples exist of BC producers that associate with animals and plants (**Table 2**). The structure, function and regulatory mechanisms of BC biofilm production are as diverse as the bacteria that produce them. Select examples of these BC-mediated inter-domain interactions are discussed below (Augimeri *et al.*, 2015).

Table 2. Environmental relationships between BC producers and various hosts. From Augimeri *et al.* (2015). *K. xylinus* is shown in bold as it is the bacterium studied in this thesis.

Bacterium	Host/Vector	Location	Relationship	Reference¹
<i>Rhizobium leguminosorum</i>	Plant	Roots	Mutualistic	Lin <i>et al.</i> (2015)
<i>Agrobacterium tumefaciens</i>	Plant	Roots	Pathogenic	Tolba and Soliman (2014)
<i>Komagataeibacter xylinus</i>	Plant	Fruit	Uncertain	Neera <i>et al.</i> (2015)
<i>Escherichia coli</i>	Human	Gut	Pathogenic	Manageiro <i>et al.</i> (2015)
	Plant	Fresh produce	Vector	Rangel-Vargas <i>et al.</i> (2015)
<i>Salmonella enterica</i>	Human	Gut	Pathogenic	Manageiro <i>et al.</i> (2015)
	Plant	Fresh produce	Vector	Rangel-Vargas <i>et al.</i> (2015)
<i>Asaia</i> sp.	Insect	Gut	Symbiotic	Favia <i>et al.</i> (2007)
<i>Aliivibrio fischeri</i>	Squid	Light Organ	Symbiotic	Boettcher and Ruby (1990)

¹References given are the most recent reports describing the isolation of the respective bacterium from its respective host or vector.

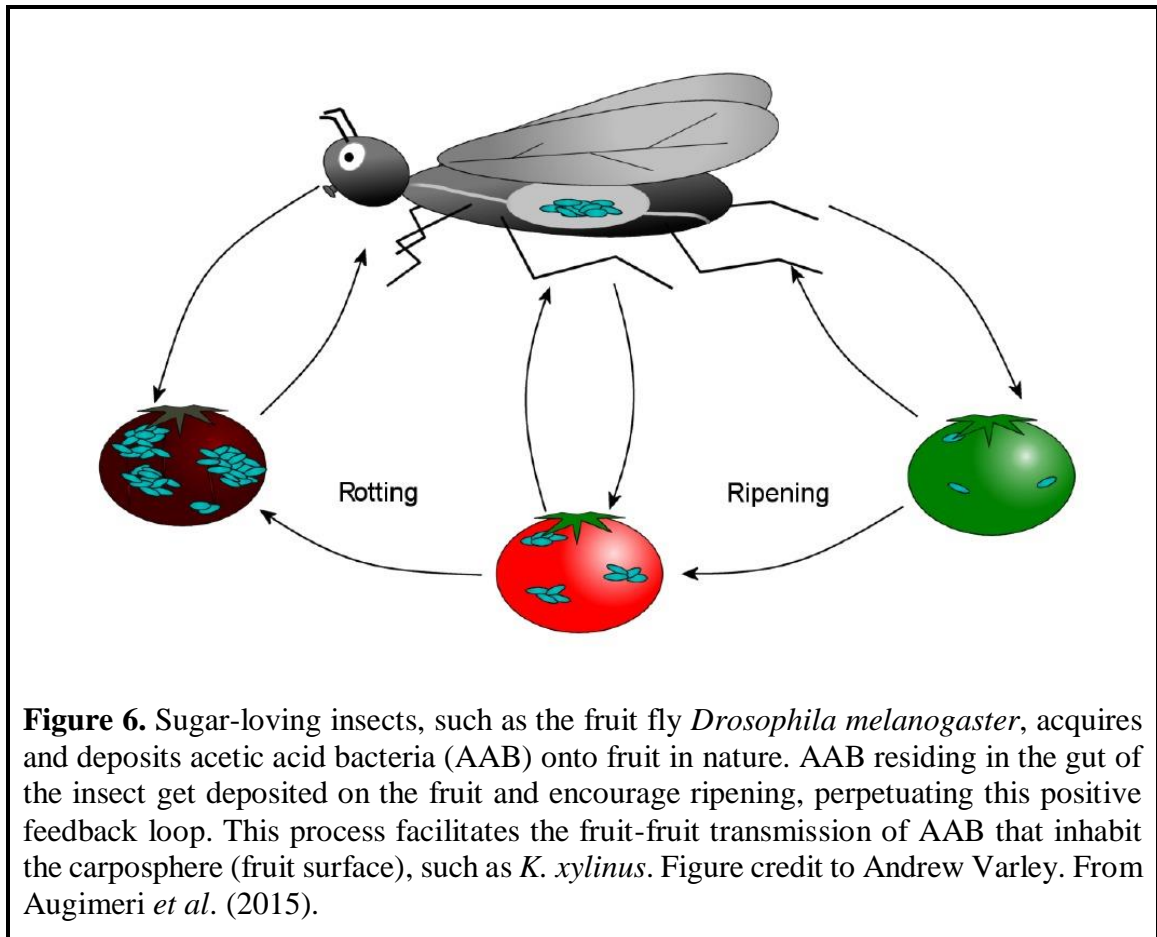
1.4.1 Insect-bacteria interactions of BC-producing acetic acid bacteria

As described in Augimeri *et al.* (2015), many BC-producing acetic acid bacteria (AAB) are secondary symbionts of insects that rely on sugar-based diets (nectars, fruit sugars, phloem sap), particularly those belonging to the orders Diptera, Hymenoptera, and Hemiptera (Crotti *et al.*, 2010). These α -proteobacteria provide their insect hosts with competitive advantages in the environment (Feldhaar and Gross, 2009). *Acetobacteraceae* are naturally found in association with the plants that these insects feed upon which facilitates environmental acquisition. The fruit fly *Drosophila melanogaster* and the pink sugarcane mealybug *Saccharicoccus sacchari* have a rich AAB microbiome consisting of *A. acetii*, *G. diazotrophicus* and *G. sacchari* (Ashbolt and Inkerman, 1990; Corby-Harris *et al.*, 2007). The BC-producing *Asaia bogorensis* (Kumagai *et al.*, 2011) was originally isolated from the nectar of tropical flowers (Yamada *et al.*, 2000) and subsequently from the gut of insects (Crotti *et al.*, 2009).

AAB typically inhabit the digestive system, salivary glands and reproductive organs of insects (Dillon and Dillon, 2004), but have also been isolated from insect surfaces (Ren *et al.*, 2007). In the digestive tract of certain insects, AAB flourish due to the aerobic environment, acidic pH and a plethora of diet-derived sugars which are ideal conditions for BC production. Transmission electron microscopy (TEM) has demonstrated that *Asaia* sp. and *Acetobacter tropicalis* embed themselves within the BC matrix to establish tight association to the host epithelium (Favia *et al.*, 2007; Kounatidis *et al.*, 2009). Consistent with observations from the human gut microbiome (Kau *et al.*, 2012), the immune system of *Drosophila* is influenced by its AAB symbionts. For example, the normal microflora of *Drosophila* suppresses the proliferation of the pathogenic commensal gut bacterium, *Gluconobacter morbifer* (Ryu *et al.*, 2008).

In addition to being a phytopathogen, BC-producing *Dickeya dadantii*, is also an insect pathogen, as it produces entomotoxins and causes septicemia and death in the pea aphid, *Acyrtosiphon pisum* (Costechareyre *et al.*, 2012). *D. dadantii* colonizes the insect gut and forms dense clusters using a BC biofilm. *A. pisum* acquires bacteria from contaminated plant leaves, serving as a vector of *D. dadantii*, and phytopathogenic and BC-producing *Pseudomonas syringae* (Stavrínides *et al.*, 2009).

Since the insect gut serves as a reservoir of AAB, sugar-loving insects act as vectors dispersing various BC-producers to plants in nature. For example, *Drosophila* could deposit and acquire AAB from unripe, ripe or rotten fruit and be responsible for their fruit-fruit transmission (**Figure 6**). This phenomenon has been demonstrated experimentally with non-pathogenic *E. coli* ATCC 11775 and human pathogenic *E. coli* O157:H7 (Berger *et al.*, 2010). Little is known about how the regulation of BC biosynthesis is affected by insect-bacteria relationships.



1.4.2 Plant-bacteria interactions of BC producers

BC biofilms contribute to numerous plant-bacteria interactions. Various BC producers inhabit the phyllosphere (above ground) and rhizosphere (beneath ground) microenvironments, where symbiotic and pathogenic relationships flourish. Some examples are discussed below (Augimeri *et al.*, 2015).

1.4.2.1 Persistence of pathogenic *Enterobacteriaceae* on fresh produce

Human pathogens, such as *E. coli* and *S. enterica*, can form biofilms on fruits and vegetables by surviving on exudate released from lysed plant cells. *Enterobacteriaceae* are found on sprouts, green leafy vegetables and fruits, such as melons and tomatoes, where they adhere to, but typically do not cause disease symptoms (Doyle and Erickson, 2008; Niemira and Zhang, 2009). However, *S. enterica* serovar Typhimurium acts as

phytopathogen in maize and mung bean plants when inoculated onto non-germinated seeds (Singh *et al.*, 2004, 2005). *S. enterica* serovar Typhimurium and the enterohemorrhagic *E. coli* O157:H7 persists for over 100 days on basil and 177 days on parsley, respectively (Islam *et al.*, 2004; Kisluk *et al.*, 2013). Contamination of fresh produce has been, and continues to be a leading source of foodborne illness and more research is required to develop more effective prevention strategies (Lynch *et al.*, 2009). The longevity of pathogens on fresh produce is largely due to EPSs and curli, which contribute to resistance against chlorine washes, a commonly used sanitizer in the food industry (Beuchat, 1997, 1999; Ryu and Beuchat, 2005; Taormina and Beuchat, 1999).

BC and curli are two main factors in adherence of *Enterbacteriaceae* on produce. *S. enterica* serovar Typhimurium mutants that were unable to produce BC or curli were found to have a one log reduction in adherence to parsley leaves (Lapidot and Yaron, 2009). The role of BC in adherence was also demonstrated by mutations in *bcsA* and *bcsC*, in which *S. enterica* serovar Enteritidis and *S. enterica* serovar Typhimurium had reduced attachment to either alfalfa sprouts and tomato fruits, respectively (Barak *et al.*, 2007; Shaw *et al.*, 2011). It is likely that the reduced colonization was caused by decreased BC synthesis and decreased BC export, in regards to the *bcsA* and *bcsC* mutants, respectively.

Other studies have shown that pre-cut produce has an increased risk of becoming contaminated, as several *S. enterica* serovars were shown to preferentially attach to cut surfaces of many types of produce (Patel and Sharma, 2010). Exposed internal surfaces supply more nutrients since numerous plant cells are lysed when the fruit is cut. In some studies, *E. coli* displays less dependence on BC for adherence. The ability for enterohemorrhagic *E. coli* O157:H7 to attach to spinach leaves was shown to be associated with curli rather than BC (Macarisin *et al.*, 2012). The highly virulent and BC non-producing *E. coli* O104:H4 was found contaminating sprouts (Buchholz *et al.*, 2011; Richter *et al.*, 2014). This strain contains a novel hyperactive DGC (GdcX), and overproduced both CsgD and curli (Richter *et al.*, 2014). This suggests that the production of curli and other c-di-GMP-dependent EPS may assist with adherence in the absence of

BC. However, these studies are not representative for all *E. coli* strains, since *E. coli* O103:H2 relies on BC for attachment to lettuce leaf surfaces, but not to their cut edges (Lee *et al.*, 2015).

A review by Yaron and Römling (2014) identified in *Enterobacteriaceae*, several plant adherence genes that encode virulence factors in animals. In *S. enterica* serovar Enteritidis, these genes include the biofilm regulator *csgD* and the curli nucleator, *csgB* (Barak *et al.*, 2005) suggesting a mechanism in which pathogens could persist in the environment and use fresh produce as vehicles to infect human hosts (Berger *et al.*, 2010).

1.4.2.2 Fruit-bacteria interactions of *Komagataeibacter xylinus*

The ability of bacteria to form BC biofilm enhances colonization of fruit substrates by serving as a molecular anchor. Two examples of BC producers that have been isolated from decaying fruit are *Enterobacter amnigenus* GH-1 (Hungund and Gupta, 2010), a human pathogen (Capdevila *et al.*, 1998), and *Komagataeibacter* spp., which has been studied in regards to its BC production and interaction with fruit.

Komagataeibacter are Gram-negative α -proteobacteria that belong to the family *Acetobacteraceae* (Cleenwerck *et al.*, 2009; Mamlouk and Gullo, 2013) and are model organisms for BC synthesis. These bacteria produce a crystalline BC pellicle at the ALI of statically grown liquid cultures (Gromet-Elhanan and Hestrin, 1963) and form biofilms on climacteric (Dellaglio *et al.*, 2005; Jahan *et al.*, 2012; Park *et al.*, 2003) and non-climacteric (Barata *et al.*, 2012; Valera *et al.*, 2011) fruit in nature. *Komagataeibacter* species are also commonly isolated from spoiled batches of wine (Bartowsky and Henschke, 2008). The natural habitat of *K. xylinus* is the carposphere (surface of fruit); its occurrence in wine is merely a result of its presence on the grapes used to make the wine. Studying the ecophysiology of *K. xylinus* will provide important clues for how the energetically costly BC is regulated and structurally influenced by its environment.

Nutrient availability on the surface of unripe fruits is limited. The small pool of plant-derived nutrients is from exudates or from wounds on the fruit surface. Bacteria are chemotactic towards exudates. For example, plant growth-promoting *Pseudomonas fluorescens* exhibits chemotaxis towards tomato root exudate, some amino acids, malic acid and citric acid, but not sugars (de Weert *et al.*, 2002). *E. coli* is chemotactic towards sugars (Adler *et al.*, 1973).

Since *K. xylinus* is an acetic acid bacterium (AAB) that colonizes fruit, it likely persists within the gut of insects (refer to section 1.4.1). The fruit fly, *Drosophila*, preferentially deposits bacteria through regurgitation on the wounds of fruit where nutrients are most plentiful (Janisiewicz *et al.*, 1999). The pH of these wounds is around 3.5 (Janisiewicz *et al.*, 1999) which is similar to the pH of *K. xylinus* cultures during exponential growth (Qureshi *et al.*, 2013). Bacterial growth within fruit wounds has been observed for a saprophytic strain of *Pseudomonas syringae* (Janisiewicz and Marchi, 1992), another plant-associated BC producer that resides in the phyllosphere (Arrebola *et al.*, 2015). As fruit ripens, stored starch and PC are degraded by endogenous plant enzymes into glucose, providing a substrate for microbial growth and BC synthesis (Ahmed and Labavitch, 1980; Brady, 1987).

Williams and Cannon (1989) investigated the environmental roles of *K. xylinus* BC production and its influence on the fruit-microbe interactions of this bacterium. When *K. xylinus* was inoculated on apple slices, it colonized the substrate and outcompeted fungi and other bacteria when BC was produced, or overproduced, compared to BC non-producers. BC protected *K. xylinus* from desiccation and from the damaging effects of UV radiation. *K. xylinus* produces BC to increase environmental fitness which differs from the notion that BC biosynthesis was required to suspend bacteria to the ALI of liquid cultures, an environment where they are not naturally found. This highlights the importance of studying the fruit-bacteria interactions of *K. xylinus*, to better understand the ecological role of BC.

The *K. xylinus* fruit-bacteria interactions described by Williams and Cannon (1989) demonstrated that BC production is required for effective colonization of apple slices. In *K. xylinus*, BC is synthesized by BcsA, BcsB, BcsC, BcsD, CcpAx, CmcAx and BglAx (refer to section 1.2) and the absence of any of these proteins results in decreased BC production (Deng *et al.*, 2013; Nakai *et al.*, 2002, 2013; Wong *et al.*, 1990). Therefore, any disruption of these proteins could be inferred to negatively impact fruit colonization. Interestingly, CmcAx is homologous to the endoglucanase, CelC2, from the endophytic bacterium, *R. leguminosarum*, which degrades the non-crystalline tip of root hairs to make a localized hole that the bacterium can penetrate (Robledo *et al.*, 2008). Similarly, secreted CmcAx (Koo *et al.*, 1998) may also function to degrade the plant cell wall so that *K. xylinus* can obtain valuable nutrients trapped inside. This mechanism may play a role in the persistence of *K. xylinus* on unripe fruit, where nutrients are scarce. This idea is supported by the fact that CmcAx is secreted by BC non-producers, suggesting a role for CmcAx that is independent of BC biosynthesis.

K. xylinus secretes large quantities of various organic acids (Zhong *et al.*, 2013, 2014). Although production of organic acids drains carbon away from *K. xylinus* BC production (Zhong *et al.*, 2013, 2014), substrate acidification serves an ecological purpose. In the context of fruit-bacteria interactions, environmental acidification through secretion of organic acids provides *K. xylinus* with a competitive advantage over less acid-tolerant organisms growing on the same substrate. This phenomenon has been observed with various vaginal lactobacilli and oral streptococci strains that acidify their environment to outcompete competitors (Graver and Wade, 2011; Quivey *et al.*, 2000). Kawano *et al.* (2002b) demonstrated that *K. xylinus* ATCC 53582, but not *K. hansenii* ATCC 23769 synthesizes BC after glucose depletion by utilizing gluconic acid as a carbon source. While gluconic acid production is correlated with a decrease in pH, gluconic acid catabolism increases culture pH (Kawano *et al.*, 2002). In the context of fruit-bacteria interactions, strains of *K. xylinus* acidify their microenvironment through gluconic acid secretion until they become the predominant organism on the fruit substrate. Once established, *K. xylinus* resorbs gluconic acid for BC production to enhance colonization. Secretion of other acids,

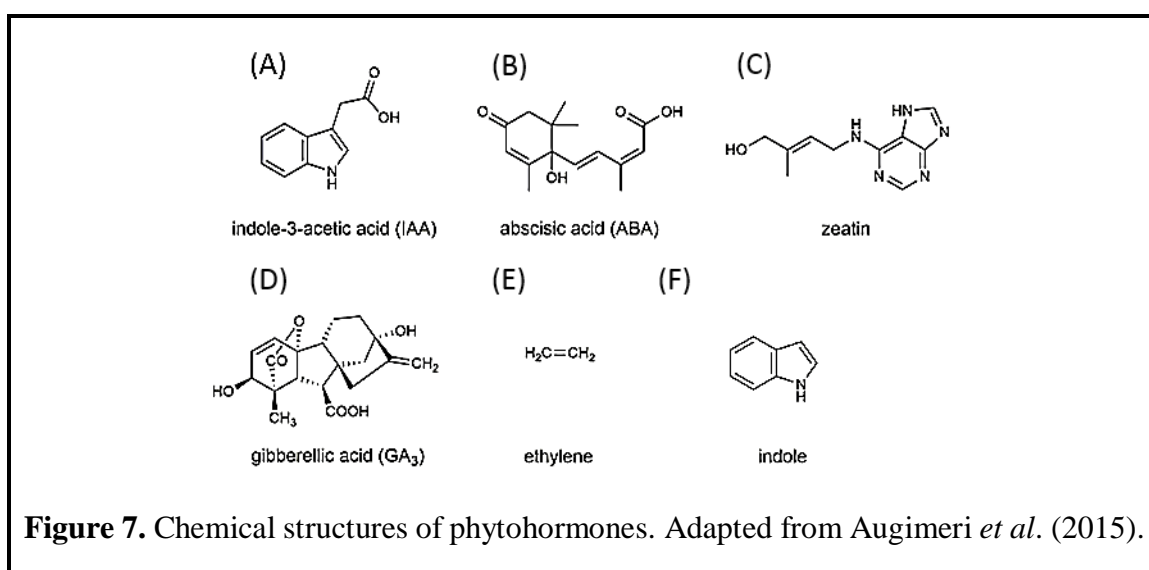
particularly acetic acid, may contribute to this process. Environmental acidification also solubilizes essential micronutrients such as phosphate and iron as previously reported for other plant-associated bacteria, including *Gluconacetobacter diazotrophicus*, *Bacillus subtilis*, and *Pseudomonas* and *Rhizobium* species (Crespo, 2011; Rodríguez and Fraga, 1999; Zhang *et al.*, 2009a).

In vitro and *in planta* biofilm production by the Gram-positive rhizosphere bacterium, *B. subtilis*, is induced by the plant cell wall polysaccharides arabinogalactan, pectin and xylan (Beauregard *et al.*, 2013), while monosaccharides have no effect. Though the *B. subtilis* biofilm has not been shown to contain BC, it does contain EPS, including the fructans levan I and II (Abdel-Fattah *et al.*, 2005; Dogsa *et al.*, 2013) and another polysaccharide containing glucose, galactose, fucose, glucuronic acid and *O*-acetyl groups in a molar ratio of about 2 : 2 : 1 : 1 : 1.5 (Morita *et al.*, 1979). Therefore, plant cell wall components (PCWCs) can have a profound effect on polysaccharide-containing biofilms. Once deposited on fruit by an insect vector, *K. xylinus* would encounter several PCWCs that would interact and structurally modify its BC (Augimeri *et al.*, 2015). Briefly, the plant cell wall polysaccharides hemicellulose (xylan, xyloglucan and glucomannan) and pectin incorporate into the BC matrix and reduce BC crystallinity (Chanliaud and Gidley, 1999; Hackney *et al.*, 1994; Hanus and Mazeau, 2006; Iwata *et al.*, 1998; Park *et al.*, 2014; Uhlin *et al.*, 1995; Whitney *et al.*, 1995, 1998; Yamamoto *et al.*, 1996; Yui *et al.*, 1992). This increases the water-holding capacity of BC and would make the BC biofilm more resistant to desiccation in an environmental setting. Lignin also incorporates into the BC matrix and forms bacterial lignocellulose (BLC) that forms a BC biofilm that is more recalcitrant and resistant to environmental cellulases (Augimeri *et al.*, 2015). The effect of PCWCs on the regulation of BC biosynthesis has not yet been investigated.

1.4.2.2.1 Phytohormone-mediated fruit-microbe interactions of *K. xylinus*

K. xylinus can be isolated from fleshy fruit where it would be exposed to various phytohormones that work in concert to control plant growth, development, and interaction with external stimuli. Indole-3-acetic acid (IAA; **Figure 7A**) is an auxin involved in nearly

every aspect of plant growth and development (Zhao, 2010). Abscisic acid (ABA; **Figure 7B**) controls root growth, seed dormancy, the opening and closing of stomata, and the adaptive stress response to biotic and abiotic factors (Cutler *et al.*, 2010). Zeatin (**Figure 7C**) is a cytokinin that regulates cytokinesis and differentiation of plant cells, and works in conjunction with IAA to control plant growth (Hitoshi, 2006). Gibberellic acid (GA₃; **Figure 7D**) encourages plant cells to increase in size through the uptake of photosynthate (Davière and Achard, 2013). Ethylene (**Figure 7E**) is a gaseous phytohormone that interacts with other phytohormones to regulate vegetative development, flowering, ripening and disease (Vandenbussche and Van Der Straeten, 2012).



Fruit growth, characterized by cell division and expansion, is initially signaled by IAA, zeatin and GA₃ sent from the seed to surrounding tissues, followed later by an increase in ABA. Fruit ripening and senescence is the final developmental stage, wherein levels of IAA, Z, and GA₃ remain low, and levels of ABA and ethylene increase.

Fruit ripening is associated with numerous physiological and biochemical changes. The sweetness of ripe fruit for example, is caused by starch hydrolysis. ABA promotes this process by upregulating ethylene production, which increases amylase activity and sugar accumulation (Agravante *et al.*, 1990; Montalvo *et al.*, 2009; Zhang *et al.*, 2009b). The fruit cell wall is weakened during ripening (Brummell, 2006). This process, triggered by

ABA and ethylene (Cantín *et al.*, 2007; Lohani *et al.*, 2004), is associated with increased activity of cell wall-degrading pectolytic and cellulolytic enzymes (Ahmed and Labavitch, 1980; Brummell and Harpster, 2001; Lohani *et al.*, 2004). Intense turgor pressure within the plant cell and weakening of the cell wall releases exudate onto the surface of the fruit leaving it more susceptible to microbial invasion.

Accumulation of sugars and weakening of the fruit cell wall during ripening provides a suitable nutrient environment for BC production and colonization. *K. xylinus* participates in numerous fruit-bacteria interactions, including the bi-directional transfer of phytohormones. While the effect of bacterially-produced phytohormones on plant physiology has been well-studied (Costacurta and Vanderleyden, 1995; Spaepen and Vanderleyden, 2011), there is limited information regarding the effect of plant-produced phytohormones on bacterial physiology.

The role of IAA in plant-bacteria interactions of rhizosphere bacteria, such as *Gluconacetobacter*, *Pseudomonas*, *Agrobacterium*, *Rhizobium*, *Bradyrhizobium*, *Enterobacter*, *Azospirillum* and *Streptomyces* (Duca *et al.*, 2014) is well-studied. Depending on the amount of IAA secreted and the sensitivity of the plant to IAA, these bacteria can have a plant-growth-promoting (Glick, 2012), or phytopathogenic effects (Spaepen and Vanderleyden, 2011). For example, crown-gall tumor formation by *A. tumefaciens* and *A. rhizogenes* depends on production of auxins and cytokinins that induce rapid cell division in plant roots. Genes for the biosynthesis of IAA, zeatin-riboside and *trans*-zeatin are found on the T-DNA region of the Ti plasmid (Akiyoshi *et al.*, 1984; Thomashow *et al.*, 1984). Unlike the rhizosphere bacterium *Gluconacetobacter diazotrophicus* (Lee and Kennedy, 2000), the closely related carposphere bacterium *K. xylinus*, does not produce endogenous IAA (Qureshi *et al.*, 2013), as it would be counter-productive for its survival; IAA inhibits fruit ripening (Aharoni *et al.*, 2002; Davies *et al.*, 1997).

Exogenous IAA stimulates the growth of *K. xylinus* but diminishes BC yield, suggesting that IAA has a direct effect on BC production (Qureshi *et al.*, 2013). The observed lower BC yield is consistent with the fruit-bacteria interactions of *K. xylinus*, since IAA inhibits ripening and signals monosaccharide building blocks are unavailable for BC synthesis. Delaying BC production preserves carbon source for growth. In nature, *K. xylinus* growth stimulation by IAA ensures cell density is at a peak once fruit ripening begins and IAA levels decrease (Jia *et al.*, 2011). Whether IAA-induced growth is a result of IAA metabolism is unknown. IAA metabolism and degradation has been observed in other bacteria (Duca *et al.*, 2014; Leveau and Gerards, 2008; Leveau and Lindow, 2005). It has been suggested that the degradation or inactivation of IAA by *K. xylinus* could decrease its effective concentration, thereby allowing fruit ripening to commence (Qureshi *et al.*, 2013). Two rhizobacteria, *Rhodococcus* sp. P1Y and *Novosphingobium* sp. P6W, metabolize ABA and decrease its concentration *in planta*, altering host-plant growth (Belimov *et al.*, 2014). Lowered BC production in the presence of IAA permits *K. xylinus* to chemotactically seek out nutrient conditions better suited for colonization (ie. wounds on fruit).

IAA and other indole derivatives act as signaling molecules in bacteria, having effects on biofilm formation (Lee *et al.*, 2007) and quorum sensing (Pillai and Jesudhasan, 2006). Similar to IAA effects on *K. xylinus* BC production, indole (**Figure 7F**) decreases biofilm formation in *E. coli* (Lee *et al.*, 2007; Martino *et al.*, 2003). The effect of indole on biofilm formation was first reported to be dependent on SdiA, an N-acyl-homoserine lactone receptor (Lee *et al.*, 2007) but recent data suggests this is not the case (Sabag-Daigle *et al.*, 2012). SdiA belongs to the LuxR family of transcriptional regulators. The genome sequence of *K. xylinus* E25 contains three genes (H845_2765, H845_67, and H845_1915) that encode LuxR family transcription factors which may be involved in *K. xylinus* quorum sensing; an area of research that has yet to be investigated.

Fruit growth occurs prior to ripening, and is regulated by zeatin and GA₃, which work with IAA to induce cytokinesis and cell enlargement, respectively. Bacterial

biosynthesis of zeatin and GA₃ is documented in numerous plant-growth promoting bacteria (Arkhipova *et al.*, 2005; Atzorn *et al.*, 1988; Bastián *et al.*, 1998; Boiero *et al.*, 2007; Bottini *et al.*, 1989; Karadeniz *et al.*, 2006; Phillips and Torrey, 1972) and bacterial phytopathogens (Akiyoshi *et al.*, 1987; Karadeniz *et al.*, 2006). These bacteria also produce IAA and influence cell division, and growth of host plants. Qureshi *et al.* (2013) showed that *K. xylinus* produces endogenous zeatin and GA₃. *B. subtilis*, when grown in association with lettuce, produces zeatin causing an increase in plant shoot and root weight (Arkhipova *et al.*, 2005). GA₃ production by various root-colonizing bacteria is also accompanied by increased plant growth (Bottini *et al.*, 2004). Inoculation with GA₃-producing *G. diazotrophicus*, or exogenous GA₃, increases monosaccharide levels in *Sorghum bicolor* (Bastian *et al.*, 1999). Exogenous GA₃ also increases the size and sugar content of grapes (Casanova *et al.*, 2009). These studies demonstrate that bacterial zeatin and GA₃ production can influence plant development, and suggest *K. xylinus* may be able to influence the growth of its fruit substrate. Exogenous zeatin and GA₃ increase *K. xylinus* growth and BC production (Qureshi *et al.*, 2013). However, the positive effect of zeatin and GA₃ on BC production is indirect because it also increases cell growth.

ABA triggers fruit ripening during the development of climacteric and non-climacteric fruit, though its effect is more pronounced in non-climacteric varieties (Li *et al.*, 2011). The climacteric stage of fruit ripening is associated with increased ethylene production and cellular respiration. Decreased IAA levels, and increased concentrations of ABA during ripening triggers the biosynthesis of ethylene (Zhang *et al.*, 2009b), initiating a cascade of physiological changes that render the fruit more suitable for colonization by *K. xylinus* (see above). ABA biosynthesis has been reported in the phytopathogens *Azospirillum brasilense* (Cohen *et al.*, 2008; Perrig *et al.*, 2007) and *A. lipoferum* (Bottini *et al.*, 2009), various plant-growth promoting bacteria such as *Bradyrhizobium japonicum*, *Rhizobium* spp., *Proteus vulgaris*, *Klebsiella pneumoniae*, *Bacillus megaterium* and *B. cereus* (Boiero *et al.*, 2007; Dangar and Basu, 1991; Karadeniz *et al.*, 2006; Tuomi and Rosenqvist, 1995) and numerous other endophytic bacteria (Sgroy *et al.*, 2009). *K. xylinus* also produces endogenous ABA (Qureshi *et al.*, 2013), which likely plays a role in its

ability to colonize fruit. *A. brasilense* Sp245 produces ABA and increases endogenous ABA levels in *Arabidopsis* (Cohen *et al.*, 2008). ABA biosynthesis by *A. lipoferum* USA 59b stimulates the growth of plants in dry soil (Bottini *et al.*, 2009). Analogously, ABA production by *K. xylinus* could accelerate fruit ripening by stimulating the fruit's endogenous ABA levels. This encourages plant ethylene production, leading to degradation of PC and starch and the liberation of free glucose providing ideal conditions for fruit colonization. ABA also plays a key role in regulating plant-pathogen interactions. In plants, there is a positive correlation between ABA levels and susceptibility to pathogens (Fan *et al.*, 2009; Mohr and Cahill, 2003; Thaler and Bostock, 2004). ABA production by *K. xylinus* may also serve to down-regulate host-plant defenses.

Qureshi *et al.* (2013) showed that exogenous ABA enhanced the growth and BC production of *K. xylinus*. Though monosaccharides in an unripe fruit are scarce, a ripe fruit provides the carbon required for growth, BC production and colonization. ABA therefore acts as a signal to *K. xylinus* indicating that the environment is suitable for colonization. In response, *K. xylinus* growth increases and causes an increase in BC synthesis, enhancing its ability to outcompete other organisms inhabiting the same fruit (Williams and Cannon, 1989). However, like zeatin and GA₃, the positive effect ABA has on BC production is an indirect result of a increased growth rate.

Based on Qureshi *et al.* (2013), IAA, zeatin and GA₃, which are present at high concentrations in unripe fruit, stimulate *K. xylinus* growth ensuring high cell density once ripening begins. IAA directly represses BC biosynthesis, since it is an indicator that fruit is not ripe. Endogenous zeatin and GA₃ production increase fruit size, providing more biomass for colonization. Higher cell densities enhance endogenous ABA production by *K. xylinus* inducing fruit ripening through the activation of plant-produced ethylene. IAA, zeatin, and GA₃ levels drop significantly concomitant with an increase in ABA during the ripening stage, a signal to *K. xylinus* that ripening has begun and that carbon source is available for BC production. Using current data, a model for this process was proposed (**Figure 10**; Augimeri *et al.*, 2015).

The periplasmic space is a region of Gram-negative bacterial cell walls located between the inner cytoplasmic membrane and the outer membrane that contains lipopolysaccharide (Mitchell, 1961). This highly viscous environment contains a thin peptidoglycan layer (Schleifer and Kandler, 1972) and acts as a buffer between the external environment and the inside of the bacterium. External signals are received and transmitted by numerous periplasmic proteins, including degradative enzymes (Cook, 1988; Li *et al.*, 2003; Minsky *et al.*, 1986), periplasmic binding proteins involved with sugar transport (Cangelosi *et al.*, 1990), chemotaxis proteins (Shilton *et al.*, 1996), and proteins that act as chaperones during cell envelope biogenesis (Zorn *et al.*, 2014). Likewise, the BCSC transverses the cell wall of *K. xylinus* and must pass the growing glucan chain through the periplasm to be exported (Römling and Galperin, 2015). Therefore, though they have not been studied to date, proteins within the periplasm of *K. xylinus* warrant investigation and represent a unique approach to investigating IAA and ABA. Determining the effect of IAA and ABA on the periplasmic protein profiles of *K. xylinus* may provide insight into the molecular mechanisms that lead to the phenotypes these hormones induce.

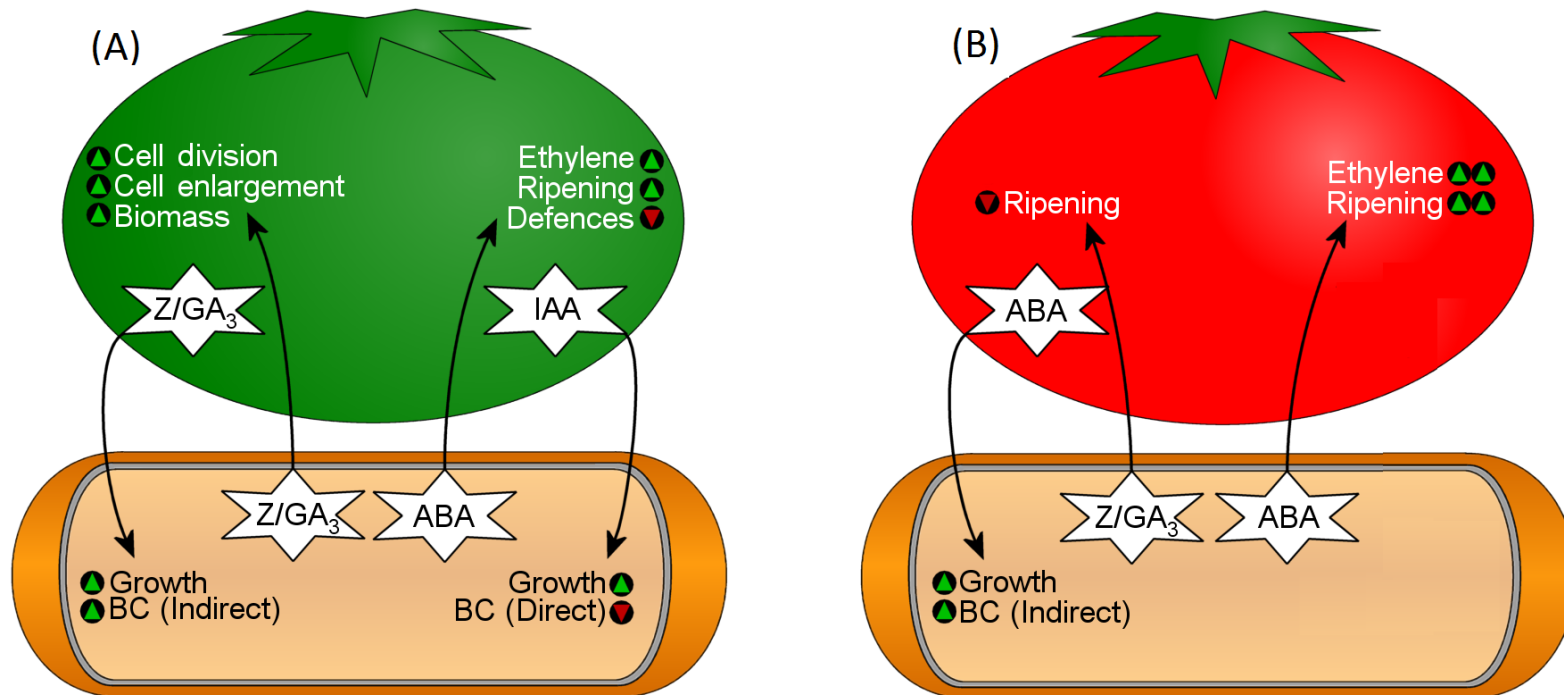


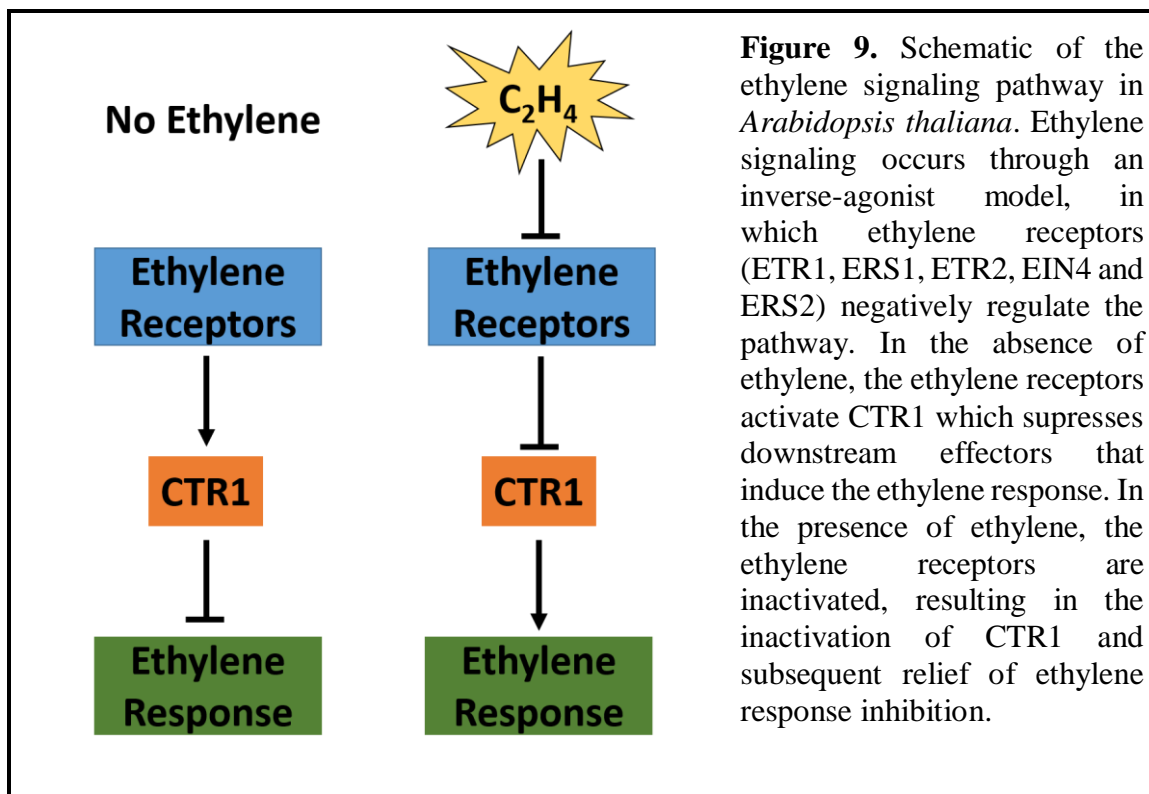
Figure 8. Proposed model of the bi-directional transfer of phytohormones which influences bacterial physiology and fruit development during *K. xylinus* fruit colonization. The fruit on the left represents an unripe fruit that contains high levels of IAA, zeatin (Z), and GA₃ (A). The fruit on the right represents a ripe fruit that contains high levels of ABA (B). Green triangles indicate that a characteristic would be promoted, while red triangles indicate that a characteristic would be reduced. Figure credit to Andrew Varley. Adapted from Augimeri *et al.* (2015).

1.5 Ethylene: Response and biosynthesis in plants and bacteria

The olefin ethylene was the first discovered phytohormone. In 1901, the graduate student, Dimitry Neljubow, from the Botanical Institute of St. Petersburg in Russia, noticed that his pea seedlings had stems that were shorter, thicker and bent sideways compared to normal pea seedlings; a phenotype later termed the triple response (Bakshi *et al.*, 2015; Guzmán and Ecker, 1990). Mr. Neljubow discovered that the abnormal morphology was caused by ethylene, a by-product from the combustion of coal gas that was being used to fuel lamps in the laboratory. Subsequent studies demonstrated that ethylene is a vital phytohormone that regulates numerous processes, such as abscission, senescence, fruit ripening, stress responses and growth (Schaller, 2012).

In *Arabidopsis thaliana*, ethylene binds to copper-containing ethylene-binding domains (EBDs) that are found within the conserved transmembrane domains of five ethylene receptors: ETR1, ERS1, ETR2, EIN4 and ERS2 (Chang *et al.*, 1993; Hua and Meyerowitz, 1998; Hua *et al.*, 1998; Sakai *et al.*, 1998). All five receptors are homodimers and are located on the membrane of the endoplasmic reticulum (Chen *et al.*, 2002; Ma *et al.*, 2006). In the cytosol, ethylene receptors contain GAF domains that mediate protein-protein interactions, as well as kinase and receiver domains that are similar to bacterial two-component signaling systems (Lacey and Binder, 2014; Schaller *et al.*, 2008). Signals are transduced through autophosphorylation of a histidine/serine/threonine residue in the kinase domain, transfer of a phosphate group to an aspartic acid residue on the receiver domain and subsequent phosphorylation of downstream effectors (Chang *et al.*, 1993; Schaller *et al.*, 2008). Two subfamilies of ethylene receptors exist: the first subfamily contains ETR1 and ERS1 that have histidine kinase activity, and the second subfamily consists of ETR2, EIN4 and ERS2 that have serine/threonine kinase activity (Gamble *et al.*, 1998; Moussatche and Klee, 2004). Ethylene signaling is believed to occur through an inverse-agonist phosphorelay model, wherein the ethylene receptors act as negative regulators of the pathway (**Figure 9**). The CTR1 (constitutive triple response-1) protein, a serine/threonine kinase that suppresses the ethylene response, is activated by the ethylene receptors in the absence of ethylene (Clark *et al.*, 1998; Kieber *et al.*, 1993). When ethylene

binds, the receptors undergo a conformational change and inactivate CTR1, which relieves the suppression of downstream effectors that induce ethylene responses.



A bioinformatics study showed that EBDs are common in plants and cyanobacteria, occur in fungi and green algae, but were absent in archaea and bacteria (Wang *et al.*, 2006). However, Kim *et al.* (2007) demonstrated that various *Pseudomonas* species, including plant-associated *P. syringae* and *P. putida*, were chemotactic towards ethylene and that a mutant with the deletion of a gene involved in chemotaxis (*cheR*) was unable to respond to ethylene. Interestingly, both prokaryotic chemoreceptors and plant ethylene receptors utilize the two-component response system. Inner membrane-bound bacterial chemoreceptors (Shapiro, 1993) detect external stimuli via sensory domains in the periplasm, and relay the signals, through the CheW linker protein, to cytoplasmic two-component signal transduction systems (Hazelbauer *et al.*, 2008). External signals are transduced to a kinase (CheA) that phosphorylates two response regulators: CheY, which controls the rotational direction of the flagellar motor, and CheB, which facilitates sensory adaptation (Hazelbauer *et al.*, 2008). Repellents activate CheA and the formation of

phospho-CheY, which binds to flagellar motor proteins and enhances clockwise rotation and random directional changes. Attractants inactivate CheA, reducing the levels of phospho-CheY, and allows the default counter-clockwise rotation of the flagellar motor to produce a forward swimming motion. Chemoreceptors respond to changes in chemoeffector concentration through reversible methylesterification of glutamate residues by the CheR methyltransferase and the CheA-activated CheB methylesterase (Bornhorst and Falke, 2003). Therefore, chemoreceptors are methyl-accepting chemotaxis proteins (MCP). A higher degree of methylesterification is correlated with an increase in attractant response. Attractants inactivate CheA, reduce CheB methylesterase activity, cause an increase in receptor methylesterification and induce a forward swimming motion (Hazelbauer *et al.*, 2008). It is possible that in *Pseudomonas*, ethylene binds to the periplasmic sensory domain of a chemoreceptor, inactivates CheA, and results in increased methylesterification and forward swimming. The absence of CheR would prevent methylesterification and inhibit the chemotactic response that *Pseudomonas* has for ethylene. No bacterial ethylene receptors have been discovered thus far, but Kim *et al.* (2007) established that bacteria have the ability to respond to exogenous ethylene, potentially through chemotaxis signaling pathways.

In addition to being able to detect ethylene, plants and microorganisms are able to synthesize ethylene. Biosynthesis of ethylene in plants occurs via the Yang cycle (Peiser *et al.*, 1984; Yang and Hoffman, 1984), wherein L-methionine is converted to S-adenosylmethionine (SAM) by SAM synthetase, and then SAM is converted to 1-aminocyclopropane-1-carboxylate (ACC) by ACC synthase (ACS). ACC is then oxidized to produce ethylene via one of the plant's ACC oxidase (ACO) enzymes, of which there are five (Yang and Hoffman, 1984). In terms of microbial ethylene biosynthesis, only a few fungal species have been shown to use the ACC pathway (Arshad and Frankenberger Jr, 2002). However, bacteria like *Escherichia coli* produce ethylene from 2-keto-4-methylthiobutyric acid (KMBA), a deaminated derivative of methionine (Ince and Knowles, 1985, 1986). In this pathway, ethylene is produced non-enzymatically by hydroxyl radicals produced from O₂ via a NADH:Fe(III)EDTA oxidoreductase-mediated

reaction. In contrast, phytopathogenic *Pseudomonas syringae* strains (Weingart and Völksch, 1997) and the fungus *Penicillium digitatum* (Chou and Yang, 1973) can produce ethylene from 2-oxoglutarate (α -ketoglutarate) using an ethylene-forming enzyme (EFE) that is classified as an O₂- and Fe(II)-dependent 2-oxoglutarate dioxygenase (2OG-dioxygenase). Interestingly, plant ACO enzymes are also members of the 2OG-dioxygenase family, suggesting a similar mechanism of ethylene formation by all EFEs. Though microorganisms can produce ethylene, an endogenous function of this compound has yet to be described.

Numerous studies have investigated the effect of bacterially-produced ethylene on plants (Baca and Elmerich, 2007; Weingart and Völksch, 1997), as well as the effect of lowering plant-produced ethylene levels by bacterially-produced 1-aminocyclopropane-1-carboxylate (ACC) deaminase enzymes (Glick, 2005). However, there is a paucity of literature regarding the effect of plant-produced ethylene on bacteria. This may be because ethylene is a gas and thus difficult to control in a laboratory setting without specialized equipment. Ethephon (2-chloroethylphosphonic acid) is an ethylene-releasing compound that produces *in situ* ethylene at a 1:1 molar ratio above pH 3.5 (Zhang and Wen, 2010). Base-catalyzed chemical degradation of ethephon results in the production of ethylene, chloride, and phosphate through a first-order reaction (Biddle *et al.*, 1976; Klein *et al.*, 1979; Warner and Leopold, 1969). The rate of ethephon decomposition is positively correlated with pH and temperature (Biddle *et al.*, 1976; Klein *et al.*, 1979). Like ethylene, numerous studies have shown that application of ethephon induces and accelerates ripening of various fruits (Ban *et al.*, 2007; Dhall and Singh, 2013; Dhillon and Mahajan, 2011; Hardie *et al.*, 1981; Jolliffe, 1975; Szyjewicz *et al.*, 1984; Zhang *et al.*, 2012), allowing ethephon to be used in agriculture as a chemical replacement for gaseous ethylene during pre- and post-harvest fruit ripening (Gill *et al.*, 2014; Khorshidi and Davarynejad, 2010; Singh and Janes, 2001).

1.6 Purpose, hypotheses, and rationale of thesis research

The study by Qureshi *et al.* (2013) revealed that IAA directly decreased BC yield in *K. xylinus*, but did not identify a phytohormone that directly increased BC yield. Qureshi *et al.* (2013) also showed that ABA increased the growth rate of *K. xylinus*. The main ripening hormone, ethylene, which is produced in plants in response to changes in IAA and ABA concentrations, was not investigated. The proposed phytohormone-mediated fruit-bacteria interaction model (**Figure 8**) is therefore lacking in this respect. The overall **purpose** of this thesis was to identify molecular mechanisms that lead to the previously observed IAA- and ABA-induced phenotypes, determine whether *K. xylinus* BC biosynthesis and gene expression is influenced by exogenous ethylene, and assess whether *K. xylinus* produces endogenous ethylene.

This thesis tested four **hypotheses**: i) *K. xylinus* periplasmic proteins are involved in mediating IAA- and ABA-induced phenotypes; ii) *K. xylinus* synthesizes endogenous ethylene; iii) Exogenous ethylene increases the yield of BC produced by *K. xylinus*; and iv) phytohormones influence the expression of *K. xylinus* genes involved in BC biosynthesis.

The **rationale** behind these hypotheses were: i) IAA and ABA exert their effects from outside of the cell, therefore periplasmic proteins are likely involved in mediating IAA- and ABA signals within the periplasm; ii) *K. xylinus* synthesizes the fruit ripening hormone ABA, thus it likely produces ethylene, another ripening hormone; iii) ripe fruit provides a more suitable nutrient environment for fruit colonization by *K. xylinus*, so ethylene may act as a signal to upregulate BC production to facilitate this process; and iv) phytohormones influence BC biosynthesis in *K. xylinus*, so it is likely that they influence the expression of BC biosynthesis-related genes.

In this thesis, periplasmic protein profiles of IAA- and ABA-treated *K. xylinus* cultures were examined using one-dimensional sodium dodecyl sulfate polyacrylamide gel electrophoresis (SDS-PAGE) to determine how periplasmic protein expression was

influenced by these phytohormones. To identify proteins involved in mediating IAA- and ABA-induced phenotypes in *K. xylinus*, protein bands displaying differential expression were excised from the gel and analyzed using liquid chromatography mass spectrometry (LC-MS). Qureshi *et al.* (2013) demonstrated *K. xylinus* endogenously produces ABA, zeatin and GA₃; phytohormones that promote fruit growth and ripening. An ethylene detection assay, inspired by the *A. thaliana* triple response assay, was developed to demonstrate that *K. xylinus* synthesizes endogenous ethylene. A method to study bacterial ethylene response using ethephon, a chemical that releases ethylene *in situ*, was developed during this research study. Using this technique, the effect of exogenous ethylene on *K. xylinus* growth, BC production and pellicle properties was assessed. To complement previous and current phenotypic studies involving IAA, ABA and ethylene, this thesis determined the effect of these phytohormones on the expression of *K. xylinus* genes involved BC biosynthesis using reverse transcription quantitative polymerase reaction (RT-qPCR) experiments. This thesis elaborates on the phytohormone-mediated fruit-bacteria interactions of *K. xylinus* and gives new insights into the transcriptional regulation of the *bcs* operon. Altogether, the data obtained from this thesis provides evidence that support the hypothesis that *K. xylinus* is a saprophytic carposphere bacterium that has the ability to effectively colonize and accelerate the rotting of fleshy fruit in the environment.

2 METHODOLOGY

2.1 Chemicals and growth medium

Indole-3-acetic acid (IAA; BioShop) and abscisic acid (ABA; BioShop) were prepared in 100% (v/v) dimethyl sulfoxide (DMSO; BioBasic). L-methionine (BioShop) was dissolved in 0.1 M HCl, while α -ketoglutarate (BioShop), Tris-HCl (BioBasic), ethylenediaminetetraacetic acid (EDTA; BioBasic; pH 8) and 1-aminocyclopropane carboxylic acid (ACC; Sigma) were prepared in ultra-pure water (18.2 M Ω water). Phenylmethylsulfonyl fluoride (PMSF; BioShop) was dissolved in 100% (v/v) ethanol. Stock solutions of ethephon (2-chloroethylphosphonic acid; Sigma), NaCl (BioBasic) and NaH₂PO₄·H₂O (BioBasic) were dissolved in acidified ultra-pure water (pH 2.5). Stock solutions (except those made in DMSO and ethanol) were filter-sterilized. All stock solutions were stored at -20°C until used. Schramm-Hestrin (SH) medium (Schramm and Hestrin, 1954) consisted of 20.0 g/L glucose, 5.0 g/L peptone, 5.0 g/L yeast extract, 2.7 g/L Na₂HPO₄·7H₂O and 1.5 g/L citric acid. SH agar plates contained 15 g/L agar. SH medium was supplemented with cellulase from *Trichoderma reesei* ATCC 26921 (Sigma) to prevent the accumulation of cellulose and to allow for a homogeneous cell solution to be produced when cultures were grown under agitated conditions. Cellulase was filter-sterilized and stored at 4°C. RNase-free water was prepared by treating ultra-pure water with 0.1% (v/v) diethylpyrocarbonate (DEPC; Sigma) for two hours at 37°C. Remaining traces of DEPC were inactivated by autoclaving for 15 minutes at 121°C.

2.2 Bacteria and starter culture growth conditions

Komagataeibacter xylinus ATCC 53582 was maintained as frozen glycerol stocks at -80°C. All starter cultures were grown by inoculating a single rough colony of *K. xylinus* from a Schramm and Hestrin (SH) agar plate streaked from glycerol stock, into 5.0 mL of SH broth (pH 5) supplemented with 0.2% (v/v) filter-sterilized cellulase. Cultures were grown in triplicate and incubated at 30°C with agitation at 150 rpm until the cells reached an OD₆₀₀ of 0.3-0.4. Cultures were harvested by centrifugation (3,500 rpm; 10 minutes; 4°C), washed twice, suspended in sterile 0.85% (w/v) NaCl and quantified with a Petroff-Hauser counting chamber.

2.3 Periplasmic protein isolation and analysis

Periplasmic proteins were extracted from *K. xylinus* using a protocol adapted from Ames *et al.* (1984). *K. xylinus* starter cultures were used to inoculate 25.0 mL of SH broth and SH broth supplemented with 0.01 μM or 10.0 μM IAA or ABA at a concentration of 10^5 cells/mL. Cultures were also supplemented with 0.2% (v/v) cellulase and were grown at 30°C and 150 rpm for 5 days. Cells were transferred to 50.0 mL screw-capped tubes, harvested via centrifugation (3,500 rpm; 10 minutes; 4°C) and washed twice with 0.85% (w/v) NaCl. Washed cell pellets were suspended in 5.0 mL of 0.85% (w/v) NaCl (5X concentrated cells) and 1.0 mL portions were aliquoted into micro-centrifuge tubes. These tubes were centrifuged (13,000 x g; 5 minutes; 4°C) and the supernatant was decanted. The cell pellets were suspended in 50 μL of chloroform, quickly vortexed and then allowed to incubate at room temperature (23°C) for 15 minutes. After incubation, 200 μL of TE buffer (10.0 mM Tris-HCl; 1.0 mM EDTA; pH 8) supplemented with PMSF (100 μM) was added to each tube (PMSF was added to the TE buffer directly before it was added to each tube, since it decomposes quickly under aqueous conditions). Periplasmic proteins were released by mixing the tubes gently by inversion for two minutes. The tubes were centrifuged (10,000 x g; 5 minutes; 4°C) to separate the aqueous and organic phases and 150 μL of the upper aqueous layer containing the periplasmic proteins in TE buffer was transferred into a micro-centrifuge tube. Periplasmic protein samples were diluted 1/10 in TE buffer (10 mM Tris-HCl; 1.0 mM EDTA; pH 8) and quantified using the Bradford assay (Bradford, 1976) with 100 $\mu\text{g}/\text{mL}$ bovine serum albumin (BSA) as the standard. Absorbance at 595 nm was measured using a Bio-Rad xMark Microplate Spectrophotometer. Samples were precipitated by adding two volumes of ice-cold acetone and overnight incubation at -20°C. Periplasmic proteins were recovered by centrifugation (13,000 x g; 15 minutes; 4°C). The supernatant was decanted completely and the protein pellet was allowed to dry at room temperature until the tubes stopped smelling of acetone (about 10 minutes). The dried protein pellet was dissolved in TE buffer (10 mM Tris-HCl; 1.0 mM EDTA; pH 8) supplemented with PMSF (100 μM) to give a protein concentration of 2.0 $\mu\text{g}/\mu\text{L}$. Unused periplasmic proteins were stored as acetone precipitates at -20°C.

SDS-PAGE was used to assess how IAA and ABA influenced the periplasmic protein profiles of *K. xylinus*. Two Bio-Rad Mini-PROTEAN TGX polyacrylamide gradient gels (4-20%) were electrophoresed with identical samples on a Bio-Rad Mini-PROTEAN Tetra System gel apparatus at 125V in 1X Tris/glycine/SDS running buffer that was diluted from a 10X stock (30.3 g/L tris base; 144.0 g/L glycine, 10.0 g/L SDS). One volume of 2X Laemmli sample buffer (120 mM Tris-HCl, pH 6.8; 4% (w/v) SDS; 20% (v/v) glycerol; 0.02% (w/v) bromophenol blue; Laemmli (1970)) was added to aliquoted periplasmic protein samples and the mixture was heated for 10 minutes at 70°C. The first gel was loaded with 5.0 µg/well of protein and was stained with silver as previously described (Gromova and Celis, 2006). The second gel was loaded with 30.0 µg/well of protein and stained (20 minutes) with 0.1% (w/v) Coomassie Blue G-250 dissolved in 50% (v/v) methanol and 10% (v/v) glacial acetic acid. The Coomassie Blue stain was filtered through Whatman #1 filter-paper. Protein bands were developed by overnight incubation in destain solution (40% (v/v) methanol and 10% (v/v) glacial acetic acid). Coomassie Blue staining and destaining were performed at room temperature with gentle agitation. Stained gels were stored in 5% glacial acetic acid and photographed using a Canon Rebel T1i digital camera on a Logan desktop light box.

Protein bands of interest (increased or decreased intensity compared to the untreated control) were excised from the gels, stored in 5% acetic acid and sent to the Sick Kids Hospital Advanced Protein Technology Centre for sequencing using LC-MS. Peptide sequences were compared to the protein database of *K. xylinus* NBRC 3288 that is published on the NCBI website. *K. xylinus* NBRC 3288 has been reclassified as *K. medellinensis* NBRC 3288 (Yamada *et al.*, 2012). Protein identification results were analyzed using Scaffold Proteome Software (www.proteomesoftware.com).

2.4 Prediction of disordered protein domains

The prediction of disordered protein domains within the MtfB protein was determined using the FoldIndex© algorithm, as previously described (Prilusky *et al.*,

2005). This program is available as a free online tool and is used by imputing the amino acid sequence of the protein of interest (<http://bip.weizmann.ac.il/fldbin/findex>).

2.5 Triple response assay

Endogenous production of ethylene from *K. xylinus* was determined using the *Arabidopsis thaliana* triple response assay (Guzmán and Ecker, 1990). Seeds of *A. thaliana* ecotype Columbia (kindly provided by Dr. Dario Bonetta) were surface-sterilized in a sealed plastic container using chlorine gas produced from the addition of 3.0 mL concentrated HCl into 100 mL of bleach. The assay was performed using sectorized polypropylene petri dishes. Growth medium for seeds was added in the quadrants adjacent to those containing SH agar (**Figure 10**). Negative controls consisted of sterile seeds plated on 1X Murashige and Skoog (MS) salts medium (4.33 g/L; pH 6.0; 0.8% agar) containing 1% (w/v) sucrose. MS medium was prepared at 75% of its required final volume so that 0.25 volumes of a 4% (w/v) sucrose stock solution (autoclaved separately) could be added. Positive controls consisted of seeds plated on the MS-sucrose medium supplemented with 10.0 μ M ACC, the precursor for ethylene biosynthesis in plants (Yang and Hoffman, 1984). After seeds were stratified at 4°C for 4 days, *K. xylinus* starter culture (20 μ L; OD₆₀₀=0.5) was spread on the two quadrants of plates containing SH medium (pH 5) with and without the addition of 4.0 mM L-methionine or α -ketoglutarate (**Figure 10**). Experiments using *K. xylinus* grown on SH medium without supplementation were also performed using glass petri dishes to rule out off-gassing as the cause of a negative result when using polypropylene petri dishes. Plates were sealed with Parafilm, wrapped in foil, exposed to light for 2 hours and then germinated in the dark for 72 hours at 23°C.

A separate triple response assay experiment was carried out to determine if ethylene was released as a result of ethephon decomposition in SH medium (pH 5 and pH 7). The assay was performed using sectorized glass petri dishes. Ethephon (1 mM) was spread on SH agar (1.5%), while seeds were plated on the adjacent MS-sucrose medium (**Figure 11**). Positive and negative control experiments, seed stratification and the germination of *A. thaliana* seeds were carried out as they were for the triple response assay with *K. xylinus*.

Both triple response assays were performed using three biological replicates (three plates per treatment). Seedlings were photographed using a Canon Rebel T1i digital camera or a USB 2.0 USB Digital Microscope (Plugable Technologies). The hypocotyl length of 60 seedlings per biological replicate (180 seedlings per treatment) was measured using ImageJ software (Schneider *et al.*, 2012). Statistics were performed using a one-way ANOVA with a Tukey's multiple comparison test. Differences were considered statistically significant if $p < 0.05$.

2.6 Gas chromatography (GC)

GC was used in an attempt to detect ethylene. NaOH (10 N), sodium phosphate buffer (pH 10) and SH broth (pH 7) were supplemented with ethephon (2.0, 20.0, 40.0 and 80.0 mM) for the production of ethylene. Ethephon decomposition was carried out in 2.0 mL GC vials that were incubated statically or at 150 rpm at 30°C for 3 days. *K. xylinus* starter cultures were grown and concentrated to an OD₆₀₀ of 0.5 in SH medium with and without the addition of 4.0 mM L-methionine or α -ketoglutarate; two precursors known to be used for bacterial ethylene biosynthesis. Five hundred microliters was added to a 2.0 mL GC vial and incubated statically or at 150 rpm at 30°C for 3 days. To determine ethylene production from cultures grown on agar, 500 μ L of SH agar was added to a 2.0 mL GC vial and 3.0 μ L of *K. xylinus* starter culture (concentrated to OD₆₀₀=0.5) was spotted. These vials were incubated statically at 30°C with the lid open for 2 days to allow for bacterial growth. The vials were then sealed and incubated in the same way for an additional 24 hours to allow for ethylene accumulation in the vial. *A. thaliana* ecotype Columbia seeds were grown in 2.0 mL GC vials containing 500 μ L MS-sucrose medium supplemented with 10.0 μ M of ACC. Vials containing *A. thaliana* seeds were initially incubated at 4°C in the dark for 3 days. Stratified seeds were then provided light for 2 hours and then incubated at 23°C in the dark for an addition 3 days to allow for germination and ethylene production. Ripening and rotting bananas produce ethylene. Therefore, slices of banana peel (0.5 x 2 cm) were added to 2.0 mL GC vials and incubated statically at 30°C for 3 days. All samples were prepared in triplicate. GC conditions (method name: Ethylene.METH) are described in **Table 3**.

Table 3. GC conditions used for the detection of ethylene.

Variable	Setting
Instrument	Varian 3900 GC
Injection volume	5.0 μ L
Split ratio	20%
Injector temperature	200°C
Run time	4.5 minutes
Column	Varian VF-23ms
Oven temperature	50°C for 2 minutes Ramp of 20°C/min Maximum of 100°C
Carrier gas	Helium
Detector	Flame-ionization detector (FID)
Detector temperature	300°C

2.7 Time-course pH analysis of ethephon-exposed cultures

The pH change during growth of *K. xylinus* cultures in the presence of ethephon was assessed. Starter cultures were used to inoculate 150 mL of SH medium (pH 7) supplemented with 0.2 % (v/v) cellulase at a concentration of 10^5 cells/mL. These cultures were incubated at 30°C and 150 rpm for 14 days. Ethephon was tested at concentrations of 0.01, 0.1 and 1.0 mM, while the untreated control culture was supplemented with an equal volume of acidified ultra-pure water (pH 2.5). An identical experiment using phosphate and chloride (0.01, 0.1 and 1.0 mM) as the test compounds was run in parallel. All flasks were covered with foil and sealed tightly with tape to prevent the escape of released ethylene. Each day, 5 mL of culture was removed and the pH was measured. Three biological replicates were tested with three technical replicates each. Statistical analysis was completed using a one-way ANOVA with Tukey's multiple comparisons test. Differences were considered significant if $p < 0.05$.

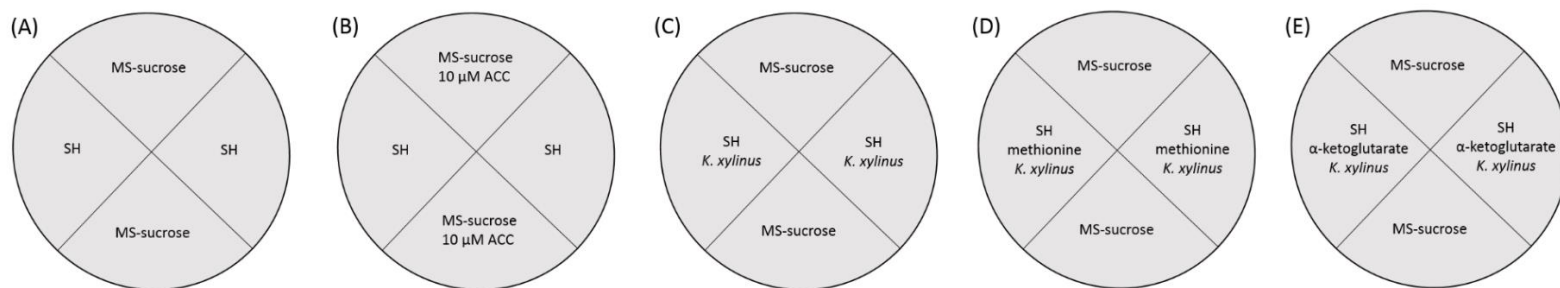


Figure 10. Plate layout for the triple response assay with *K. xylinus*. A schematic illustrates the composition of each quadrant in the negative control (A), positive control (B) and experimental plates (C-E).

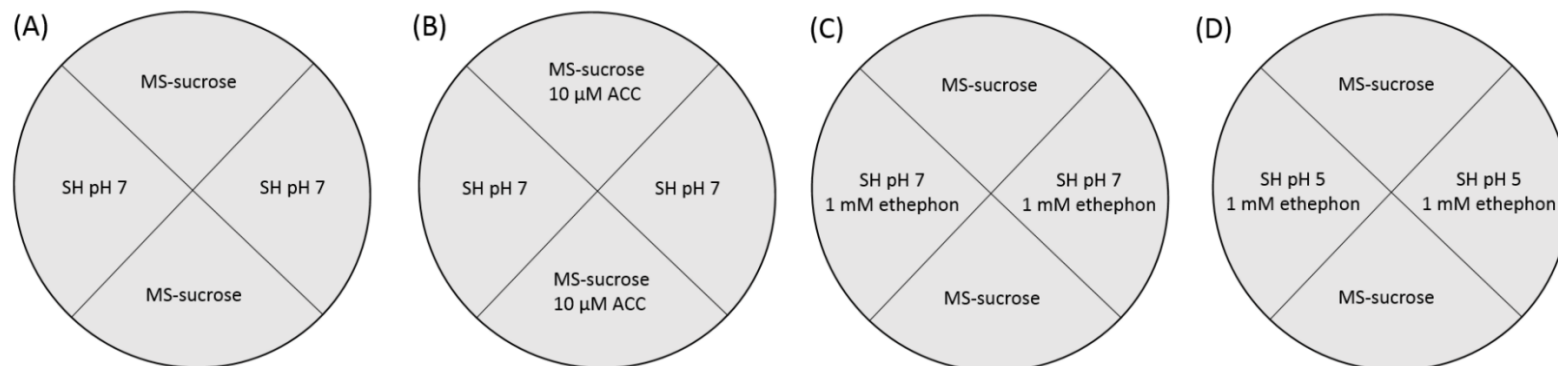


Figure 11. Plate layout for the triple response assay with ethephon as an *in situ* source of ethylene. A schematic illustrates the composition of each quadrant in the negative control (A), positive control (B) and experimental plates (C and D).

2.8 Minimum inhibitory concentration (MIC) assay

MIC assays were performed in sterile 96-well plates using the two-fold serial broth dilution MIC method (Witebsky *et al.*, 1979) to determine the lowest concentration of ethephon that prevented visible growth of *K. xylinus*. Ethephon was tested using a concentration range of 0.195-100 mM and was diluted in SH broth (pH 7). Wells were inoculated with *K. xylinus* starter cultures at a concentration of 10^5 cells/mL in a final volume of 150 μ L. Growth controls without ethephon and sterile controls were included. Plates were sealed with Parafilm and incubated statically for five days. Clear wells were an indication of growth inhibition. To ensure the results were caused by ethylene and not by chloride or phosphate, the two by-products that result from ethephon decomposition, the same experiment was performed using phosphate and chloride at the same concentrations as ethephon was tested. Three biological replicates were tested with one technical replicate each.

2.9 Growth kinetics

The effect of ethephon on the growth of agitated *K. xylinus* cultures was determined in 96-well plates that were inoculated, in triplicate, with *K. xylinus* starter cultures at a concentration of 10^5 cells/mL in a final volume of 200 μ L of SH medium (pH 7) supplemented with 0.4% (v/v) cellulase. Three biological replicates and sterile controls, each with six technical replicates, were included for each treatment. Ethephon concentrations of 0.01, 0.1 and 1.0 mM, along with an untreated control plate that was supplemented with sterile ultra-pure water (pH 2.5), were all tested using separate plates. All unused wells contained sterile water to limit evaporation of test wells. Two experiments were conducted; one in which ethephon or acidified ultra-pure water (pH 2.5) was added only at the beginning of the experiment, while the second included the addition of ethephon or ultra-pure water (pH 2.5) every two days. The latter was conducted to control for the possible loss of ethylene gas, since plates needed to be opened to read the OD. All plates were sealed with Parafilm and incubated at 30°C and 150 rpm. OD₆₀₀ was recorded using a Bio-Rad xMark™ Microplate Absorbance Spectrophotometer. Growth was followed for 335 hours.

The effect of IAA and ABA on the agitated growth of *K. xylinus* was also assessed. Cultures were inoculated at a concentration of 10^5 cells/mL in 25 mL of SH broth supplemented with 0.2% (w/v) cellulase and 0.01 μ M and 10.0 μ M of IAA and ABA. Untreated and DMSO-treated cultures were grown in parallel as controls. All treated cultures contained a final DMSO concentration of 0.02% (v/v) and were grown at 30°C and 150 rpm for 14 days. Each day, 1.0 mL of culture was removed and 100 μ L aliquots were added to the wells of a 96-well plate. Sterile growth medium containing cellulase was used as a blank. OD₆₀₀ was recorded using a Bio-Rad xMark microplate spectrophotometer. All cultures were grown in triplicate, each having their OD₆₀₀ calculated using the mean of six technical replicates. Statistical analysis was carried out using a repeated measures one-way ANOVA with the Greenhouse-Geisser correction.

2.10 Pellicle assays and analysis

K. xylinus pellicles grown in the presence of ethephon were characterized to determine the effect of ethylene on BC production under static conditions. Pellicle assays were conducted in sterile 24-well plates using a final well volume of 2.0 mL SH broth (pH 7). Wells were inoculated with *K. xylinus* starter cultures using three biological replicates, each with six technical replicates, at a concentration of 10^5 cells/mL. Ethephon stock solution was added to obtain final ethephon concentrations of 0.01, 0.1 and 1.0 mM. Each plate contained a row of sterile control wells that consisted of only medium and ethephon to control for contamination. All plates were sealed with Parafilm and incubated statically at 30°C for 7 days. Untreated control plates, as well as phosphate-chloride (0.01, 0.1 and 1.0 mM) control plates were run in parallel. Each treatment was run in its own plate to prevent crossover of ethylene. Additionally, control- and ethephon-treated plates were spatially separated by growing them in different incubators.

The thickness of *K. xylinus* pellicles was measured without the removal of water at the time of harvest. All pellicles, aligned with a ruler, were photographed from the side and measured at three different positions using ImageJ software (Schneider *et al.*, 2012). These

values were averaged to get one value for each technical replicate, which were averaged to obtain one value for each biological replicate.

Pellicle water-holding capacity and BC yield was determined by measuring the wet weights and dry weights, respectively. Pellicle wet weights were determined by removing pellicles from the plates and then holding them on paper towel for three seconds to remove excess medium before weighing. BC yield was determined by treating the pellicles with 0.1 N NaOH at 80°C for 20 minutes to lyse cells. Pellicles were neutralized by shaking in ultra-pure water for 24 hours with two water changes and then dried in micro-centrifuge tubes at 50°C to constant weight before being weighed for pellicle dry weight. Pellicle hydration was calculated by subtracting the dry weight from the wet weight.

The crystallinity index, CI(IR), of untreated *K. xylinus* pellicles as well as those formed in the presence of 0.01, 0.1 and 1.0 mM ethephon and phosphate-chloride, were assessed using Fourier-transform infrared spectroscopy (FT-IR). Pellicles from each treatment that had been NaOH-treated, washed and dried were used for FT-IR analysis on a Perkin Elmer Precisely Spectrum 100 FT-IR spectrometer with a horizontal attenuated total reflectance sampling accessory. For each treatment, three technical replicates for each of the three biological replicates were analyzed using 32 scans with a resolution of 4 cm⁻¹ in the range of 4000 to 650 cm⁻¹. Background correction was performed prior to collecting sample data. OriginPro 2016 software was used for baseline correction and to normalize baseline-corrected transmittance values from 0 to 100. CI(IR) was calculated by converting the transmittance values for the bands at 1437 cm⁻¹ (crystallinity band) and 895 cm⁻¹ (amorphous band) to absorbance values and determining the A_{1437}/A_{895} as previously described (Czaja *et al.*, 2004)

Values for technical replicates of pellicles were averaged to get one value for each biological replicate, which was used for statistical analysis. The means of ethephon-treated cultures were normalized to the mean of the control cultures and presented as the percent

of the control. A one-way ANOVA with a Tukey's multiple comparison test was used. Differences were considered statistically significant if $p < 0.05$.

2.11 Colony morphology

The effect of ethephon-derived ethylene on the morphology of *K. xylinus* colonies was assessed using an agar plate assay. Plates were made with 25 mL of SH agar (pH 7) and ethephon or phosphate-chloride were spread onto plates at concentrations of 0.01, 0.1 and 1.0 mM. Untreated and solvent control plates which consisted of no amendments and the spreading of acidified ultra-pure water (pH 2.5), respectively, were also performed. Triplicate *K. xylinus* starter cultures were grown, washed and inoculated onto agar plates that were sealed with Parafilm and incubated statically for five days. Colonies were photographed with a USB 2.0 USB Digital Microscope (Plugable Technologies). All treatments included three biological replicates.

2.12 Reverse-transcription quantitative polymerase chain reaction (RT-qPCR)

2.12.1 Growth conditions

The effects of IAA and ABA on the steady-state expression levels of *K. xylinus* genes was assessed by performing a seven day time-course RT-qPCR experiment. Triplicate *K. xylinus* starter cultures were pooled and used to inoculate 80 mL of SH broth (10^5 cells/mL) that was supplemented with 0.2% (v/v) cellulase and 0.01 or 10.0 μ M IAA or ABA. A control culture that was treated with an equal volume of 100% (v/v) DMSO was run in parallel and was considered the untreated culture. These master-mix cultures were separated into triplicate 25 mL cultures that were incubated at 30°C and 150 rpm for seven days. Cells were harvested by centrifugation (3,500 rpm; 10 minutes; 4°C) after 3 (72 h), 4 (96 h), 5 (120 h), 6 (144 h) and 7 days (168 h) of growth. Medium-free cell pellets were flash-frozen in liquid nitrogen and stored at -80°C until RNA extraction could be completed (no longer than 7 days). All treatments included three biological replicates.

Ethephon, ABA and IAA were utilized for an RT-qPCR pulse experiment that was completed to assess the effect these hormones had on the expression of certain *K. xylinus* genes. For ethephon- and phosphate-chloride-treated cultures, triplicate *K. xylinus* starter cultures were grown, pooled, washed and quantified. A 2.0 L Erlenmeyer flask, containing 1.0 L of SH broth (pH 5) with 0.2 % (v/v) cellulase was inoculated with 10^5 cells/mL and incubated at 30°C and 150 rpm until an OD₆₀₀ of 0.4-0.5 was reached. Cells were harvested by centrifugation (3,500 rpm; 10 minutes; 4°C), washed twice with room temperature SH broth (pH 7), and suspended in 1.0 L of SH broth (pH 7). This synchronized culture was then separated into triplicate 25 mL cultures that were supplemented with 10.0 µM ethephon, 10.0 µM phosphate-chloride, or an equal volume of acidified ultra-pure water (pH 2.5) for the control. These cultures were incubated for 24 hours to allow for the decomposition of ethephon, and subsequent release of ethylene before being harvested. Flasks were covered with foil and tightly sealed with tape to trap released ethylene. Cultures treated with IAA and ABA were inoculated similarly to those treated with ethephon. After the OD₆₀₀ reached 0.4-0.5, the culture was separated into triplicate 25 mL cultures and supplemented with IAA or ABA at a concentration of 10.0 µM. A control experiment consisting of DMSO-treated cultures was performed in parallel. Cultures were harvested 1 hour after being treated with hormone and medium-free cell pellets were flash-frozen in liquid nitrogen and stored at -80°C until RNA extraction could be completed (no longer than 7 days). All treatments included three biological replicates.

2.12.2 RNA purification, quality control and first-strand cDNA synthesis

Flash-frozen cell pellets (10^9 cells) were subject to total RNA extraction and purification using the Norgen Biotek RNA Purification Plus Kit following manufacturer instructions. Cells were not allowed to thaw prior to treatment with lysis buffer to ensure no change in mRNA levels occurred. Genomic DNA (gDNA) was removed by passing the crude RNA through a gDNA-removal column provided in the kit. Samples were stored at -80°C as RNA precipitates, obtained by the addition of 2.5 volumes of ice-cold 100% (v/v) ethanol, a 1/10 volume of 3.0 M sodium acetate (pH 5.2) and 10.0 µg of glycogen. Precipitated samples were centrifuged (13,000 x g; 30 minutes; 4°C) to recover the RNA.

Pellets were washed with ice-cold 70% (v/v) ethanol and dried at room temperature. Samples were suspended in DEPC-treated Tris-HCl (10 mM; pH 6.0) as soon as the pellets changed from opaque to translucent.

Quality control of RNA was completed on the same day of cDNA synthesis. RNA quality was determined by agarose gel electrophoresis using a 2.0% (w/v) agarose gel. RNA concentration and purity was determined spectrophotometrically on a Cary 50 UV-Visible Spectrophotometer (Varian), by measuring the A_{260} and A_{260}/A_{280} values, respectively. RNA samples were diluted 1/200 in DEPC-treated Tris-HCl (10 mM; pH 6.0; the same buffer the RNA is suspended in) and read in a quartz cuvette. Only samples with A_{260}/A_{280} values within 1.9-2.1 were used for cDNA synthesis. All samples were diluted to the same concentration using sterile DEPC-treated ultra-pure water.

In a reaction volume of 40 μ L, 2.0 μ g of RNA from each sample was converted to first-strand cDNA using the Bio-Rad iScript Select cDNA Synthesis Kit using random hexamer primers according to manufacturer instructions. An initial master mix was made containing all reaction components except for the RNA template. This master mix was aliquoted into 200 μ L polymerase chain reaction (PCR) tubes and RNA samples were added. Three samples were chosen at random from each experiment, and were subject to a mock-cDNA reaction that contained all components except reverse transcriptase, to assess RNA samples for genomic DNA (gDNA) contamination using RT-qPCR. All cDNA samples were stored at -20°C.

2.12.3 Bioinformatic identification of *crp/fnr*_{Kx}

A transcription factor belonging to the CRP/FNR family was shown to positively regulate BC biosynthesis in *K. hansenii* ATCC 23769 (Deng et al., 2013). This prompted investigation of the *K. xylinus* genome for potential homologous genes. BlastN analysis (Altschul et al., 1990) was used to compare the nucleotide sequence of *crp/fnr*_{Kh} (GXY_00863) from *K. hansenii* ATCC 23769 to the *K. xylinus* E25 genome sequence (accession: CP004360.1). This analysis revealed the presence of a *crp/fnr*_{Kx} gene

(H845_3156) that is 79% similar ($E=4^{-175}$; 97% query coverage) to *crp/fnr_{Kh}*. BlastX analysis showed that the encoded protein sequences have 81% identity ($E=1^{-121}$; 94% query coverage). This high level of similarity suggested that CRP/FNR_{Kx} may regulate BC biosynthesis in *K. xylinus* ATCC 53582, similar to the results of Deng *et al.* (2013) that showed CRP/FNR_{Kh} regulates BC biosynthesis in *K. hansenii* ATCC 23769. Therefore, *crp/fnr_{Kx}* expression was analyzed in the RT-qPCR studies.

2.12.4 Primer Design

RT-qPCR primers were designed and validated for seven genes involved in *K. xylinus* BC production (*bcsA*, *bcsB*, *bcsC*, *bcsD*, *cmcAx*, *ccpAx* and *bglAx*; **Table 4**), one gene identified bioinformatically (*crp/fnr_{Kx}*), one gene identified from the periplasmic protein experiment (*oprB*; **Table 4**) and seven reference genes from five different functional class (**Table 4**). Since the *K. xylinus* ATCC 53582 genome sequence is not published, primers for *crp/fnr_{Kx}*, *oprB*, *23SrRNA* and *gyrB* were designed using the nucleotide sequence of identical genes from other *K. xylinus* strains (**Table 5**). End-point PCR was conducted using all primer sets and *K. xylinus* ATCC 53582 gDNA as the template to ensure the expected amplicons were produced. Primer specificity was assessed empirically by end-point PCR using *K. xylinus* ATCC 53582 gDNA as the template and by RT-qPCR melt-curve analysis. PCR products were run on a 2.0% (w/v) agarose to verify amplicon size and primer specificity. All primer sets were designed using Primer3Plus (Untergasser *et al.*, 2007) to be 20-27 base-pairs in length, have a GC content of 45-55%, a melting temperature (T_m) of 55-65°C, and to produce an amplicon of 90-300 base-pairs. Sequences were checked to be specific *in silico* using the Primer-Blast program (<http://www.ncbi.nlm.nih.gov/tools/primer-blast/>) to compare primer sequences to the genome sequences of various *K. xylinus* strains. The mfold web server (<http://mfold.rna.albany.edu/?q=mfold/dna-folding-form>) was used to check primers and amplicons for potential secondary structures. Validated primer sequences are given (**Table 5**).

Table 4. Function of proteins encoded by genes analyzed by RT-qPCR in this study. See introduction for details.

	Gene Name	Encoded Protein	Protein Function
Reference Genes	<i>23SrRNA</i>	23S ribosomal RNA subunit	Structural component of ribosome
	<i>16SrRNA</i>	16S ribosomal RNA subunit	Structural component of ribosome
	<i>gyrB</i>	DNA gyrase B subunit (GyrB)	DNA replication
	<i>gapdh</i>	Glyceraldehyde-3-phosphate dehydrogenase (GAPDH)	Glycolytic enzyme
	<i>rho</i>	Termination factor (Rho)	Transcription termination factor
	<i>rpoA</i>	RNA polymerase α subunit (RpoA)	Transcription initiation
	<i>rpoD</i>	RNA polymerase β subunit (RpoD)	Transcription initiation and binding of RNA polymerase
Target Genes	<i>bcsA</i>	BC synthase A subunit (BcsA)	Glycosyltransferase/BC synthesis
	<i>bcsB</i>	BC synthase B subunit (BcsB)	Carbohydrate binding/BC chaperone
	<i>bcsC</i>	BC synthase C subunit (BcsC)	Outer-membrane pore/BC export
	<i>bcsD</i>	BC synthase D subunit (BcsD)	BC crystallization
	<i>cmcAx</i>	Endo- β -1,4-glucanase (CmcAx)	BC hydrolysis/regulation
	<i>ccpAx</i>	Cellulose-complimenting protein (CcpAx)	BC crystallization/regulation
	<i>bglAx</i>	β -glucosidase (BglAx)	BC hydrolysis/regulation
	<i>crp/fnr_{Kx}</i>	Cyclic-AMP receptor protein/fumarate-nitrate reductase (CRP/FNR _{Kx})	Transcription factor
<i>oprB</i>	Carbohydrate selective porin B (OprB)	Cellular uptake of carbohydrates	

Table 5. Details of primer sets used in this study

Type	Gene	Design Strain ¹	Accession/Locus Tag ³	Amplicon length (bp)	Forward primer sequence (5'→3')	Reverse primer sequence (5'→3')
Reference Genes	<i>23S</i> rRNA	NBRC 3288 ²	GLX_r0020 ⁴	255	TGAGCTGGGTTTAGAACGTCGTG	ACACCTGGCCTATTGACGTGATG
	<i>16S</i> rRNA	Consensus	Consensus	273	TGGGTGGGGGATAACTTTGG	CGAAAACCTTCTCACACACGC
	<i>gyrB</i>	E25	H845_869 ⁵	108	TCTCGTCACAGACCAAGGACAAG	CTTCCTGGGGTGGGTTTCAAAC
	<i>gapdh</i>	E25	H845_402 ⁴	103	GTGGAGGTCGGGATCATGTTCA	TCACCATCCATTCTATACCGGC
	<i>rho</i>	NBRC 3288 ²	GLX_18850 ⁴	190	GTTGTGCCCTCATCGGGTAA	TTACCCGTGCCCTTGAATC
	<i>rpoA</i>	NBRC 3288 ²	GLX_10430 ⁴	116	GGACTTCCTTGATCTCGTTGAG	CTGCCTGAAGAACGACAACATC
	<i>rpoD</i>	E25	H845_2170 ⁵	126	CACCAGCTTGTGTGATCGTCTCG	CGTGGCTACAAGTTCTCGACCTA
Target Genes	<i>bcsA</i>	ATCC 53582	X54676 ⁶	184	ACAATGGGCTGGATGGTCGA	ACCCGCAAAAAGAAGGTCGA
	<i>bcsB</i>	ATCC 53582	X54676.1 ⁶	197	AATGCGTTCATCTTGGGCTTGAC	ATCAGGTCAAGATAGGCGCCAACA
	<i>bcsC</i>	ATCC 53582	X54676.1 ⁶	103	TACCAGTCGCATATCGGCAATCGT	GCAGGTCGTCAACTGGCTTTCAT
	<i>bcsD</i>	ATCC 53582	X54676.1 ⁶	153	TCACCCTGTTTCTTCAGACCCTGT	TCAGTTCGATCTGCAGCTTGCCA
	<i>cmcAx</i>	ATCC 53582	AB091058.1 ⁶	98	CACCAACCTGCAGCATACCAATGA	CGCCATCTGTGGCATTGTTCTTGT
	<i>ccpAx</i>	ATCC 53582	AB091058.1 ⁶	191	TGTTGCCGATGAATGGAGTCCTGT	TGTCTGTCTTGGTCATGCTGGTCA
	<i>bglAx</i>	ATCC 53582	AB091059.1 ⁶	116	TACCGATCAGGAACTTGTCTAT	CAAAAGTGGTGTAGGTCAGG
	<i>crp/fur_{Kx}</i>	E25	H845_3156 ⁵	138	TCAGGCAGCGCCTTGAACAGCTTGACC	TGACATTTCCCGCTGTCCGAAGCAGC
	<i>oprB</i>	NBRC 3288 ²	GLX_01170 ⁴	289	GACAGTCCGTAATCACCAACAGA	CTTACCAGCACCATGGATAGAT

¹Represents the strains of *K. xylinus* whose genome sequences were used to design each primer set.

²*K. xylinus* NBRC 3288 has been renamed to *K. medellinensis* NBRC 3288 (Yamada *et al.*, 2012).

³These locus tags identify each gene and can be found within the genome sequences of the respective *K. xylinus* strain.

⁴Locus tag- Genome accession: AP012159.1

⁵Locus tag- Genome accession: CP004360.1

⁶Gene accession numbers

2.12.5 RT-qPCR

The relative expression levels of these genes (**Table 4** and **Table 5**) were determined after treatment with 10.0 μ M ethephon, IAA, and ABA using the CFX Connect Real-Time PCR Detection System (Bio-Rad). RT-qPCR reactions (10.0 μ L) included the SsoFast™ EvaGreen® Supermix (Bio-Rad), 300 nM or 500 nM primers (**Table 6**) and 4.0 μ L of the appropriate cDNA sample. To minimize technical variation, a master-mix was made that contained Supermix, primers and ultra-pure water. This master-mix was aliquoted into separate tubes and the template of each sample was added to the sub-master-mixes. Aliquots (10.0 μ L; one reaction) of sub-master-mix was then loaded into triplicate wells in the 96-well qPCR plate. Annealing temperature gradients were performed to empirically determine the optimal annealing temperature ($T_{a, opt.}$) for each primer set. The template for annealing temperature gradients consisted of aliquots of cDNA from each sample that were pooled and diluted 1/20 in Tris-HCl (10.0 mM; pH 8). The $T_{a, opt.}$ was chosen as the annealing temperature that resulted in the lowest C_t value and caused specific amplification as shown by melt-curve analysis. Standard curves were completed to ensure the PCR amplification efficiency (E) of each primer set at their optimal annealing temperature was between 90-110% (**Table 6**), as per the minimum information for publication of quantitative real-time PCR experiments (MIQE) guidelines (Bustin *et al.*, 2009; Taylor *et al.*, 2010). The same pooled and 1/20-diluted cDNA were subject to a minimum of four serial dilutions and used as the template for standard curves. The fold-dilution (**Table 6**) depended on the expression level of each gene, as determined from annealing temperature gradients. The cDNA template concentration used for expression analysis (**Table 6**) was determined by the linear dynamic range (LDR) of each primer set (**Table 6**) as determined from the standard curves. Samples to be compared were diluted to the middle range of the LDR of each primer set. Every run included a no template control (NTC) containing Tris-HCl (10.0 mM; pH 8) as the template to check for reagent contamination and a no reverse-transcriptase (NRT) control containing the pooled mock cDNA reaction as the template to check for gDNA contamination. The qPCR reaction conditions were as follows: 2 minutes at 95.0°C, 40 cycles of 95.0°C for 5 seconds, the $T_{a, opt.}$ (**Table 6**) for 15 seconds, and 72.0°C for 5 seconds. Melt-curve analysis was carried out

at the end of every run with an initial denaturation at 95.0°C for 10.0 seconds, and then a temperature gradient from 65.0-95.0°C by steps of 0.5°C every 5 seconds. Plates were loaded using the sample maximization strategy as previously described (Hellemans *et al.*, 2007), by analyzing all samples with a particular gene on one plate to prevent the need for inter-run calibration. Each RT-qPCR was run in triplicate for three biological replicates per treatment.

2.12.6 Analysis and selection of reference genes

K. xylinus reference genes were analyzed using three commonly used gene stability algorithms: geNorm (Vandesompele *et al.*, 2002), NormFinder (Andersen *et al.*, 2004) and RefFinder (Xie *et al.*, 2012). This analysis was completed for each time-point studied using RT-qPCR.

Analysis using geNorm was conducted by exporting raw C_t values from the CFX Manager Software in the form of an RDML file and importing it for analysis into qbase+ version 3.0 software (Hellemans *et al.*, 2007; Vandesompele *et al.*, 2002). Outlier technical replicates were removed prior to analysis. The geNorm algorithm uses a pairwise comparison approach to calculate a gene stability value (M) to determine the most stably expressed genes. For every combination of reference genes and samples, an array consisting of log-transformed expression ratios is calculated. The standard deviation of each array element is defined as the pairwise variation (V) value, and the arithmetic mean of all pairwise variations is termed M . Step-wise exclusion of the least stable gene, and recalculation of the M value identifies the most stably expressed gene. A gene is considered stable if the M value is below 0.5 for homogeneously-derived samples, such as bacterial samples (Hellemans *et al.*, 2007). To determine the optimal number of reference genes to use, the pairwise variation ratio (V_n/V_{n+1}) was calculated (n corresponds to the number of reference genes). A threshold value of 0.15 for V_n/V_{n+1} is suggested, at which the inclusion of another reference gene is not required since it does not significantly improve the normalization factor (Vandesompele *et al.*, 2002). The geNorm algorithm assumes reference genes are not co-regulated, since the expression ratios of co-regulated genes will

result in a low M value regardless of expression stability, due to a low pair-wise variation. As such, reference gene stability was also completed using NormFinder which utilizes an algorithm that does not employ such assumptions.

NormFinder analysis was conducted using the freely-accessible Excel macro (<http://moma.dk/normfinder-software>). Raw C_t values from CFX Manager Software were converted to efficiency-corrected relative linear quantities (RLQ) by normalizing the C_t values for all samples of each gene (C_{t2}) to the sample that produced the lowest C_t value (C_{t1}). The following formula was used:

$$RLQ = \frac{1}{E^{C_{t2}-C_{t1}}}$$

Where,

$$E = (\% \text{ efficiency} \times 0.01) + 1$$

This normalized data was then log-transformed by the macro and analyzed. NormFinder software employs a model-based approach to measure gene stability using intra- and inter-group variations from defined sample groups. These variations are then used to calculate a stability value, where a lower value represents a more stably expressed gene.

RefFinder is a web-based tool (<http://fulxie.0fees.us/>) that integrates the four major computational programs used to determine reference gene stability (geNorm, NormFinder, BestKeeper (Pfaffl *et al.*, 2004) and the comparative $\Delta\Delta C_t$ method (Silver *et al.*, 2006). C_t values from CFX Manager Software were efficiency-corrected in Excel and entered into the RefFinder and analyzed. Based on the rankings from each program, RefFinder assigns an appropriate weight to individual genes and calculates the geometric mean of these weights for their overall final ranking. This final ranking provides a comprehensive expression stability value; this was used to determine the reference genes for data normalization. The number of these reference genes to use was determined by the geNorm V value.

Table 6. RT-qPCR assay optimization.

	Gene	[Primer] (nM)	T _{a, opt.} (°C)	E (%) ¹	Standard Curve (Fold dilution)	LDR (dilution factor)	[Template] (dilution factor)
Reference Genes	<i>16SrRNA</i>	300	60	90.1	10	20-200,000	2000
	<i>23SrRNA</i>	300	62	100.0	10	20-200,000	2000
	<i>gapdh</i>	500	60	100.5	4	4-1024	100
	<i>gyrB</i>	500	60	106.7	4	4-1024	100
	<i>rho</i>	500	58	107.8	3	9-243	100
	<i>rpoA</i>	500	56	91.4	3	27-729	100
	<i>rpoD</i>	500	60	103.1	4	16-1024	100
	Target Genes	<i>bcsA</i>	500	66.4	95.2	3	3-243
<i>bcsB</i>		300	62.4	99.6	3	3-243	100
<i>bcsC</i>		500	60	99.0	4	4-256	100
<i>bcsD</i>		500	60	98.8	4	4-256	100
<i>cmcAx</i>		500	56.7	94.5	4	16-1024	100
<i>ccpAx</i>		500	60	99.4	4	4-256	100
<i>bglAx</i>		500	62	105.0	3	3-243	100
<i>crp/fnr_{Kx}</i>		500	60	105.2	3	36-324	100
<i>oprB</i>		300	60	92.0	3	9-243	100

¹Calculated from the slope of the standard curve: $E=(X-1) \times 100$, where $X=10^{-(1/\text{slope})}$

2.12.7 RT-qPCR quality control, data analysis and statistics

Raw C_t values were exported from CFX Manager Software as RDML files and imported into qbase+, where amplification efficiencies were used to correct C_t values. Technical replicates were excluded if the standard deviation of their C_t values was over 0.2, but the mean of at least two technical replicates for each sample was used for comparison. Data analysis was carried out using the $\Delta\Delta C_t$ method (Livak and Schmittgen, 2001) employed in the Bio-Rad CFX Manager 3.1 Gene Study software using efficiency-corrected C_t values. For the time-course experiment with IAA and ABA, data for each time-point was made relative to the DMSO-treated control sample from the same time-point and validated reference genes were used for normalization. For the pulse experiment, C_t values from ethephon and phosphate-chloride RT-qPCR assays were made relative to C_t values obtained from the acidified ultra-pure water (pH 2.5) control samples, while C_t values from IAA and ABA RT-qPCR assays were made relative to C_t values from their respective DMSO-treated controls. The data obtained from the pulse experiment was normalized to the geometric mean of the efficiency-corrected expression data of the validated reference genes. Results from the gene study were imported into GraphPad Prism 6.0 software and the data was plotted. Expression differences were tested for statistical significance in qbase+ using an unpaired, two-tailed t -test. Differences were considered statistically significant if $p < 0.05$.

3 RESULTS

3.1 IAA and ABA influence the periplasmic protein profiles of *K. xylinus*

K. xylinus has been shown to be affected by IAA and ABA (Qureshi et al., 2013), but a molecular basis for these effects has yet to be described. The periplasmic space acts as a buffer between the extracellular and intracellular environment, and likely contains proteins involved in IAA and ABA signalling. Thus, the effect of IAA and ABA on the expression of *K. xylinus* periplasmic proteins was assessed. *K. xylinus* cultures supplemented with 0.01 μM and 10.0 μM IAA and ABA were subjected to periplasmic protein extraction and SDS-PAGE analysis. Numerous differences in protein band intensity was observed when *K. xylinus* was grown in the presence of IAA and ABA (**Figure 12**). Differences in band intensity were more obvious on the silver-stained gel (**Figure 12A**) compared to the Coomassie-stained gel (**Figure 12B**) due to silver-staining being a more sensitive staining method (Chevalier, 2010) or because the ionization states of silver and Coomassie Blue are different during staining. For example, the protein bands at a molecular weight greater than 212 kDa were stained by silver-stained (**Figure 12A**) but were negatively stained by Coomassie Blue (**Figure 12B**).

Proteins corresponding to the bands labelled SS-261 (261 kDa) and SS-278 (278 kDa) were only expressed in the presence of IAA (**Figure 12A**) and showed increasing intensity with a higher IAA concentration (10.0 μM). These proteins were absent in the untreated- and ABA-treated samples and could only be observed with the more sensitive silver stain (**Figure 12A**), suggesting the protein concentration was too low to be detected by Coomassie Blue staining (**Figure 12B**). The protein band labelled as PB-29 was also only affected by IAA. As clearly illustrated in the silver-stained gel (**Figure 12A**), the intensity of PB-29 was greater in the lane containing the 10.0 μM IAA sample compared to the lanes containing the untreated- and ABA-treated samples. This suggests that IAA may upregulate the expression of the protein(s) within the PB-29 band.

In contrast, protein bands PB-25 and CS-36 were only affected by ABA (**Figure 12A**) exhibiting greater intensity in the ABA-treated samples compared to the untreated-

and IAA-treated samples suggesting that the protein(s) that constitute PB-25 and CS-36 may be upregulated by ABA.

Interestingly, the protein bands designated CS-46 and PB-55 were affected by both IAA and ABA (**Figure 12A**). In comparison to the untreated control, these protein bands were less abundant in the lanes containing IAA-treated samples and more abundant in the lanes containing ABA-treated samples.

The protein bands designated CS-36 and CS-46 were excised from the Coomassie-stained gel and represent protein(s) that were affected by only ABA and both IAA and ABA, respectively. Bands SS-261 and SS-278 were extracted from the silver-stained gel and represent protein(s) that were only affected by IAA. These proteins were identified by mass spectrometry.

The protein containing bands that differed in intensity due to IAA or ABA treatment were excised from the gel and subjected to LC-MS analysis to identify the constituent proteins. The CS-36 and CS-46 protein bands were excised from the Coomassie-stained SDS-PAG gel. Twelve proteins were identified from band CS-36 (**Table 7**) with molecular weights (MW) in the range of 33-40 kDa. CS-36 showed an increased intensity in ABA-treated samples compared to the untreated control (**Figure 12**). The proteins identified in the CS-36 band belong to various functional classes including sugar and alcohol metabolism, redox reactions, branched-chain amino acid biosynthesis, S-methyl-5'-thioadenosine degradation and terpenoid biosynthesis. Singular protein(s) affected by ABA could not be determined from this experiment.

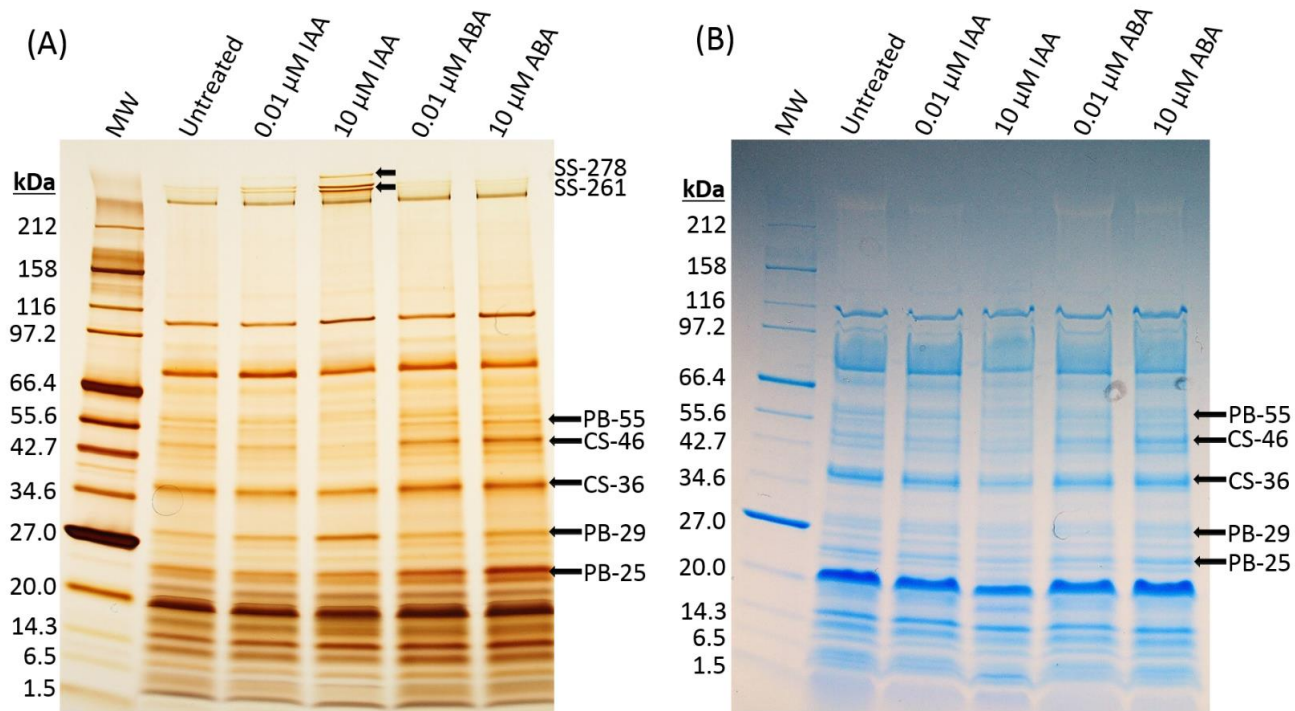


Figure 12. IAA and ABA influence the periplasmic protein profiles of *K. xylinus*. Cultures were grown for five days in SH medium that was either untreated or supplemented with 0.01 μM or 10.0 μM of IAA or ABA. Periplasmic proteins were extracted with chloroform (see methods for details) and analyzed using Bio-Rad Mini-PROTEAN TGX polyacrylamide gradient gels (4-20%) and SDS-PAGE. The gel on the left was loaded with 5.0 μg of protein and stained with silver (A). The gel on the right was loaded with 30 μg of protein and stained with Coomassie Blue (B). Black arrows show protein bands whose intensities are altered by IAA and/or ABA. Molecular weight (MW); Silver-stained (SS); Coomassie-stained (CS); Protein band (PB).

Table 7. Proteins identified in the CS-36 protein band by LC-MS.

Identified Protein	Accession Number	Molecular Weight (kDa)	% Coverage	Protein Function
Pyruvate dehydrogenase E1 component α subunit	GLX_27610	34	17	Sugar metabolism
Pyruvate dehydrogenase E1 component β subunit	GLX_27620	37	36	Sugar metabolism
Fructose-1,6-bisphosphatase	GLX_02870	35	17	Sugar metabolism
6-phosphogluconate dehydrogenase	GLX_20720	36	25	Sugar metabolism
Glyceraldehyde 3-Phosphate dehydrogenase	GLX_24640	36	32	Sugar metabolism
Isocitrate dehydrogenase	GLX_27020	37	24	Sugar metabolism
Alcohol dehydrogenase zinc-dependant	GLX_07290	37	16	Alcohol metabolism
Alcohol dehydrogenase zinc-dependant	GLX_06680	40	41	Alcohol metabolism
Ketol-acid reductoisomerase	GLX_16830	37	34	Amino acid biosynthesis
D-isomer-specific 2-hydroxyacid dehydrogenase	GLX_01160	33	30	Redox reactions
S-methyl-5'-thioadenosine phosphorylase	GLX_26470	33	25	S-methyl-5'-thioadenosine degradation
4-hydroxy-3-methylbut-2-enyl diphosphate reductase	GLX_09340	40	15	Terpenoid Biosynthesis

The CS-46 protein band was more abundant in ABA-treated samples and less abundant with IAA-treated samples compared to the untreated control (**Figure 12**). LC-MS analysis identified 19 different proteins with a MW range of 37-55 kDa (**Table 8**). Similar to the CS-36 protein band, numerous proteins involved with many areas of fundamental bacterial metabolism (sugar, amino acid, protein, fatty acid, nucleotide, DNA, alcohol) were identified. The functions of other identified proteins include S-adenosyl-L-methionine and S-adenosyl-L-homocysteine metabolism, periplasmic protein turnover and cellular uptake of carbohydrates. The specific protein(s) affected by IAA and ABA could not be determined from this experiment since proteins of similar molecular weight could not be sufficiently resolved by one-dimensional gel electrophoresis.

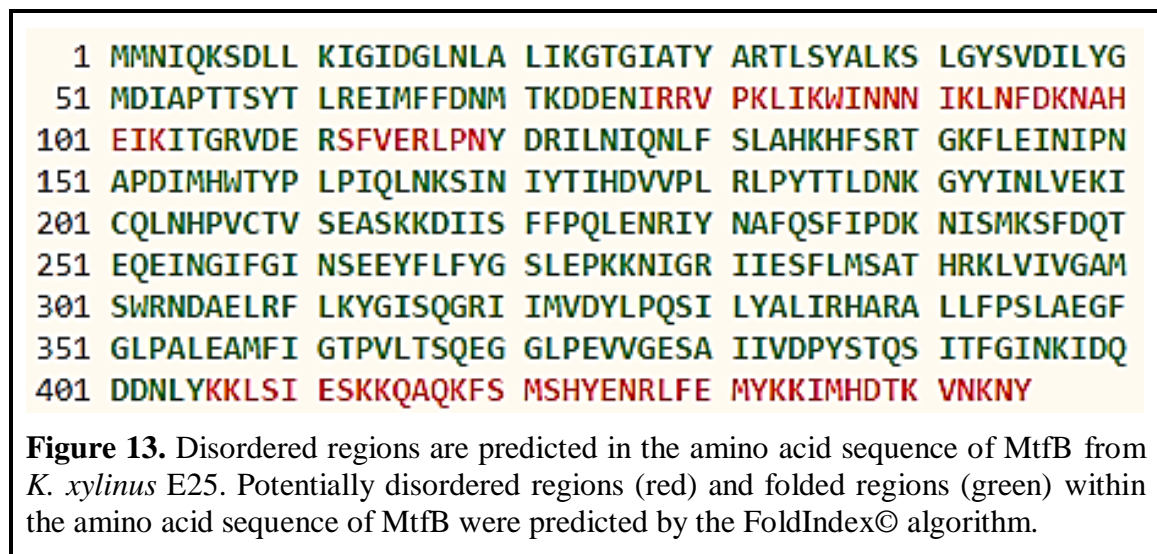
Table 8. Proteins identified in the CS-46 protein band by LC-MS.

Identified Protein	Accession Number	Molecular Weight (kDa)	% Coverage	Protein Function
Isocitrate dehydrogenase	GLX_27020	37	22	Sugar metabolism
Isocitrate dehydrogenase [NADP]	GLX_15100	46	31	Sugar metabolism
Pyruvate dehydrogenase E1 component β subunit	GLX_27620	37	27	Sugar metabolism
Enolase	GLX_05920	45	31	Sugar metabolism
Acetyl-CoA hydrolase	GLX_06800	55	18	Acetyl-CoA metabolism
DNA polymerase III subunit β	GLX_00020	40	14	DNA replication
Adenylosuccinate synthetase	GLX_25000	46	33	Purine biosynthesis
Transcription termination factor Rho	GLX_18850	48	21	Transcription termination
Threonine synthase	GLX_26260	51	13	Amino acid metabolism
Aldehyde/betaine dehydrogenase	GLX_24740	52	23	Amino acid metabolism
Elongation factor Tu	GLX_10690	43	58	Protein synthesis
Aspartyl/glutamyl-tRNA amidotransferase subunit B	GLX_05220	53	18	Protein synthesis
Argininosuccinate synthase	GLX_06620	45	18	Nitrogen metabolism
Adenosyl-homocysteinase	GLX_14510	47	21	S-adenosyl-homocysteine metabolism
S-adenosyl-methionine synthase	GLX_18200	43	23	S-adenosyl-methionine metabolism
Acetyl-CoA carboxylase	GLX_19250	49	15	Fatty acid metabolism
Aldehyde dehydrogenase	GLX_16210	50	21	Alcohol metabolism
Endopeptidase DegP/Do	GLX_19020	54	16	Periplasmic protease
Porin B carbohydrate selective	GLX_01170	55	22	Carbohydrate uptake

The SS-261 and SS-278 protein bands were only observed in silver-stained IAA-treated samples. A single protein with a MW of 51 kDa was identified (13% coverage) in the SS-261 band was a mannosyltransferase B (*mtfB*; GLX_18490) that is closely related to the GT-1 family of glycosyltransferases. No other proteins were identified in the SS-261 band suggesting that IAA induces the expression of MtfB in *K. xylinus*. Interestingly, the SS-261 band ran at a calculated MW of 261 kDa on the SDS-PAGE but was identified as a 51 kDa protein. No proteins were identified in SS-278 band; this is likely due to a low protein concentration.

3.2 The MtfB protein from *K. xylinus* has predicted disordered regions

The aberrant migration of MtfB through the SDS-PAGE gel prompted investigation of possible disordered regions within the proteins sequence. The IDP prediction algorithm FoldIndex© found four regions of disorder within the MtfB sequence (**Figure 13**).



3.3 *K. xylinus* produces low levels of endogenous ethylene

K. xylinus was assessed for endogenous ethylene production using GC and the *Arabidopsis thaliana* triple response assay (Guzmán and Ecker, 1990). Multiple attempts to detect ethylene using GC failed. This is likely due to *K. xylinus* producing ethylene concentrations below the limit of detection by GC analysis, as well as non-ideal GC conditions. However, the triple response assay showed that *K. xylinus* produces low

concentrations of ethylene (**Figure 14**). *A. thaliana* seedlings were grown in the dark in sectored petri dishes in the presence of *K. xylinus* grown on adjacent plate sections (**Figure 10**). Seedlings displayed a full triple response phenotype (shorter and thicker hypocotyl with exaggerated apical hook) when grown in the presence of ACC and an intermediate response in the presence of *K. xylinus* (**Figure 14A**). The hypocotyl length of seedlings grown in the presence of ACC and *K. xylinus* were significantly shorter than the untreated control, but hypocotyl shortening was significantly greater in the presence of ACC compared to *K. xylinus* (**Figure 14B**). Due to the dose-dependent nature of the triple response phenotype (Larsen and Chang, 2001), this suggests that *K. xylinus* produces low levels of endogenous ethylene that induces a slight triple response in dark-grown *A. thaliana* seedlings. Off gassing was not an issue when using plastic petri dishes since comparable results were obtained when *K. xylinus* was plated on SH agar in plastic and glass plates.

3.4 *K. xylinus* has proteins similar to other ethylene-forming enzymes

All ethylene-forming enzymes (EFEs) are members of the 2-oxoglutarate dioxygenase (2OG-dioxygenase) family. BlastP analysis comparing the protein sequence of the *P. syringae* pathovar pisi EFE (Q9Z3T0) to the *K. xylinus* E25 genome sequence reveals two similar *K. xylinus* proteins: 1) Fe(II)-dependent 2OG-dioxygenase (WP_025437122.1; E = 1^{-23} ; 28% identities, 40% positives with 88% query coverage), and 2) iron/ascorbate oxidoreductase (WP_025439960.1; E = 1^{-16} ; 27% identities, 40% positives with 84% query coverage). A similar search using the *A. thaliana* ACC oxidase 1 enzyme (ACO1) sequence identified the same two *K. xylinus* proteins: 1) Fe(II)-dependent 2OG-dioxygenase (WP_025437122.1; E = 8^{-17} ; 24% identities, 39% positives with 88% query coverage), and 2) iron/ascorbate oxidoreductase (WP_025439960.1; E = 2^{-24} ; 26% identities, 44% positives with 87% query coverage).

3.5 Ethylene is produced from ethephon decomposition in SH medium (pH 7)

The production of ethylene from ethephon decomposition on SH medium (pH 5 and pH 7) was assessed using GC and the *A. thaliana* triple response assay. Ethylene could not

be detected using GC. However, ethylene production from ethephon was verified using the triple response assay. *A. thaliana* seedlings were grown in sectored petri dishes in the presence of no ethylene source, an endogenous ethylene source (ACC) and an exogenous ethylene source (ethephon; **Figure 11**). The growth of seedlings in medium containing ACC allowed ethylene production and induction of the triple response phenotype (**Figure 15A**). Ethephon decomposition was performed on SH agar (pH 5 and pH 7) in the sectored petri dishes containing *A. thaliana* seeds on MS-sucrose agar. The hypocotyl thickness was increased and the apical hook was exaggerated for seedlings grown in the presence of ethylene produced from ethephon decomposition on pH 7 SH agar compared to the untreated control (**Figure 15A**). In addition, the hypocotyl length of seedlings grown in the presence of ACC and ethephon (decomposed on pH 7 SH agar) were significantly shorter than the untreated control (**Figure 15B**). The triple response was not induced in seedlings grown on plates where ethephon was spread onto pH 5 SH agar, indicating the rate and efficiency of ethephon decomposition was higher on pH 7 SH agar. This result confirms that ethephon decomposition occurs in SH medium (pH 7) and that sufficient ethylene is released to induce a biological response at this pH.

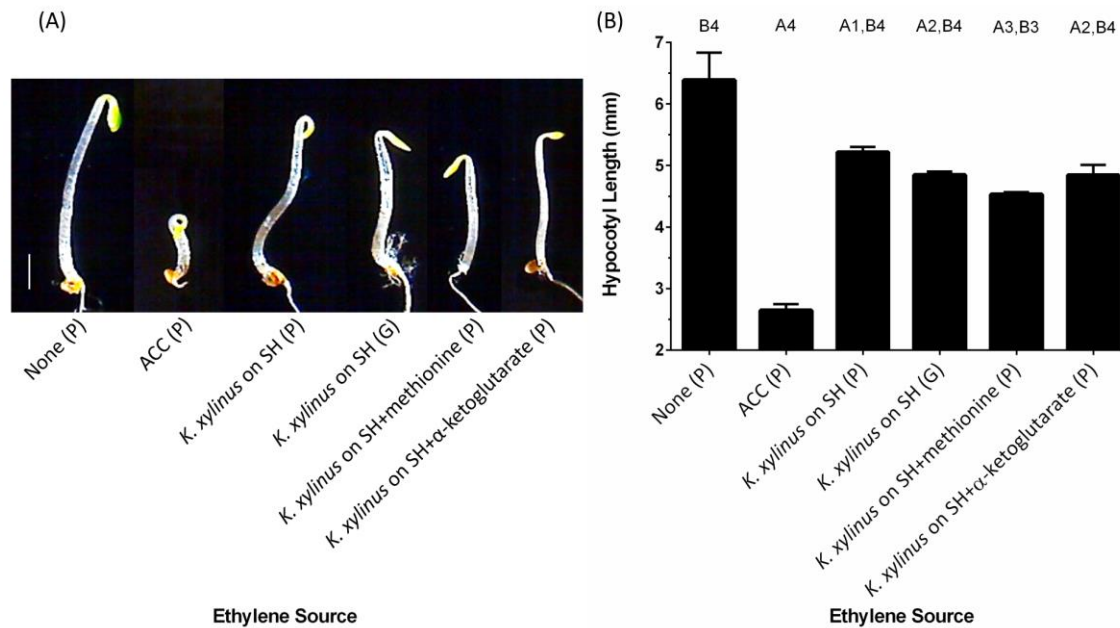


Figure 14. *K. xylinus* produces low-levels of endogenous ethylene. Dark-grown *A. thaliana* seedlings display the triple response phenotype (shorter and thicker hypocotyl with exaggerated apical hook) when grown in the presence of ACC (full response) and *K. xylinus* (intermediate response) compared to the untreated control (A). The hypocotyl length of seedlings grown in the presence of ACC and *K. xylinus* were significantly shorter than the untreated control, while hypocotyl shortening was significantly greater in the presence of ACC compared to *K. xylinus* (B). Scale bar represents 1 mm. Different treatments containing *K. xylinus* were not statistically different from each other. Plastic petri dishes (P) and glass petri dishes (G) were used for the assay. “A” indicates a treatment is significantly different from the untreated control. “B” indicates a treatment is significantly different than the ACC-treated positive control. 1 = $p < 0.05$; 2 = $p < 0.01$; 3 = $p < 0.001$; 4 = $p < 0.0001$. Error bars show SD ($n = 3$).

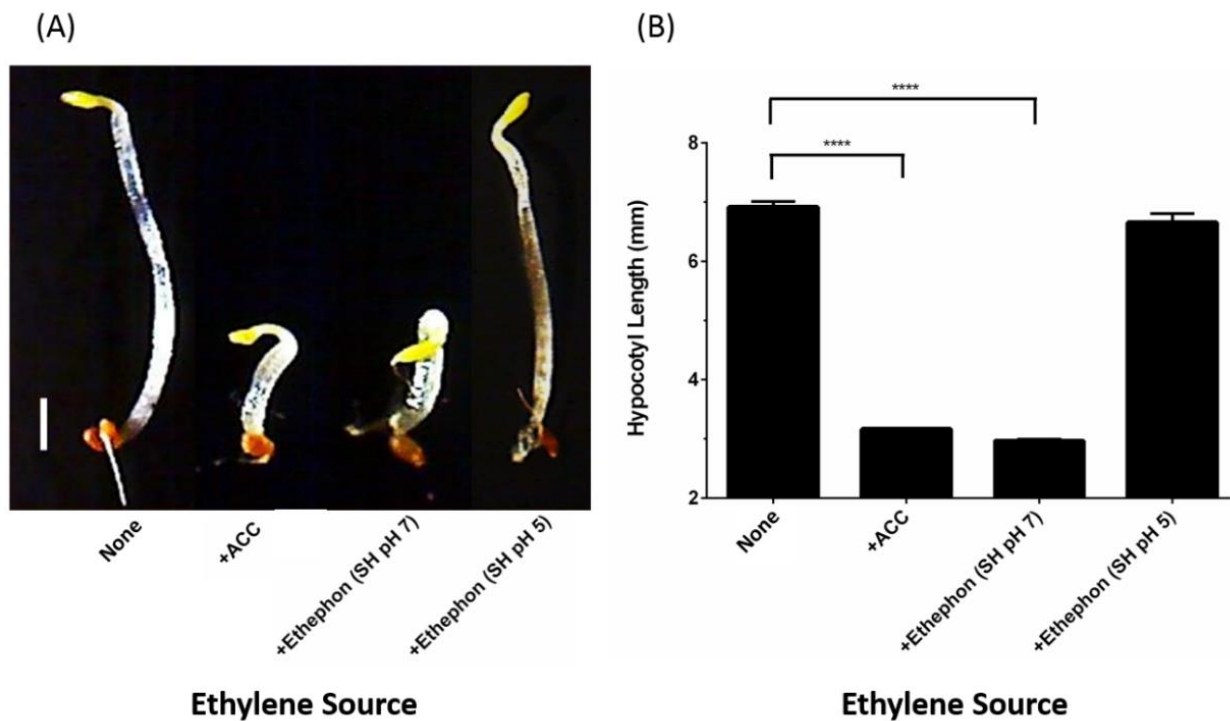


Figure 15. Ethylene is released by ethephon decomposition in SH medium (pH 7). Dark-grown *A. thaliana* seedlings exhibit the triple response phenotype (shorter and thicker hypocotyl with exaggerated apical hook) when grown in the presence of ACC and when ethephon is decomposed into ethylene on SH medium at pH 7 but not SH medium at pH 5 compared to the untreated control (A). Scale bar represents 1 mm. The hypocotyl length of seedlings grown in the presence of ACC and ethephon-derived ethylene were significantly shorter than the untreated control (B). Error bars show SD ($n = 3$). **** $p < 0.0001$. From Augimeri and Strap (2015).

3.6 *K. xylinus* culture pH allows for ethephon decomposition

K. xylinus is an acetic acid bacterium and is known to decrease the pH of its culture medium (Kawano *et al.*, 2002b). Therefore, a time-course pH analysis was performed over a 14 day period to ensure the culture pH remained above 3.5 so that ethephon decomposition into ethylene would proceed unimpaired. This experiment was conducted using SH medium at pH 7 which was shown to facilitate ethephon decomposition into ethylene (**Figure 15**). The pH of all cultures decreased from pH 7 to approximately pH 5.5 for the first 7 days, wherein the pH increased back to pH 7 (**Figure 16A**). Thus, acidification of the culture medium by *K. xylinus* would not have significantly affected ethephon decomposition and consequently, ethylene evolution. Comparable results were obtained for cultures treated with phosphate and chloride (**Figure 16B**). However, when *K. xylinus* was cultured in SH medium (pH 5), the pH dropped to about 4 (**Appendix Figure A1**), which may have a negative impact on ethephon decomposition.

3.7 *K. xylinus* cultures have an increased final pH in the presence of ethylene

The pH of *K. xylinus* cultures treated with ethephon and phosphate-chloride were assessed over a 14-day period (**Figure 16**). Ethephon-treated cultures had a significantly higher final pH compared to the untreated control (**Figure 17A**). The final pH of cultures treated with phosphate and chloride were not different from the control (**Figure 17B**), indicating that the higher final pH observed with ethephon-treated cultures was due to the presence of ethylene.

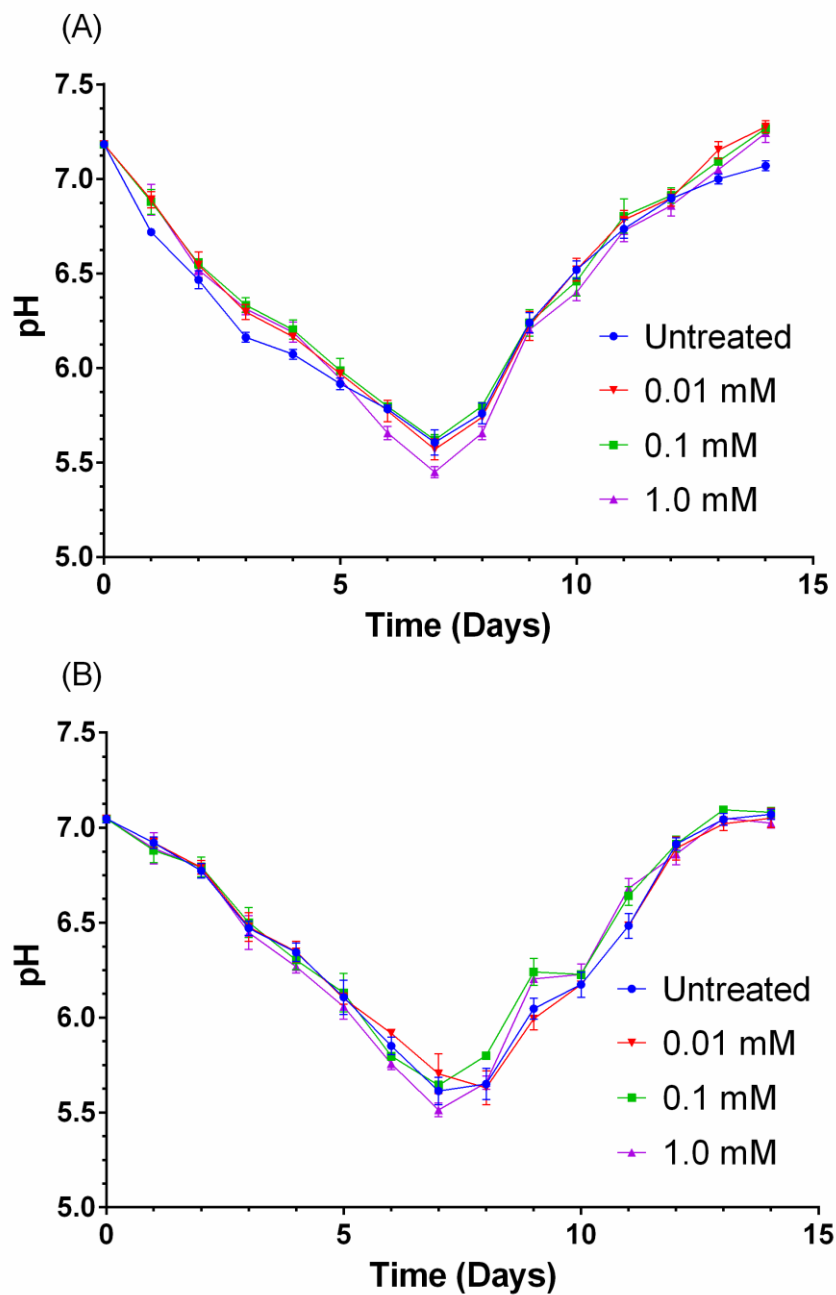


Figure 16. The pH of *K. xylinus* cultures grown in SH medium (pH 7) stays above 3.5, allowing for efficient decomposition of ethephon into ethylene. *K. xylinus* was grown at 30°C and 150 rpm in SH medium (pH 7) that was supplemented with 0.2% (v/v) cellulase, as well as ethephon (A) or phosphate and chloride (B). The change in culture pH was monitored for 14 days. Note that the y-axis begins at pH 5. Error bars show SD ($n = 3$). From Augimeri and Strap (2015).

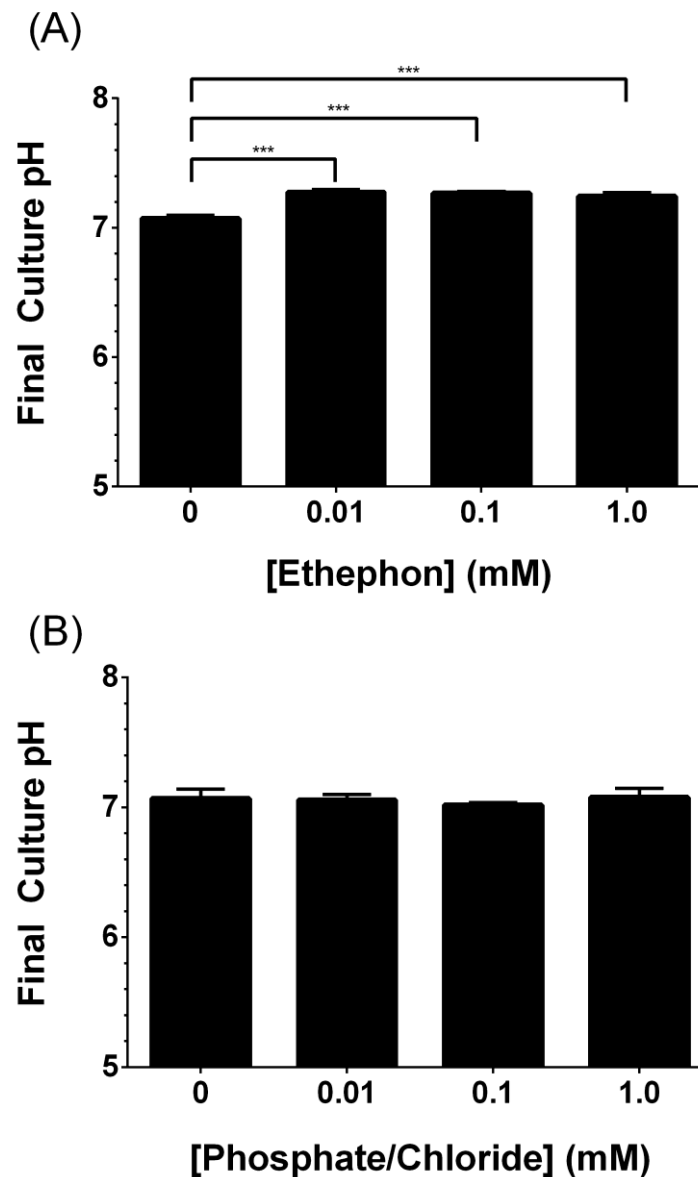
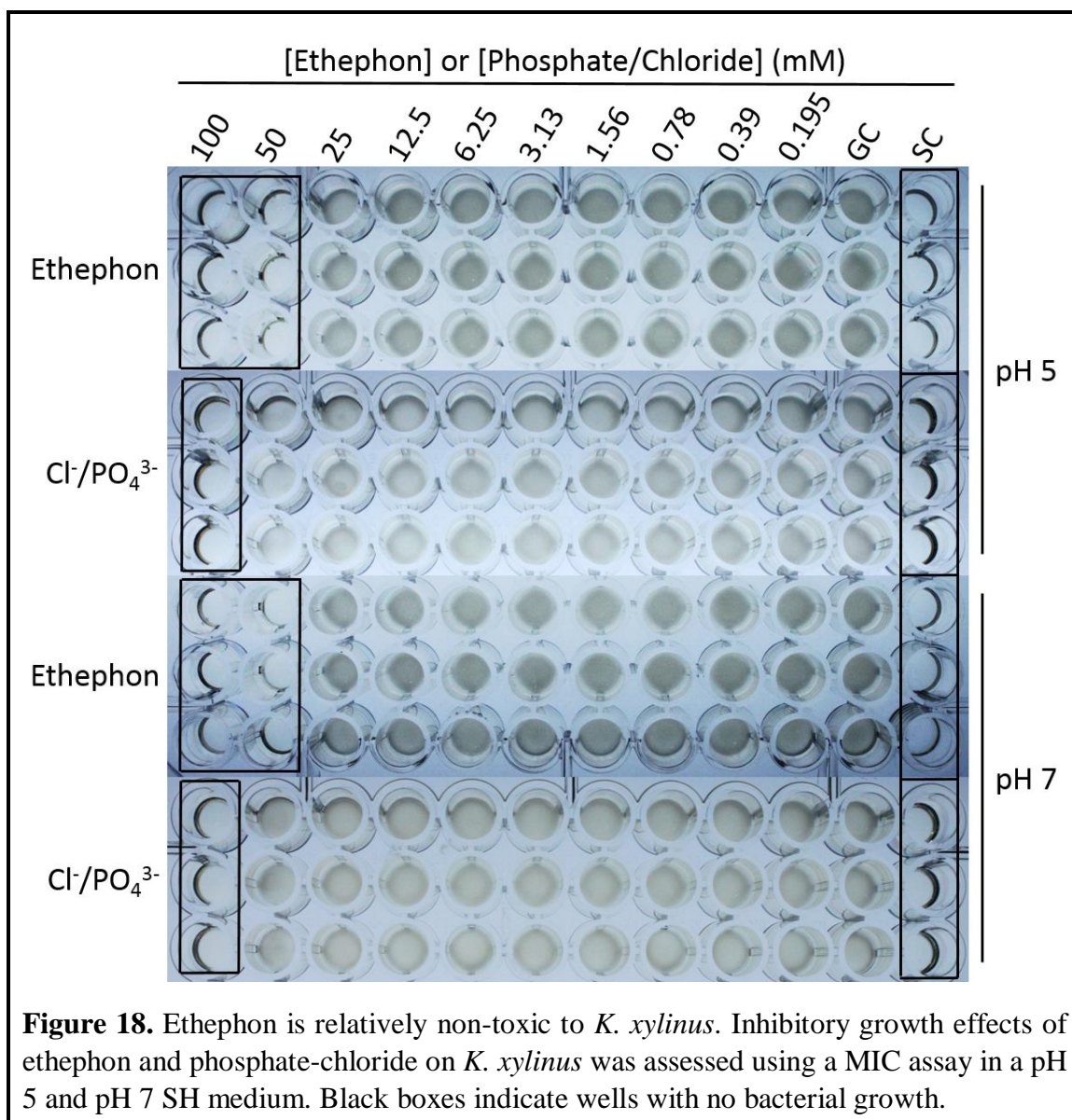


Figure 17. Ethephon-derived ethylene causes an increase in the final pH of *K. xylinus* broth cultures. Cultures were grown at 30°C and 150 rpm in SH broth (pH 7) supplemented with ethephon (A) or phosphate-chloride (B) and 0.2% (v/v) cellulase. The final culture pH of phosphate-chloride-treated cultures was not different from the untreated control, indicating that the increased final pH of ethephon-treated cultures was caused by the presence of ethylene. Data presented indicates the final culture pH after 14 days of growth and was normalized to, and expressed as percent of the untreated control. Note that the y-axis begins at pH = 5. Error bars show SD ($n = 3$). *** $p < 0.001$.

3.8 Ethephon is relatively non-toxic to *K. xylinus*

An MIC assay was performed to assess whether ethephon concentrations of 0.195 to 100 mM inhibited the growth of *K. xylinus*. In both a pH 5 and pH 7 SH medium, *K. xylinus* growth was prevented with ethephon and phosphate-chloride at a concentration of 100 mM (**Figure 18**). In contrast, growth was inhibited with 50 mM ethephon but not phosphate-chloride at the same concentration. This suggests that ethylene prevents the growth of *K. xylinus* when it is cultured in the presence of 50 mM ethephon in both SH media. This result is contradicted by the *A. thaliana* triple response assay (**Figure 15**), which indicated that ethylene was not liberated from ethephon on a pH 5 SH medium. However, ethephon decomposition for the triple response assay was conducted on solid medium and was spatially separated from the seedlings. For the MIC assay, ethylene liberation was performed using broth and occurred locally with the bacteria present. It is possible that more ethylene is released at pH 5 when ethephon is decomposed in a liquid compared to solid medium. In addition, the triple response assay utilized an ethephon concentration of 1 mM, while growth inhibition was observed using 50 mM ethephon during the MIC assay. Therefore, it is also possible that more ethylene was released during the MIC assay compared to the triple response assay and prevented *K. xylinus* growth. It cannot be ruled out that the observed growth inhibition in the 100 mM chloride-phosphate treatment may be due to the Na⁺ counter-ion. Since NaCl and NaH₂PO₄ were both added at 100 mM, the [Na⁺] would have been 200 mM, which could have prevented the growth of *K. xylinus* due to osmolarity effects. Therefore, phosphate and chloride may not be responsible for *K. xylinus* growth inhibition. All subsequent experiments utilized non-inhibitory ethephon concentrations.



3.9 Ethylene does not affect the growth of *K. xylinus* in agitated broth cultures

The effect of ethephon-derived ethylene on the growth of agitated *K. xylinus* broth cultures grown in SH medium (pH 7) was investigated. Since ethylene is a gas and the 96-well plates had to be opened to read the optical density, some ethylene was inevitably lost during this process. To determine if this loss was a significant factor, ethephon was added only on the day of inoculation or on the day of inoculation and every two days thereafter.

When compared to controls, no significant difference in growth was observed when ethephon was added to cultures at the time of inoculation (**Figure 19A**) or when ethephon was added every two days (**Figure 19B**). The same result was obtained when comparing the ethephon-treated cultures to phosphate-chloride controls (**Figure 19C** and **Figure 19D**). Therefore, ethylene does not influence *K. xylinus* growth in agitated culture.

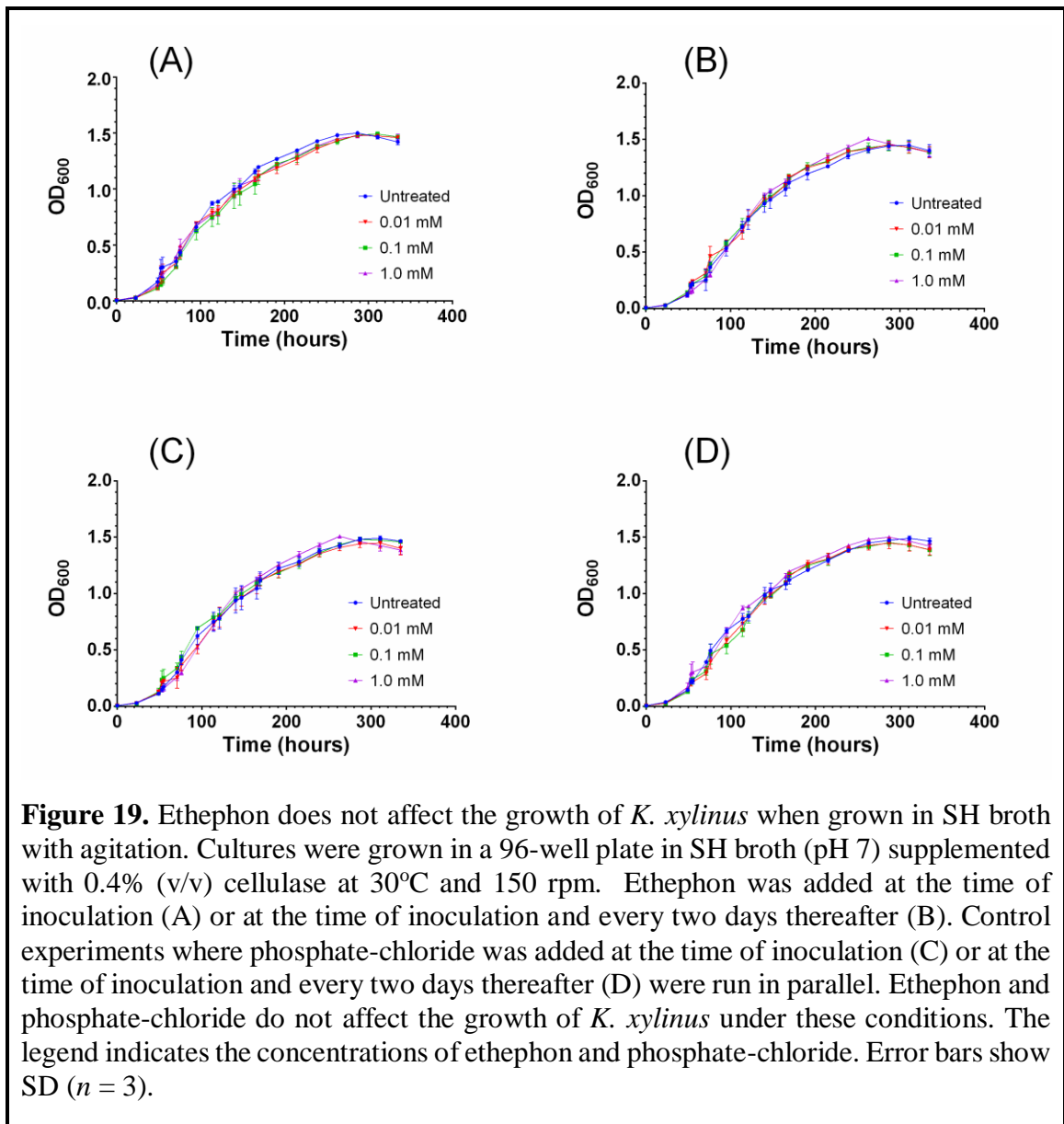


Figure 19. Ethephon does not affect the growth of *K. xylinus* when grown in SH broth with agitation. Cultures were grown in a 96-well plate in SH broth (pH 7) supplemented with 0.4% (v/v) cellulase at 30°C and 150 rpm. Ethephon was added at the time of inoculation (A) or at the time of inoculation and every two days thereafter (B). Control experiments where phosphate-chloride was added at the time of inoculation (C) or at the time of inoculation and every two days thereafter (D) were run in parallel. Ethephon and phosphate-chloride do not affect the growth of *K. xylinus* under these conditions. The legend indicates the concentrations of ethephon and phosphate-chloride. Error bars show SD ($n = 3$).

3.10 Ethylene increases BC yield and decreases *K. xylinus* pellicle hydration due to an increase in crystallinity

Pellicles formed by *K. xylinus* grown in the presence of ethephon-derived ethylene were analyzed in regards to their wet weight, thickness, dry weight, hydration and crystallinity. The wet weight of pellicles were obtained after harvest, before removal of water and were affected by ethephon-derived ethylene when cultured in SH medium at pH 7; ethylene was shown to be produced by ethephon decomposition in this medium (**Figure 15**). The wet weight of pellicles produced in the presence of ethephon was decreased by 10% with 0.01 mM ethephon, 14% in the presence of 0.1 mM ethephon and 9% with 1.0 mM ethephon, in comparison to the untreated control (**Figure 20A**). The relationship between ethephon concentration and wet weight was not linear, and differences between ethephon treatments were not significant. Ethephon did not influence the thickness of *K. xylinus* pellicles (**Figure 20B**).

Pellicle dry weights were obtained after cells were removed by lysis in NaOH, neutralization and drying to constant weight. Similar to the wet weights, pellicle dry weight was affected by ethephon-derived ethylene. All concentrations of ethephon resulted in a significant increase in pellicle dry weight (**Figure 20C**), which increased linearly with ethephon concentration. Differences between ethephon treatments were not statistically significant. In comparison to the untreated control, a 23% increase in BC yield was observed when *K. xylinus* was grown in the presence of 0.01 mM ethephon, while a 27% and 29% increase was observed after ethephon treatment at concentrations of 0.1 mM and 1.0 mM, respectively. Phosphate and chloride did not influence pellicle wet weight (**Figure 20D**), thickness (**Figure 20E**) or dry weight (**Figure 20F**), further supporting the conclusion that the decreased wet weight and increased dry weight observed with ethephon treatment was caused by ethylene.

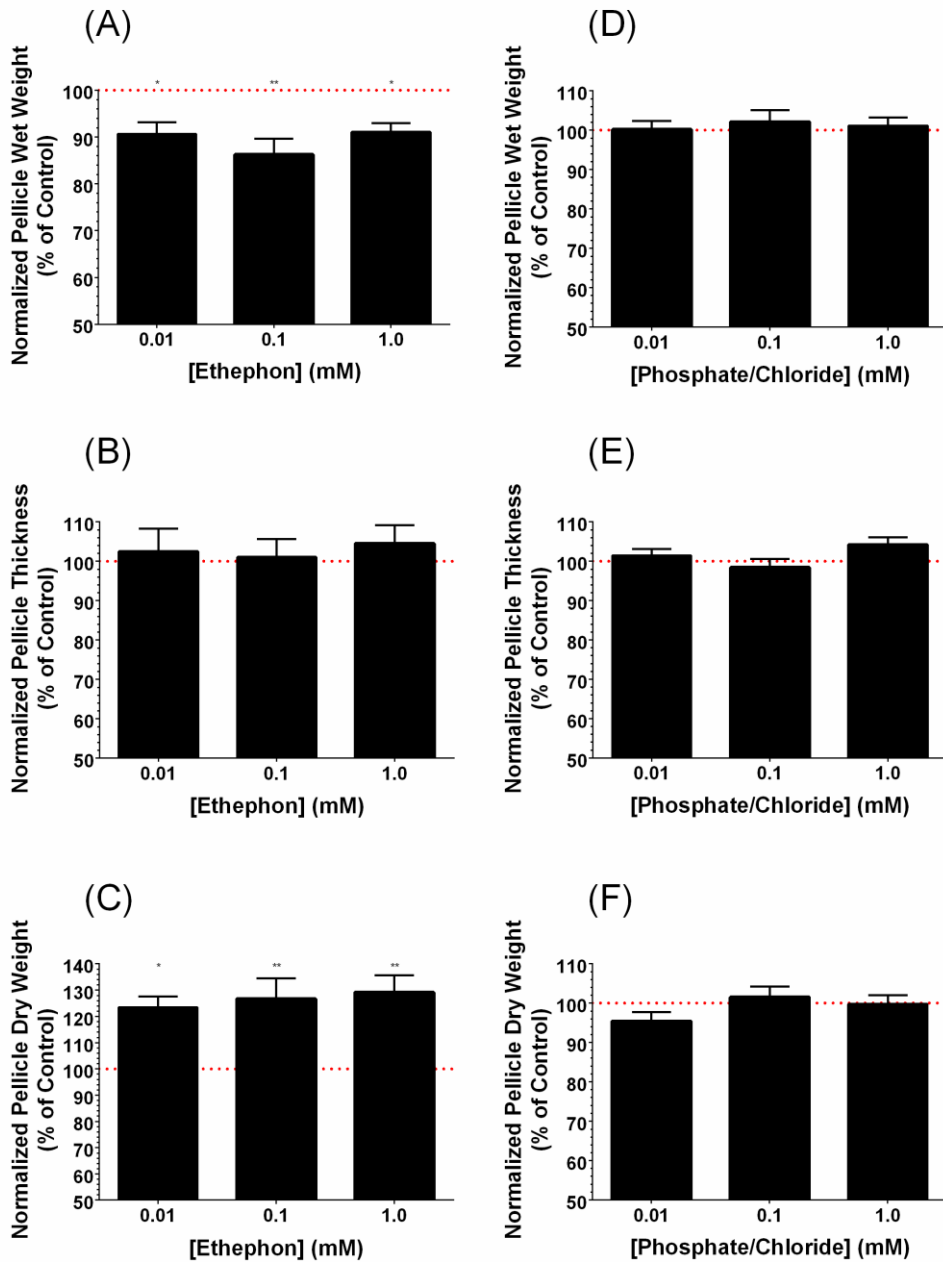
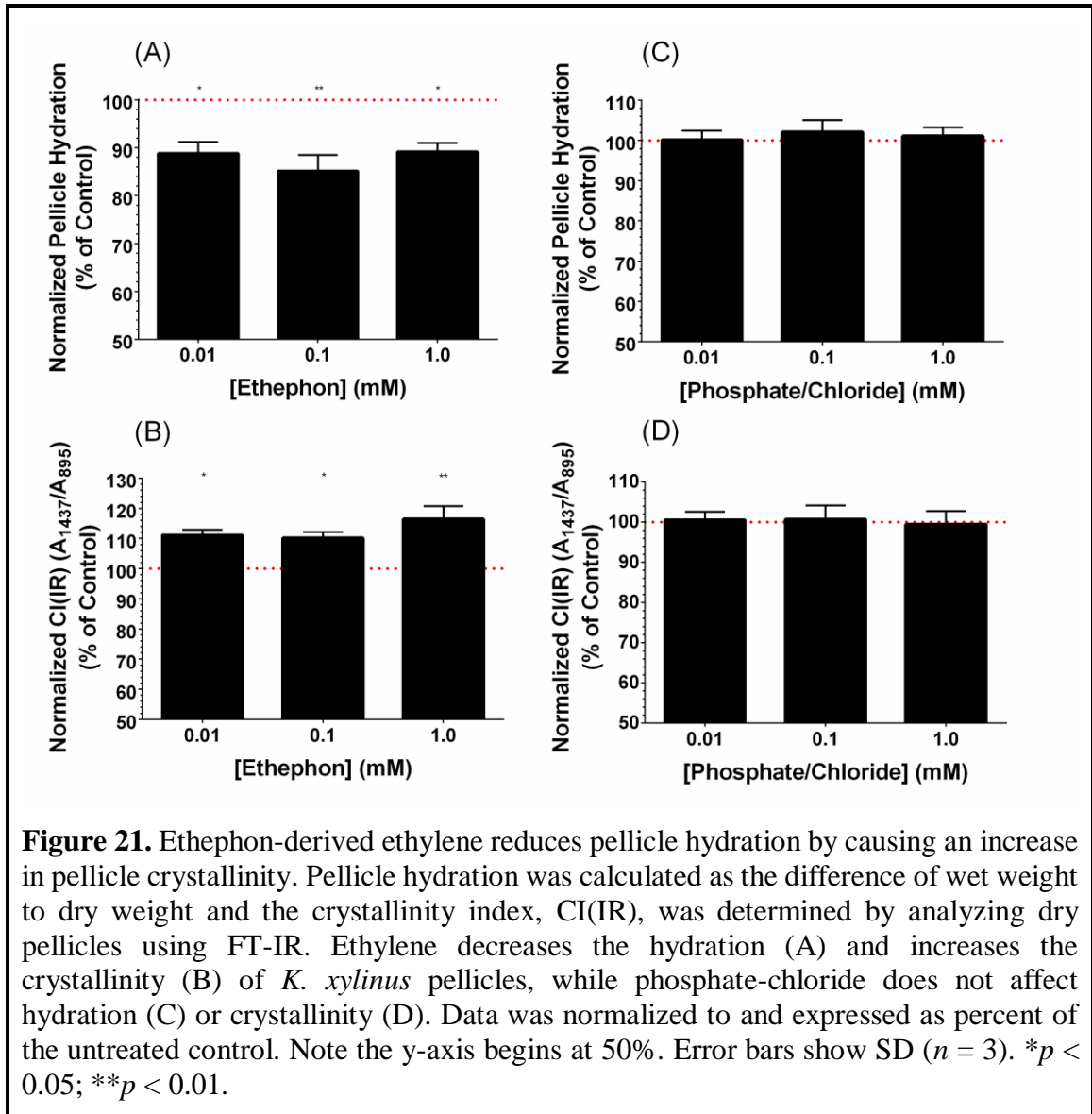


Figure 20. Ethephon-derived ethylene influences the properties and yield of *K. xylinus* BC pellicles. Cultures were grown statically in SH broth (pH 7) and incubated at 30°C for 7 days before pellicles were harvested and analyzed. Ethephon-derived ethylene decreases the wet weight (A), has no effect on thickness (B) and increases the dry weight of pellicles (C). Phosphate-chloride does not affect the wet weight (D), thickness (E) or dry weight (F) of *K. xylinus* pellicles. Data was normalized to and expressed as percent of the untreated control. Note the y-axis begins at 50%. Error bars show SD ($n = 3$). * $p < 0.05$; ** $p < 0.01$.

Pellicle hydration was assessed by subtracting pellicle dry weight from the wet weight. Ethephon-derived ethylene caused a significant decrease in pellicle hydration compared to the untreated control (**Figure 21A**). It was hypothesized that the decrease in pellicle hydration was related to differences in crystallinity, so the crystallinity index of *K. xylinus* pellicles produced in the presence of ethephon was determined using FT-IR.



Representative FT-IR spectra of an untreated BC pellicle (**Figure 22A**) show peaks indicative of microcrystalline cellulose (Ciolacu *et al.*, 2011). An O-H stretching vibration peak at 3343 cm^{-1} indicates the presence of hydroxyl groups. Bands indicative of C-H

stretching vibrations were obtained at 2924 cm^{-1} and 2899 cm^{-1} , and represent amorphous and crystalline cellulose, respectively. Water bound to the BC pellicle produced a peak at 1590 cm^{-1} . Alterations in cellulose crystallinity do not influence this peak (Ciolacu *et al.*, 2011). A peak at 1437 cm^{-1} represents symmetric CH_2 bending vibrations and is referred to as the crystallinity band since its intensity decreases in amorphous samples (Ciolacu *et al.*, 2011). The BC pellicle produced transmittance bands from approximately 1500 cm^{-1} to 900 cm^{-1} and indicates it is crystalline cellulose; these bands are strongly reduced in intensity or absent with amorphous cellulose (Ciolacu *et al.*, 2011). A band at 895 cm^{-1} is indicative of the C-O-C stretching vibrations caused by the β -1,4-glycosidic bonds that connect glucopyranose monomers and is referred to as the amorphous band since its intensity increases in amorphous cellulose samples (Ciolacu *et al.*, 2011). Similar to the untreated BC pellicle, those synthesized by *K. xylinus* grown in the presence of ethephon produced numerous bands indicative of microcrystalline cellulose (**Figure 22B**). Interestingly, the peaks of the O-H stretching bands from the ethephon-treated BC samples are shifted to a lower wavenumber, which is characteristic of cellulose that is more crystalline (Ciolacu *et al.*, 2011). This is due to the differences in intermolecular hydrogen between crystalline and amorphous cellulose. Pellicles synthesized by ethephon-treated *K. xylinus* cultures produced C-H stretching vibration bands at 2924 cm^{-1} and 2899 cm^{-1} with a greater intensity than the control pellicle.

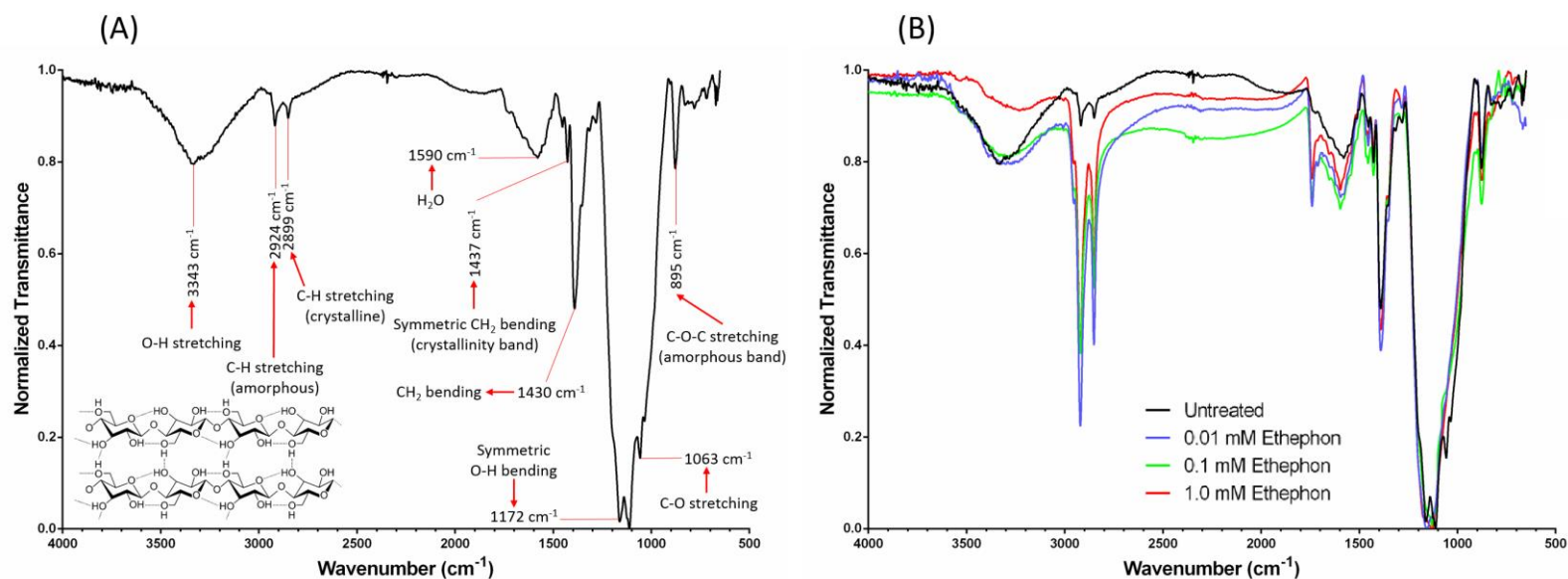


Figure 22. FT-IR spectra of BC pellicles produced by *K. xylinus*. A representative FT-IR spectrum of a BC pellicle produced by *K. xylinus* under untreated conditions (A) shows numerous bands indicative of the functional groups that make up the cellulose structure (inset). Representative FT-IR spectra of BC pellicles produced by ethephon-treated *K. xylinus* cultures also show bands indicative of cellulose with slight alterations (B). See text for details.

Compared to the untreated control, pellicles grown in the presence of all concentrations of ethephon had a higher crystallinity (**Figure 21B**). The CI(IR) of untreated pellicles was 0.62, while pellicles grown with ethephon treatments of 0.01 mM, 0.1mM and 1.0 mM had a significantly increased CI(IR) of 0.69, 0.68 and 0.73, respectively. Therefore pellicle crystallinity increased by 11%, 10% and 16% when synthesized in the presence of 0.01 mM, 0.1 mM, and 1.0 mM ethephon, respectively. This is consistent with the decrease in pellicle hydration observed after ethephon treatment. In the presence of ethephon, the pellicles were more crystalline and therefore less able to retain water. Phosphate-chloride did not affect pellicle hydration (**Figure 21C**) or crystallinity (**Figure 21D**), indicating that the differences obtained with ethephon treatment were due to the presence of ethylene.

Furthermore, pellicle wet weight (**Appendix Figure A2A**), thickness (**Appendix Figure A2B**), dry weight (**Appendix Figure A2C**) and crystallinity (**Appendix Figure A2D**) were not affected by ethephon treatment when *K. xylinus* was grown in a pH 5 SH medium. Decomposition of 1.0 mM ethephon was demonstrated to be insignificant when on a pH 5 SH medium (**Figure 15**), suggesting that ethephon itself does not affect these pellicle properties.

3.11 Ethylene increases *K. xylinus* BC production on solid medium

In order to assess how ethylene affected *K. xylinus* colony morphology and BC production on solid medium, agar plates were pre-treated with ethephon, acidified ultra-pure water (pH 2.5), or phosphate-chloride, then streaked for isolated colonies. **Figure 23** shows representative colonies from the various treatments. Colonies formed under control conditions (untreated) were about 1 mm in diameter, convex in elevation, irregular in form, and slightly orange in color (**Figure 23A**). All treatments, including the acidified water (**Figure 23B**) and phosphate-chloride (**Figure 23C, D and E**) controls influenced BC production of agar-grown cultures. Colonies grown on untreated plates produced some BC, as shown by the hazy material surrounding the central part of the colony (**Figure 23A**). Interestingly, when plates were pre-treated with acidified ultra-pure water (**Figure 23B**) or phosphate-chloride (**Figure 23C, D and E**), *K. xylinus* colonies produced minimal BC. Colonies grown in the presence of ethephon (**Figure 23F, G and H**) produced more BC than all of the controls, with the largest increase being caused by 0.01 mM ethephon (**Figure 23F**). Colonies grown on the phosphate-chloride control plates were similar to those grown with acidified ultra-pure water, demonstrating that the ethephon-induced BC overproduction phenotype was caused by ethylene. This result is reinforced by the increased BC yield observed for statically grown liquid cultures exposed to ethylene (**Figure 20**). Colonial morphologies were generally not affected, except that colonies grown with ethephon (**Figure 23F, G and H**) were slightly smaller than colonies grown on the control medium (**Figure 23A**).

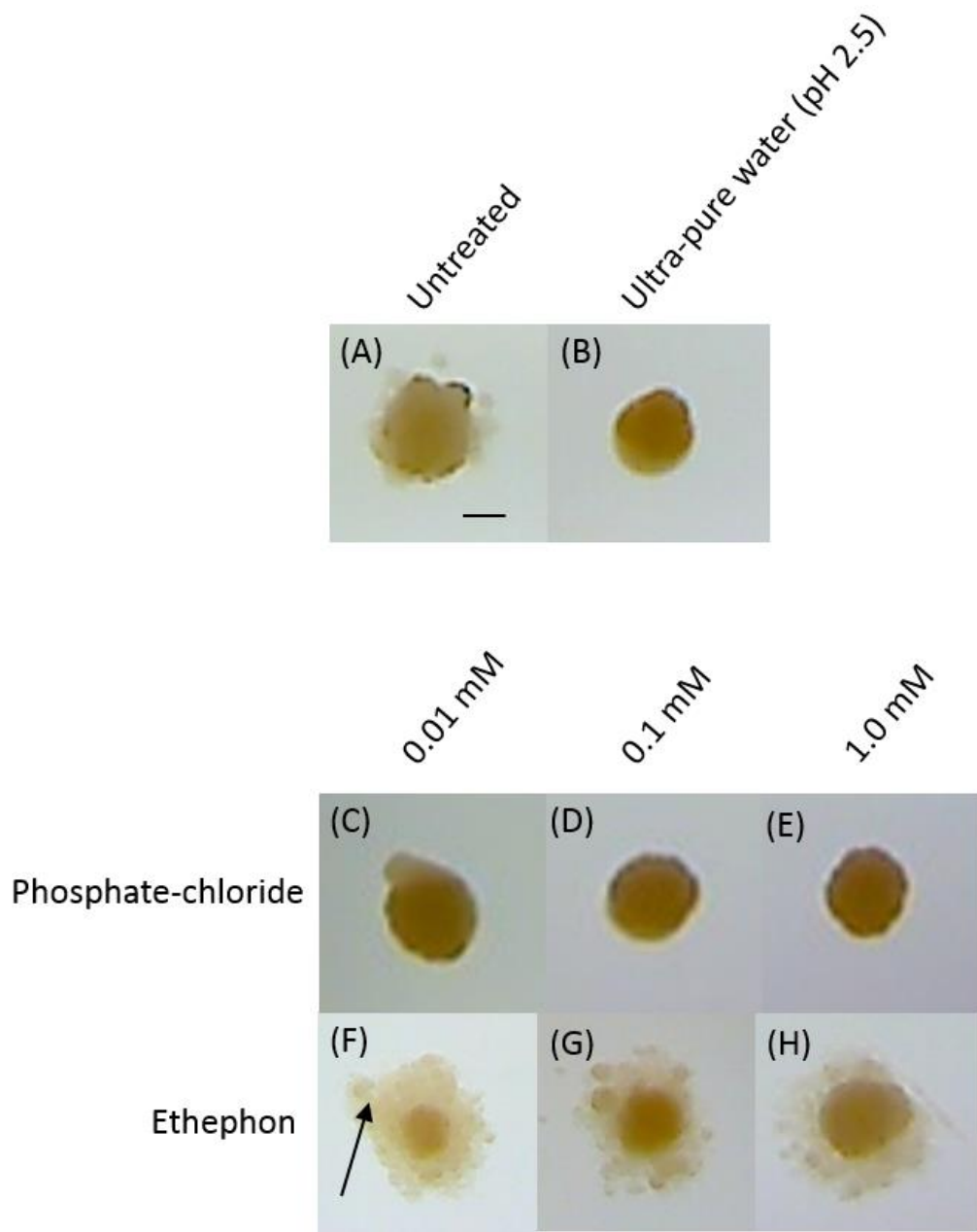


Figure 23. Ethepon enhances *K. xylinus* BC production when grown on solid medium. *K. xylinus* was streaked onto SH agar plates (pH 7) that were untreated (A), or pre-treated with ultra-pure water (pH 2.5; B), phosphate and chloride (C-E) or ethepon (F-H). Plates were incubated at 30°C for 7 days. Representative colonies are shown. The arrow shows BC, seen as the hazy substance around the central cell colony. Scale bar represents 0.5 mm.

3.12 The genome of *K. xylinus* contains potential ethylene-receptor genes

The observation that *K. xylinus* responds to exogenous ethylene prompted investigation of its genome for potential ethylene receptors. The most well-characterized ethylene receptors are ETR1, ERS1, ETR2, EIN4 and ERS2 from *A. thaliana*. Comparison of the amino acid sequences of these proteins to the *K. xylinus* E25 proteome revealed the presence of two potential ethylene receptors in *K. xylinus* (**Table 9**). ETR1 and ERS1 from *A. thaliana* showed similarity to a PAS/PAC sensor hybrid histidine kinase and a two-component sensor histidine kinase from *K. xylinus*. No *K. xylinus* proteins showed significant sequence similarity to the *A. thaliana* ETR2, EIN4 and ERS2 receptors.

Table 9. DELTA-Blast results comparing the *K. xylinus* E25 proteome to protein sequences of known ethylene receptors from *Arabidopsis thaliana*. *K. xylinus* proteins shown are those that produced max scores over 180 and had over 20% sequence identity. N/A indicates no hits were obtained.

<i>A. thaliana</i> Protein	<i>K. xylinus</i> Protein Name	<i>K. xylinus</i> Protein Accession	Max Score	Query Coverage (%)	E value	Identity (%)
Ethylene receptor 1 (ETR1)	PAS/PAC sensor hybrid histidine kinase	AHI26059.1	223	56	2 ⁻⁶²	21
	Two-component sensor histidine kinase	WP_051459895.1	184	33	7 ⁻⁵²	23
Ethylene response sensor 1 (ERS1)	Two-component sensor histidine kinase	WP_051459895.1	185	39	8 ⁻⁵³	21
Ethylene receptor 2 (ETR2)	N/A	N/A	N/A	N/A	N/A	N/A
Ethylene Insensitive Protein (EIN4)	N/A	N/A	N/A	N/A	N/A	N/A
Ethylene response sensor 2 (ERS2)	N/A	N/A	N/A	N/A	N/A	N/A

3.13 RT-qPCR

3.13.1 Steady-state mRNA levels are affected by IAA and ABA in *K. xylinus*

The effect of IAA and ABA on the steady-state expression of nine *K. xylinus* genes (**Table 4**) was assessed using a seven day time-course RT-qPCR experiment. *K. xylinus* cultures were supplemented with 0.01 μM and 10.0 μM IAA and ABA at the time of inoculation and were harvested and subjected to RNA extraction after 3 (72 h), 4 (96 h), 5 (120 h), 6 (144 h) and 7 days (168 h) of growth. These time-points correspond to different phases of *K. xylinus* growth as determined from growth curve analysis with IAA and ABA (**Appendix Figure A16**). Early log phase corresponds to day 3, mid-log phase to day 4, late log phase to day 5, early stationary phase to day 6 and stationary phase to day 7. RNA was converted to first-strand cDNA and analyzed using optimized RT-qPCR assays. Data was normalized using the optimal reference genes as determined from the reference gene analysis studies (**Appendix Table A2**) and the C_t values of IAA- and ABA-treated samples were made relative to the C_t values of the respective untreated (DMSO-treated) controls.

3.13.1.1 IAA and ABA induce differential steady-state expression of *bcs* operon genes that depends on hormone concentration and bacterial growth phase

Genes within the *bcs* operon (*bcsA*, *bcsB*, *bcsC* and *bcsD*) produce proteins that are directly responsible for the synthesis, translocation and crystallization of BC by *K. xylinus* (Römling and Galperin, 2015). Though these genes were thought to belong to an operon and that they were co-regulated, the time-course RT-qPCR results demonstrate their differential gene expression depending on the type of hormone, the concentration of hormone and the phase of growth.

None of the *bcs* genes were affected by IAA or ABA at day 4 (**Figure 24B**), day 6 (**Figure 24D**) or day 7 (**Figure 24E**). However, *bcsA* was downregulated 2-fold ($p < 0.05$) by 0.01 μM and 10.0 μM IAA after 3 days of growth (**Figure 24A**), which corresponds to early log phase (**Appendix Figure A16**). Though not affected by IAA, the expression of *bcsD* was downregulated 2-fold ($p < 0.05$) by both concentrations of ABA at day 3 (**Figure 24A**). Neither *bcsB* nor *bcsC* were affected by IAA or ABA at this time-point.

Furthermore, *bcsB* was upregulated 2-fold ($p < 0.05$) by 0.01 μM IAA and 0.01 μM ABA at the day 5 time-point (**Figure 24C**), which corresponds to mid-log phase of growth (**Appendix Figure A16**). Similar to *bcsB*, the expression of *bcsC* was upregulated 2-fold ($p < 0.05$) by IAA and 3-fold ($p < 0.01$) by ABA at day 5 (**Figure 24C**). Both *bcsA* and *bcsD* were not affected by IAA or ABA at this time-point. Overall, the *bcs* operon genes display differential expression in response to IAA and ABA that is dependent on hormone concentration and bacterial growth phase.

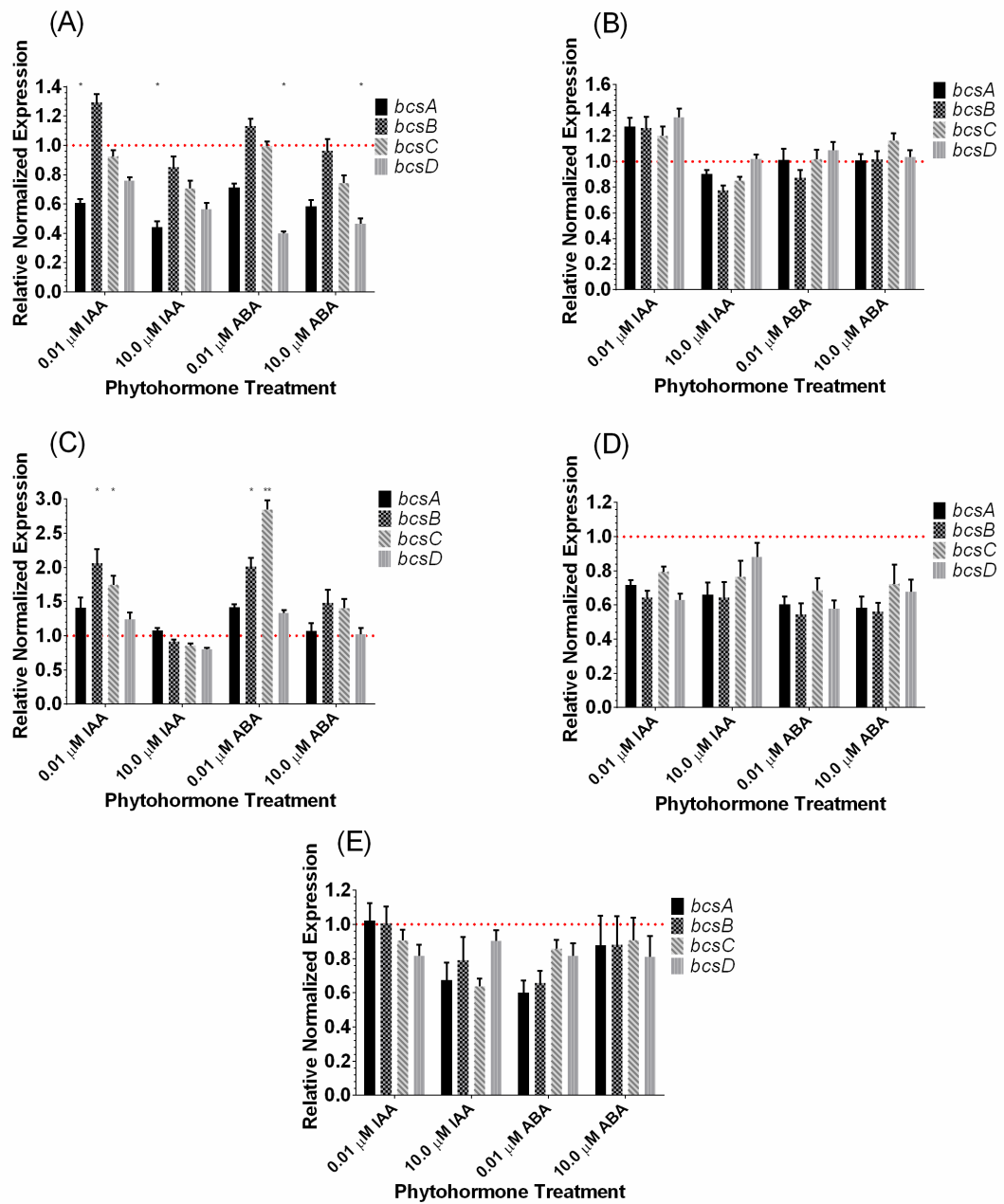


Figure 24. IAA and ABA influence the steady-state expression levels of genes within the *bcs* operon. RT-qPCR was used to measure the relative normalized expression of *bcsA*, *bcsB*, *bcsC* and *bcsD* in cDNA samples made from RNA extracted from *K. xylinus* after 3 (A), 4 (B), 5 (C), 6 (D) and 7 days (E) of growth in the presence of IAA and ABA. Expression values were made relative to the respective untreated (DMSO-treated) controls and normalized using validated reference genes (**Appendix Table A2**). The dotted line indicates the relative normalized expression of the untreated control. Error bars show SD ($n = 3$). * $p < 0.05$; ** $p < 0.01$.

3.13.1.2 IAA and ABA affect the steady-state expression levels of *bglAx*, but do not affect expression of *cmcAx* and *ccpAx*

Upstream of the *bcs* operon are *cmcAx* and *ccpAx*, which encode proteins that are involved in the crystallization and regulation of *K. xylinus* BC biosynthesis (**Table 4**). In addition, *bglAx* is found down downstream of the *bcs* operon and its gene product has a role in the regulation of BC biosynthesis (**Table 4**). The steady-state expression of these genes was assessed as part of the RT-qPCR time-course experiment. The expression of *cmcAx* and *ccpAx* were not affected by IAA or ABA at any time-point (**Figure 25**). However, similar to the *bcs* operon genes, *bglAx* was expressed differentially depending on the type of hormone, the hormone concentration and bacterial growth phase (**Figure 25**). The expression of *bglAx* was downregulated 1.8-fold ($p < 0.05$) by 0.01 μM ABA after 3 days of growth (early log phase; **Figure 25A**). Interestingly, *bglAx* expression in response to ABA was not different than the control at day 4, was upregulated 2-fold ($p < 0.01$) by the treatment at day 5, significantly ($p < 0.01$) downregulated again by both ABA concentrations at day 6, and finally not affected by ABA at day 7. The fluctuation in steady-state expression levels of *bglAx* may be attributed to the different growth phases that correspond to the different time-points analyzed during the time-course RT-qPCR study (**Appendix Figure A16**). The expression of *bglAx* was affected by IAA only at the 6 day time-point (**Figure 25D**), wherein it was significantly ($p < 0.05$) downregulated 1.8-fold by 0.01 μM IAA. This suggest that IAA influences *bglAx* expression during early stationary phase (**Appendix Figure A16**).

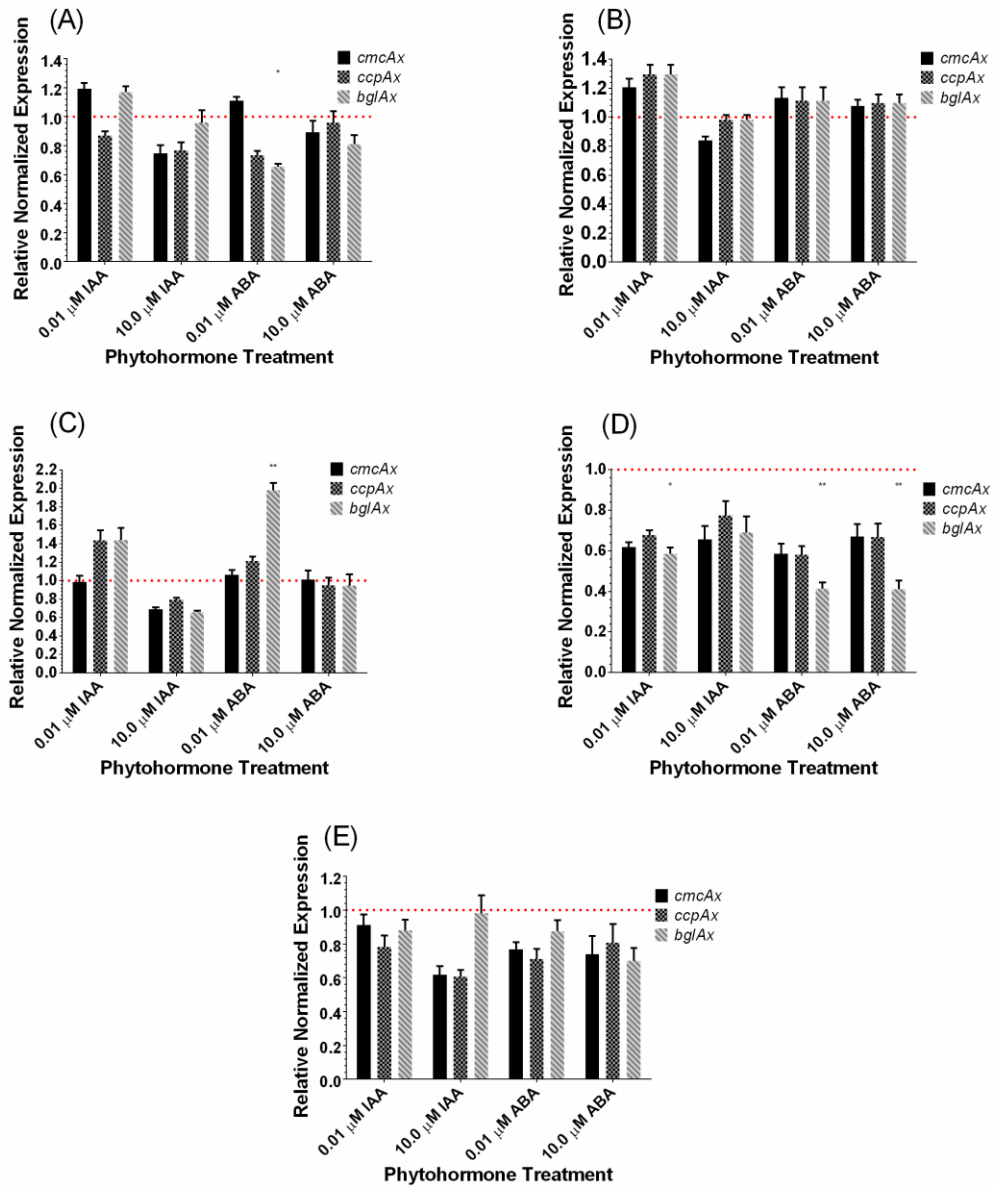


Figure 25. IAA and ABA influence the steady-state expression level of *bglAx*. RT-qPCR was used to measure the relative normalized expression of *ccpAx*, *cmcAx* and *bglAx* in cDNA samples made from RNA extracted from *K. xylinus* after 3 (A), 4 (B), 5 (C), 6 (D) and 7 days (E) of growth in the presence of IAA and ABA. Expression values were made relative to the respective untreated (DMSO-treated) controls and normalized using validated reference genes (**Appendix Table A2**). The dotted line indicates the relative normalized expression of the untreated control. Error bars show SD ($n = 3$). * $p < 0.05$; ** $p < 0.01$.

3.13.1.3 IAA and ABA upregulate the steady-state levels of *crp/fnr*_{Kx} during the exponential growth phase of *K. xylinus*

The steady-state expression levels of *crp/fnr*_{Kx} was also assessed during the RT-qPCR time-course experiment. This gene was bioinformatically identified in the *K. xylinus* E25 genome based on high sequence similarity to a CRP/FNR transcription factor gene from *K. hansenii* ATCC 23769. CRP/FNR_{Kh} was demonstrated to control BC biosynthesis at a transcriptional level in *K. hansenii* (Deng *et al.*, 2013) and it was hypothesized to have a similar function in *K. xylinus*. The expression of *crp/fnr*_{Kx} was upregulated 1.6-fold ($p < 0.05$) in response to 0.01 μ M IAA and upregulated 1.9 fold ($p < 0.05$) by 10.0 μ M ABA after 5 days of growth (**Figure 26A**). IAA and ABA did not affect *crp/fnr*_{Kx} expression at any other time-point. This suggests that IAA and ABA influence the steady-state expression level of *crp/fnr*_{Kx} during the exponential growth phase (**Appendix Figure A16**).

3.13.1.4 The steady-state expression levels of *oprB* are downregulated by IAA and upregulated by ABA during the early stages of *K. xylinus* growth

The *oprB* gene was identified in *K. xylinus* from analysis of periplasmic profiles obtained after treatment with IAA and ABA. SDS-PAGE revealed numerous periplasmic proteins whose intensities were altered by IAA and ABA treatment (**Figure 12**). Select protein bands were excised from the SDS-PAGE gel and the proteins within them were identified by LC-MS. The OprB protein was identified within the CS-46 protein band (**Table 8**) whose intensity varied inversely with IAA- and ABA-treatment (**Figure 12**). OprB is a porin that is involved in cellular carbohydrate uptake, therefore, it was of interest to examine the steady-state expression levels of *oprB* during the time-course RT-qPCR experiment. Interestingly, *oprB* expression correlated with the intensity of the protein band, CS-46 from which it was identified. The expression of *oprB* was downregulated by ~2-fold ($p < 0.05$ and $p < 0.01$) by both concentrations of IAA, and upregulated 2-fold ($p < 0.05$ and $p < 0.01$) by 10.0 μ M ABA at the 3, 4, and 5 day time-points (**Figure 26B**). This suggests that IAA and ABA influence *oprB* expression during exponential growth (**Appendix Figure A16**). The gene expression data supports the hypothesis that the hormone-induced differential intensity of the CS-46 protein band (**Figure 12**) was caused by alterations in OprB expression, rather than changes in the expression of other proteins

identified in the CS-46 band. This hypothesis is further supported since the periplasmic proteins used for SDS-PAGE analysis were harvested 5 days after treatment with hormone and *oprB* expression was influenced between day 3 and 5. Therefore, the changes in *oprB* expression on days 3 and 4 could have resulted in altered OprB expression on day 5.

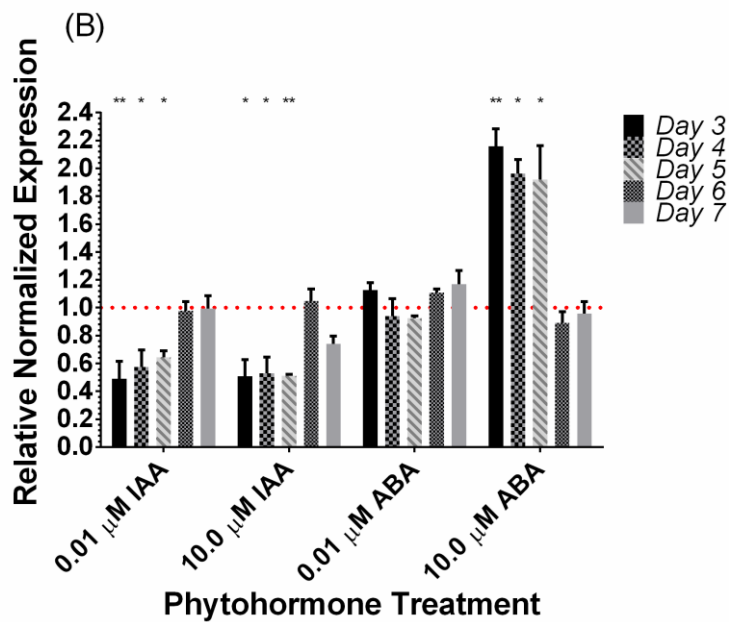
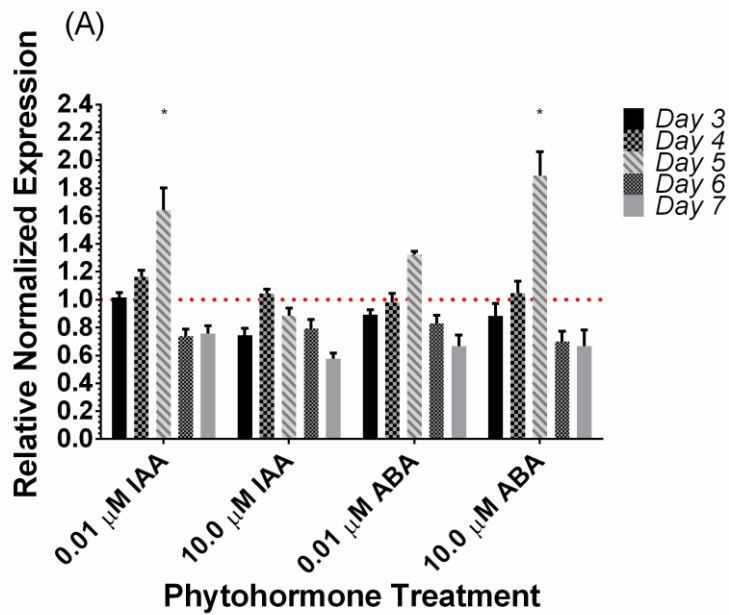


Figure 26. IAA and ABA influence the steady-state expression levels of *crp/fnr_{Kx}* and *oprB*. RT-qPCR was used to measure the relative normalized expression of *crp/fnr_{Kx}* (A) and *oprB* (B) in cDNA samples made from RNA extracted from *K. xylinus* after 3, 4, 5, 6 and 7 days of growth in the presence of IAA and ABA. Expression values were made relative to the respective untreated (DMSO-treated) controls and normalized using validated reference genes (**Appendix Table A2**). The dotted line indicates the relative normalized expression of the untreated control. Error bars show SD ($n = 3$). * $p < 0.05$; ** $p < 0.01$.

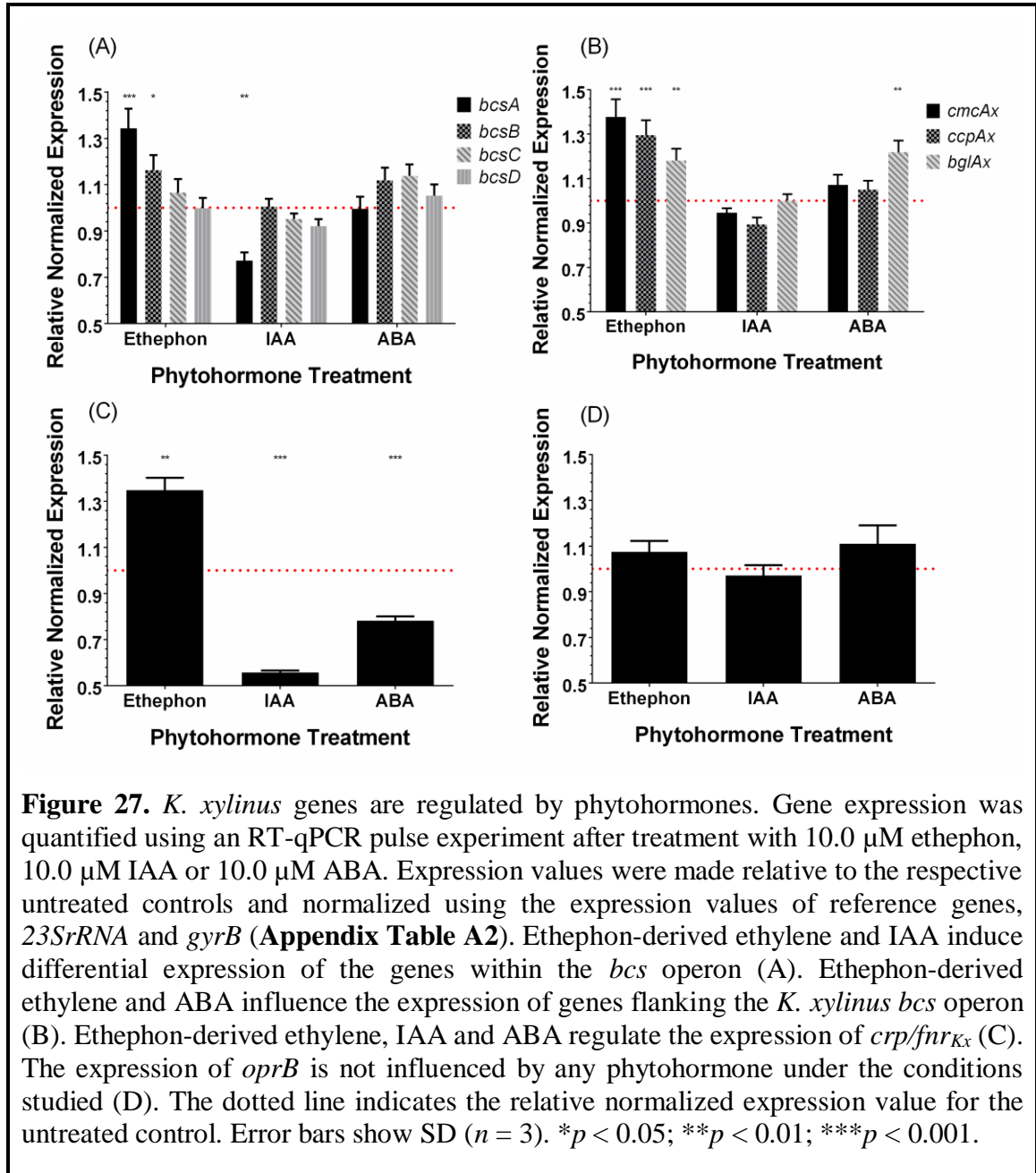
3.13.2 Phytohormones influence the active mRNA levels of *K. xylinus* genes

The levels of actively produced mRNA of *K. xylinus* genes (**Table 4**) in response to IAA, ABA and ethylene were assessed using an RT-qPCR experiment in which early-log phase cultures were supplemented with hormone and quickly harvested. This was done to compliment the RT-qPCR time-course experiment that measured steady-state gene expression levels in response to IAA and ABA. RT-qPCR data was normalized using the optimal reference genes as determined from the reference gene analysis studies (**Appendix Table A2**). The C_t values of IAA- and ABA-treated samples were made relative to the C_t values of the respective untreated (DMSO-treated) controls and the C_t values of ethephon-treated samples were made relative to the C_t values of the acidified water control samples.

3.13.2.1 Ethylene and IAA cause differential expression of *bcs* operon genes

The expression of the *bcs* operon genes (*bcsA*, *bcsB*, *bcsC* and *bcsD*) encoding proteins that form the BC synthesis complex responsible for BC biosynthesis (**Table 4**) were analyzed from *K. xylinus* cultures grown in the presence of 10.0 μ M ethephon, 10.0 μ M IAA and 10.0 μ M ABA using an RT-qPCR experiment. When cultures were treated with ethephon, *bcsA* and *bcsB* were upregulated by 1.4-fold ($p < 0.001$) and 1.2-fold ($p < 0.05$), respectively, compared to the untreated control (**Figure 27A**). Interestingly, *bcsC* and *bcsD* were not affected. The phosphate-chloride control treatment had no effect on the expression of the *bcs* operon genes (**Appendix Figure A17**), supporting the conclusion that the observed differential expression of these genes was caused by ethephon-derived ethylene. IAA treatment significantly downregulated *bcsA* by 1.3-fold ($p < 0.01$) compared to the untreated control, while the expression of *bcsB*, *bcsC* and *bcsD* were not affected (**Figure 27A**). The expression of all *bcs* operon genes were unaffected by ABA treatment (**Figure 27A**). Ethylene and IAA therefore, uniquely cause differential expression of the genes within the *K. xylinus* *bcs* operon. Ethylene upregulates *bcsA* and *bcsB*, which is consistent with the increase in BC yield observed in liquid (**Figure 20**) and solid (**Figure 23**) medium. IAA downregulates *bcsA* while ABA has no effect on the expression of *bcs* genes which is consistent with the previous observation that IAA directly decreases BC

production, while ABA has an indirect effect on BC yield in *K. xylinus* (Qureshi *et al.*, 2013).



3.13.2.2 Ethylene and ABA affect the expression of genes flanking the *bcs* operon

Three other genes known to be involved in *K. xylinus* BC biosynthesis were also analyzed during the RT-qPCR pulse experiment. The *ccpAx* and *cmcAx* genes form an operon upstream, while *bglAx* is located downstream of the *bcs* operon. Ethephon-derived

ethylene significantly upregulated *ccpAx*, *cmcAx* and *bglAx* 1.3-fold ($p < 0.001$), 1.4-fold ($p < 0.001$) and 1.2-fold ($p < 0.01$), respectively, compared to the untreated control (**Figure 27B**). These genes were not affected by phosphate-chloride (**Appendix Figure A17**), indicating these ethephon-induced phenotypes were caused by ethylene. The expression of *bglAx* was upregulated 1.2-fold ($p < 0.01$) compared to the control after treatment with ABA, while IAA had no effect on these genes (**Figure 27B**).

3.13.2.3 The CRP/FNR_{Kx} transcription factor gene is hormonally-regulated

The expression of the *crp/fnr_{Kx}* gene, bioinformatically identified in the genome of *K. xylinus* E25, was assessed during the RT-qPCR pulse study to ascertain if it is regulated by ethylene, IAA or ABA. This gene was studied since it has high similarity to a *crp/fnr_{Kh}* gene in *K. hansenii* ATCC 23769 that has recently been shown to be essential for BC biosynthesis (Deng *et al.*, 2013). The expression of *crp/fnr_{Kx}* in *K. xylinus* is regulated by ethylene, IAA and ABA (**Figure 27C**). Compared to the untreated controls, ethephon-derived ethylene upregulated *crp/fnr_{Kx}* 1.4-fold ($p < 0.01$), while IAA and ABA downregulated its expression by 1.5-fold ($p < 0.001$) and 1.2-fold ($p < 0.001$), respectively. The expression of *crp/fnr_{Kx}* was not affected by phosphate-chloride (**Appendix Figure A17**) confirming that ethephon-induced effects were caused by ethylene. Taken together, these results indicate that *crp/fnr_{Kx}* is phytohormonally-regulated. Ethylene directly increases BC production (**Figure 20 and Figure 23**) and upregulates *crp/fnr_{Kx}* expression (**Figure 27C**), while IAA directly decreases BC production (Qureshi *et al.*, 2013) and downregulates *crp/fnr_{Kx}* expression (**Figure 27C**). This suggests that like CRP/FNR_{Kh} in *K. hansenii* ATCC 23769 (Deng *et al.*, 2013), CRP/FNR_{Kx} may directly regulate BC biosynthesis in *K. xylinus* ATCC 53582.

4 DISCUSSION

The overall goal of this thesis was to elaborate on the potential interactions that *Komagataeibacter xylinus* has with fruit in the environment using *in vitro* experiments. Phytohormones involved with fruit ripening influence the growth and BC production of *K. xylinus* when added exogenously to cultures. IAA enhances bacterial growth while decreasing BC production, while ABA increases growth and indirectly increases BC yield (Qureshi *et al.*, 2013). One goal of this work was to establish a molecular basis to explain the previously observed IAA- and ABA-induced phenotypes in *K. xylinus*. In plants, ethylene is produced in response to changes in IAA and ABA concentrations (Zhang *et al.*, 2009b). Therefore, another goal of this research was to assess *K. xylinus* for endogenous ethylene production, to determine the effect of exogenous ethylene on its growth and BC production and to expand on the proposed model of phytohormone-mediated fruit-bacteria interactions. Novel protocols to study bacterial ethylene response using ethephon were developed accordingly.

The effect of IAA and ABA on the expression of *K. xylinus* periplasmic proteins was assessed using SDS-PAGE to determine if these hormones induced differential expression changes compared to the untreated control. Indeed, the *K. xylinus* periplasmic protein profiles were markedly influenced by IAA and ABA (**Figure 12**). The intensity of various proteins was altered in response to hormones compared to the DMSO-treated control, indicating that IAA and ABA signaling occurs in the periplasm. One protein from a 261 kDa protein band (SS-261) was induced by IAA treatment and identified as a 51 kDa α -mannosyltransferase B (MtfB; **Figure 12A**). This enzyme is closely related to the GT-1 family of glycosyltransferases. Numerous attempts to make RT-qPCR primers for *mtfB* were unsuccessful, likely because the sequence of *mtfB* is not evolutionarily conserved, and primers were designed using the genome sequence of *K. medellinensis* NBRC 3288 (formerly *K. xylinus* NBRC 3288) since the genome sequence of *K. xylinus* ATCC 53582 has not been published. The genome of *K. xylinus* E25 was not published at the time when *mtfB* primers were being designed and no attempts were made after it was.

In *E. coli*, *mtfB* is found within the *mtfABC* operon and encodes a protein that directs the growth of the O9-specific polysaccharide chain of LPS (Kido *et al.*, 1995). Similar to the BCSC, MtfB is a part of an enzyme complex that synthesizes a polysaccharide at the cytoplasmic face of the inner membrane. MtfB-mediated polymerization of the O9-specific polysaccharide chain is coupled to its export through an ABC transport system (Kido *et al.*, 1995). LPS was demonstrated to be vital for pellicle formation in the wrinkly spreader isolate of *Pseudomonas fluorescens* which produces an acetylated BC matrix (Spiers and Rainey, 2005; Spiers *et al.*, 2003). A LPS-deficient mutant of *P. fluorescens* produced wildtype levels of BC but formed very weak pellicles, indicating that interactions between LPS and the BC matrix are required for biofilm strength (Spiers and Rainey, 2005). Therefore, induction of MtfB expression by IAA may alter the LPS composition of *K. xylinus* in a way that weakens its BC pellicle (Qureshi *et al.*, 2013). MtfB has not been implicated in *K. xylinus* BC biosynthesis or biofilm formation. Future studies should consider knocking out *mtfB* (GLX_18490 in *K. medellenensis* NBRC 3288; H845_RS13330 in *K. xylinus* E25) or other genes involved in LPS biogenesis from the *K. xylinus* genome and analyze pellicle production from the mutants.

Furthermore, *mtfB* from *E. coli* is similar to *aceA* from *K. xylinus* (Petroni and Ielpi, 1996). AceA is an α -mannosyltransferase that adds mannose residues during the synthesis of acetan, a soluble EPS that contains four glucoses, one mannose, one glucuronic acid and one rhamnose (Petroni and Ielpi, 1996). Alternatively, IAA may induce MtfB expression to increase acetan production and divert carbon away from BC production, resulting in decreased BC yield as observed previously (Qureshi *et al.*, 2013). The effect of IAA on acetan production was not assessed by Qureshi *et al.* (2013), nor in this study but warrants further investigation. IAA may also induce MtfB to incorporate mannose into the *K. xylinus* pellicle. Pellicles produced by *Shewanella oneidensis* are rich in mannose (Liang *et al.*, 2010). Therefore, the sugar composition of pellicles produced in the presence of IAA should be determined. Incorporation of mannose into the *K. xylinus* biofilm would deplete pools of UDP-mannose, which is a substrate for bacterial N-glycosylation (Nothaft and

Szymanski, 2013). Reducing the amount of N-glycosylation could result in decreased cellulose production, as has been observed in *Arabidopsis thaliana* (Lukowitz *et al.*, 2001).

K. xylinus has not been shown to contain curli fimbriae, described as extracellular proteinaceous appendages involved in bacterial adhesion to biotic and abiotic substrates. Curli fimbriae are vital to *E. coli* and *S. enterica* biofilms by facilitating cell to cell adherence (Jonas *et al.*, 2007; Macarisin *et al.*, 2012) and contain a terminal oligomannose-binding FimH adhesin (Knudsen and Klemm, 1998; Krogfelt *et al.*, 1990). Binding of oligomannose by FimH inhibits biofilm formation by *E. coli* by preventing cell to cell adherence (Wellens *et al.*, 2008). Consistently, the fimbriae of Pseudomonad-like bacteria isolated from chicken carcasses bind oligomannoses, resulting in the formation of weak pellicles that are easily dispersed (Heath, 1990). Whether curli fimbriae are present on the surface of *K. xylinus* cells should be determined in future studies. It is possible that IAA-induced MtfB may synthesize oligomannoses that bind *K. xylinus* curli fimbriae, preventing cell to cell adhesion and cause the formation of the weak pellicle previously shown to be produced in the presence of IAA (Qureshi *et al.*, 2013).

Interestingly, MtfB migrated as a 261 kDa protein on SDS-PAGE gels, but was identified as a 51 kDa protein by LC-MS. This abnormal mobility is typical of intrinsically disordered proteins (IDPs) due to their significantly polar amino acid composition that binds less SDS (Rath *et al.*, 2009; Uversky and Dunker, 2012). For example, the intrinsically disordered *Xeroderma pigmentosum* group A protein (XPA) of *Xenopus* electrophoresed as a 42 kDa protein during SDS-PAGE (denaturing), but was identified as a 31 kDa protein by MS. Therefore, the aberrant migration of MtrB through the SDS-PAGE gel may have been caused by its predicted disordered regions (**Figure 13**). Furthermore, numerous glycosyltransferase-type proteins from animals and bacteria contain disordered regions with various functions, such as excluding water from the catalytic center, and chaperoning substrates to the active site (Breton *et al.*, 2006; Brockhausen, 2014; Uversky and Dunker, 2012; Yazer and Palcic, 2005). Proteins with post-translational modifications and those bound to oligosaccharides and nucleic acids can also experience abnormal

mobility on SDS-PAGE gels (Hellman and Fried, 2007; Shi *et al.*, 2012). Therefore, it is possible that MtfB was bound to an oligomannose chain or contains post-translational modifications that affect its electrophoretic mobility.

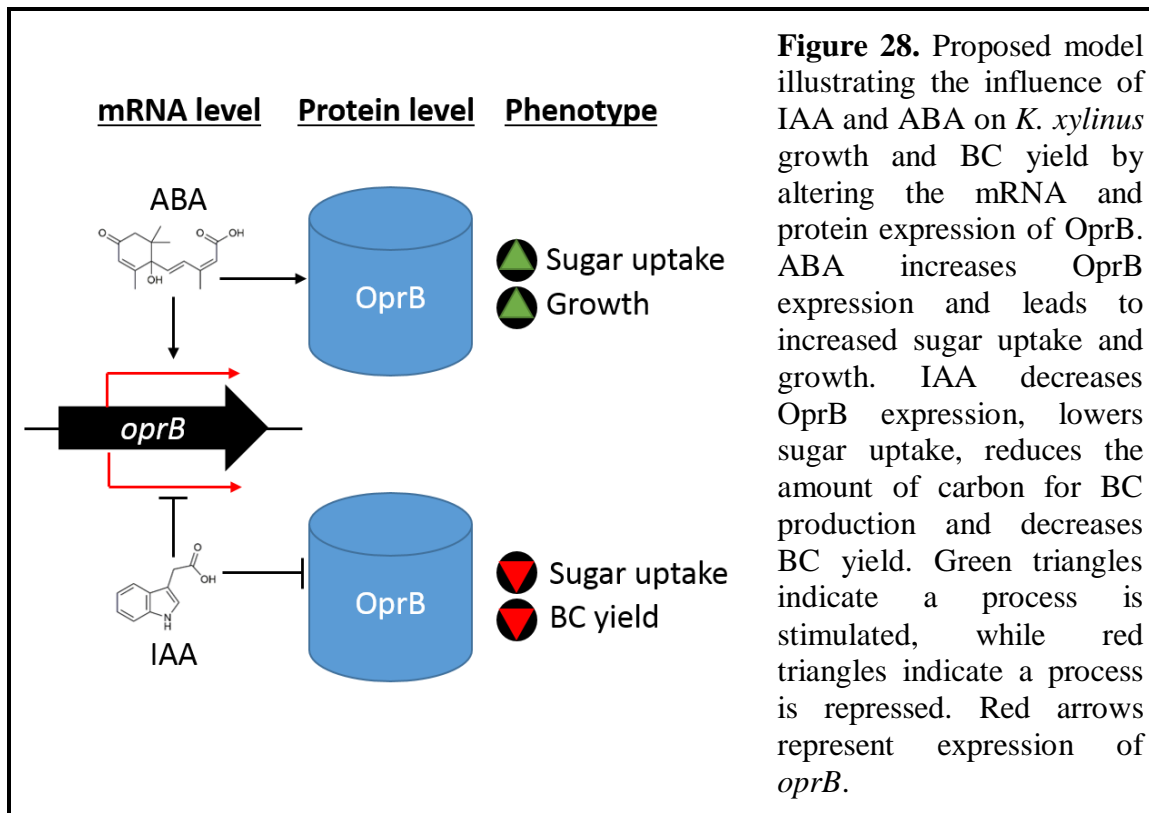
Numerous other protein bands displayed differential intensities in samples derived from IAA- and ABA-treated cultures (**Figure 12**). A 36 kDa band (CS-36) showed greater intensity in ABA-treated samples compared to IAA-treated or untreated samples (**Figure 12A**), suggesting that ABA increases the expression of one or more of the proteins within the band. A 46 kDa protein band (CS-46) displayed greater intensity upon ABA-treatment and less intensity from IAA-treated samples compared to protein derived from the untreated control (**Figure 12A**), suggesting ABA and IAA increase and decrease the expression of one or more proteins within the CS-46 band, respectively. Numerous proteins central to bacterial metabolism were identified in the CS-36 and CS-46 bands, including glyceraldehyde-3-phosphate dehydrogenase (GAPDH) and enolase, respectively (**Table 7**). Interestingly, GAPDH and enolase are well-studied moonlighting enzymes; proteins that perform a variety of often unrelated functions without altering the structure of their domains (Huberts and van der Klei, 2010). For example, in addition to being a cytoplasmic glycolytic enzyme, GAPDH from virulent *E. coli* strains is also found on the bacterial surface where it binds human plasminogen and fibrinogen, and acts as a virulent adhesin (Egea *et al.*, 2007). Similarly, enolase of *Borrelia burgdorferi* is released from membrane vesicles and acts as a plasminogen receptor that aids in pathogen survival (Floden *et al.*, 2011; Toledo *et al.*, 2012). Therefore, it is possible that ABA increases the expression of one or more of the potential moonlighting proteins identified in the CS-36 and CS-46 protein bands. Future studies are required to confirm this possibility.

A terpenoid biosynthesis protein (TBP; GLX_09340) was also identified in the CS-36 band (**Table 7**). Pentacyclic C₃₅ terpenes were identified in *K. xylinus* (Foster *et al.*, 1973) and were demonstrated to aid in the alignment of BC microfibrils in the extracellular space (Haigh, 1973). The terpenoid biosynthesis protein identified in the CS-36 band may therefore be upregulated by ABA to assist with microfibril orientation during BC

crystallization. It would be interesting to knock out the terpenoid biosynthesis gene from the *K. xylinus* genome and assess how pellicle production is affected. Terpene synthases are widely distributed in bacteria, but the functions of the produced terpenes are not known (Cane and Ikeda, 2011; Yamada *et al.*, 2015). Additional experiments are required to determine if the *K. xylinus* TBP is upregulated by ABA, and if the TBP plays a role in BC biosynthesis.

A carbohydrate-selective porin (OprB; 55 kDa) was also identified in the CS-46 protein band (**Table 8**). OprB acts as a glucose-inducible and carbohydrate-selective outer-membrane porin that facilitates the diffusion of various monosaccharides into the periplasm in *Pseudomonas aeruginosa* and plant-associated *P. putida* (van den Berg, 2012; Saravolac *et al.*, 1991; Wylie and Worobec, 1995; Wylie *et al.*, 1993). The present study demonstrated that *K. xylinus* OprB was isolated from a protein band that showed increased and decreased intensity in response to ABA and IAA treatment, respectively (**Figure 12**). Moreover, the time-course RT-qPCR experiment showed the steady-state expression of *oprB* was increased and decreased during exponential growth in response to ABA and IAA treatment, respectively (**Figure 26B**). Consistency between IAA- and ABA-induced effects on OprB expression at the mRNA and protein levels suggests that OprB is a direct target of these hormones and may contribute to the phenotypes they elicit from *K. xylinus*. IAA downregulates the expression of *oprB* beginning at the initiation of exponential growth (**Figure 26 and Appendix Figure A16**) and leads to decreased OprB expression by late-log phase (**Figure 12 and Table 8**). This reduces monosaccharide uptake and the amount of carbon source available for BC production, resulting in available carbon being used for enhanced growth and a decreased BC yield (Qureshi *et al.*, 2013). Similar to the repression of *K. xylinus* OprB by heteroaromatic IAA, *P. putida* OprB is repressed by various aromatic compounds that also downregulate intracellular glucose-metabolizing enzymes to encourage utilization of the aromatic compound (Shrivastava *et al.*, 2011). In contrast to IAA, ABA upregulates the expression of *oprB* during exponential growth (**Figure 26 and Appendix Figure A16**) and leads to increased OprB expression by late-log phase. This enhances monosaccharide uptake and the amount of carbon source

available to increase *K. xylinus* growth rate (Qureshi *et al.*, 2013). A proposed model for this process is shown in **Figure 28**. Future studies should consider determining carbohydrate uptake by OprB in response to IAA and ABA treatment to verify this model.



Qureshi *et al.* (2013) demonstrated that *K. xylinus* produces endogenous ABA, zeatin and GA₃, but not IAA, which may play a role in its interaction with fruit in the environment. Production of phytohormones may allow *K. xylinus* to increase their endogenous concentrations in fruit and alter developmental traits. For example, production of ABA may accelerate the ripening process to produce a substrate more suitable for colonization, while production of zeatin and GA₃ may increase fruit size to produce more biomass to colonize (Augimeri *et al.*, 2015). In the present study, endogenous ethylene production was assessed using a novel modification of the *A. thaliana* triple response assay, wherein *K. xylinus* was inoculated onto sectorized petri dishes containing *A. thaliana* seedlings (**Figure 10**). The length of *A. thaliana* seedling hypocotyls are negatively correlated with ethylene concentration in a dose dependent manner (Guzmán and Ecker,

1990). Seedlings exposed to ethylene produced by *K. xylinus* were shorter than the untreated seedlings, but longer than the ACC-treated positive control seedlings (**Figure 14**), indicating that only low levels of ethylene were produced. Plants and some fungi are known to produce ethylene from L-methionine (Arshad and Frankenberger Jr, 2002; Yang and Hoffman, 1984), *E. coli* produces ethylene from the methionine derivative KMBA (Ince and Knowles, 1985, 1986), and *P. syringae* and *Penicillium digitatum* use α -ketoglutarate as a biosynthetic precursor. Supplementation of L-methionine and α -ketoglutarate to the growth medium did not enhance *K. xylinus* ethylene production, suggesting that they are not used as biosynthetic precursors by this bacterium, or that the growth conditions used were not suitable for ethylene production. The direct precursor of ethylene biosynthesis in plants, ACC, was not tested as a potential precursor for *K. xylinus* ethylene production, but should be considered in future studies. Blast analysis revealed that *K. xylinus* contains potential ethylene-forming enzymes (EFEs) similar to that of *P. syringae* and *A. thaliana*. The similarity values obtained were above the 25% twilight zone threshold (Rost, 1999), indicating that these proteins may be responsible for ethylene biosynthesis in *K. xylinus*. Future studies should consider knocking-out or overexpressing the genes that encode these potential EFes in *K. xylinus*.

Application of exogenous ethylene is well known to promote fruit ripening (Brady, 1987; Dhall and Singh, 2013; Dhillon and Mahajan, 2011; Lohani *et al.*, 2004; Pech *et al.*, 2008). The ability to produce endogenous ethylene would provide *K. xylinus* with a survival advantage in its natural niche in the carposphere by allowing it to accelerate the ripening of the fruit it is colonizing. Exposing fruit to ethylene leads to increased production of pectinases that weaken the plant cell wall (Brummell and Harpster, 2001; Brummell, 2006), as well as amylases and cellulases that degrade starch and cellulose in soluble monosaccharides (Ahmed and Labavitch, 1980; Lohani *et al.*, 2004), respectively. All of these features make fruit more susceptible to colonization by bacteria like *K. xylinus*. However, no studies have evaluated the ability of plant-associated ethylene-producing bacteria to accelerate ripening *in planta*.

Ethephon, an ethylene-releasing compound, was used to investigate the effect of ethylene on *K. xylinus* ATCC 53582 growth, BC production, pellicle properties and gene expression. *K. xylinus* is a plant-associated carposphere bacterium (Dellaglio *et al.*, 2005; Jahan *et al.*, 2012; Neera *et al.*, 2015; Park *et al.*, 2003). This close association with fruit exposes *K. xylinus* to a plethora of plant-derived compounds, including phytohormones that regulate plant growth and development when present at low concentrations (Davies, 2010). Ethylene is the main ripening hormone in climacteric fruit and is released in high concentrations during the ripening stage (McAtee *et al.*, 2013; Pech *et al.*, 2008). In non-climacteric fruit, ABA is believed to be the most important ripening hormone (Jia *et al.*, 2011; Li *et al.*, 2011; McAtee *et al.*, 2013). However, recent data has shown that even non-climacteric fruit, such as strawberry, grapes and citrus respond to ethylene and experience a spike in ethylene production during ripening, though the magnitude of response and production is cultivar-dependent (Chervin *et al.*, 2004; Iannetta *et al.*, 2006; Paul *et al.*, 2012; Trainotti *et al.*, 2005). Nevertheless, *K. xylinus* would be exposed to exogenous ethylene when it inhabits both climacteric and non-climacteric fruit in the environment.

The ripening stage of fruit development is characterized by modulation of endogenous hormone levels (McAtee *et al.*, 2013). Numerous metabolic changes occur that result in the fruit being sweeter, due to starch hydrolysis by amylase (Agravante *et al.*, 1990) and softer, due to the activity of pectinase and cellulase enzymes that degrade the fruit cell wall (Ahmed and Labavitch, 1980; Lohani *et al.*, 2004; Sitrit and Bennett, 1998). Due to the intense turgor pressure in plant cells, weakening of the cell wall results in the release of exudate onto the fruit surface (Brummell and Harpster, 2001; Brummell, 2006), providing an attractive nutrient environment for microorganisms. The levels of ethylene are typically low during fruit growth and maturation, but spike at the onset of ripening (McAtee *et al.*, 2013). Ethylene, due to its positive role in fruit ripening, would therefore be a signal indicating an ideal nutrient environment for *K. xylinus* as fruit at this developmental stage contain high levels of soluble monosaccharides that can be used for growth and BC production.

Investigations using ethephon in plants have shown ethylene-dependent phenotypes even though the dosage and magnitude of ethephon decomposition was not precisely controlled (Zhang and Wen, 2010; Zhang *et al.*, 2010). In this study, ethephon was used as a convenient vehicle to produce *in situ* ethylene when added to *K. xylinus* cultures growing in SH medium. Ethephon decomposition is linear, in that the amount of ethylene produced is proportional to the amount of ethephon used (Klein *et al.*, 1979; Zhang and Wen, 2010). The half-life in aqueous medium at 30°C is 5.1 ± 0.9 hours at pH 7 and 6.0 ± 0.9 hours at pH 6 (Klein *et al.*, 1979). Biddle *et al.* (1976) demonstrated that ethephon decomposition below pH 5 is extremely slow, while the rate is greatly increased at pH 7 and above. The *A. thaliana* triple response assay verified that ethephon decomposition and ethylene production occurred in a pH SH medium (**Figure 15**) and time-course pH analysis showed that the decrease in culture pH would not have hampered this process (**Appendix Figure A1**). Ethylene evolution was not significant on the pH 5 SH medium, likely because this pH resulted in extremely slow ethephon decomposition. Phosphate and chloride ions are produced in addition to the desired ethylene during ethephon decomposition. Therefore, control experiments using phosphate-chloride were completed alongside the ethephon experiments. In all cases, the effects of phosphate and chloride were insignificant, supporting our conclusion that the observed results were due to ethylene.

The analysis of pH changes over the course of *K. xylinus* growth revealed that the final culture pH is higher after treatment with ethylene. We observed a decrease in pH during exponential growth and then an increase in pH during stationary growth phase. This was also observed by Kawano *et al.* (2002b), who correlated this trend in pH alteration to glucose oxidation into gluconic acid, and subsequent resorption of gluconic acid. They also showed that unlike *K. hansenii* ATCC 23769, *K. xylinus* ATCC 53582 is able to synthesize BC after glucose depletion by using gluconic acid as carbon source. Keshk (2014) reported that this occurs after treatment with 0.5% (w/v) ascorbic acid, indicating that ascorbic acid enhances the ability of *K. xylinus* to utilize gluconic acid for BC production. The higher final pH and increased production of BC observed in this study may therefore be attributed

in part to increased gluconic acid metabolism in the presence of ethylene. However, this requires further investigation.

MIC assays were performed to ensure ethephon was not toxic to *K. xylinus*. Ethephon concentrations of 50 and 100 mM prevented *K. xylinus* growth (**Figure 18**). Control assays revealed that the bacterium could grow when chloride and phosphate concentrations were at 50 mM but not 100 mM, suggesting that ethylene was responsible for *K. xylinus* growth inhibition when the medium was supplemented with 50 mM ethephon. To our knowledge, this is the first time ethephon has been used to treat bacteria with ethylene. However, there are numerous literature reports that describe treating plants with millimolar concentrations of ethephon (Denney and Martin, 1994; Dhillon and Mahajan, 2011; Khan, 2004; Kong *et al.*, 2009; Wang *et al.*, 2013). Burg *et al.* (1962) showed that ethylene production levels in fruit vary depending on the cultivar. The internal ethylene concentration of various fruit varieties is in the micromolar range, with the exception of apples and passion fruit which produce ethylene in the high micromolar to low millimolar range. Furthermore, Wheeler *et al.* (2004) demonstrated that the peak ethylene concentration in ripening tomatoes is approximately 10 μ M. Based on this, an ethylene concentration of 50 mM is not physiologically relevant, and therefore the non-toxic ethephon-derived ethylene concentrations of 0.01, 0.1 and 1.0 mM were utilized in this study.

Ethylene reduced pellicle hydration by increasing pellicle crystallinity (**Figure 21**), suggesting a higher degree of hydrogen bonding between adjacent glucan chains that resulted in a reduced ability to hydrogen bond to water. Qureshi *et al.* (2013) showed that exogenous IAA, ABA, GA₃ and zeatin influenced the hydration and crystallinity of *K. xylinus* pellicles in a concentration-dependant manner. In contrast, all concentrations of ethylene decreased hydration and increased the crystallinity of the pellicles in this study. Increased crystallinity enhances the recalcitrance of BC, which provides a survival advantage to *K. xylinus* in the environment since it would be less susceptible to cellulase-producing microorganisms.

Increased BC yield by *K. xylinus* is a direct result of exposure to ethylene in both liquid (**Figure 20**) and solid media (**Figure 23**); growth is not affected (**Figure 19**). An increase in BC production after ethylene treatment was observed, further supporting the conclusion that it has a direct effect on BC biosynthesis. This is in contrast to ABA, zeatin and GA₃ which indirectly enhance BC production due to an increased growth rate (Qureshi *et al.*, 2013). Hu and Catchmark (2010) investigated the effect of 1-methylcyclopropene (1-MCP), a known inhibitor of ethylene-dependant responses in plants (Tassoni *et al.*, 2006), on the growth and BC production of *K. xylinus*. This compound is thought to antagonistically bind ethylene receptors and blocks ethylene response in plants (Sisler, 1991). Though an ethylene receptor has not been reported in *K. xylinus*, Hu and Catchmark (2010) showed that 1-MCP decreased *K. xylinus* growth rate and increased BC yield, indicating that similar to ethylene, 1-MCP has a direct effect on BC biosynthesis. This suggests that an ethylene receptor exists in *K. xylinus* and that ethylene and 1-MCP act as agonists since they induce similar phenotypes. This is in contrast to their effects on fruit, since treatment with 1-MCP inhibits ethylene-dependent ripening phenotypes (Tassoni *et al.*, 2006).

The direct target of ethylene and 1-MCP in *K. xylinus* has not yet been identified. However, it should be noted that although ethylene receptors have not been identified in bacteria, ethylene receptors in plants are highly similar to the two-component regulatory systems in bacteria (Chang *et al.*, 1993). Interestingly, Delta-Blast comparison of the amino acid sequences of the *A. thaliana* ETR1 and ERS1 ethylene receptors to the proteome of *K. xylinus* E25 revealed two potential ethylene receptors that resemble two-component regulatory proteins (**Table 9**). Therefore, future studies should investigate these two-component systems as mediators of the ethylene-induced phenotypes in *K. xylinus*.

It is also possible that proteins involved *K. xylinus* chemotaxis may be involved in the ethylene response, as they are in *Pseudomonas aeruginosa* (Kim *et al.*, 2007). Interestingly, the *P. pseudoalcaligenes* KF707 histidine kinase (CheA) involved in chemotaxis is also required for biofilm formation (Tremaroli *et al.*, 2011), suggesting a link between

chemotaxis and biofilm development. It is possible that chemoreceptors are involved in *K. xylinus* ethylene response and that this signaling pathway is connected to BC biosynthesis. However, more research is required to investigate this possibility.

The effect of IAA, ABA and ethylene on *K. xylinus* gene expression was assessed using optimized RT-qPCR assays. First, a time-course RT-qPCR study was performed to assess how IAA and ABA influenced the steady-state expression levels of *K. xylinus* genes involved in BC biosynthesis (**Table 4**). Next, an RT-qPCR pulse experiment was completed to determine how these genes responded to IAA, ABA and ethylene treatment at mid-log phase. The differences in yield (**Appendix Table A1**) and quality (**Appendix Figure A4 and Appendix Figure A5**) between the time-course and pulse RNA samples was caused by variability in the Norgen Biotek RNA Purification Plus kits that were used. The RNA-binding column used to purify the time-course RNA samples would elute silica carbide resin during the RNA elution step, which likely affected the RNA yield. This malfunction was corrected by the manufacturer by adding another O-ring to the RNA-binding columns. This updated RNA purification kit was used at a later date to extract the RNA used in the pulse experiment and was demonstrated to isolate a higher yield of RNA that contained more small RNAs.

RT-qPCR reference genes were also thoroughly validated for both RT-qPCR studies. Interestingly, geNorm assigned M values below 0.5 for all reference genes and all time points, indicating that all reference genes were considered stable using the geNorm model. NormFinder and RefFinder produced different stability rankings in some cases, but all programs generally agreed on what genes were most and least stable. Therefore, the use of multiple algorithms to assess reference gene stability in future studies may not be necessary. The geNorm algorithm provides a cut-off value of 0.5 for reference gene stability (M) and 1.5 for pair-wise variation values (V ; Hellemans *et al.*, 2007), which provide an indication of how many reference genes should be used for data normalization. Therefore, geNorm is the best program for determining reference gene stability since it provides a reference to which gene stability can be compared, while simultaneously

determining the required number of reference genes needed for accurate gene expression analysis.

In this study, only two reference genes were required in all cases. In retrospect, a small-scale RT-qPCR pilot experiment should be performed with multiple reference genes to determine the number and identity of reference genes required for a large-scale experiment. This will reduce the number of assays required for the large-scale RT-qPCR study, and will save time and reagents.

The time-course RT-qPCR experiment was performed over seven days, wherein RNA samples were extracted from IAA- and ABA-treated cultures after 3, 4, 5, 6 and 7 days. These time-points correspond to different growth phases of *K. xylinus* (**Appendix Figure A16**). Genes within the *bcs* operon were only affected at the 3 day and 5 day time points (**Figure 24**). IAA downregulated *bcsA* during early log phase (day 3) which may contribute to the decreased BC yield observed with IAA treatment (Qureshi *et al.*, 2013), since BcsA is the enzyme responsible for BC synthesis (Morgan *et al.*, 2013; Omadjela *et al.*, 2013). Downregulation of *bcsD* by ABA during early log phase (day 3) may reduce the activity of the BCSC, since BcsD is required for optimal BC production (McManus *et al.*, 2016). Reduced rates of BC biosynthesis may leave more carbon available to be used to increase *K. xylinus* growth (Qureshi *et al.*, 2013). However, ABA was not shown to decrease BC yield, but rather, it increased it (Qureshi *et al.*, 2013). It is possible that decreases in BC yield are hidden by an increase in growth rate when *K. xylinus* is grown in the presence of ABA. If the magnitude of the reduction in BC biosynthesis rate was less than the magnitude of the increased growth rate, it is possible that an indirect increase in BC yield could be observed since there would be more cells producing BC. This corresponds to the observed indirect effect of ABA on *K. xylinus* BC production (Qureshi *et al.*, 2013).

By mid-log phase (day 5), IAA upregulated *bcsB* and *bcsC* which seems to contradict previous results, since increasing the expression of these two genes would be expected to increase BC production, but IAA decreases it. It is possible that the steady-state levels of

bcsB and *bcsC* mRNA do not correspond to the levels of their encoded proteins as observed for numerous others due to differential mRNA stability (Mikulits *et al.*, 2000). ABA upregulated *bcsC* at mid-log phase (day 5). Since the effect of ABA on *K. xylinus* BC production is indirect (Augimeri *et al.*, 2015; Qureshi *et al.*, 2013), the physiological consequence of ABA-induced *bcsC* upregulation is not known. Overall, the time-course RT-qPCR experiment demonstrated that the steady-state expression levels of *bcs* operon genes are different, possibly due to differential mRNA stability. However, future studies are required to confirm this hypothesis.

The steady-state level of *bglAx*, located downstream of the *bcs* operon (Saxena *et al.*, 1994), was influenced by IAA and ABA (**Figure 25**). In response to ABA, *bglAx* was downregulated at early log phase (day 3), upregulated at mid log phase (day 5), and downregulated again at early stationary phase (day 6). Fluctuations in *bglAx* expression was likely caused by effects of different growth stages. It is possible that the requirement for BglAx under ABA-treated conditions may be temporally sensitive. The *bglAx* gene was downregulated during early stationary phase (day 6) by IAA, which may play a role in causing IAA-induced decreases in BC yield (Qureshi *et al.*, 2013) since BglAx is required for optimal BC production (Deng *et al.*, 2013). The genes upstream of the *bcs* operon, *cmcAx* and *ccpAx*, were not affected by IAA or ABA during the RT-qPCR time-course.

A transcription factor belonging to the CRP/FNR family was previously identified in *K. hansenii* ATCC 23769 and shown positively regulate BC biosynthesis (Deng *et al.*, 2013). A homologous protein was identified bioinformatically in *K. xylinus* during this thesis. The steady-state expression level of *crp/fnr_{Kx}* mRNA was upregulated by IAA and ABA during the exponential growth phase (**Figure 26**). However, since IAA decreases BC yield and ABA has no direct effect on BC biosynthesis, it is likely that CRP/FNR_{Kx} affects other processes in *K. xylinus* that are independent of BC biosynthesis. Analysis of the steady-state expression of a transcription factor is not the best way to determine how it is affected by a certain treatment, since they tend to exert their effects quickly in response to

changing environmental conditions. Thus, *crp/fnr_{Kx}* expression was also analyzed using pulse RT-qPCR experiments.

Using data from the RT-qPCR pulse experiments, the differential expression of genes within the *K. xylinus* *bcs* operon is reported for the first time. This operon encodes proteins that comprise the complex responsible for BC production in *K. xylinus*. The *bcs* operon in *K. xylinus* encodes four genes (*bcsABCD*) to form a polycistronic mRNA. However, little is known in regards to how the *bcs* operon is regulated, particularly how relative gene expression is affected by external signals. Ethylene upregulated the expression of *bcsA* and *bcsB* which encode enzymes responsible for BC biosynthesis, but not *bcsC* and *bcsD*, which encode enzymes for BC export and crystallization. Therefore, an increase in BC production only requires additional synthesis proteins (BcsA and BcsB), but not increased levels of export/crystallization proteins (BcsC and BcsD). Similarly, IAA downregulated *bcsA* but did not affect the other *bcs* genes. Since *bcsA* encodes the BC synthase (BcsA) that is responsible for synthesis of BC, it follows that its downregulation results in decreased BC production as observed with IAA, and that its upregulation results in increased BC production as observed with ethylene. This data indicates that ethylene and IAA directly influence BC biosynthesis at a transcriptional level. In order to increase BC biosynthesis, both *bcsA* and *bcsB* must be upregulated, since functional BcsA is stabilized by BcsB in the periplasm (Morgan *et al.*, 2013). However, decreasing BC biosynthesis only requires the downregulation of *bcsA*, since its protein product is enzymatically responsible for BC biosynthesis. It is possible that *K. xylinus* preserves cellular energy by maintaining constitutive levels of *bcsB* transcription so that the transcript is readily available for translation into BcsB once *bcsA* repression is relieved.

The differential relative expression of genes within operons is especially useful for regulating encoded proteins that serve different functions, such as the protein products of the *bcs* operon genes. Recall that BcsA synthesizes BC, BcsB chaperones BC chains through the periplasm, BcsC facilitates export of BC into the extracellular environment and BcsD is responsible for crystallization of BC. In some cases, differential relative expression

of genes within an operon can be attributed to different translation efficiencies of operon-encoded mRNA due to variations in ribosome-binding sites (Vellanoweth, 1993). Inhibition of individual genes in a polycistronic mRNA by anti-sense RNA causes differential relative gene expression of the *E. coli* galactose operon (Møller *et al.*, 2002) and various other operons, including those regulated by excludons (Lasa and Villanueva, 2014; Sesto *et al.*, 2013). Lastly, polycistronic mRNA can undergo RNase cleavage and produce individual mRNAs that differ in terms of stability, leading to differential protein expression. For example, the genes within the *Escherichia coli atp* operon that encode proteins that make up the ATP synthase (Gay and Walker, 1981) are differentially regulated (McCarthy *et al.*, 1991). Like the BC synthesis complex, the ATP synthase is made up of numerous protein subunits and is embedded in the cell membrane of Gram-negative bacteria. The differential expression of the *atpIBEFHAGDC* operon genes has been attributed to segmental differences in mRNA stability (Lagoni *et al.*, 1993; McCarthy *et al.*, 1991), in that the mRNA of the first two genes of the operon are rapidly degraded by RNase enzymes (Ziemke and McCarthy, 1992), while the remaining seven genes are more stable (McCarthy *et al.*, 1991). In addition, the translational efficiencies of mRNA from the *atp* genes vary (Brusilow *et al.*, 1982) so that the differential expression of the operon is controlled at two post-transcriptional levels. This type of regulation has also been observed for the *malEFG* operon in *E. coli* (Newbury *et al.*, 1987), the *gap-pgk* operon of *Zymomonas mobilis* (Burchhardt *et al.*, 1993; Eddy *et al.*, 1991) and *Clostridium acetobutylicum* (Schreiber and Dürre, 2000), the *dnaK* operon of *B. subtilis* (Homuth *et al.*, 1999), the *puf* operon in *Rhodobacter capsulatus* (Belasco *et al.*, 1985; Klug *et al.*, 1987) and the uropathogenic *E. coli pap* operon (Båga *et al.*, 1988; Nilsson *et al.*, 1996). It is therefore possible that the *bcs* operon in *K. xylinus* is differentially-regulated through one of these mechanisms. However, determining the mechanism that is responsible requires further investigation.

The deletion of *ccpAx* in *K. hansenii* ATCC 23769 significantly decreased levels of BcsB and BcsC, but not BcsA, which are controlled by the same promoter (Deng *et al.*, 2013; McManus *et al.*, 2016). The expression of *bcsD* is regulated by a different promoter

(Deng *et al.*, 2013) supporting the notion that differential expression of the genes that make up the BCSC does occur. Therefore, it is possible that in *K. hansenii*, *ccpAx* plays a role in regulating differential relative expression of the *bcsABC* operon, resulting in the differential protein expression observed in the study by Deng *et al.* (2013).

Ethylene also upregulated *cmcAx* and *ccpAx* which form their own operon upstream of the *bcs* operon (Kawano *et al.*, 2002b; Sunagawa *et al.*, 2013). CcpAx is essential for BC biosynthesis (Standal *et al.*, 1994) and is believed to be involved in crystallizing BC due to its localization with BcsD (Sunagawa *et al.*, 2013). The precise function and transcriptional regulation of CcpAx is not known. Similarly, the exact function of CmcAx is not known. However, it is required for BC biosynthesis as CmcAx inhibition by antibodies results in decreased BC production (Koo *et al.*, 1998) and addition of minute amounts of CmcAx, or its overexpression increases BC production (Kawano *et al.*, 2002a, 2008; Tonouchi *et al.*, 1995). CmcAx is believed to play a role in editing distorted glucan chains since *cmcAx* deletion results in the formation of highly twisted ribbons (Nakai *et al.*, 2013). Expression of *cmcAx* is induced by gentiobiose produced by BglAx (Kawano *et al.*, 2008). The expression of *bglAx* is induced by the CRP/FNR_{Kh} transcription factor in *K. hansenii* ATCC 23769 (Deng *et al.*, 2013). We demonstrated that ethylene and ABA upregulate the expression of *bglAx*. The ethylene-dependant upregulation of all three genes may be required to cope with the enhancement of BC biosynthesis. In addition, upregulation of *cmcAx* and *bglAx* may lead to increased levels of secreted CmcAx and BglAx which have cellulose-hydrolyzing activity (Kawano *et al.*, 2002b; Tahara *et al.*, 1998; Tajima *et al.*, 2001). These proteins may aid in the degradation of plant cellulose in order to weaken the fruit cell wall and provide more glucose for BC production.

The CRP/FNR family of transcription factors regulate the expression of genes critical to bacterial growth and survival in response to changing environmental conditions (Körner *et al.*, 2003). Ethylene upregulated *crp/fnr_{Kx}* expression and increased BC production. IAA downregulated *crp/fnr_{Kx}* expression and decreased BC production. Together, these results suggest that CRP/FNR_{Kx} directly regulates BC biosynthesis in *K. xylinus* at a

transcriptional level, similar to how CRP/FNR_{Kh} regulates BC biosynthesis in *K. hansenii* (Deng *et al.*, 2013). Positive regulation of biofilm formation by CRP/FNR family protein, CRP, has also been observed in *E. coli* (Jackson *et al.*, 2002) and *Shewanella oneidensis* (Thormann *et al.*, 2005) when bound to cAMP. In contrast, CRP-cAMP negatively regulates transcription of genes involved in the biosynthesis of *Vibrio* polysaccharide (VPS) in *Vibrio cholerae* (Fong and Yildiz, 2008). Contradictory to the hypothesis that CRP/FNR_{Kx} positively regulates BC production in *K. xylinus* is the observation that ABA downregulates *crp/fnr_{Kx}* but does not decrease BC yield (Qureshi *et al.*, 2013). However, our study only focused on a small subset of genes. Therefore, it is possible that ABA regulates a yet to be identified gene whose protein product counteracts the downregulation of *crp/fnr_{Kx}*. This unknown protein may mitigate the negative effect that *crp/fnr_{Kx}* downregulation would have on BC biosynthesis. However, this requires further investigation.

The CRP/FNR family transcription factor, Bcam1349, binds c-di-GMP and regulates biofilm formation by enhancing the production of BC and curli fimbriae in *Burkholderia cenocepacia* (Fazli *et al.*, 2011). Binding of c-di-GMP enhanced the ability of Bcam1349 to bind the promoter region and increase the expression of *bcs* operon genes (Fazli *et al.*, 2011) and the *Bcam1330-Bcam1341* gene cluster that is involved with exopolysaccharide production (Fazli *et al.*, 2013). Interestingly, various diguanylate cyclase and phosphodiesterase proteins that are involved with c-di-GMP metabolism, are regulated by the CRP/FNR family protein, CRP, in *V. cholerae* (Fong and Yildiz, 2008). Therefore, we postulate that CRP/FNR_{Kx} may have the ability to bind c-di-GMP and increase the expression of genes within the *K. xylinus bcs* operon. Furthermore, the CRP/FNR family transcription factor, Lmo0753, has been shown to regulate biofilm formation in *Listeria monocytogenes* (Salazar *et al.*, 2013).

CRP/FNR_{Kh} regulates BC biosynthesis in *K. hansenii* ATCC 23769 by positively regulating the expression of *bglAx* and other genes required for BC production that have yet to be identified (Deng *et al.*, 2013). This is consistent with the effects of ethylene, which

upregulates both *crp/fnr_{Kx}* and *bglAx*. This provides evidence that active CRP/FNR_{Kx} may positively regulate *bglAx* transcription in *K. xylinus*. In contrast, ABA induces inverse expression of *crp/fnr_{Kx}* and *bglAx*, while IAA down-regulates *crp/fnr_{Kx}*, but has no effect on *bglAx*. This suggests that the mechanisms involved in CRP/FNR_{Kx}-mediated transcriptional regulation are influenced differently by ethylene, IAA and ABA. This may be explained by the complex regulatory role that CRP/FNR family transcription factors have in bacteria, due to their ability to regulate numerous target genes depending on activation by a ligand. For example, the *E. coli* CRP transcription factor activates the transcription of over 100 promoters (Brown and Callan, 2004; Harman, 2001; Kolb *et al.*, 1993). The activation of CRP is dependent on allosteric binding of cAMP (Harman, 2001). Apo-CRP has low DNA binding affinity and displays minimal sequence specificity. Binding of cAMP results in conformational changes that result in high affinity, sequence-specific DNA binding and interaction with RNA polymerase (Won *et al.*, 2009). Sigma factors produced under the specific conditions then coordinate sequence-specific gene expression mediated by active CRP and RNA polymerase (Colland *et al.*, 2000). Therefore, it is possible that ethylene, IAA and ABA alter the DNA binding specificity of CRP/FNR_{Kx} resulting in differential regulation of *bglAx*. To our knowledge, this is the first report of a bacterial CRP/FNR family transcription factor that is regulated by phytohormones.

Based on the results of the current study, as well as data provided by Qureshi *et al.* (2013), an update to the model for the phytohormone-mediated fruit-bacteria interactions of *K. xylinus* is proposed (**Figure 29**). On unripe fruit (**Figure 29A**), *K. xylinus* is exposed to high concentrations of IAA, zeatin (Z) and GA₃. As a fruit ripening inhibitor (Davies *et al.*, 1997; Frenkel and Dyck, 1973; Symons *et al.*, 2012; Ziliotto *et al.*, 2012), IAA directly inhibits energetically-costly BC biosynthesis by downregulating *bcsA*, since carbon source is limited on unripe fruit. Exogenous IAA, zeatin and GA₃ increase *K. xylinus* growth, enhancing bacterial production of zeatin and GA₃. These two hormones increase fruit size by controlling cytokinesis (zeatin) and cell enlargement (GA₃; McAtee *et al.*, 2013). Previous studies showed that rhizosphere bacteria that produce endogenous zeatin and GA₃ can enhance plant growth (Arkhipova *et al.*, 2005; Bottini *et al.*, 2004) and that application

of GA₃ increases the size of grape berries (Casanova *et al.*, 2009) and tomatoes (Serrani *et al.*, 2007). Therefore, we postulate that endogenous production of zeatin and GA₃ by *K. xylinus* may contribute to the pool of endogenous hormone levels in the fruit so that there is more biomass to colonize once ripening begins. Endogenous production of ABA and ethylene is also increased as a result of enhanced cell growth. Exposing fruit to exogenous ABA and ethylene increases their endogenous levels in fruit tissues, triggering ethylene biosynthesis and inducing ripening (Leng *et al.*, 2014; McAtee *et al.*, 2013; Zhang *et al.*, 2009b). ABA and ethylene production by *K. xylinus* may therefore play a role in triggering and accelerating ripening, resulting in a preferred growth environment compared to unripe fruit. Furthermore, IAA-, ABA-, zeatin- and GA₃-mediated growth enhancement ensures that cell density is at its peak when ripening begins. On ripe fruit (**Figure 29B**), *K. xylinus* would be exposed to high concentrations of ABA and ethylene (McAtee *et al.*, 2013). Fruit-produced ABA increases *K. xylinus* growth (Qureshi *et al.*, 2013), increasing bacterial production of ABA and ethylene, which in turn upregulates plant-produced ethylene and accelerates ripening, respectively (Zhang *et al.*, 2009b). Our hypothesis that ABA does not directly influence BC biosynthesis is supported by the observation that it did not affect the expression of genes within the *bcs* operon during the RT-qPCR pulse experiment. In contrast, exogenous ethylene directly enhances BC biosynthesis in *K. xylinus* by upregulating the expression of *bcsA* and *bcsB*. Therefore, ABA and ethylene act together as environmental signals to promote colonization of ripe fruit by *K. xylinus* through increased cell growth and direct enhancement of BC biosynthesis. Overproduction of BC provides a competitive advantage to *K. xylinus* as shown by apple colonization studies (Williams and Cannon, 1989). Enhancement of BC production and crystallization by ethylene therefore increases the environmental fitness of *K. xylinus* within the carposphere.

In contrast to phytopathogens, saprophytes generally do not enter the intracellular space of plant cells. This leaves them more susceptible to environmental stresses. Thus, they must employ strategies that confer increased resistance to an ever changing environment (Beattie and Lindow, 1995); *K. xylinus* produces a BC biofilm that increases its epiphytic fitness (Williams and Cannon, 1989). Saprophytic organisms typically require

an abundance of water (BC helps retain water), oxygen (*K. xylinus* is aerobic), acidic conditions (*K. xylinus* is an acetic acid bacterium) and temperatures of 1-35°C (*K. xylinus* grows optimally at 28-30°C). In addition, saprophytes typically have an ability to resist host defenses; *K. xylinus* produces ABA which suppresses plant immunity, and forms a biofilm that can protect it from chemical defenses. Thus, based on the current data, it is reasonable to suggest that *K. xylinus* is an epiphytic and saprophytic bacterium that exists within the carposphere. This is consistent with the observation that *K. xylinus* is heterotrophic. However, in addition to actively breaking down plant biomass, *K. xylinus* produces ethylene and ABA, increasing their levels in fruit, which results in the production of degradative enzymes that produce soluble nutrients that the bacteria can metabolize.

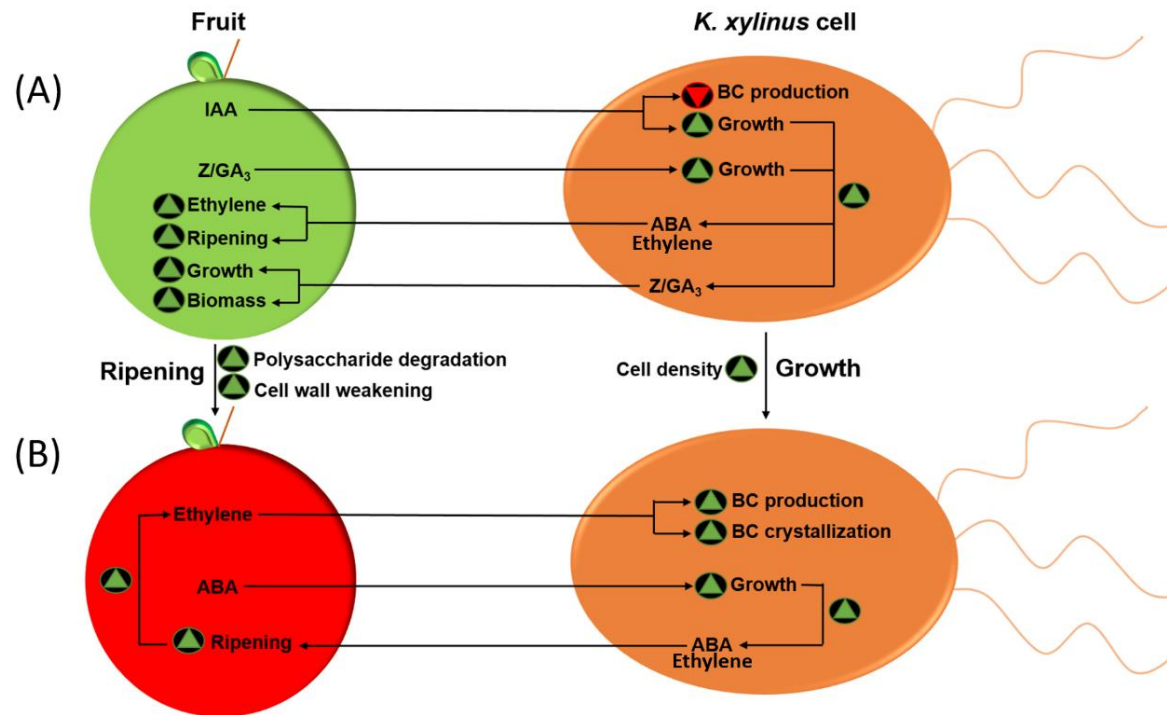


Figure 29. Updated model for the phytohormone-mediated fruit-bacteria interactions of *K. xylinus*. Only direct effects are shown. Unripe fruit (A) contain high concentrations of IAA, zeatin (Z) and GA₃. IAA decreases *K. xylinus* BC production, while IAA, zeatin and GA₃ increase bacterial cell growth enhancing endogenous production of ABA, ethylene, zeatin and GA₃ by *K. xylinus*. These hormones increase fruit size and induce ripening, characterized by degradation of polysaccharides and weakening of the fruit cell wall. On ripe fruit (B), plant-produced ethylene up-regulates biosynthesis and crystallization of BC. Exogenous ABA increases *K. xylinus* growth, allowing it to accelerate the fruit ripening process by increasing endogenous ABA and ethylene production, which facilitates colonization. Green triangles, and inverted red triangles indicate a process is enhanced or repressed, respectively. Adapted from Augimeri and Strap (2015).

5 CONCLUSIONS AND FUTURE DIRECTIONS

In summary, this thesis has demonstrated that ethylene produced through the *in situ* decomposition of ethephon can be used to study the effects of this hormone on bacteria. Ethylene directly increased *K. xylinus* BC biosynthesis by upregulating the expression of *bcsA* and *bcsB* and indirectly by upregulating the expression of *cmcAx*, *ccpAx* and *bglAx*. IAA decreases BC biosynthesis directly by downregulating *bcsA* expression. It was also demonstrated that the *bcs* operon in *K. xylinus* is differentially regulated by ethylene and IAA. Altogether, this thesis has expanded on the putative fruit-bacteria interactions of *K. xylinus*, provided new insights into the transcriptional regulation of the *bcs* operon and identified a new phytohormone-regulated CRP/FNR_{Kx} transcription factor that plays a role in BC biosynthesis in *K. xylinus* ATCC 53582.

Future studies should attempt to identify receptors for IAA, ABA and ethylene in *K. xylinus*; no receptors for these hormones have been discovered in bacteria to date. In addition, it should be determined how these hormones affect DGCs and PDEs in *K. xylinus*, as well as c-di-GMP concentration. Since IAA directly decreases BC yield and ethylene directly increases BC production, it can be hypothesized that IAA-treated cultures will have lower c-di-GMP concentrations, while ethylene-treated cultures will have higher c-di-GMP concentrations than the untreated controls.

Studies regarding the phytohormone-mediated fruit-bacteria interactions of *K. xylinus* have only been performed *in vitro* and were used to develop a model for how *K. xylinus* behaves when growing on rotting fruit in the environment. Future studies should consider testing the model *in planta* to confirm whether the observed phenotypes are replicated. In terms of endogenous hormone production, *K. xylinus* was shown to produce ABA in a previous study (Qureshi *et al.*, 2013), and ethylene in the present study. This suggests that *K. xylinus* could accelerate fruit ripening by increasing endogenous ABA and ethylene concentrations in the fruit it has colonized. This could be tested *in planta* using methods similar to those used to determine whether an *E. coli* strain, genetically-modified to produce large quantities of ethylene, could ripen fruit (Digiacomio *et al.*, 2014). Briefly, *K.*

xylinus cultures could be grown in Büchner flasks and connected with tubing to sterilized glass jars containing surface-sterilized fruit. This would allow the fruit to be exposed to headspace gas from *K. xylinus* cultures. After set time-points, the fruit would be assessed for different ripening characteristics, such as a change in color, sugar concentration and firmness. This would determine if *K. xylinus* can ripen fruit through ethylene production. In addition, if an ABA non-producing mutant of *K. xylinus* was obtained, the mutant and wildtype strains could be inoculated onto fruit. The ripening characteristics of fruit from each group could then be assessed. If the fruit inoculated with the ABA-producing wildtype strain is riper than the fruit inoculated with the ABA non-producing mutant, *K. xylinus* would be shown to accelerate ripening through ABA production. These types of studies could provide data that could immensely strengthen the model proposed in this thesis.

Altogether, this thesis has elaborated on the fruit-bacteria interactions of *K. xylinus* by demonstrating that it has the ability to respond to and synthesize ethylene. This information is relevant to the agriculture industry in regards to post-harvest crop management, since fruit containing *K. xylinus* on its surface would ripen at a faster rate due to endogenous ethylene production by the bacterium. This research study has established a molecular basis for the effect that IAA, ABA and ethylene have on *K. xylinus*, and proved the effectiveness of using ethephon as a tool to study bacterial ethylene response. In addition, the aforementioned data has shed new light on the regulation of the *bcs* operon in *K. xylinus* by establishing that it can be differentially-regulated. Evidence has been provided that suggests CRP/FNR_{Kx} positively regulates BC biosynthesis and represents the first transcription factor implicated in this process in *K. xylinus*. This thesis has significantly contributed to the field of BC biosynthesis and the study of *K. xylinus* ecophysiology, and has inspired numerous avenues for promising future research.

6 REFERENCES

- Abdel-Fattah, A. F., Mahmoud, D. R., and Esawy, M. T. (2005). Production of levansucrase from *Bacillus subtilis* NRC 33a and enzymic synthesis of levan and fructo-oligosaccharides. *Curr. Microbiol.* 51, 402–407. doi:10.1007/s00284-005-0111-1.
- Abeer, M. M., Mohd Amin, M. C. I., and Martin, C. (2014). A review of bacterial cellulose-based drug delivery systems: Their biochemistry, current approaches and future prospects. *J. Pharm. Pharmacol.* 66, 1047–1061. doi:10.1111/jphp.12234.
- Adler, J., Hazelbauer, G. L., and Dahl, M. M. (1973). Chemotaxis toward sugars in *Escherichia coli*. *J. Bacteriol.* 115, 824–847.
- Agravante, J. U., Matsui, T., and Kitagawa, H. (1990). Starch breakdown and changes in amylase activity during ripening of ethylene and ethanol treated bananas. *Acta Hort.* 269, 133–140.
- Aharoni, A., Keizer, L. C. P., Van Den Broeck, H. C., Blanco-Portales, R., Muñoz-Blanco, J., Bois, G., et al. (2002). Novel insight into vascular, stress, and auxin-dependent and -independent gene expression programs in strawberry, a non-climacteric fruit. *Plant Physiol.* 129, 1019–1031. doi:10.1104/pp.003558.
- Ahmed, A. E., and Labavitch, J. M. (1980). Cell wall metabolism in ripening fruit: II. Changes in carbohydrate-degrading enzymes in ripening Bartlett pears. *Plant Physiol.* 65, 1014–1016. doi:10.1104/pp.65.5.1014.
- Akiyoshi, D. E., Klee, H., Amasino, R. M., Nester, E. W., and Gordon, M. P. (1984). T-DNA of *Agrobacterium tumefaciens* encodes an enzyme of cytokinin biosynthesis. *Proc. Natl. Acad. Sci. U. S. A.* 81, 5994–5998. doi:10.1073/pnas.81.19.5994.
- Akiyoshi, D. E., Regier, D. A., and Gordon, M. P. (1987). Cytokinin production by *Agrobacterium* and *Pseudomonas* spp. *J. Bacteriol.* 169, 4242–4248.
- Altschul, S. F., Gish, W., Miller, W., Myers, E. W., and Lipman, D. J. (1990). Basic local alignment search tool. *J. Mol. Biol.* 215, 403–410.
- Ames, G. F., Prody, C., and Kustu, S. (1984). Simple, rapid, and quantitative release of periplasmic proteins by chloroform. *J. Bacteriol.* 160, 1181–1183.
- Amikam, D., and Benziman, M. (1989). Cyclic diguanylic acid and cellulose synthesis in *Agrobacterium tumefaciens*. *J. Bacteriol.* 171, 6649–6655.
- Amikam, D., and Galperin, M. Y. (2006). PilZ domain is part of the bacterial c-di-GMP binding protein. *Bioinformatics* 22, 3–6. doi:10.1093/bioinformatics/bti739.
- Andersen, C. L., Jensen, J. L., and Ørntoft, T. F. (2004). Normalization of real-time quantitative reverse transcription-PCR data: a model-based variance estimation approach to identify genes suited for normalization, applied to bladder and colon cancer data sets. *Cancer Res.* 64, 5245–5250.

- Arkhipova, T. N., Veselov, S. U., Melentiev, A. I., Martynenko, E. V., and Kudoyarova, G. R. (2005). Ability of bacterium *Bacillus subtilis* to produce cytokinins and to influence the growth and endogenous hormone content of lettuce plants. *Plant Soil* 272, 201–209. doi:10.1007/s11104-004-5047-x.
- Armitano, J., Méjean, V., and Jurlin-Castelli, C. (2014). Gram-negative bacteria can also form pellicles. *Environ. Microbiol. Rep.* 6, 534–544. doi:10.1111/1758-2229.12171.
- Arrebola, E., Carrion, V. J., Gutierrez-Barranquero, J. A., Perez-Garcia, A., Robriguez-Palenzuela, P., Cazorla, F. M., et al. (2015). Cellulose production in *Pseudomonas syringae* pv. *syringae*: a compromise between epiphytic and pathogenic lifestyles. *FEMS Microbiol. Ecol.* doi:http://dx.doi.org/10.1093/femsec/fiv071.
- Arshad, M., and Frankenberger Jr, W. T. (2002). “Biochemistry of Microbial Production of Ethylene,” in *Ethylene* (Springer), 51–96.
- Aschner, M., and Hestrin, S. (1946). Fibrillar structure of cellulose of bacterial and animal origin. *Nature* 157, 659. doi:10.1038/157659b0.
- Ashbolt, N. J., and Inkerman, P. A. (1990). Acetic acid bacterial biota of the pink sugar cane mealybug, *Saccharococcus sacchari*, and its environs. *Appl. Environ. Microbiol.* 56, 707–712.
- Atzorn, R., Crozier, A., Wheeler, C. T., and Sandberg, G. (1988). Production of gibberellins and indole-3-acetic acid by *Rhizobium phaseoli* in relation to nodulation of *Phaseolus vulgaris* roots. *Planta* 175, 532–538. doi:10.1007/BF00393076.
- Augimeri, R. V., and Strap, J. L. (2015). The phytohormone ethylene enhances bacterial cellulose production, regulates CRP/FNRKx transcription and causes differential gene expression within the cellulose synthesis operon of *Komagataeibacter (Gluconacetobacter) xylinus* ATCC 53582. *Front. Microbiol.* 6, 1459.
- Augimeri, R. V., Varley, A. J., and Strap, J. L. (2015). Establishing a role for bacterial cellulose in environmental interactions: lessons learned from diverse biofilm-producing *Proteobacteria*. *Front. Microbiol.* 6, 1282. doi:10.3389/fmicb.2015.01282.
- Baca, B. E., and Elmerich, C. (2007). “Microbial production of plant hormones,” in *Associative and endophytic nitrogen-fixing bacteria and cyanobacterial associations*, eds. C. Elmerich and W. E. Newton (Springer Netherlands), 113–143. doi:10.1007/1-4020-3546-2.
- Båga, M., Göransson, M., Normark, S., and Uhlin, B. E. (1988). Processed mRNA with differential stability in the regulation of *E. coli* pilin gene expression. *Cell* 52, 197–206.
- Bakshi, A., Shemansky, J. M., Chang, C., and Binder, B. M. (2015). History of research on the plant hormone ethylene. *J. Plant Growth Regul.* 34, 809–827.

- Ban, T., Kugishima, M., Ogata, T., Shiozaki, S., Horiuchi, S., and Ueda, H. (2007). Effect of ethephon (2-chloroethylphosphonic acid) on the fruit ripening characters of rabbiteye blueberry. *Sci. Hortic. (Amsterdam)*. 112, 278–281.
- Barak, J. D., Gorski, L., Naraghi-arani, P., Charkowski, O., and Charkowski, A. O. (2005). *Salmonella enterica* virulence genes are required for bacterial attachment to plant tissue. *Appl. Environ. Microbiol.* 71, 5685–5691. doi:10.1128/AEM.71.10.5685.
- Barak, J. D., Jahn, C. E., Gibson, D. L., and Charkowski, A. O. (2007). The role of cellulose and O-antigen capsule in the colonization of plants by *Salmonella enterica*. *Mol. Plant. Microbe. Interact.* 20, 1083–1091. doi:10.1094/MPMI-20-9-1083.
- Barata, A., Malfeito-Ferreira, M., and Loureiro, V. (2012). Changes in sour rotten grape berry microbiota during ripening and wine fermentation. *Int. J. Food Microbiol.* 154, 152–161. doi:10.1016/j.ijfoodmicro.2011.12.029.
- Bartowsky, E. J., and Henschke, P. A. (2008). Acetic acid bacteria spoilage of bottled red wine- A review. *Int. J. Food Microbiol.* 125, 60–70. doi:10.1016/j.ijfoodmicro.2007.10.016.
- Bassis, C. M., and Visick, K. L. (2010). The cyclic-di-GMP phosphodiesterase Bina negatively regulates cellulose-containing biofilms in *Vibrio fischeri*. *J. Bacteriol.* 192, 1269–1278. doi:10.1128/JB.01048-09.
- Bastián, F., Cohen, A., Piccoli, P., Luna, V., Baraldi, R., and Bottini, R. (1998). Production of indole-3-acetic acid and gibberellins A1 and A3 by *Acetobacter diazotrophicus* and *Herbaspirillum seropedicae* in chemically-defined culture media. *Plant Growth Regul.* 24, 7–11. doi:10.1023/A:1005964031159.
- Bastian, F., Rapparini, F., Baraldi, R., Piccoli, P., and Bottini, R. (1999). Inoculation with *Acetobacter diazotrophicus* increases glucose and fructose content in shoots of *Sorghum bicolor* (L.) Moench. *Symbiosis* 27, 147–156.
- Beattie, G. A., and Lindow, S. E. (1995). The secret life of foliar bacterial pathogens on leaves. *Annu. Rev. Phytopathol.* 33, 145–172.
- Beauregard, P. B., Chai, Y., Vlamakis, H., Losick, R., and Kolter, R. (2013). *Bacillus subtilis* biofilm induction by plant polysaccharides. *Proc. Natl. Acad. Sci. U. S. A.* 110, E1621–E1630. doi:10.1073/pnas.1218984110.
- Belasco, J. G., Beatty, J. T., Adams, C. W., von Gabain, A., and Cohen, S. N. (1985). Differential expression of photosynthesis genes in *R. capsulata* results from segmental differences in stability within the polycistronic *rxcA* transcript. *Cell* 40, 171–181.
- Belimov, A. A., Dodd, I. C., Safronova, V. I., Dumova, V. A., Shaposhnikov, A. I., Ladatko, A. G., et al. (2014). Abscisic acid metabolizing rhizobacteria decrease ABA concentrations in planta and alter plant growth. *Plant Physiol. Biochem.* 74, 84–91. doi:10.1016/j.plaphy.2013.10.032.

- Benziman, M., Haigler, C. H., Brown, R. M., White, A. R., and Cooper, K. M. (1980). Cellulose biogenesis: polymerization and crystallization are coupled processes in *Acetobacter xylinum*. *Proc. Natl. Acad. Sci.* 77, 6678–6682.
- van den Berg, B. (2012). Structural Basis for Outer Membrane Sugar Uptake in Pseudomonads. *J. Biol. Chem.* 287, 41044–41052. doi:10.1074/jbc.M112.408518.
- Berger, C. N., Sodha, S. V., Shaw, R. K., Griffin, P. M., Pink, D., Hand, P., et al. (2010). Fresh fruit and vegetables as vehicles for the transmission of human pathogens. *Environ. Microbiol.* 12, 2385–2397. doi:10.1111/j.1462-2920.2010.02297.x.
- Beuchat, L. R. (1997). Comparison of chemical treatments to kill *Salmonella* on alfalfa seeds destined for sprout production. *Int. J. Food Microbiol.* 34, 329–333. doi:10.1016/S0168-1605(96)01202-0.
- Beuchat, L. R. (1999). Survival of enterohemorrhagic *Escherichia coli* O157:H7 in bovine feces applied to lettuce and the effectiveness of chlorinated water as a disinfectant. *J. Food Prot.* 62, 845–849.
- Biddle, E., Kerfoot, D. G. S., Kho, Y. H., and Russell, K. E. (1976). Kinetic studies of the thermal decomposition of 2-chloroethylphosphonic acid in aqueous solution. *Plant Physiol.* 58, 700–702.
- Blatch, G. L., and Lässle, M. (1999). The tetratricopeptide repeat: a structural motif mediating protein-protein interactions. *Bioessays* 21, 932–939.
- Boettcher, K. J., and Ruby, E. G. (1990). Depressed light-emission by symbiotic *Vibrio fischeri* of the sepiolid squid *Euprymna scolopes*. *J. Bacteriol.* 172, 3701–3706.
- Boiero, L., Perrig, D., Masciarelli, O., Penna, C., Cassán, F., and Luna, V. (2007). Phytohormone production by three strains of *Bradyrhizobium japonicum* and possible physiological and technological implications. *Appl. Microbiol. Biotechnol.* 74, 874–880. doi:10.1007/s00253-006-0731-9.
- Bornhorst, J. A., and Falke, J. J. (2003). Quantitative analysis of aspartate receptor signaling complex reveals that the homogeneous two-state model is inadequate: development of a heterogeneous two-state model. *J. Mol. Biol.* 326, 1597–1614.
- Bottini, R., Cassán, F., and Piccoli, P. (2004). Gibberellin production by bacteria and its involvement in plant growth promotion and yield increase. *Appl. Microbiol. Biotechnol.* 65, 497–503. doi:10.1007/s00253-004-1696-1.
- Bottini, R., Cohen, A. C., Travaglia, C. N., and Piccoli, P. N. (2009). Participation of abscisic acid and gibberellins produced by endophytic *Azospirillum* in the alleviation of drought effects in maize. *Botany-Botanique* 87, 455–462.
- Bottini, R., Fulchieri, M., Pearce, D., and Pharis, R. P. (1989). Identification of gibberellins A(1), A(3), and Iso-A(3) in cultures of *Azospirillum lipoferum*. *Plant Physiol.* 90, 45–47. doi:10.1104/pp.90.1.45.
- Bradford, M. M. (1976). A rapid and sensitive method for the quantitation of microgram

- quantities of protein utilizing the principle of protein-dye binding. *Anal. Biochem.* 72, 248–254.
- Brady, C. J. (1987). Fruit ripening. *Annu. Rev. Plant Physiol.* 38, 155–178.
doi:10.1146/annurev.pp.38.060187.001103.
- Breton, C., Šnajdrová, L., Jeanneau, C., Koča, J., and Imberty, A. (2006). Structures and mechanisms of glycosyltransferases. *Glycobiology* 16, 29R–37R.
- Brockhausen, I. (2014). Crossroads between bacterial and mammalian glycosyltransferases. *Front. Immunol.* 5.
- Brown, C. T., and Callan, C. G. (2004). Evolutionary comparisons suggest many novel cAMP response protein binding sites in *Escherichia coli*. *Proc. Natl. Acad. Sci. U. S. A.* 101, 2404–2409.
- Brown, R. M., and Montezinos, D. (1976). Cellulose microfibrils: visualization of biosynthetic and orienting complexes in association with the plasma membrane. *Proc. Natl. Acad. Sci.* 73, 143–147.
- Brown, R. M., Willison, J. H., and Richardson, C. L. (1976). Cellulose biosynthesis in *Acetobacter xylinum*: visualization of the site of synthesis and direct measurement of the *in vivo* process. *Proc. Natl. Acad. Sci. U. S. A.* 73, 4565–4569.
doi:10.1073/pnas.73.12.4565.
- Brummell, D. A. (2006). Cell wall disassembly in ripening fruit. *Funct. Plant Biol.* 33, 103–119.
- Brummell, D. A., and Harpster, M. H. (2001). Cell wall metabolism in fruit softening and quality and its manipulation in transgenic plants. *Plant Mol. Biol.* 47, 311–340.
doi:10.1023/A:1010656104304.
- Brusilow, W. S., Klionsky, D. J., and Simoni, R. D. (1982). Differential polypeptide synthesis of the proton-translocating ATPase of *Escherichia coli*. *J. Bacteriol.* 151, 1363–1371.
- Buchholz, U., Bernard, H., Werber, D., Böhmer, M. M., Remschmidt, C., Wilking, H., et al. (2011). German outbreak of *Escherichia coli* O104:H4 associated with sprouts. *N. Engl. J. Med.* 365, 1763–1770. doi:10.1056/NEJMoa1106482.
- Burchhardt, G., Keshav, K. F., Yomano, L., and Ingram, L. O. (1993). Mutational analysis of segmental stabilization of transcripts from the *Zymomonas mobilis gap-pgk* operon. *J. Bacteriol.* 175, 2327–2333.
- Bureau, T. E., and Brown, R. M. (1987). *In vitro* synthesis of cellulose II from a cytoplasmic membrane fraction of *Acetobacter xylinum*. *Proc. Natl. Acad. Sci.* 84, 6985–6989.
- Burg, S. P., and Burg, E. A. (1962). Role of ethylene in fruit ripening. *Plant Physiol.* 37, 179.

- Bustin, S. A., Benes, V., Garson, J. A., Hellemans, J., Huggett, J., Kubista, M., et al. (2009). The MIQE guidelines: minimum information for publication of quantitative real-time PCR experiments. *Clin. Chem.* 55, 611–622.
- Cane, D. E., and Ikeda, H. (2011). Exploration and mining of the bacterial terpenome. *Acc. Chem. Res.* 45, 463–472.
- Cangelosi, G. A., Ankenbauer, R. G., and Nester, E. W. (1990). Sugars induce the *Agrobacterium* virulence genes through a periplasmic binding protein and a transmembrane signal protein. *Proc. Natl. Acad. Sci.* 87, 6708–6712.
- Cantín, C. M., Fidelibus, M. W., and Crisosto, C. H. (2007). Application of abscisic acid (ABA) at veraison advanced red color development and maintained postharvest quality of “Crimson Seedless” grapes. *Postharvest Biol. Technol.* 46, 237–241. doi:10.1016/j.postharvbio.2007.05.017.
- Capdevila, J. A., Bisbe, V., Gasser, I., Zuazu, J., Olivé, T., Fernández, F., et al. (1998). *Enterobacter amnigenus*. An unusual human pathogen. *Enferm. Infecc. Microbiol. Clin.* 16, 364–366.
- Casanova, L., Casanova, R., Moret, A., and Agustí, M. (2009). The application of gibberellic acid increases berry size of “Emperatriz” seedless grape. *Spanish J. Agric. Res.* 7, 919–927. doi:1695-971-X.
- Chang, A. L., Tuckerman, J. R., Gonzalez, G., Mayer, R., Weinhouse, H., Volman, G., et al. (2001). Phosphodiesterase A1, a regulator of cellulose synthesis in *Acetobacter xylinum*, is a heme-based sensor. *Biochemistry* 40, 3420–3426. doi:10.1021/bi0100236.
- Chang, C., Kwok, S. F., Bleecker, A. B., and Meyerowitz, E. M. (1993). *Arabidopsis* ethylene-response gene ETR1: similarity of product to two-component regulators. *Science* (80-.). 262, 539–544.
- Chanliaud, E., and Gidley, M. J. (1999). *In vitro* synthesis and properties of pectin/*Acetobacter xylinus* cellulose composites. *Plant J.* 20, 25–35.
- Chen, Y.-F., Randlett, M. D., Findell, J. L., and Schaller, G. E. (2002). Localization of the ethylene receptor ETR1 to the endoplasmic reticulum of *Arabidopsis*. *J. Biol. Chem.* 277, 19861–19866.
- Chervin, C., El-Kereamy, A., Roustan, J. P., Latché, A., Lamon, J., and Bouzayen, M. (2004). Ethylene seems required for the berry development and ripening in grape, a non-climacteric fruit. *Plant Sci.* 167, 1301–1305. doi:10.1016/j.plantsci.2004.06.026.
- Chevalier, F. (2010). Standard dyes for total protein staining in gel-based proteomic analysis. *Materials (Basel)*. 3, 4784–4792.
- Chou, T. W., and Yang, S. F. (1973). The biogenesis of ethylene in *Penicillium digitatum*. *Arch. Biochem. Biophys.* 157, 73–82.

- Ciolacu, D., Ciolacu, F., and Popa, V. I. (2011). Amorphous cellulose—structure and characterization. *Cellul. Chem. Technol.* 45, 13–21.
- Clark, K. L., Larsen, P. B., Wang, X., and Chang, C. (1998). Association of the *Arabidopsis* CTR1 Raf-like kinase with the ETR1 and ERS ethylene receptors. *Proc. Natl. Acad. Sci.* 95, 5401–5406.
- Cleenwerck, I., De Wachter, M., González, Á., De Vuyst, L., and De Vos, P. (2009). Differentiation of species of the family *Acetobacteraceae* by AFLP DNA fingerprinting: *Gluconacetobacter kombuchae* is a later heterotypic synonym of *Gluconacetobacter hansenii*. *Int. J. Syst. Evol. Microbiol.* 59, 1771–1786. doi:10.1099/ijs.0.005157-0.
- Cohen, A. C., Bottini, R., and Piccoli, P. N. (2008). *Azospirillum brasilense* Sp 245 produces ABA in chemically-defined culture medium and increases ABA content in *Arabidopsis* plants. *Plant Growth Regul.* 54, 97–103. doi:10.1007/s10725-007-9232-9.
- Colland, F., Barth, M., Hengge-Aronis, R., and Kolb, A. (2000). σ factor selectivity of *Escherichia coli* RNA polymerase: role for CRP, IHF and Lrp transcription factors. *EMBO J.* 19, 3028–3037.
- Cook, R. A. (1988). Periplasmic proteases of *Escherichia coli*. *Crit. Rev. Biotechnol.* 8, 159–175.
- Corby-Harris, V., Pontaroli, A. C., Shimkets, L. J., Bennetzen, J. L., Habel, K. E., and Promislow, D. E. L. (2007). Geographical distribution and diversity of bacteria associated with natural populations of *Drosophila melanogaster*. *Appl. Environ. Microbiol.* 73, 3470–3479. doi:10.1128/AEM.02120-06.
- Cortajarena, A. L., and Regan, L. (2006). Ligand binding by TPR domains. *Protein Sci.* 15, 1193–1198.
- Costacurta, A., and Vanderleyden, J. (1995). Synthesis of phytohormones by plant-associated bacteria. *Crit. Rev. Microbiol.* 21, 1–18. doi:10.3109/10408419509113531.
- Costechareyre, D., Balmand, S., Condemine, G., and Rahbé, Y. (2012). *Dickeya dadantii*, a plant pathogenic bacterium producing cyt-like entomotoxins, causes septicemia in the pea aphid *Acyrtosiphon pisum*. *PLoS One* 7, e30702. doi:10.1371/journal.pone.0030702.
- Costerton, J. W., Lewandowski, Z., Caldwell, D. E., Korber, D. R., and Lappin-Scott, H. M. (1995). Microbial biofilms. *Annu. Rev. Microbiol.* 49, 711–745. doi:10.1146/annurev.mi.49.100195.003431.
- Cousins, S. K., and Brown, R. M. (1995). Cellulose I microfibril assembly: computational molecular mechanics energy analysis favours bonding by van der Waals forces as the initial step in crystallization. *Polymer (Guildf)*. 36, 3885–3888.

- Crespo, J. M. (2011). Mineral phosphate solubilization activity of *Gluconacetobacter diazotrophicus* under P-limitation and plant root environment. *Agric. Sci.* 02, 16–22. doi:10.4236/as.2011.21003.
- Crotti, E., Damiani, C., Pajoro, M., Gonella, E., Rizzi, A., Ricci, I., et al. (2009). *Asaia*, a versatile acetic acid bacterial symbiont, capable of cross-colonizing insects of phylogenetically distant genera and orders. *Environ. Microbiol.* 11, 3252–3264. doi:10.1111/j.1462-2920.2009.02048.x.
- Crotti, E., Rizzi, A., Chouaia, B., Ricci, I., Favia, G., Alma, A., et al. (2010). Acetic acid bacteria, newly emerging symbionts of insects. *Appl. Environ. Microbiol.* 76, 6963–6970. doi:10.1128/AEM.01336-10.
- Cutler, S. R., Rodriguez, P. L., Finkelstein, R. R., and Abrams, S. R. (2010). Abscisic acid: emergence of a core signaling network. *Annu. Rev. Plant Biol.* 61, 651–679. doi:10.1146/annurev-arplant-042809-112122.
- Czaja, W., Romanovicz, D., and Brown, R. M. (2004). Structural investigations of microbial cellulose produced in stationary and agitated culture. *Cellulose* 11, 403–411. doi:10.1023/b:cell.0000046412.11983.61.
- Dangar, T. K., and Basu, P. S. (1991). Abscisic acid production in culture by some *Rhizobium* spp. of leguminous trees and pulses. *Folia Microbiol. (Praha)*. 36, 527–532. doi:10.1007/BF02884031.
- Davière, J.-M., and Achard, P. (2013). Gibberellin signaling in plants. *Development* 140, 1147–1151. doi:10.1242/dev.087650.
- Davies, C., Boss, P. K., and Robinson, S. P. (1997). Treatment of grape berries, a nonclimacteric fruit with a synthetic auxin, retards ripening and alters the expression of developmentally regulated genes. *Plant Physiol.* 115, 1155–1161. doi:115/3/1155 [pii].
- Davies, P. J. (2010). “The plant hormones: their nature, occurrence, and functions,” in *Plant hormones* (Springer), 1–15.
- Dellaglio, F., Cleenwerck, I., Felis, G. E., Engelbeen, K., Janssens, D., and Marzotto, M. (2005). Description of *Gluconacetobacter swingsii* sp. nov. and *Gluconacetobacter rhaeticus* sp. nov., isolated from Italian apple fruit. *Int. J. Syst. Evol. Microbiol.* 55, 2365–2370. doi:10.1099/ijs.0.63301-0.
- Delmer, D. P. (1999). Cellulose biosynthesis: exciting times for a difficult field of study. *Annu. Rev. Plant Physiol. Plant Mol. Biol.* 50, 245–276. doi:10.1146/annurev.arplant.50.1.245.
- Deng, Y., Nagachar, N., Fang, L., Luan, X., Catchmark, J., Tien, M., et al. (2015). Isolation and characterization of two cellulose morphology mutants of *Gluconacetobacter hansenii* ATCC23769 producing cellulose with lower crystallinity. *PLoS One* 10.

- Deng, Y., Nagachar, N., Xiao, C., Tien, M., and Kao, T. H. (2013). Identification and characterization of non-cellulose-producing mutants of *Gluconacetobacter hansenii* generated by Tn5 transposon mutagenesis. *J. Bacteriol.* 195, 5072–5083. doi:10.1128/JB.00767-13.
- Denney, J. O., and Martin, G. C. (1994). Ethephon tissue penetration and harvest effectiveness in olive as a function of solution pH, application time, and BA or NAA addition. *J. Am. Soc. Hortic. Sci.* 119, 1185–1192.
- Desprez, T., Juraniec, M., Crowell, E. F., Jouy, H., Pochylova, Z., Parcy, F., et al. (2007). Organization of cellulose synthase complexes involved in primary cell wall synthesis in *Arabidopsis thaliana*. *Proc. Natl. Acad. Sci.* 104, 15572–15577.
- Dhall, R. K., and Singh, P. (2013). Effect of ethephon and ethylene gas on ripening and quality of tomato (*Solanum lycopersicum* L.) during cold storage. *J. Nutr. Food Sci.* 3, 1.
- Dhillon, W. S., and Mahajan, B. V. C. (2011). Ethylene and ethephon induced fruit ripening in pear. *J. Stored Prod. Postharvest Res.* 2, 45–51.
- Digiacomio, F., Girelli, G., Aor, B., Marchioretti, C., Pedrotti, M., Perli, T., et al. (2014). Ethylene-producing bacteria that ripen fruit. *ACS Synth. Biol.* 3, 935–938.
- Dillon, R. J., and Dillon, V. M. (2004). The gut bacteria of insects: nonpathogenic interactions. *Annu. Rev. Entomol.* 49, 71–92. doi:10.1146/annurev.ento.49.061802.123416.
- Doblin, M. S., Kurek, I., Jacob-Wilk, D., and Delmer, D. P. (2002). Cellulose biosynthesis in plants: from genes to rosettes. *Plant Cell Physiol.* 43, 1407–1420.
- Dogsca, I., Brloznic, M., Stopar, D., and Mandic-Mulec, I. (2013). Exopolymer diversity and the role of levan in *Bacillus subtilis*. *PLoS One* 8, e62044. doi:10.1371/journal.pone.0062044.
- Doyle, M. P., and Erickson, M. C. (2008). Summer meeting 2007 - the problem with fresh produce: an overview. *J. Appl. Microbiol.* 105, 317–330.
- Duca, D., Lorv, J., Patten, C. L., Rose, D., and Glick, B. R. (2014). Indole-3-acetic acid in plant-microbe interactions. *Antonie Van Leeuwenhoek* 106, 85–125.
- Eddy, C. K., Keshav, K. F., An, H., Utt, E. A., Mejia, J. P., and Ingram, L. O. (1991). Segmental message stabilization as a mechanism for differential expression from the *Zymomonas mobilis* gap operon. *J. Bacteriol.* 173, 245–254.
- Egea, L., Aguilera, L., Gimenez, R., Sorolla, M. A., Aguilar, J., Badia, J., et al. (2007). Role of secreted glyceraldehyde-3-phosphate dehydrogenase in the infection mechanism of enterohemorrhagic and enteropathogenic *Escherichia coli*: interaction of the extracellular enzyme with human plasminogen and fibrinogen. *Int. J. Biochem. Cell Biol.* 39, 1190–1203.
- Ellermann, M., Huh, E. Y., Liu, B., Carroll, I. M., Tamayo, R., and Sartor, R. B. (2015).

- Adherent-invasive *Escherichia coli* production of cellulose influences iron-induced bacterial aggregation, phagocytosis and induction of colitis. *Infect. Immun.*
- Even, S., Burguière, P., Auger, S., Soutourina, O., Danchin, A., and Martin-Verstraete, I. (2006). Global control of cysteine metabolism by CymR in *Bacillus subtilis*. *J. Bacteriol.* 188, 2184–2197.
- Fan, J., Hill, L., Crooks, C., Doerner, P., and Lamb, C. (2009). Abscisic acid has a key role in modulating diverse plant-pathogen interactions. *Plant Physiol.* 150, 1750–1761. doi:10.1104/pp.109.137943.
- Fang, L., and Catchmark, J. (2014). Characterization of water-soluble exopolysaccharides from *Gluconacetobacter xylinus* and their impacts on bacterial cellulose formation. *Biomacromolecules* 21, 3965–3978. doi:10.1007/s10570-014-0443-8.
- Fang, L., and Catchmark, J. M. (2015). Characterization of cellulose and other exopolysaccharides produced from *Gluconacetobacter* strains. *Carbohydr. Polym.* 115, 663–669.
- Favia, G., Ricci, I., Damiani, C., Raddadi, N., Crotti, E., Marzorati, M., et al. (2007). Bacteria of the genus *Asaia* stably associate with *Anopheles stephensi*, an Asian malarial mosquito vector. *Proc. Natl. Acad. Sci. U. S. A.* 104, 9047–9051. doi:10.1073/pnas.0610451104.
- Fazli, M., McCarthy, Y., Givskov, M., Ryan, R. P., and Tolker-Nielsen, T. (2013). The exopolysaccharide gene cluster *Bcam1330–Bcam1341* is involved in *Burkholderia cenocepacia* biofilm formation, and its expression is regulated by c-di-GMP and *Bcam1349*. *Microbiologyopen* 2, 105–122.
- Fazli, M., O’Connell, A., Nilsson, M., Niehaus, K., Dow, J. M., Givskov, M., et al. (2011). The CRP/FNR family protein *Bcam1349* is a c-di-GMP effector that regulates biofilm formation in the respiratory pathogen *Burkholderia cenocepacia*. *Mol. Microbiol.* 82, 327–341.
- Feldhaar, H., and Gross, R. (2009). Insects as hosts for mutualistic bacteria. *Int. J. Med. Microbiol.* 299, 1–8. doi:10.1016/j.ijmm.2008.05.010.
- Flemming, H.-C., and Wingender, J. (2010). The biofilm matrix. *Nat. Rev. Microbiol.* 8, 623–633. doi:10.1080/0892701031000072190.
- Floden, A. M., Watt, J. A., and Brissette, C. A. (2011). *Borrelia burgdorferi* enolase is a surface-exposed plasminogen binding protein. *PLoS One* 6, e27502.
- Fong, J. C. N., and Yildiz, F. H. (2008). Interplay between cyclic AMP-cyclic AMP receptor protein and cyclic di-GMP signaling in *Vibrio cholerae* biofilm formation. *J. Bacteriol.* 190, 6646–6659.
- Foster, H. J., Biemann, K., Haigh, W. G., Tattrie, N. H., and Calvin, J. R. (1973). The structure of novel C35 pentacyclic terpenes from *Acetobacter xylium*. *Biochem. J.* 135, 133–143.

- Frenkel, C., and Dyck, R. (1973). Auxin inhibition of ripening in Bartlett pears. *Plant Physiol.* 51, 6–9.
- Galperin, M. Y., Nikolskaya, A. N., and Koonin, E. V (2001). Novel domains of the prokaryotic two-component signal transduction systems. *FEMS Microbiol. Lett.* 203, 11–21.
- Gamble, R. L., Coonfield, M. L., and Schaller, G. E. (1998). Histidine kinase activity of the ETR1 ethylene receptor from *Arabidopsis*. *Proc. Natl. Acad. Sci.* 95, 7825–7829.
- Gay, N. J., and Walker, J. E. (1981). The *atp* operon: nucleotide sequence of the promoter and the genes for the membrane proteins, and the δ subunit of *Escherichia coli* ATP-synthase. *Nucleic Acids Res.* 9, 3919–3926.
- Geesey, G. G., Mutch, R., Costerton, J. W., and Green, R. B. (1978). Sessile bacteria: An important component of the microbial population in small mountain streams. *Limnol. Oceanogr.* 23, 1214–1223. doi:10.4319/lo.1978.23.6.1214.
- Gill, P. S., Jawandha, S. K., Singh, N., Kaur, N., and Verma, A. (2014). Influence of postharvest applications of ethephon on fruit ripening in mango. *Int. J. Adv. Biol. Res.* 4, 438–441.
- Gilles-Gonzalez, M.-A., and Gonzalez, G. (2004). Signal transduction by heme-containing PAS-domain proteins. *J. Appl. Physiol.* 96, 774–783.
- Glick, B. R. (2005). Modulation of plant ethylene levels by the bacterial enzyme ACC deaminase. *FEMS Microbiol. Lett.* 251, 1–7. doi:10.1016/j.femsle.2005.07.030.
- Glick, B. R. (2012). Plant growth-promoting bacteria: Mechanisms and applications. *Scientifica (Cairo)*. vol. 2012, 1–15.
- Graver, M. A., and Wade, J. J. (2011). The role of acidification in the inhibition of *Neisseria gonorrhoeae* by vaginal lactobacilli during anaerobic growth. *Ann. Clin. Microbiol. Antimicrob.* 10, 8. doi:10.1186/1476-0711-10-8.
- Gromet-Elhanan, Z., and Hestrin, S. (1963). Synthesis of cellulose by *Acetobacter xylinum* VI. Growth on citric acid-cycle intermediates. *J. Bacteriol.* 85, 284–292.
- Gromova, I., and Celis, J. E. (2006). Protein detection in gels by silver staining: a procedure compatible with mass-spectrometry. *Cell Biol. A Lab. Handb.* 4, 421–429.
- Guzmán, P., and Ecker, J. R. (1990). Exploiting the triple response of *Arabidopsis* to identify ethylene-related mutants. *Plant Cell* 2, 513–523. doi:10.1105/tpc.2.6.513.
- Hackney, J. M., Atalla, R. H., and VanderHart, D. L. (1994). Modification of crystallinity and crystalline structure of *Acetobacter xylinum* cellulose in the presence of water-soluble beta-1,4-linked polysaccharides: ¹³C-NMR evidence. *Int. J. Biol. Macromol.* 16, 215–218. doi:10.1016/0141-8130(94)90053-1.
- Haigh, W. G. (1973). Induction of orientation of bacterial cellulose microfibrils by a novel terpenoid from *Acetobacter xylinum*. *Biochem. J* 135, 145–149.

- Haigler, C. H., Brown, R. M., and Benziman, M. (1980). Calcofluor white ST alters the in vivo assembly of cellulose microfibrils. *Science*. 210, 903–906.
- Hanus, J., and Mazeau, K. (2006). The xyloglucan-cellulose assembly at the atomic scale. *Biopolymers* 82, 59–73. doi:10.1002/bip.20460.
- Hardie, W. J., Johnson, J. O., and Weaver, R. J. (1981). The influence of vine water regime on ethephon-enhanced ripening of Zinfandel. *Am. J. Enol. Vitic.* 32, 115–121.
- Harman, J. G. (2001). Allosteric regulation of the cAMP receptor protein. *Biochim. Biophys. Acta (BBA)-Protein Struct. Mol. Enzymol.* 1547, 1–17.
- Harris, D. M., Corbin, K., Wang, T., Gutierrez, R., Bertolo, A. L., Petti, C., et al. (2012). Cellulose microfibril crystallinity is reduced by mutating C-terminal transmembrane region residues CESA1A903V and CESA3T942I of cellulose synthase. *Proc. Natl. Acad. Sci.* 109, 4098–4103.
- Hazelbauer, G. L., Falke, J. J., and Parkinson, J. S. (2008). Bacterial chemoreceptors: high-performance signaling in networked arrays. *Trends Biochem. Sci.* 33, 9–19.
- Heath, J. L. (1990). Effect of D-mannose on fimbriae of bacterial isolates from chicken carcasses. *Poult. Sci.* 69, 1582–1589.
- Heins, V. (1944). John Mercer and mercerization, 1844. *J. Chem. Educ.* 21, 430.
- Hellemans, J., Mortier, G., De Paepe, A., Speleman, F., and Vandesompele, J. (2007). qBase relative quantification framework and software for management and automated analysis of real-time quantitative PCR data. *Genome Biol.* 8, R19. doi:10.1186/gb-2007-8-2-r19.
- Hellman, L. M., and Fried, M. G. (2007). Electrophoretic mobility shift assay (EMSA) for detecting protein–nucleic acid interactions. *Nat. Protoc.* 2, 1849–1861.
- Hentzer, M., Teitzel, G. M., Balzer, G. J., Heydorn, A., Molin, S., Givskov, M., et al. (2001). Alginate Overproduction Affects *Pseudomonas aeruginosa* Biofilm Structure and Function. *J. Bacteriol.* 183, 5395–5401. doi:10.1128/JB.183.18.5395-5401.2001.
- Hestrin, S., Aschner, M., and Mager, J. (1947). Synthesis of cellulose by resting cells of *Acetobacter xylinum*. *Nature* 159, 64. doi:10.1038/159064a0.
- Hitoshi, S. (2006). Cytokinins: Activity, biosynthesis, and translocation. *Annu. Rev. Plant Biol.* 57, 431–449.
- Homuth, G., Mogk, A., and Schumann, W. (1999). Post-transcriptional regulation of the *Bacillus subtilis dnaK* operon. *Mol. Microbiol.* 32, 1183–1197.
- Hsu, W.-L., Oldfield, C., Meng, J., Huang, F., Xue, B., Uversky, V. N., et al. (2012). Intrinsic protein disorder and protein-protein interactions. *Pac. Symp. Biocomput.* 3, 116–27. Available at: <http://www.ncbi.nlm.nih.gov/pubmed/22174268>.

- Hu, S. Q., Gao, Y. G., Tajima, K., Sunagawa, N., Zhou, Y., Kawano, S., et al. (2010). Structure of bacterial cellulose synthase subunit D octamer with four inner passageways. *Proc. Natl. Acad. Sci. U. S. A.* 107, 17957–17961. doi:10.1073/pnas.1000601107.
- Hu, Y., and Catchmark, J. M. (2010). Influence of 1-methylcyclopropene (1-MCP) on the production of bacterial cellulose biosynthesized by *Acetobacter xylinum* under the agitated culture. *Lett. Appl. Microbiol.* 51, 109–113. doi:10.1111/j.1472-765X.2010.02866.x.
- Hua, J., and Meyerowitz, E. M. (1998). Ethylene responses are negatively regulated by a receptor gene family in *Arabidopsis thaliana*. *Cell* 94, 261–271.
- Hua, J., Sakai, H., Nourizadeh, S., Chen, Q. G., Bleecker, A. B., Ecker, J. R., et al. (1998). EIN4 and ERS2 are members of the putative ethylene receptor gene family in *Arabidopsis*. *Plant Cell* 10, 1321–1332.
- Huberts, D. H. E. W., and van der Klei, I. J. (2010). Moonlighting proteins: an intriguing mode of multitasking. *Biochim. Biophys. Acta (BBA)-Molecular Cell Res.* 1803, 520–525.
- Hungund, B. S., and Gupta, S. G. (2010). Improved production of bacterial cellulose from *Gluconacetobacter persimmonis* GH-2. *J. Microb. Biochem. Technol.* 02, 127–133. doi:10.4172/1948-5948.1000037.
- Iannetta, P. P. M., Laarhoven, L., Medina-Escobar, N., James, E. K., McManus, M. T., Davies, H. V., et al. (2006). Ethylene and carbon dioxide production by developing strawberries show a correlative pattern that is indicative of ripening climacteric fruit. *Physiol. Plant.* 127, 247–259.
- Iguchi, M., Yamanaka, S., and Budhiono, A. (2000). Bacterial cellulose - a masterpiece of nature's arts. *J. Mater. Sci.* 35, 261–270. doi:10.1023/A:1004775229149.
- Ince, J. E., and Knowles, C. J. (1985). Ethylene formation by cultures of *Escherichia coli*. *Arch. Microbiol.* 141, 209–213. doi:10.1007/BF00408060.
- Ince, J. E., and Knowles, C. J. (1986). Ethylene formation by cell-free extracts of *Escherichia coli*. *Arch. Microbiol.* 146, 151–158.
- Islam, M., Morgan, J., Doyle, M. P., Phatak, S. C., Millner, P., and Jiang, X. (2004). Persistence of *Salmonella enterica* serovar Typhimurium on lettuce and parsley and in soils on which they were grown in fields treated with contaminated manure composts or irrigation water. *Foodborne Pathog. Dis.* 1, 27–35. doi:10.1089/153531404772914437.
- Iwata, T., Indrarti, L., and Azuma, J. I. (1998). Affinity of hemicellulose for cellulose produced by *Acetobacter xylinum*. *Cellulose* 5, 215–228. doi:10.1023/A:1009237401548.
- Iyer, P. R., Catchmark, J., Brown, N. R., and Tien, M. (2011). Biochemical localization

- of a protein involved in synthesis of *Gluconacetobacter hansenii* cellulose. *Cellulose* 18, 739–747. doi:10.1007/s10570-011-9504-4.
- Jackson, D. W., Simecka, J. W., and Romeo, T. (2002). Catabolite repression of *Escherichia coli* biofilm formation. *J. Bacteriol.* 184, 3406–3410.
- Jahan, F., Kumar, V., Rawat, G., and Saxena, R. K. (2012). Production of microbial cellulose by a bacterium isolated from fruit. *Appl. Biochem. Biotechnol.* 167, 1157–1171. doi:10.1007/s12010-012-9595-x.
- Jahn, C. E., Selimi, D. A., Barak, J. D., and Charkowski, A. O. (2011). The *Dickeya dadantii* biofilm matrix consists of cellulose nanofibres, and is an emergent property dependent upon the type III secretion system and the cellulose synthesis operon. *Microbiology* 157, 2733–2744. doi:10.1099/mic.0.051003-0.
- Janisiewicz, W. J., Conway, W. S., Brown, M. W., Sapers, G. M., Fratamico, P., and Buchanan, R. L. (1999). Fate of *Escherichia coli* O157: H7 on fresh-cut apple tissue and its potential for transmission by fruit flies. *Appl. Environ. Microbiol.* 65, 1–5.
- Janisiewicz, W. J., and Marchi, A. (1992). Control of storage rots on various pear cultivars with saprophytic strain of *Pseudomonas syringae*. *Plant Dis.* 76, 555–560.
- Jia, H. F., Chai, Y. M., Li, C. L., Lu, D., Luo, J. J., Qin, L., et al. (2011). Abscisic Acid plays an important role in the regulation of strawberry fruit ripening. *Plant Physiol.* 157, 188–199. doi:10.1104/pp.111.177311.
- Jolliffe, P. A. (1975). Effects of ethephon on raspberry fruit ripeness, fruit weight and fruit removal. *Can. J. Plant Sci.* 55, 429–437. doi:10.4141/cjps75-067.
- Jonas, K., Tomenius, H., Kader, A., Normark, S., Römling, U., Belova, L. M., et al. (2007). Roles of curli, cellulose and BapA in *Salmonella* biofilm morphology studied by atomic force microscopy. *BMC Microbiol.* 7, 70. doi:10.1186/1471-2180-7-70.
- Jørgensen, H., Kristensen, J. B., and Felby, C. (2007). Enzymatic conversion of lignocellulose into fermentable sugars: Challenges and opportunities. *Biofuels, Bioprod. Biorefining* 1, 119–134. doi:10.1002/bbb.4.
- Karadeniz, A., Topcuoğlu, Ş. F., and Inan, S. (2006). Auxin, gibberellin, cytokinin and abscisic acid production in some bacteria. *World J. Microbiol. Biotechnol.* 22, 1061–1064. doi:10.1007/s11274-005-4561-1.
- Kau, A. L., Ahern, P. P., Griffin, N. W., Goodman, A. L., and Jeffrey, I. (2012). Human nutrition, the gut microbiome, and immune system: envisioning the future. *Nature* 474, 327–336. doi:10.1038/nature10213.Human.
- Kawano, S., Tajima, K., Kono, H., Erata, T., Munekata, M., and Takai, M. (2002a). Effects of endogenous endo-beta-1,4-glucanase on cellulose biosynthesis in *Acetobacter xylinum* ATCC23769. *J. Biosci. Bioeng.* 94, 275–281.
- Kawano, S., Tajima, K., Kono, H., Numata, Y., Yamashita, H., Satoh, Y., et al. (2008).

- Regulation of endoglucanase gene (*cmcax*) expression in *Acetobacter xylinum*. *J. Biosci. Bioeng.* 106, 88–94. doi:10.1263/jbb.106.88.
- Kawano, S., Tajima, K., Uemori, Y., Yamashita, H., Erata, T., Munekata, M., et al. (2002b). Cloning of cellulose synthesis related genes from *Acetobacter xylinum* ATCC23769 and ATCC53582: Comparison of cellulose synthetic ability between strains. *DNA Res.* 9, 149–156. doi:10.1093/dnares/9.5.149.
- Keshk, S. M. A. S. (2014). Vitamin C enhances bacterial cellulose production in *Gluconacetobacter xylinus*. *Carbohydr. Polym.* 99, 98–100. doi:10.1016/j.carbpol.2013.08.060.
- Khan, N. A. (2004). An evaluation of the effects of exogenous ethephon, an ethylene releasing compound, on photosynthesis of mustard (*Brassica juncea*) cultivars that differ in photosynthetic capacity. *BMC Plant Biol.* 4, 21. doi:10.1186/1471-2229-4-21.
- Khorshidi, S., and Davarynejad, G. (2010). Influence of preharvest ethephon spray on fruit quality and chemical attributes of “Cigany” sour cherry cultivar. *Fruits* 4, 133–141.
- Kido, N., Torgov, V. I., Sugiyama, T., Uchiya, K., Sugihara, H., Komatsu, T., et al. (1995). Expression of the O9 polysaccharide of *Escherichia coli*: sequencing of the *E. coli* O9 *rfb* gene cluster, characterization of mannosyl transferases, and evidence for an ATP-binding cassette transport system. *J. Bacteriol.* 177, 2178–2187.
- Kieber, J. J., Rothenberg, M., Roman, G., Feldmann, K. A., and Ecker, J. R. (1993). CTR1, a negative regulator of the ethylene response pathway in *Arabidopsis*, encodes a member of the RAF family of protein kinases. *Cell* 72, 427–441.
- Kim, H.-E., Shitashiro, M., Kuroda, A., Takiguchi, N., and Kato, J. (2007). Ethylene chemotaxis in *Pseudomonas aeruginosa* and other *Pseudomonas* species. *Microbes Environ.* 22, 186–189. doi:10.1264/jsme2.22.186.
- Kimura, S., Chen, H. P., Saxena, I. M., Brown, R. M., and Itoh, T. (2001). Localization of c-di-GMP-binding protein with the linear terminal complexes of *Acetobacter xylinum*. *J. Bacteriol.* 183, 5668–5674. doi:10.1128/JB.183.19.5668-5674.2001.
- Kimura, S., and Itoh, T. (2007). “Biogenesis and function of cellulose in the tunicates,” in *Cellulose: molecular and structural biology*, eds. M. R. Brown Jr. and I. M. Saxena (Netherlands: Springer), 217–236. doi:10.1007/978-1-4020-5380-1_13.
- Kimura, S., Laosinchai, W., Itoh, T., Cui, X., Linder, C. R., and Brown, R. M. (1999). Immunogold labeling of rosette terminal cellulose-synthesizing complexes in the vascular plant *Vigna angularis*. *Plant Cell* 11, 2075–2085.
- Kisluk, G., Kalily, E., and Yaron, S. (2013). Resistance to essential oils affects survival of *Salmonella enterica* serovars in growing and harvested basil. *Environ. Microbiol.* 15, 2787–2798. doi:10.1111/1462-2920.12139.

- Klein, I., Lavee, S., and Ben-Tal, Y. (1979). Effect of water vapor pressure on the thermal decomposition of 2-chloroethylphosphonic acid. *Plant Physiol.* 63, 474–477.
- Klug, G., Adams, C. W., Belasco, J., Doerge, B., and Cohen, S. N. (1987). Biological consequences of segmental alterations in mRNA stability: effects of deletion of the intercistronic hairpin loop region of the *Rhodobacter capsulatus puf* operon. *EMBO J.* 6, 3515.
- Knudsen, T. B., and Klemm, P. (1998). Probing the receptor recognition site of the FimH adhesin by fimbriae-displayed FimH--FocH hybrids. *Microbiology* 144, 1919–1929.
- Kolb, A., Busby, S., Buc, I. I., Garges, S., and Adhya, S. (1993). Transcriptional regulation by cAMP and its receptor protein. *Annu. Rev. Biochem.* 62, 749–797.
- Kong, Y., Wang, Z., Chen, J., Pan, X.-T. T., Liu, D.-T. T., Zhang, E.-J. J., et al. (2009). Effects of ethephon on aerenchyma formation in rice roots. *Rice Sci.* 16, 210–216. doi:10.1016/S1672-6308(08)60081-5.
- Koo, H. M., Song, S. H., Pyun, Y. R., and Kim, Y. S. (1998). Evidence that a beta-1,4-endoglucanase secreted by *Acetobacter xylinum* plays an essential role for the formation of cellulose fiber. *Biosci. Biotechnol. Biochem.* 62, 2257–2259. doi:10.1271/bbb.62.2257.
- Körner, H., Sofia, H. J., and Zumft, W. G. (2003). Phylogeny of the bacterial superfamily of CRP-FNR transcription regulators: exploiting the metabolic spectrum by controlling alternative gene programs. *FEMS Microbiol. Rev.* 27, 559–592.
- Kounatidis, I., Crotti, E., Sapountzis, P., Sacchi, L., Rizzi, A., Chouaia, B., et al. (2009). *Acetobacter tropicalis* is a major symbiont of the olive fruit fly (*Bactrocera oleae*). *Appl. Environ. Microbiol.* 75, 3281–3288. doi:10.1128/AEM.02933-08.
- Krogfelt, K. A., Bergmans, H., and Klemm, P. (1990). Direct evidence that the FimH protein is the mannose-specific adhesin of *Escherichia coli* type 1 fimbriae. *Infect. Immun.* 58, 1995–1998.
- Kudlicka, K., and Brown, R. M. (1996). Cellulose biosynthesis in higher plants. *Acta Soc. Bot. Pol.* 65, 17–24. doi:10.1016/S1360-1385(96)80050-1.
- Kumagai, A., Mizuno, M., Kato, N., Nozaki, K., Togawa, E., Yamanaka, S., et al. (2011). Ultrafine cellulose fibers produced by *Asaia bogorensis*, an acetic acid bacterium. *Biomacromolecules* 12, 2815–2821. doi:10.1021/bm2005615.
- Kumar, M., and Turner, S. (2014). Plant cellulose synthesis: CESA proteins crossing kingdoms. *Phytochemistry* 112, 91–99. doi:10.1016/j.phytochem.2014.07.009.
- Lacey, R. F., and Binder, B. M. (2014). How plants sense ethylene gas - The ethylene receptors. *J. Inorg. Biochem.* 133, 58–62. doi:10.1016/j.jinorgbio.2014.01.006.
- Laemmli, U. K. (1970). Cleavage of structural proteins during the assembly of the head

- of bacteriophage T4. *Nature* 227, 680–685.
- Lagoni, O. R., von Meyenburg, K., and Michelsen, O. (1993). Limited differential mRNA inactivation in the *atp (unc)* operon of *Escherichia coli*. *J. Bacteriol.* 175, 5791–5797.
- Lapidot, A., and Yaron, S. (2009). Transfer of *Salmonella enterica* serovar Typhimurium from contaminated irrigation water to parsley is dependent on curli and cellulose, the biofilm matrix components. *J. Food Prot.* 72, 618–623.
- Larsen, P. B., and Chang, C. (2001). The *Arabidopsis eer1* Mutant Has Enhanced Ethylene Responses in the Hypocotyl and Stem. *Plant Physiol.* 125, 1061–1073. Available at: <http://www.ncbi.nlm.nih.gov/pmc/articles/PMC64905/>.
- Lasa, I., and Villanueva, M. (2014). Overlapping transcription and bacterial RNA removal. *Proc. Natl. Acad. Sci.* 111, 2868–2869.
- Laus, M. C., van Brussel, A. A. N., and Kijne, J. W. (2005). Role of cellulose fibrils and exopolysaccharides of *Rhizobium leguminosarum* in attachment to and infection of *Vicia sativa* root hairs. *Mol. Plant. Microbe. Interact.* 18, 533–538. doi:10.1094/MPMI-18-0533.
- Lee, C.-C., Chen, J., and Frank, J. F. (2015). Role of cellulose and colanic acid in attachment of shiga toxin-producing *Escherichia coli* to lettuce and spinach in different water hardness environments. *J. Food Prot.* 78, 1461–1466.
- Lee, J., Jayaraman, A., and Wood, T. K. (2007). Indole is an inter-species biofilm signal mediated by SdiA. *BMC Microbiol.* 7, 42. doi:10.1186/1471-2180-7-42.
- Lee, S., and Kennedy, C. (2000). “Characterization of indole-3-acetic acid (IAA) produced by the sugarcane endophyte *Acetobacter diazotrophicus*, in sugarcane growth,” in *Nitrogen Fixation: From Molecules to Crop Productivity* (Springer), 421.
- Lejeune, A., and Deprez, T. (2010). *Cellulose: Structure and Properties, Derivatives and Industrial Uses*. New York: Nova Science Publishers Available at: <http://books.google.com/books?id=Oq-VQQAACAAJ&pgis=1>.
- Leng, P., Yuan, B., Guo, Y., and Chen, P. (2014). The role of abscisic acid in fruit ripening and responses to abiotic stress. *J. Exp. Bot.*, eru204.
- Leveau, J. H. J., and Gerards, S. (2008). Discovery of a bacterial gene cluster for catabolism of the plant hormone indole 3-acetic acid. *FEMS Microbiol. Ecol.* 65, 238–250. doi:10.1111/j.1574-6941.2008.00436.x.
- Leveau, J. H. J., and Lindow, S. E. (2005). Utilization of the plant hormone indole-3-acetic acid for growth by *Pseudomonas putida* strain 1290. *Appl. Environ. Microbiol.* 71, 2365–2371. doi:10.1128/AEM.71.5.2365.
- Li, C., Hor, L., Chang, Z., Tsai, L., Yang, W., and Yuan, H. S. (2003). DNA binding and cleavage by the periplasmic nuclease Vvn: a novel structure with a known active

- site. *EMBO J.* 22, 4014–4025.
- Li, C., Jia, H., Chai, Y., and Shen, Y. (2011). Abscisic acid perception and signaling transduction in strawberry: A model for non-climacteric fruit ripening. *Plant Signal. Behav.* 6, 1950–1953. doi:10.4161/psb.6.12.18024.
- Li, S., Bashline, L., Lei, L., and Gu, Y. (2014). Cellulose synthesis and its regulation. *Arabidopsis Book* 12, e0169. doi:10.1199/tab.0169.
- Liang, Y., Gao, H., Chen, J., Dong, Y., Wu, L., He, Z., et al. (2010). Pellicle formation in *Shewanella oneidensis*. *BMC Microbiol.* 10, 291.
- Lin, F. C., Brown, R. M., Drake, R. R., and Haley, B. E. (1990). Identification of the uridine 5'-diphosphoglucose (UDP-Glc) binding subunit of cellulose synthase in *Acetobacter xylinum* using the photoaffinity probe 5-azido-UDP-Glc. *J. Biol. Chem.* 265, 4782–4784.
- Lin, S.-Y., Hung, M.-H., Hameed, A., Liu, Y.-C., Hsu, Y.-H., Wen, C.-Z., et al. (2015). *Rhizobium capsici* sp. nov., isolated from root tumor of a green bell pepper (*Capsicum annuum* var. *grossum*) plant. *Antonie Van Leeuwenhoek* 107, 773–784.
- Livak, K. J., and Schmittgen, T. D. (2001). Analysis of relative gene expression data using real-time quantitative PCR and the 2⁻($\Delta\Delta C(T)$) method. *Methods* 25, 402–408. doi:http://dx.doi.org/10.1006/meth.2001.1262.
- Lohani, S., Trivedi, P. K., and Nath, P. (2004). Changes in activities of cell wall hydrolases during ethylene-induced ripening in banana: Effect of 1-MCP, ABA and IAA. *Postharvest Biol. Technol.* 31, 119–126. doi:10.1016/j.postharvbio.2003.08.001.
- Lukowitz, W., Nickle, T. C., Meinke, D. W., Last, R. L., Conklin, P. L., and Somerville, C. R. (2001). *Arabidopsis cyt1* mutants are deficient in a mannose-1-phosphate guanylyltransferase and point to a requirement of N-linked glycosylation for cellulose biosynthesis. *Proc. Natl. Acad. Sci.* 98, 2262–2267.
- Lynch, M. F., Tauxe, R. V., and Hedberg, C. W. (2009). The growing burden of foodborne outbreaks due to contaminated fresh produce: risks and opportunities. *Epidemiol. Infect.* 137, 307–315.
- Ma, B., Cui, M.-L., Sun, H.-J., Takada, K., Mori, H., Kamada, H., et al. (2006). Subcellular localization and membrane topology of the melon ethylene receptor CmERS1. *Plant Physiol.* 141, 587–597.
- Macarisin, D., Patel, J., Bauchan, G., Giron, J. A., and Sharma, V. K. (2012). Role of curli and cellulose expression in adherence of *Escherichia coli* O157:H7 to spinach leaves. *Foodborne Pathog. Dis.* 9, 160–167. doi:10.1089/fpd.2011.1020.
- Mamlouk, D., and Gullo, M. (2013). Acetic acid bacteria: physiology and carbon sources oxidation. *Indian J. Microbiol.* 53, 377–384. doi:10.1007/s12088-013-0414-z.
- Manageiro, V., Ferreira, E., Pinto, M., Fonseca, F., Ferreira, M., Bonnet, R., et al. (2015).

- Two novel CMY-2-type β -lactamases encountered in clinical *Escherichia coli* isolates. *Ann. Clin. Microbiol. Antimicrob.* 14, 12.
- Marchler-Bauer, A., Anderson, J. B., Cherukuri, P. F., DeWeese-Scott, C., Geer, L. Y., Gwadz, M., et al. (2005). CDD: A Conserved Domain Database for protein classification. *Nucleic Acids Res.* 33, D192–D196. doi:10.1093/nar/gki069.
- Martino, P. Di, Fursy, R., Bret, L., Sundararaju, B., and Phillips, R. S. (2003). Indole can act as an extracellular signal to regulate biofilm formation of *Escherichia coli* and other indole-producing bacteria. *Can. J. Microbiol.* 49, 443–449. doi:10.1139/W03-056.
- Matsui, M., Tomita, M., and Kanai, A. (2013). Comprehensive computational analysis of bacterial CRP/FNR superfamily and its target motifs reveals stepwise evolution of transcriptional networks. *Genome Biol. Evol.* 5, 267–282.
- Matthysse, A. G., Holmes, K. V., and Gurlitz, R. H. G. (1981). Elaboration of cellulose fibrils by *Agrobacterium tumefaciens* during attachment to carrot cells. *J. Bacteriol.* 145, 583–595.
- Matthysse, A., White, S., and Lightfoot, R. (1995). Genes required for cellulose synthesis in *Agrobacterium tumefaciens*. *J. Bacteriol.* 177, 1069–1075. Available at: <http://jb.asm.org/content/177/4/1069.short>.
- McAtee, P., Karim, S., Schaffer, R., and David, K. (2013). A dynamic interplay between phytohormones is required for fruit development, maturation, and ripening. *Front. Plant Sci.* 4, 79. doi:10.3389/fpls.2013.00079.
- McCarthy, J. E. G., Gerstel, B., Surin, B., Wiedemann, U., and Ziemke, P. (1991). Differential gene expression from the *Escherichia coli atp* operon mediated by segmental differences in mRNA stability. *Mol. Microbiol.* 5, 2447–2458.
- McManus, J. B., Deng, Y., Nagachar, N., Kao, T., and Tien, M. (2016). AcsA–AcsB: The core of the cellulose synthase complex from *Gluconacetobacter hansenii* ATCC23769. *Enzyme Microb. Technol.* 82, 58–65.
- Mikulits, W., Pradet-Balade, B., Habermann, B., Beug, H., Garcia-Sanz, J. A., and Mullner, E. W. (2000). Isolation of translationally controlled mRNAs by differential screening. *FASEB J.* 14, 1641–1652.
- Minsky, A., Summers, R. G., and Knowles, J. R. (1986). Secretion of beta-lactamase into the periplasm of *Escherichia coli*: evidence for a distinct release step associated with a conformational change. *Proc. Natl. Acad. Sci.* 83, 4180–4184.
- Mitchell, P. (1961). Approaches to the analysis of specific membrane transport. *Biol. Struct. Funct.* 2, 581–599.
- Mohr, P. G., and Cahill, D. M. (2003). Abscisic acid influences the susceptibility of *Arabidopsis thaliana* to *Pseudomonas syringae* pv. tomato and *Peronospora parasitica*. *Funct. Plant Biol.* 30, 461–469. doi:10.1071/FP02231.

- Møller, T., Franch, T., Udesen, C., Gerdes, K., and Valentin-Hansen, P. (2002). Spot 42 RNA mediates discoordinate expression of the *E. coli* galactose operon. *Genes Dev.* 16, 1696–1706.
- Montalvo, E., Adame, Y., García, H. S., Tovar, B., and Mata, M. (2009). Changes of sugars, β -carotene and firmness of refrigerated *Ataulfo* mangoes treated with exogenous ethylene. *J. Agric. Sci.* 147, 193. doi:10.1017/S0021859608008320.
- Morgan, J. L. W., McNamara, J. T., and Zimmer, J. (2014). Mechanism of activation of bacterial cellulose synthase by cyclic di-GMP. *Nat. Struct. Mol. Biol.* 21, 489–96. doi:10.1038/nsmb.2803.
- Morgan, J. L. W., Strumillo, J., and Zimmer, J. (2013). Crystallographic snapshot of cellulose synthesis and membrane translocation. *Nature* 493, 181–6. doi:10.1038/nature11744.
- Morita, N., Takagi, M., and Murao, S. (1979). A new gel-forming polysaccharide produced by *Bacillus subtilis* FT-3 its structure and its physical and chemical characteristics. *Bull. Univ. Osaka Prefect. Ser. B* 31, 27–41.
- Moussatche, P., and Klee, H. J. (2004). Autophosphorylation activity of the *Arabidopsis* ethylene receptor multigene family. *J. Biol. Chem.* 279, 48734–48741.
- Nakai, T., Nishiyama, Y., Kuga, S., Sugano, Y., and Shoda, M. (2002). *ORF2* gene involves in the construction of high-order structure of bacterial cellulose. *Biochem. Biophys. Res. Commun.* 295, 458–462. doi:10.1016/S0006-291X(02)00696-4.
- Nakai, T., Sugano, Y., Shoda, M., Sakakibara, H., Oiwa, K., Tuzi, S., et al. (2013). Formation of highly twisted ribbons in a carboxymethylcellulase gene-disrupted strain of a cellulose-producing bacterium. *J. Bacteriol.* 195, 958–964. doi:10.1128/JB.01473-12.
- Neera, Ramana, K. V., and Batra, H. V. (2015). Occurrence of cellulose-producing *Gluconacetobacter* spp. in fruit samples and kombucha tea, and production of the biopolymer. *Appl. Biochem. Biotechnol.* 176, 1162–1173. doi:10.1007/s12010-015-1637-8.
- Newbury, S. F., Smith, N. H., and Higgins, C. F. (1987). Differential mRNA stability controls relative gene expression within a polycistronic operon. *Cell* 51, 1131–1143.
- Nicol, F., His, I., Jauneau, A., Vernhettes, S., Canut, H., and Höfte, H. (1998). A plasma membrane-bound putative endo-1, 4- β -D-glucanase is required for normal wall assembly and cell elongation in *Arabidopsis*. *EMBO J.* 17, 5563–5576.
- Niemira, B. A., and Zhang, H. Q. (2009). “Advanced technologies for detection and elimination of pathogens,” in *The Produce Contamination Problem* (Academic Press), 425–443. doi:10.1016/B978-0-12-374186-8.00017-3.
- Nilsson, P., Naureckiene, S., and Uhlin, B. E. (1996). Mutations affecting mRNA processing and fimbrial biogenesis in the *Escherichia coli* *pap* operon. *J. Bacteriol.*

178, 683–690.

- Nobles, D. R., and Brown, R. M. (2004). The pivotal role of cyanobacteria in the evolution of cellulose synthases and cellulose synthase-like proteins. *Cellulose* 11, 437–448. doi:10.1023/B:CELL.0000046339.48003.0e.
- Nobles, D. R., and Brown, R. M. (2008). Transgenic expression of *Gluconacetobacter xylinus* strain ATCC 53582 cellulose synthase genes in the cyanobacterium *Synechococcus leopoliensis* strain UTCC 100. *Cellulose* 15, 691–701. doi:10.1007/s10570-008-9217-5.
- Nobles, D. R., Romanovicz, D. K., and Brown, R. M. (2001). Cellulose in cyanobacteria. Origin of vascular plant cellulose synthase? *Plant Physiol.* 127, 529–542. doi:10.1104/pp.010557.
- Nothaft, H., and Szymanski, C. M. (2013). Bacterial protein N-glycosylation: new perspectives and applications. *J. Biol. Chem.* 288, 6912–6920.
- Nwodo, U. U., Green, E., and Okoh, A. I. (2012). Bacterial exopolysaccharides: Functionality and prospects. *Int. J. Mol. Sci.* 13, 14002–14015. doi:10.3390/ijms131114002.
- O’Sullivan, A. (1997). Cellulose: the structure slowly unravels. *Cellulose* 4, 173–207.
- Okano, T., and Sarko, a. (1985). Mercerization of Cellulose, Ii. Alkali-Cellulose Intermediates and a Possible Mercerization Mechanism. *J. Appl. Polym. Sci.* 30, 325–332. doi:10.1002/app.1985.070300128.
- Omadjela, O., Narahari, A., Strumillo, J., Mérida, H., Mazur, O., Bulone, V., et al. (2013). BcsA and BcsB form the catalytically active core of bacterial cellulose synthase sufficient for *in vitro* cellulose synthesis. *Proc. Natl. Acad. Sci. U. S. A.* 110, 17856–61. doi:10.1073/pnas.1314063110.
- Paredez, A. R., Somerville, C. R., and Ehrhardt, D. W. (2006). Visualization of cellulose synthase demonstrates functional association with microtubules. *Science* 312, 1491–1495.
- Park, J. K., Park, Y. H., and Jung, J. Y. (2003). Production of bacterial cellulose by *Gluconacetobacter hansenii* PJK isolated from rotten apple. *Biotechnol. Bioprocess Eng.* 8, 83–88. doi:10.1007/BF02940261.
- Park, Y. B., Lee, C. M., Kafle, K., Park, S., Cosgrove, D. J., and Kim, S. H. (2014). Effects of plant cell wall matrix polysaccharides on bacterial cellulose structure studied with vibrational sum frequency generation spectroscopy and x-ray diffraction. *Biomacromolecules* 15, 2718–2724.
- Patel, J., and Sharma, M. (2010). Differences in attachment of *Salmonella enterica* serovars to cabbage and lettuce leaves. *Int. J. Food Microbiol.* 139, 41–47. doi:10.1016/j.ijfoodmicro.2010.02.005.
- Paul, V., Pandey, R., and Srivastava, G. C. (2012). The fading distinctions between

- classical patterns of ripening in climacteric and non-climacteric fruit and the ubiquity of ethylene-An overview. *J. Food Sci. Technol.* 49, 1–21. doi:10.1007/s13197-011-0293-4.
- Pech, J. C., Bouzayen, M., and Latché, A. (2008). Climacteric fruit ripening: ethylene-dependent and independent regulation of ripening pathways in melon fruit. *Plant Sci.* 175, 114–120.
- Peiser, G. D., Wang, T.-T., Hoffman, N. E., Yang, S. F., Liu, H., and Walsh, C. T. (1984). Formation of cyanide from carbon 1 of 1-aminocyclopropane-1-carboxylic acid during its conversion to ethylene. *Proc. Natl. Acad. Sci.* 81, 3059–3063.
- Perrig, D., Boiero, M. L., Masciarelli, O. A., Penna, C., Ruiz, O. A., Cassán, F. D., et al. (2007). Plant-growth-promoting compounds produced by two agronomically important strains of *Azospirillum brasilense*, and implications for inoculant formulation. *Appl. Microbiol. Biotechnol.* 75, 1143–1150. doi:10.1007/s00253-007-0909-9.
- Petroni, E. A., and Ielpi, L. (1996). Isolation and nucleotide sequence of the GDP-mannose: cellobiosyl-diphosphopolyrenol alpha-mannosyltransferase gene from *Acetobacter xylinum*. *J. Bacteriol.* 178, 4814–4821.
- Pfaffl, M. W., Tichopad, A., Prgomet, C., and Neuvians, T. P. (2004). Determination of stable housekeeping genes, differentially regulated target genes and sample integrity: BestKeeper - Excel-based tool using pair-wise correlations. *Biotechnol. Lett.* 26, 509–515. doi:10.1023/B:BILE.0000019559.84305.47.
- Phillips, D. A., and Torrey, J. G. (1972). Studies on cytokinin production by *Rhizobium*. *Plant Physiol.* 49, 11–15. doi:10.1104/pp.49.1.11.
- Pillai, S. D., and Jesudhasan, P. R. (2006). Quorum sensing: How bacteria communicate. *Food Technol.* 60, 42–50.
- Prilusky, J., Felder, C. E., Zeev-Ben-Mordehai, T., Rydberg, E. H., Man, O., Beckmann, J. S., et al. (2005). FoldIndex©: a simple tool to predict whether a given protein sequence is intrinsically unfolded. *Bioinformatics* 21, 3435–3438.
- Qi, Y., Rao, F., Luo, Z., and Liang, Z. X. (2009). A flavin cofactor-binding PAS domain regulates c-di-GMP synthesis in AxDGC2 from *Acetobacter xylinum*. *Biochemistry* 48, 10275–10285. doi:10.1021/bi901121w.
- Quivey, R. G., Kuhnert, W. L., and Hahn, K. (2000). Adaptation of oral streptococci to low pH. *Adv. Microb. Physiol.* 42, 239–274. doi:DOI: 10.1016/S0065-2911(00)42004-7.
- Qureshi, O., Sohail, H., Latos, A., and Strap, J. L. (2013). The effect of phytohormones on the growth, cellulose production and pellicle properties of *Gluconacetobacter xylinus* ATCC 53582. *Acetic Acid Bact.* 2, 39–46. doi:10.4081/aab.2013.s1.e7.
- Rangel-Vargas, E., Gómez-Aldapa, C. A., Torres-Vitela, M., Villarruel-López, A.,

- Gordillo-Martínez, A. J., and Castro-Rosas, J. (2015). Presence and correlation of some enteric indicator bacteria, diarrheagenic *Escherichia coli* pathotypes, and *Salmonella* serotypes in alfalfa sprouts from local retail markets in Pachuca, Mexico. *J. Food Prot.* 78, 609–614.
- Rath, A., Glibowicka, M., Nadeau, V. G., Chen, G., and Deber, C. M. (2009). Detergent binding explains anomalous SDS-PAGE migration of membrane proteins. *Proc. Natl. Acad. Sci.* 106, 1760–1765.
- Recouvreux, D. O. S., Carminatti, C. A., Pitlovanciv, A. K., Rambo, C. R., Porto, L. M., and Antônio, R. V. (2008). Cellulose biosynthesis by the *beta*-proteobacterium, *Chromobacterium violaceum*. *Curr. Microbiol.* 57, 469–476. doi:10.1007/s00284-008-9271-0.
- Ren, C., Webster, P., Finkel, S. E., and Tower, J. (2007). Increased internal and external bacterial load during *Drosophila* aging without life-span trade-off. *Cell Metab.* 6, 144–152. doi:10.1016/j.cmet.2007.06.006.
- Richmond, T. A., and Somerville, C. R. (2000). The cellulose synthase superfamily. *Plant Physiol.* 124, 495–498. doi:10.1104/pp.124.2.495.
- Richter, A. M., Povolotsky, T. L., Wieler, L. H., and Hengge, R. (2014). Cyclic-di-GMP signalling and biofilm-related properties of the shiga toxin-producing 2011 German outbreak *Escherichia coli* O104: H4. *EMBO Mol. Med.* 6, 1622 – 1637.
- Robledo, M., Jiménez-Zurdo, J. I., Velázquez, E., Trujillo, M. E., Zurdo-Piñeiro, J. L., Ramírez-Bahena, M. H., et al. (2008). *Rhizobium* cellulase CelC2 is essential for primary symbiotic infection of legume host roots. *Proc. Natl. Acad. Sci. U. S. A.* 105, 7064–7069. doi:10.1073/pnas.0802547105.
- Rodríguez, H., and Fraga, R. (1999). Phosphate solubilizing bacteria and their role in plant growth promotion. *Biotechnol. Adv.* 17, 319–339. doi:10.1016/S0734-9750(99)00014-2.
- Römling, U. (2002). Molecular biology of cellulose production in bacteria. *Res. Microbiol.* 153, 205–212. doi:10.1016/S0923-2508(02)01316-5.
- Römling, U., and Galperin, M. Y. (2015). Bacterial cellulose biosynthesis: diversity of operons, subunits, products, and functions. *Trends Microbiol.* 9, 545–557. doi:10.1016/j.tim.2015.05.005.
- Römling, U., Galperin, M. Y., and Gomelsky, M. (2013). Cyclic di-GMP: the first 25 years of a universal bacterial second messenger. *Microbiol. Mol. Biol. Rev.* 77, 1–52. doi:10.1128/MMBR.00043-12.
- Römling, U., Lünsdorf, H., and Lu, H. (2004). Characterization of cellulose produced by *Salmonella enterica* serovar Typhimurium. *Cellulose* 11, 413–418.
- Ross, P., Mayer, R., and Benziman, M. (1991). Cellulose biosynthesis and function in bacteria. *Microbiol. Rev.* 55, 35–58. doi:10.1016/j.bbalip.2012.08.009.

- Ross, P., Weinhouse, H., Aloni, Y., Michaeli, D., Weinberger-Ohana, P., Mayer, R., et al. (1987). Regulation of cellulose synthesis in *Acetobacter xylinum* by cyclic diguanylic acid. *Nature* 325, 279–281. doi:10.1038/325279a0.
- Rost, B. (1999). Twilight zone of protein sequence alignments. *Protein Eng.* 12, 85–94.
- Ryjenkov, D. A., Simm, R., Römling, U., and Gomelsky, M. (2006). The PilZ domain is a receptor for the second messenger c-di-GMP: The PilZ domain protein YcgR controls motility in enterobacteria. *J. Biol. Chem.* 281, 30310–30314. doi:10.1074/jbc.C600179200.
- Ryu, J., and Beuchat, L. R. (2005). Biofilm formation by *Escherichia coli* O157 : H7 on stainless steel: Effect of exopolysaccharide and curli production on its resistance to chlorine. *Appl. Environ. Microbiol.* 71, 247–254. doi:10.1128/AEM.71.1.247.
- Ryu, J.-H., Kim, S.-H., Lee, H.-Y., Bai, J. Y., Nam, Y.-D., Bae, J.-W., et al. (2008). Innate immune homeostasis by the homeobox gene caudal and commensal-gut mutualism in *Drosophila*. *Science* 319, 777–782. doi:10.1126/science.1149357.
- Sabag-Daigle, A., Soares, J. A., Smith, J. N., Elmasry, M. E., and Ahmer, B. M. M. (2012). The acyl homoserine lactone receptor, SdiA, of *Escherichia coli* and *Salmonella enterica* serovar Typhimurium does not respond to indole. *Appl. Environ. Microbiol.* 78, 5424–5431. doi:10.1128/AEM.00046-12.
- Sakai, H., Hua, J., Chen, Q. G., Chang, C., Medrano, L. J., Bleecker, A. B., et al. (1998). ETR2 is an ETR1-like gene involved in ethylene signaling in *Arabidopsis*. *Proc. Natl. Acad. Sci.* 95, 5812–5817.
- Salazar, J. K., Wu, Z., Yang, W., Freitag, N. E., Tortorello, M. L., Wang, H., et al. (2013). Roles of a novel Crp/Fnr family transcription factor Lmo0753 in soil survival, biofilm production and surface attachment to fresh produce of *Listeria monocytogenes*. *PLoS One* 8. doi:10.1371/journal.pone.0075736.
- Saldaña, Z., Xicohtencatl-Cortes, J., Avelino, F., Phillips, A. D., Kaper, J. B., Puente, J. L., et al. (2009). Synergistic role of curli and cellulose in cell adherence and biofilm formation of attaching and effacing *Escherichia coli* and identification of Fis as a negative regulator of curli. *Environ. Microbiol.* 11, 992–1006. doi:10.1111/j.1462-2920.2008.01824.x.
- Saravolac, E. G., Taylor, N. F., Benz, R., and Hancock, R. E. (1991). Purification of glucose-inducible outer membrane protein OprB of *Pseudomonas putida* and reconstitution of glucose-specific pores. *J. Bacteriol.* 173, 4970–4976.
- Sarkar, P., Bosneaga, E., and Auer, M. (2009). Plant cell walls throughout evolution: Towards a molecular understanding of their design principles. *J. Exp. Bot.* 60, 3615–3635. doi:10.1093/jxb/erp245.
- Saxena, I. M., Brown Jr, R. M., Fevre, M., Geremia, R. A., and Henrissat, B. (1995). Multidomain architecture of beta-glycosyl transferases: implications for mechanism of action. *J. Bacteriol.* 177, 1419.

- Saxena, I. M., Kudlicka, K., Okuda, K., and Brown, R. M. (1994). Characterization of genes in the cellulose-synthesizing operon (*acs* operon) of *Acetobacter xylinum*: Implications for cellulose crystallization. *J. Bacteriol.* 176, 5735–5752.
- Saxena, I. M., Lin, F. C., and Brown, R. M. (1990). Cloning and sequencing of the cellulose synthase catalytic subunit gene of *Acetobacter xylinum*. *Plant Mol. Biol.* 15, 673–683.
- Schaller, G. E. (2012). Ethylene and the regulation of plant development. *BMC Biol.* 10, 9.
- Schaller, G. E., Kieber, J. J., and Shiu, S.-H. (2008). Two-component signaling elements and histidyl-aspartyl phosphorelays. *Arab. Book/American Soc. Plant Biol.* 6.
- Schleifer, K. H., and Kandler, O. (1972). Peptidoglycan types of bacterial cell walls and their taxonomic implications. *Bacteriol. Rev.* 36, 407–477. Available at: <http://www.ncbi.nlm.nih.gov/pmc/articles/PMC408328/>.
- Schneider, C. A., Rasband, W. S., and Eliceiri, K. W. (2012). NIH Image to ImageJ: 25 years of image analysis. *Nat. Methods* 9, 671–675. doi:10.1038/nmeth.2089.
- Schramm, M., and Hestrin, S. (1954). Factors affecting production of cellulose at the air/liquid interface of a culture of *Acetobacter xylinum*. *J. Gen. Microbiol.* 11, 123–129. doi:10.1099/00221287-11-1-123.
- Schreiber, W., and Dürre, P. (2000). Differential expression of genes within the *gap* operon of *Clostridium acetobutylicum*. *Anaerobe* 6, 291–297.
- Serrani, J. C., Sanjuán, R., Ruiz-Rivero, O., Fos, M., and García-Martínez, J. L. (2007). Gibberellin regulation of fruit set and growth in tomato. *Plant Physiol.* 145, 246–257. doi:10.1104/pp.107.098335.
- Sesto, N., Wurtzel, O., Archambaud, C., Sorek, R., and Cossart, P. (2013). The excludon: a new concept in bacterial antisense RNA-mediated gene regulation. *Nat. Rev. Microbiol.* 11, 75–82.
- Sethaphong, L., Haigler, C. H., Kubicki, J. D., Zimmer, J., Bonetta, D., DeBolt, S., et al. (2013). Tertiary model of a plant cellulose synthase. *Proc. Natl. Acad. Sci. U. S. A.* 110, 7512–7517. doi:10.1073/pnas.1301027110.
- Sgroy, V., Cassán, F., Masciarelli, O., Papa, M. F. Del, Lagares, A., and Luna, V. (2009). Isolation and characterization of endophytic plant growth-promoting (PGPB) or stress homeostasis-regulating (PSHB) bacteria associated to the halophyte *Prosopis strombulifera*. *Appl. Microbiol. Biotechnol.* 85, 371–381.
- Shapiro, L. (1993). Polar location of the chemoreceptor complex in the *Escherichia coli* cell. *Science* 259, 1717–1723.
- Shaw, R. K., Lasa, I., García, B. M., Pallen, M. J., Hinton, J. C. D., Berger, C. N., et al. (2011). Cellulose mediates attachment of *Salmonella enterica* serovar Typhimurium to tomatoes. *Environ. Microbiol. Rep.* 3, 569–573. doi:10.1111/j.1758-

2229.2011.00263.x.

- Shepard, W., Soutourina, O., Courtois, E., England, P., Haouz, A., and Martin-Verstraete, I. (2011). Insights into the Rrf2 repressor family - The structure of CymR, the global cysteine regulator of *Bacillus subtilis*. *FEBS J.* 278, 2689–2701. doi:10.1111/j.1742-4658.2011.08195.x.
- Shi, Y., Mowery, R. A., Ashley, J., Hentz, M., Ramirez, A. J., Bilgicer, B., et al. (2012). Abnormal SDS-PAGE migration of cytosolic proteins can identify domains and mechanisms that control surfactant binding. *Protein Sci.* 21, 1197–1209. doi:10.1002/pro.2107.
- Shilton, B. H., Flocco, M. M., Nilsson, M., and Mowbray, S. L. (1996). Conformational changes of three periplasmic receptors for bacterial chemotaxis and transport: the maltose-, glucose/galactose- and ribose-binding proteins. *J. Mol. Biol.* 264, 350–363.
- Shrivastava, R., Basu, B., Godbole, A., Mathew, M. K., Apte, S. K., and Phale, P. S. (2011). Repression of the glucose-inducible outer-membrane protein OprB during utilization of aromatic compounds and organic acids in *Pseudomonas putida* CSV86. *Microbiology* 157, 1531–1540.
- Silver, N., Best, S., Jiang, J., and Thein, S. L. (2006). Selection of housekeeping genes for gene expression studies in human reticulocytes using real-time PCR. *BMC Mol. Biol.* 7, 33. doi:10.1186/1471-2199-7-33.
- Simm, R., Morr, M., Kader, A., Nimtz, M., and Römling, U. (2004). GGDEF and EAL domains inversely regulate cyclic di-GMP levels and transition from sessility to motility. *Mol. Microbiol.* 53, 1123–1134. doi:10.1111/j.1365-2958.2004.04206.x.
- Singh, B. R., Agarwal, R., and Chandra, M. (2004). Pathogenic effects of *Salmonella enterica* subspecies enterica serovar Typhimurium on sprouting and growth of maize. *Indian J. Exp. Biol.* 42, 1100–1106.
- Singh, B. R., Chandra, M., and Agarwal, R. (2005). Interaction of *Salmonella enterica* subspecies enterica serovar Typhimurium and mung bean (*Phaseolus aureus*) plants. *J. Food Prot.* 68, 476–481.
- Singh, Z., and Janes, J. (2001). Effects of postharvest application of ethephon on fruit ripening, quality and shelf life of mango under modified atmosphere packaging. *Acta Hortic.* 553, 599–602.
- Siró, I., and Plackett, D. (2010). Microfibrillated cellulose and new nanocomposite materials: A review. *Cellulose* 17, 459–494. doi:10.1007/s10570-010-9405-y.
- Sisler, E. C. (1991). “Ethylene binding components in plants,” in *The plant hormone ethylene*, eds. A. Mattoo and J. Suttle (CRC Press Boca Raton, Florida, USA), 81–99.
- Sitrit, Y., and Bennett, A. B. (1998). Regulation of tomato fruit polygalacturonase mRNA accumulation by ethylene: a re-examination. *Plant Physiol.* 116, 1145–1150.

- Somerville, C. (2006). Cellulose synthesis in higher plants. *Annu. Rev. Cell Dev. Biol.* 22, 53–78. doi:10.1146/annurev.cellbio.22.022206.160206.
- Spaepen, S., and Vanderleyden, J. (2011). Auxin and plant-microbe interactions. *Cold Spring Harb. Perspect. Biol.* 3, 1–13.
- Spiers, A. J., Bohannon, J., Gehrig, S. M., and Rainey, P. B. (2003). Biofilm formation at the air-liquid interface by the *Pseudomonas fluorescens* SBW25 wrinkly spreader requires an acetylated form of cellulose. *Mol. Microbiol.* 50, 15–27. doi:10.1046/j.1365-2958.2003.03670.x.
- Spiers, A. J., and Rainey, P. B. (2005). The *Pseudomonas fluorescens* SBW25 wrinkly spreader biofilm requires attachment factor, cellulose fibre and LPS interactions to maintain strength and integrity. *Microbiology* 151, 2829–2839.
- Standal, R., Iversen, T. G., Coucheron, D. H., Fjaervik, E., Blatny, J. M., and Valla, S. (1994). A new gene required for cellulose production and a gene encoding cellulolytic activity in *Acetobacter xylinum* are colocalized with the *bcs* operon. *J. Bacteriol.* 176, 665–672.
- Stavriniades, J., McCloskey, J. K., and Ochman, H. (2009). Pea aphid as both host and vector for the phytopathogenic bacterium *Pseudomonas syringae*. *Appl. Environ. Microbiol.* 75, 2230–2235. doi:10.1128/AEM.02860-08.
- Stone, B. (2005). *Cellulose: Structure and distribution*. Wiley Online Library doi:10.1038/npg.els.0003892.
- Strap, J. L., Latos, A., Shim, I., and Bonetta, D. T. (2011). Characterization of pellicle inhibition in *Gluconacetobacter xylinus* 53582 by a small molecule, pellicin, identified by a chemical genetics screen. *PLoS One* 6, e28015. doi:10.1371/journal.pone.0028015. doi:10.1371/journal.pone.0028015.
- Sunagawa, N., Fujiwara, T., Yoda, T., Kawano, S., Satoh, Y., Yao, M., et al. (2013). Cellulose complementing factor (Ccp) is a new member of the cellulose synthase complex (terminal complex) in *Acetobacter xylinum*. *J. Biosci. Bioeng.* 115, 607–612. doi:10.1016/j.jbiosc.2012.12.021.
- Symons, G. M., Chua, Y. J., Ross, J. J., Quittenden, L. J., Davies, N. W., and Reid, J. B. (2012). Hormonal changes during non-climacteric ripening in strawberry. *J. Exp. Bot.* 63, 4741–4750.
- Szyjewicz, E., Rosner, N., and Kliewer, W. M. (1984). Ethephon ((2-chloroethyl) phosphonic acid, Ethrel, CEPA) in viticulture—a review. *Am. J. Enol. Vitic.* 35, 117–123.
- Tahara, N., Tonouchi, N., and Yano, H. (1998). Purification and characterization of exo-1, 4-glucosidase from *Acetobacter xylinum* BPR2001. *J. Ferment.* 85, 589–594.
- Tajima, K., Nakajima, K., Yamashita, H., Shiba, T., Munekata, M., and Takai, M. (2001). Cloning and sequencing of the beta-glucosidase gene from *Acetobacter xylinum*

- ATCC 23769. *DNA Res.* 8, 263–269.
- Tal, R., Wong, H. C., Calhoon, R., Gelfand, D., Fear, A. L., Volman, G., et al. (1998). Three *cdg* operons control cellular turnover of cyclic di-GMP in *Acetobacter xylinum*: Genetic organization and occurrence of conserved domains in isoenzymes. *J. Bacteriol.* 180, 4416–4425.
- Taormina, P. J., and Beuchat, L. R. (1999). Comparison of chemical treatments to eliminate enterohemorrhagic *Escherichia coli* O157:H7 on alfalfa seeds. *J. Food Prot.* 62, 318–324.
- Tarutina, M., Ryjenkov, D. A., and Gomelsky, M. (2006). An unorthodox bacteriophytochrome from *Rhodobacter sphaeroides* involved in turnover of the second messenger c-di-GMP. *J. Biol. Chem.* 281, 34751–34758. doi:10.1074/jbc.M604819200.
- Tassoni, A., Watkins, C. B., and Davies, P. J. (2006). Inhibition of the ethylene response by 1-MCP in tomato suggests that polyamines are not involved in delaying ripening, but may moderate the rate of ripening or over-ripening. *J. Exp. Bot.* 57, 3313–3325.
- Taylor, N. G., Howells, R. M., Huttly, A. K., Vickers, K., and Turner, S. R. (2003). Interactions among three distinct CesA proteins essential for cellulose synthesis. *Proc. Natl. Acad. Sci.* 100, 1450–1455.
- Taylor, S., Wakem, M., Dijkman, G., Alsarraj, M., and Nguyen, M. (2010). A practical approach to RT-qPCR-Publishing data that conform to the MIQE guidelines. *Methods* 50, S1–S5. doi:10.1016/j.ymeth.2010.01.005.
- Thaler, J. S., and Bostock, R. M. (2004). Interactions between abscisic-acid-mediated responses and plant resistance to pathogens and insects. *Ecology* 85, 48–58. doi:10.1890/02-0710.
- Thomashow, L. S., Reeves, S., and Thomashow, M. F. (1984). Crown gall oncogenesis: evidence that a T-DNA gene from the *Agrobacterium* Ti plasmid pTiA6 encodes an enzyme that catalyzes synthesis of indoleacetic acid. *Proc. Natl. Acad. Sci. U. S. A.* 81, 5071–5075. doi:10.1073/pnas.81.16.5071.
- Thormann, K. M., Saville, R. M., Shukla, S., and Spormann, A. M. (2005). Induction of rapid detachment in *Shewanella oneidensis* MR-1 biofilms. *J. Bacteriol.* 187, 1014–1021.
- Tolba, I. H., and Soliman, M. A. (2014). Phenotypic and molecular characterization of tumorigenic *Agrobacterium tumefaciens* strains isolated from rose plant in Egypt. *Middle East J.* 3, 1002–1014.
- Toledo, A., Coleman, J. L., Kuhlow, C. J., Crowley, J. T., and Benach, J. L. (2012). The enolase of *Borrelia burgdorferi* is a plasminogen receptor released in outer membrane vesicles. *Infect. Immun.* 80, 359–368.
- Tonouchi, N., Tahara, N., Tsuchida, T., Yoshinaga, F., Beppu, T., and Horinouchi, S.

- (1995). Addition of a small amount of an endoglucanase enhances cellulose production by *Acetobacter xylinum*. *Biosci. Biotechnol. Biochem.* 59, 805–808.
- Trainotti, L., Pavanello, A., and Casadoro, G. (2005). Different ethylene receptors show an increased expression during the ripening of strawberries: does such an increment imply a role for ethylene in the ripening of these non-climacteric fruits? *J. Exp. Bot.* 56, 2037–2046.
- Tremaroli, V., Fedi, S., Tamburini, S., Viti, C., Tatti, E., Ceri, H., et al. (2011). A histidine-kinase *cheA* gene of *Pseudomonas pseudoalcaligenes* KF707 not only has a key role in chemotaxis but also affects biofilm formation and cell metabolism. *Biofouling* 27, 33–46. doi:10.1080/08927014.2010.537099.
- Tsekos, I. (1999). The sites of cellulose synthesis in algae: diversity and evolution of cellulose-synthesizing enzyme complexes. *J. Phycol.* 35, 635–655.
- Tuomi, T., and Rosenqvist, H. (1995). Detection of abscisic, gibberellic and indole-3-acetic acid from plants and microbes. *Plant Physiol Biochem* 33, 725–734.
- Uhlin, K. I., Atalla, R. H., and Thompson, N. S. (1995). Influence of hemicelluloses on the aggregation patterns of bacterial cellulose. *Cellulose* 2, 129–144. doi:10.1007/BF00816385.
- Untergasser, A., Nijveen, H., Rao, X., Bisseling, T., Geurts, R., and Leunissen, J. A. M. (2007). Primer3Plus, an enhanced web interface to Primer3. *Nucleic Acids Res.* 35, W71–74. doi:10.1093/nar/gkm306.
- Uversky, V. N., and Dunker, A. K. (2012). Multiparametric analysis of intrinsically disordered proteins: looking at intrinsic disorder through compound eyes. *Anal. Chem.* 84, 2096–2104.
- Valera, M. J., Laich, F., González, S. S., Torija, M. J., Mateo, E., and Mas, A. (2011). Diversity of acetic acid bacteria present in healthy grapes from the Canary Islands. *Int. J. Food Microbiol.* 151, 105–112. doi:10.1016/j.ijfoodmicro.2011.08.007.
- Vandenbussche, F., and Van Der Straeten, D. (2012). The role of ethylene in plant growth and development. *Annu. Plant Rev. Plant Horm. Ethyl.* 44, 222.
- Vandesompele, J., De Preter, K., Pattyn, F., Poppe, B., Van Roy, N., De Paepe, A., et al. (2002). Accurate normalization of real-time quantitative RT-PCR data by geometric averaging of multiple internal control genes. *Genome Biol.* 3, 1–11. doi:10.1186/gb-2002-3-7-research0034.
- Vellanoweth, R. L. (1993). “Translation and its regulation in Gram-positive bacteria,” in *Bacillus subtilis and Other Gram-positive Bacteria: Physiology, Biochemistry and Molecular Biology*, eds. J. Hoch, R. Losick, and A. Sonenshein (ASM), 699–711.
- Vlamakis, H., Chai, Y., Beaugerard, P., Losick, R., and Kolter, R. (2013). Sticking together: building a biofilm the *Bacillus subtilis* way. *Nat. Rev. Microbiol.* 11, 157–68. doi:10.1038/nrmicro2960.

- Vu, B., Chen, M., Crawford, R. J., and Ivanova, E. P. (2009). Bacterial extracellular polysaccharides involved in biofilm formation. *Molecules* 14, 2535–2554.
- Wang, A. Q., Huang, W. J., Niu, J. Q., Liu, M., Yang, L. T., and Li, Y. R. (2013). Effects of ethephon on key enzymes of sucrose metabolism in relation to sucrose accumulation in sugarcane. *Sugar Tech* 15, 177–186. doi:10.1007/s12355-012-0202-9.
- Wang, W., Esch, J. J., Shiu, S.-H., Agula, H., Binder, B. M., Chang, C., et al. (2006). Identification of important regions for ethylene binding and signaling in the transmembrane domain of the ETR1 ethylene receptor of *Arabidopsis*. *Plant Cell* 18, 3429–3442. doi:10.1105/tpc.106.044537.
- Warner, H. L., and Leopold, A. C. (1969). Ethylene evolution from 2-chloroethylphosphonic acid. *Plant Physiol.* 44, 156–158.
- de Weert, S., Vermeiren, H., Mulders, I. H. M., Kuiper, I., Hendrickx, N., Bloemberg, G. V., et al. (2002). Flagella-driven chemotaxis towards exudate components is an important trait for tomato root colonization by *Pseudomonas fluorescens*. *Mol. Plant. Microbe. Interact.* 15, 1173–1180. doi:10.1094/MPMI.2002.15.11.1173.
- Weingart, H., and Völksch, B. (1997). Ethylene production by *Pseudomonas syringae* pathovars *in vitro* and *in planta*. *Appl. Environ. Microbiol.* 63, 156–161.
- Weinhouse, H., Sapir, S., Amikam, D., Shilo, Y., Volman, G., Ohana, P., et al. (1997). C-di-GMP-binding protein, a new factor regulating cellulose synthesis in *Acetobacter xylinum*. *FEBS Lett.* 416, 207–211. doi:10.1016/S0014-5793(97)01202-7.
- Wellens, A., Garofalo, C., Nguyen, H., Van Gerven, N., Slattegard, R., Hernalsteens, J.-P., et al. (2008). Intervening with urinary tract infections using anti-adhesives based on the crystal structure of the FimH-oligomannose-3 complex. *PLoS One* 3, e2040.
- Wheeler, R. M., Peterson, B. V., and Stutte, G. W. (2004). Ethylene production throughout growth and development of plants. *Hort. Science* 39, 1541–1545.
- Whitney, S. E. C., Brigham, J. E., Darke, A. H., Reid, J. S. G., and Gidley, M. J. (1995). *In vitro* assembly of cellulose/xyloglucan networks: ultrastructural and molecular aspects. *Plant J.* 8, 491–504. doi:10.1046/j.1365-313X.1995.8040491.x.
- Whitney, S. E. C., Brigham, J. E., Darke, A. H., Reid, J. S. G., and Gidley, M. J. (1998). Structural aspects of the interaction of mannan based polysaccharides with bacterial cellulose. *Carbohydr. Res.* 307, 299–309. doi:10.1016/S0008-6215(98)00004-4.
- Williams, W. S., and Cannon, R. E. (1989). Alternative environmental roles for cellulose produced by *Acetobacter xylinum*. *Appl. Environ. Microbiol.* 55, 2448–2452.
- Witebsky, F. G., Maclowry, J. D., and French, S. S. (1979). Broth dilution minimum inhibitory concentrations : Rationale for use of selected antimicrobial concentrations. *J. Clin. Microbiol.* 9, 589–595.
- Won, H. S., Lee, Y. S., Lee, S. H., and Lee, B. J. (2009). Structural overview on the

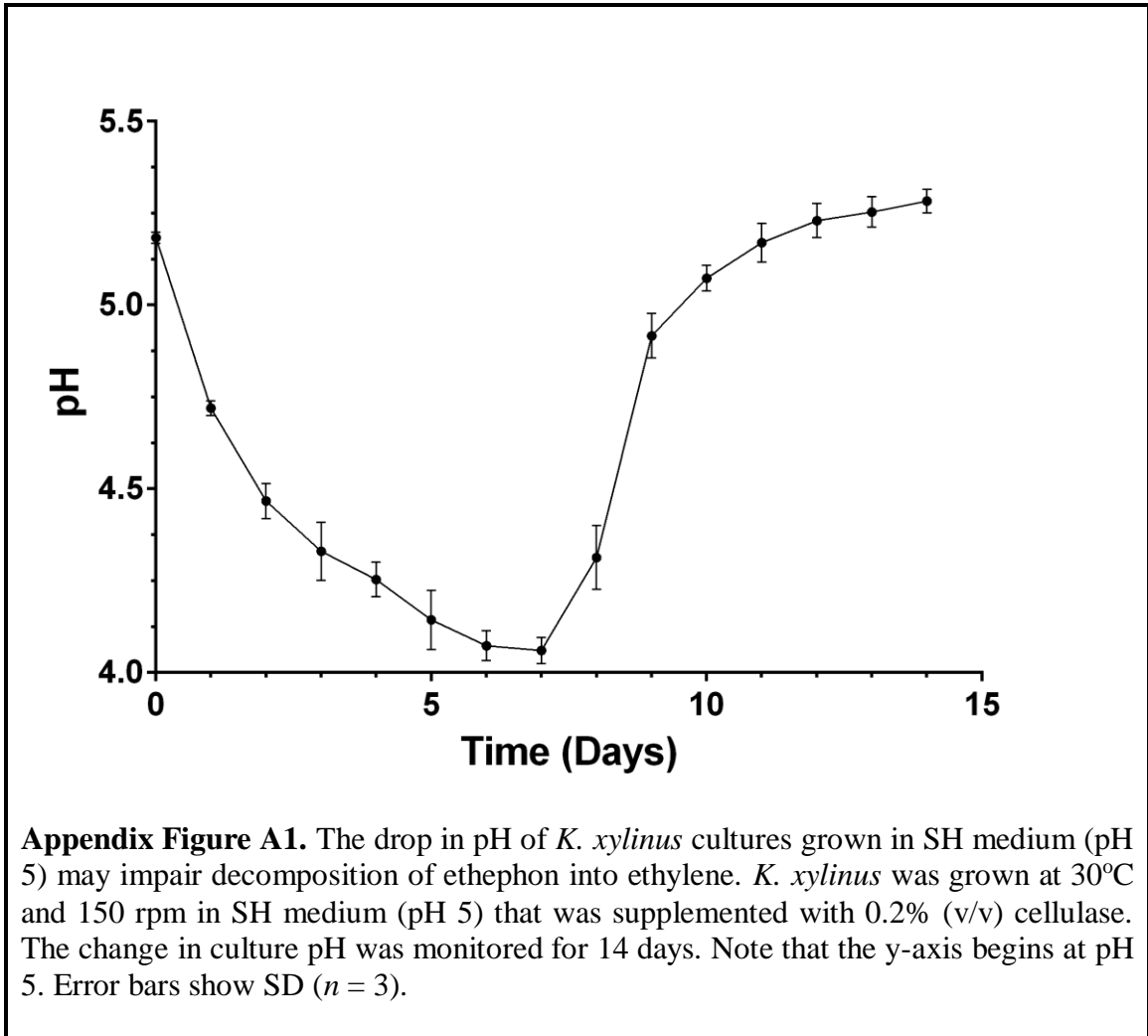
- allosteric activation of cyclic AMP receptor protein. *Biochim. Biophys. Acta (BBA)-Proteins Proteomics* 1794, 1299–1308.
- Wong, H. C., Fear, A. L., Calhoun, R. D., Eichinger, G. H., Mayer, R., Amikam, D., et al. (1990). Genetic organization of the cellulose synthase operon in *Acetobacter xylinum*. *Proc. Natl. Acad. Sci. U. S. A.* 87, 8130–8134. doi:10.1073/pnas.87.20.8130.
- Wylie, J. L., Bernegger-Egli, C., O’Neil, J. D. J., and Worobec, E. A. (1993). Biophysical characterization of OprB, a glucose-inducible porin of *Pseudomonas aeruginosa*. *J. Bioenerg. Biomembr.* 25, 547–556.
- Wylie, J. L., and Worobec, E. A. (1995). The OprB porin plays a central role in carbohydrate uptake in *Pseudomonas aeruginosa*. *J. Bacteriol.* 177, 3021–3026. Available at: <http://www.ncbi.nlm.nih.gov/pmc/articles/PMC176988/>.
- Xie, F., Xiao, P., Chen, D., Xu, L., and Zhang, B. (2012). miRDeepFinder: A miRNA analysis tool for deep sequencing of plant small RNAs. *Plant Mol. Biol.* 80, 75–84. doi:10.1007/s11103-012-9885-2.
- Yamada, Y., Katsura, K., Kawasaki, H., Widyastuti, Y., Saono, S., Seki, T., et al. (2000). *Asaia bogorensis* gen. nov., sp. nov., an unusual acetic acid bacterium in the *alpha-Proteobacteria*. *Int. J. Syst. Evol. Microbiol.* 50, 823–829. doi:10.1099/00207713-50-2-823.
- Yamada, Y., Kuzuyama, T., Komatsu, M., Shin-ya, K., Omura, S., Cane, D. E., et al. (2015). Terpene synthases are widely distributed in bacteria. *Proc. Natl. Acad. Sci.* 112, 857–862.
- Yamada, Y., Yukphan, P., Vu, H. T. L., Muramatsu, Y., Ochaikul, D., Tanasupawat, S., et al. (2012). Description of *Komagataeibacter* gen. nov., with proposals of new combinations (*Acetobacteraceae*). *J. Gen. Appl. Microbiol.* 58, 397–404.
- Yamamoto, H., Horii, F., and Hirai, A. (1996). *In situ* crystallization of bacterial cellulose II. Influences of different polymeric additives on the formation of celluloses Ia and Ib at the early stage of incubation. *Cellulose* 3, 229–242. doi:10.1007/BF02228804.
- Yang, S. F., and Hoffman, N. E. (1984). Ethylene Biosynthesis and its Regulation in Higher Plants. *Annu. Rev. Plant Physiol.* 35, 155–189. doi:10.1146/annurev.pp.35.060184.001103.
- Yaron, S., and Römling, U. (2014). Biofilm formation by enteric pathogens and its role in plant colonization and persistence. *Microb. Biotechnol.* 7, 496–516. doi:10.1111/1751-7915.12186.
- Yasutake, Y., Kawano, S., Tajima, K., Yao, M., Satoh, Y., Munekata, M., et al. (2006). Structural characterization of the *Acetobacter xylinum* endo- β -1,4-glucanase CMCax required for cellulose biosynthesis. *Proteins Struct. Funct. Bioinforma.* 64, 1069–1077.

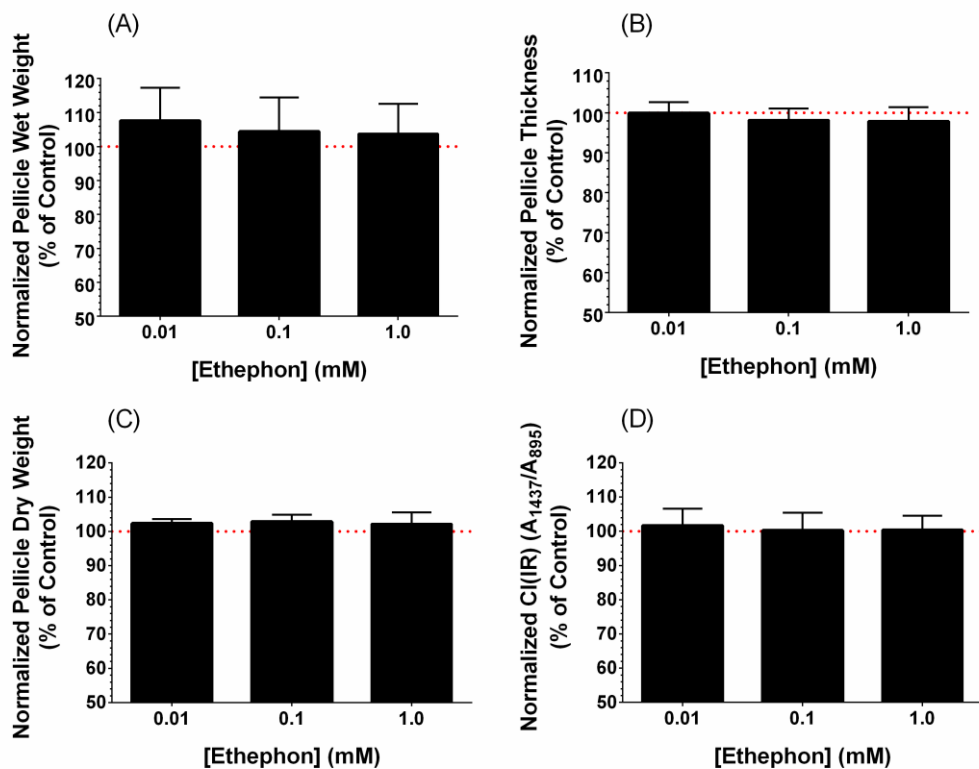
- Yazer, M. H., and Palcic, M. M. (2005). The importance of disordered loops in ABO glycosyltransferases. *Transfus. Med. Rev.* 19, 210–216.
- Yui, T., Ogawa, K., and Sarko, a. (1992). Molecular and crystal structure of konjac glucomannan in the mannan II polymorphic form. *Carbohydr. Res.* 229, 41–55. doi:10.1016/S0008-6215(00)90479-8.
- Zhang, H., Sun, Y., Xie, X., Kim, M. S., Dowd, S. E., and Paré, P. W. (2009a). A soil bacterium regulates plant acquisition of iron via deficiency-inducible mechanisms. *Plant J.* 58, 568–577. doi:10.1111/j.1365-313X.2009.03803.x.
- Zhang, L., Li, S., Liu, X., Song, C., and Liu, X. (2012). Effects of ethephon on physicochemical and quality properties of kiwifruit during ripening. *Postharvest Biol. Technol.* 65, 69–75. doi:10.1016/j.postharvbio.2011.11.004.
- Zhang, M., Yuan, B., and Leng, P. (2009b). The role of ABA in triggering ethylene biosynthesis and ripening of tomato fruit. *J. Exp. Bot.* 60, 1579–1588. doi:10.1093/jxb/erp026.
- Zhang, T., Mahgoudy-Louyeh, S., Tittmann, B., and Cosgrove, D. J. (2014). Visualization of the nanoscale pattern of recently-deposited cellulose microfibrils and matrix materials in never-dried primary walls of the onion epidermis. *Cellulose* 21, 853–862.
- Zhang, W., Hu, W., and Wen, C. K. (2010). Ethylene preparation and its application to physiological experiments. *Plant Signal. Behav.* 5, 453–457.
- Zhang, W., and Wen, C. K. (2010). Preparation of ethylene gas and comparison of ethylene responses induced by ethylene, ACC, and ethephon. *Plant Physiol. Biochem.* 48, 45–53. doi:10.1016/j.plaphy.2009.10.002.
- Zhao, C., Li, Z., Li, T., Zhang, Y., Bryant, D. A., and Zhao, J. (2015). High-yield production of extracellular type-I cellulose by the cyanobacterium *Synechococcus* sp. PCC 7002. *Cell Discov.* 1.
- Zhao, Y. (2010). Auxin biosynthesis and its role in plant development. *Annu. Rev. Plant Biol.* 61, 49–64. doi:10.1146/annurev-arplant-042809-112308.
- Zhong, C., Fei, L., Miao, L., Xiao-Ning, Y., Hui-Xia, Z., Yuan-Yuan, J., et al. (2014). Revealing differences in metabolic flux distributions between a mutant strain and its parent strain *Gluconacetobacter xylinus* CGMCC 2955. *PLoS One* 9. doi:10.1371/journal.pone.0098772.
- Zhong, C., Zhang, G. C., Liu, M., Zheng, X. T., Han, P. P., and Jia, S. R. (2013). Metabolic flux analysis of *Gluconacetobacter xylinus* for bacterial cellulose production. *Appl. Microbiol. Biotechnol.* 97, 6189–6199. doi:10.1007/s00253-013-4908-8.
- Ziemke, P., and McCarthy, J. E. G. (1992). The control of mRNA stability in *Escherichia coli*: manipulation of the degradation pathway of the polycistronic *atp* mRNA.

Biochim. Biophys. Acta (BBA)-Gene Struct. Expr. 1130, 297–306.

- Ziliotto, F., Corso, M., Rizzini, F. M., Rasori, A., Botton, A., and Bonghi, C. (2012). Grape berry ripening delay induced by a pre-véraison NAA treatment is paralleled by a shift in the expression pattern of auxin- and ethylene-related genes. *BMC Plant Biol.* 12, 185. doi:10.1186/1471-2229-12-185.
- Zorn, M., Ihling, C. H., Golbik, R., Sawers, R. G., and Sinz, A. (2014). Mapping cell envelope and periplasm protein interactions of *Escherichia coli* respiratory formate dehydrogenases by chemical cross-linking and mass spectrometry. *J. Proteome Res.* 13, 5524–5535.

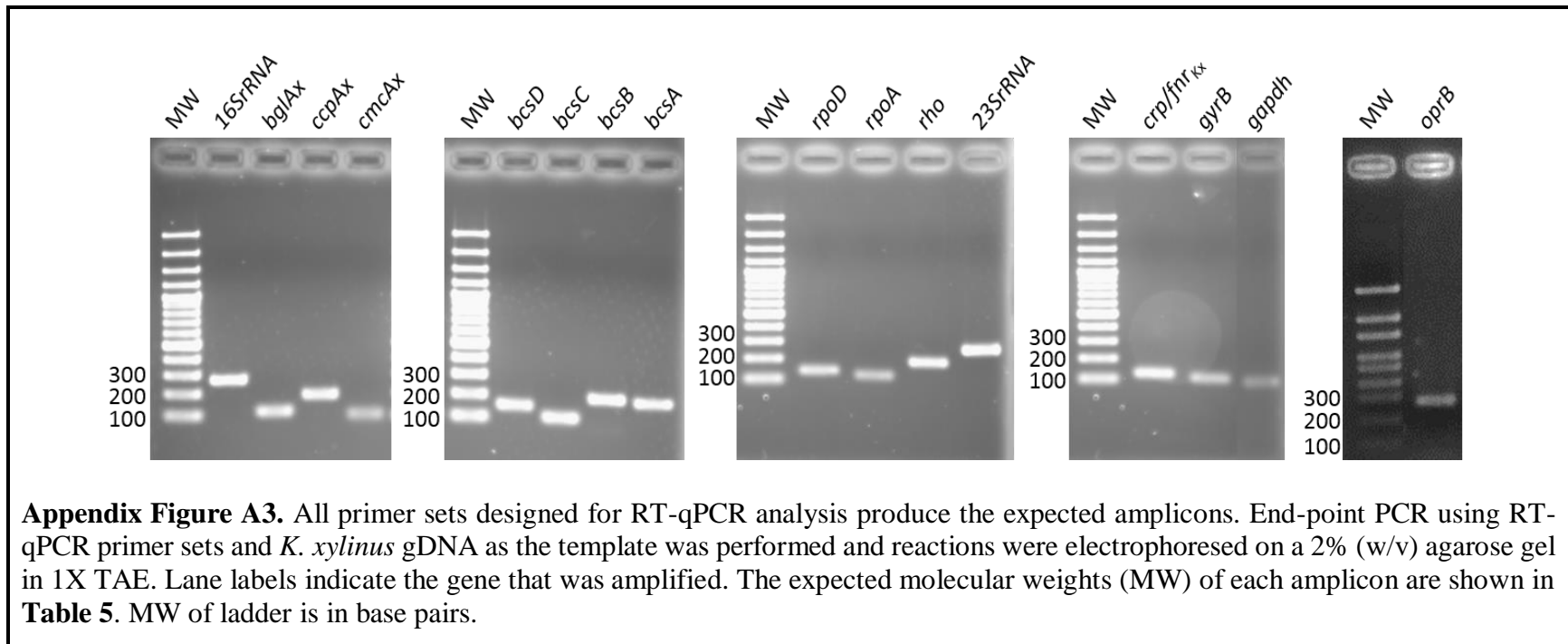
7 APPENDIX





Appendix Figure A2. Ethephon itself does not affect the properties of *K. xylinus* pellicles. *K. xylinus* was cultured in SH medium (pH 5) and grown statically at 30°C for 7 days before pellicles were harvested and analyzed. Ethephon had no effect on the wet weight (A), thickness (B), dry weight (C) or crystallinity of *K. xylinus* pellicles when they are grown in a pH 5 SH medium. Ethephon decomposition was shown to be insignificant in a pH 5 SH medium (**Figure 15**), indicating ethephon itself does not influence these pellicle properties. Data was normalized to and expressed as percent of the untreated control. Note how the y-axis begins at 50%. Error bars show SD ($n = 3$).

All primer sets designed for RT-qPCR analysis of various *K. xylinus* genes (**Table 4**) were tested by end-point PCR to ensure they produced amplicons of the expected size (**Table 5**). PCR samples were electrophoresed on 2% (w/v) agarose gels and showed that all primer sets produced the expected amplicons (**Appendix Figure A3**). This result verified that all primer sets amplify the correct genes and that they could be used for RT-qPCR analysis.

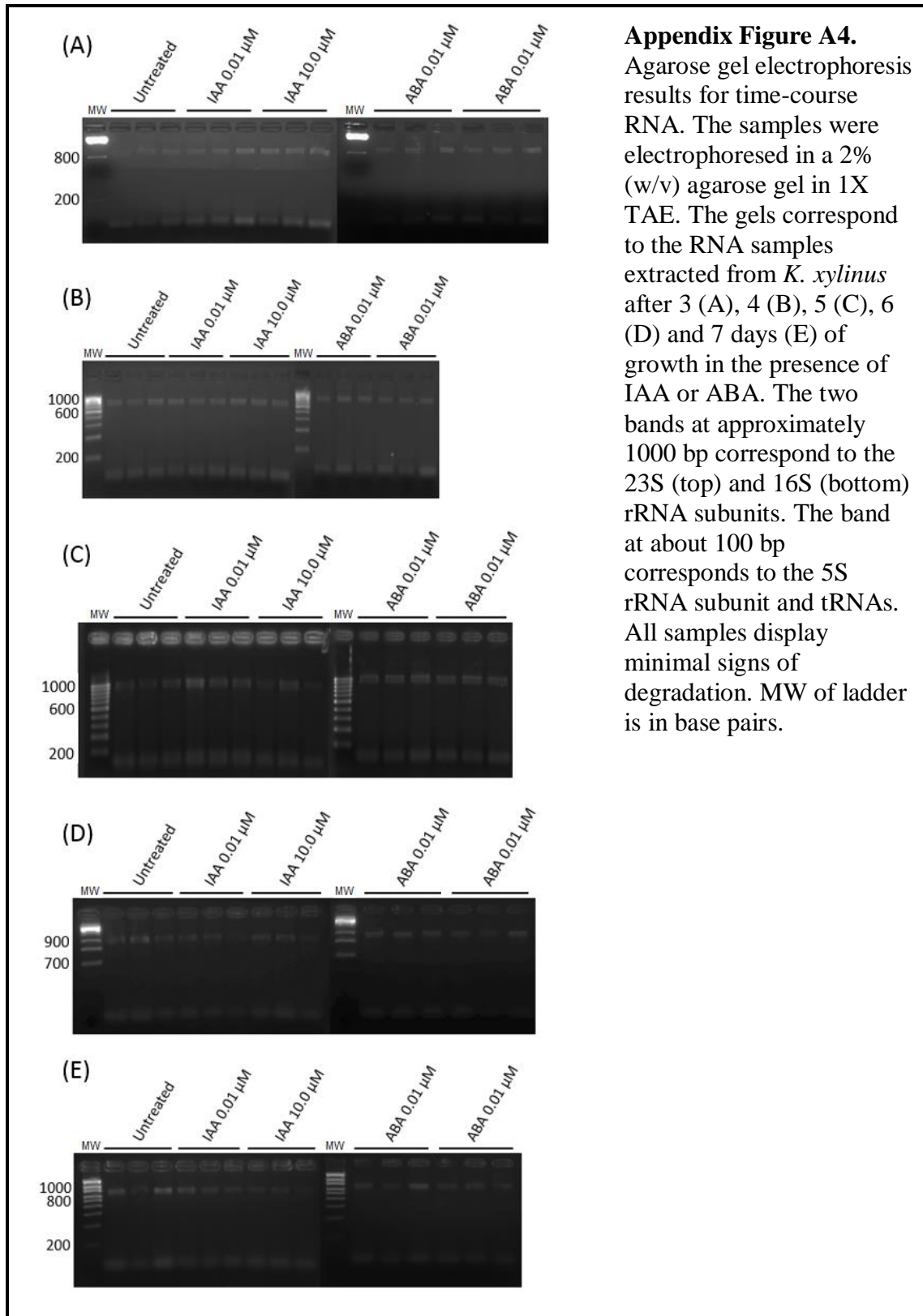


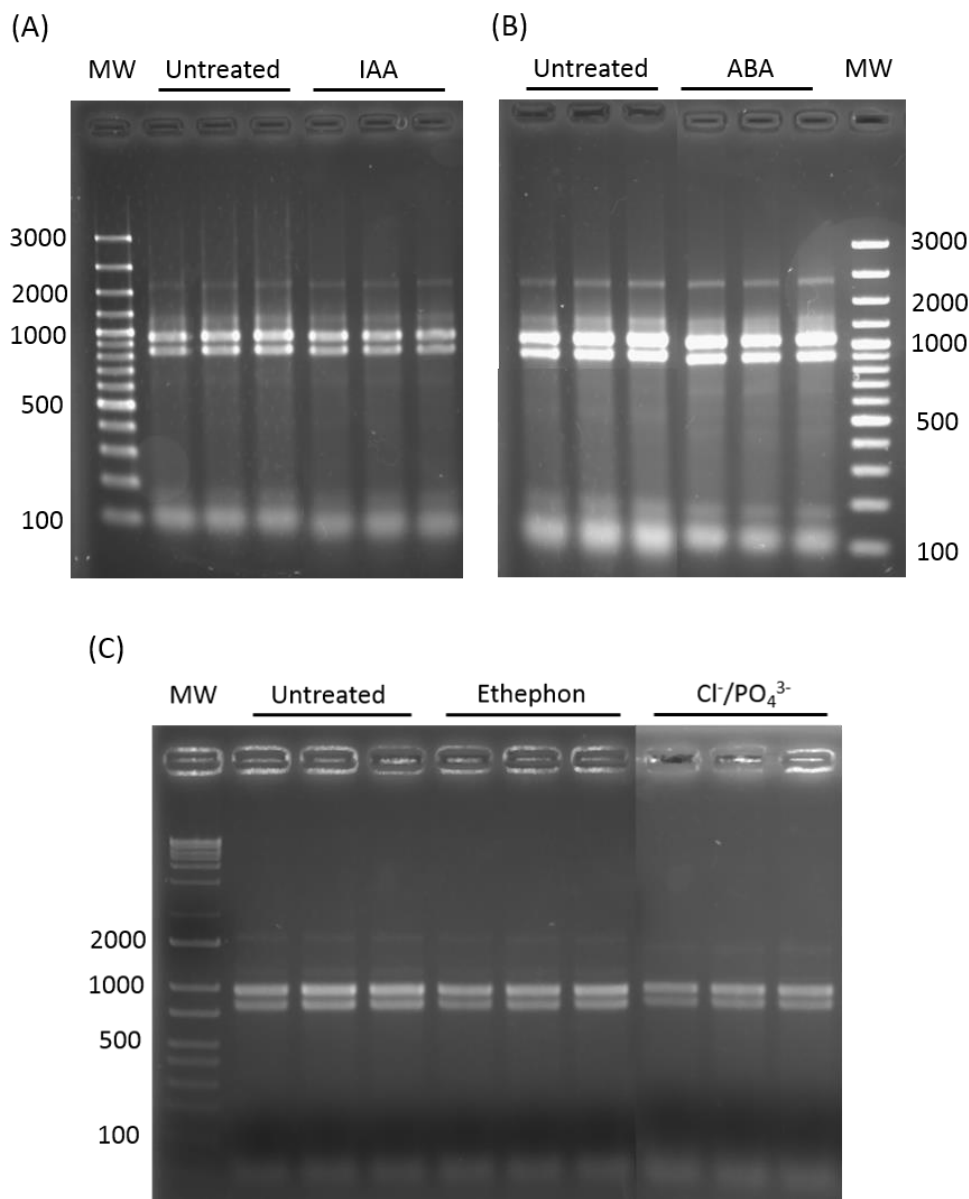
The quality and purity of each RNA sample was assessed using agarose gel electrophoresis and UV-visible spectrophotometry, respectively. Electrophoresis results for the time-course (**Appendix Figure A4**) and pulse (**Appendix Figure A5**) RNA samples show the presence of bands corresponding to the 5S, 16S and 23S rRNA subunits. All RNA samples showed no sign of significant degradation or genomic DNA contamination. However, the RNA samples from the pulse experiment (**Appendix Figure A5**) have much more distinct bands compared to the time-course RNA samples (**Appendix Figure A4**), indicating they contain higher quality RNA. The band above the 23S rRNA band likely corresponds to rRNA traveling as a certain secondary structure that impedes its movement through the agarose gel since it was performed using non-denaturing conditions. UV-visible spectrophotometry showed that all time-course and pulse RNA samples produced A_{260}/A_{280} values of 1.9-2.3 (data not shown), indicating high purity and limited protein contamination. The average A_{260}/A_{280} values were similar for both the time-course and pulse samples, but the average concentration of pulse RNA was significantly higher ($p < 0.001$) and more variable than the time-course RNA (**Appendix Table A1**). Taken together, these results verify that all RNA samples were suitable for cDNA synthesis and RT-qPCR analysis.

Appendix Table A1. Average A_{260}/A_{280} values and RNA concentrations of time-course and pulse RNA samples. Error shown is SD ($n = 75$ for time-course and $n = 21$ for pulse).

Experiment	Average A_{260}/A_{280}	Average [RNA] (ng/μL)¹
Time-course	2.032 \pm 0.008	184 \pm 6.71
Pulse	2.092 \pm 0.093	325 \pm 102

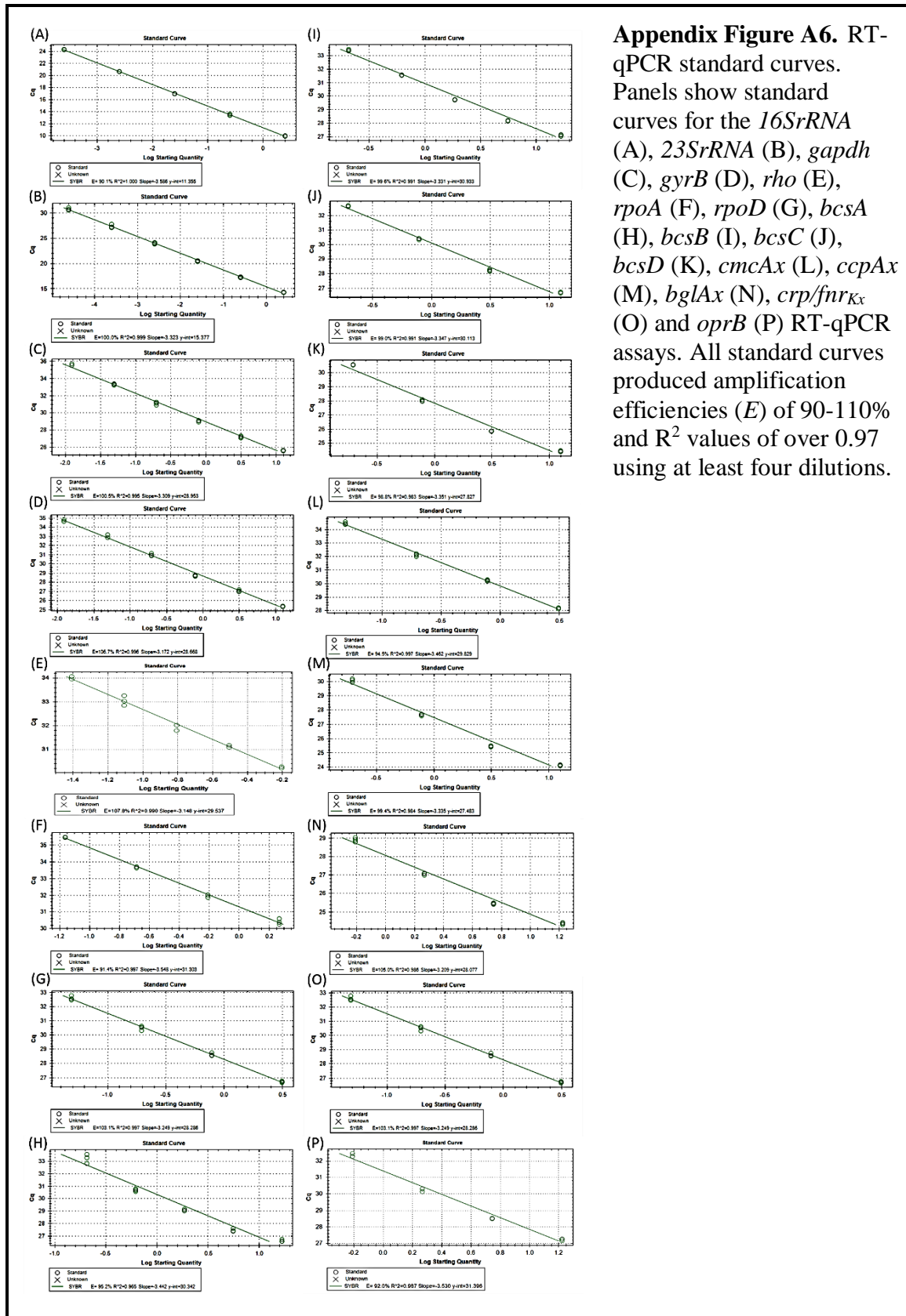
¹ Difference between time-course and pulse average [RNA] is significant ($p < 0.001$) as determined by an unpaired, two-tailed Student's *t*-test.



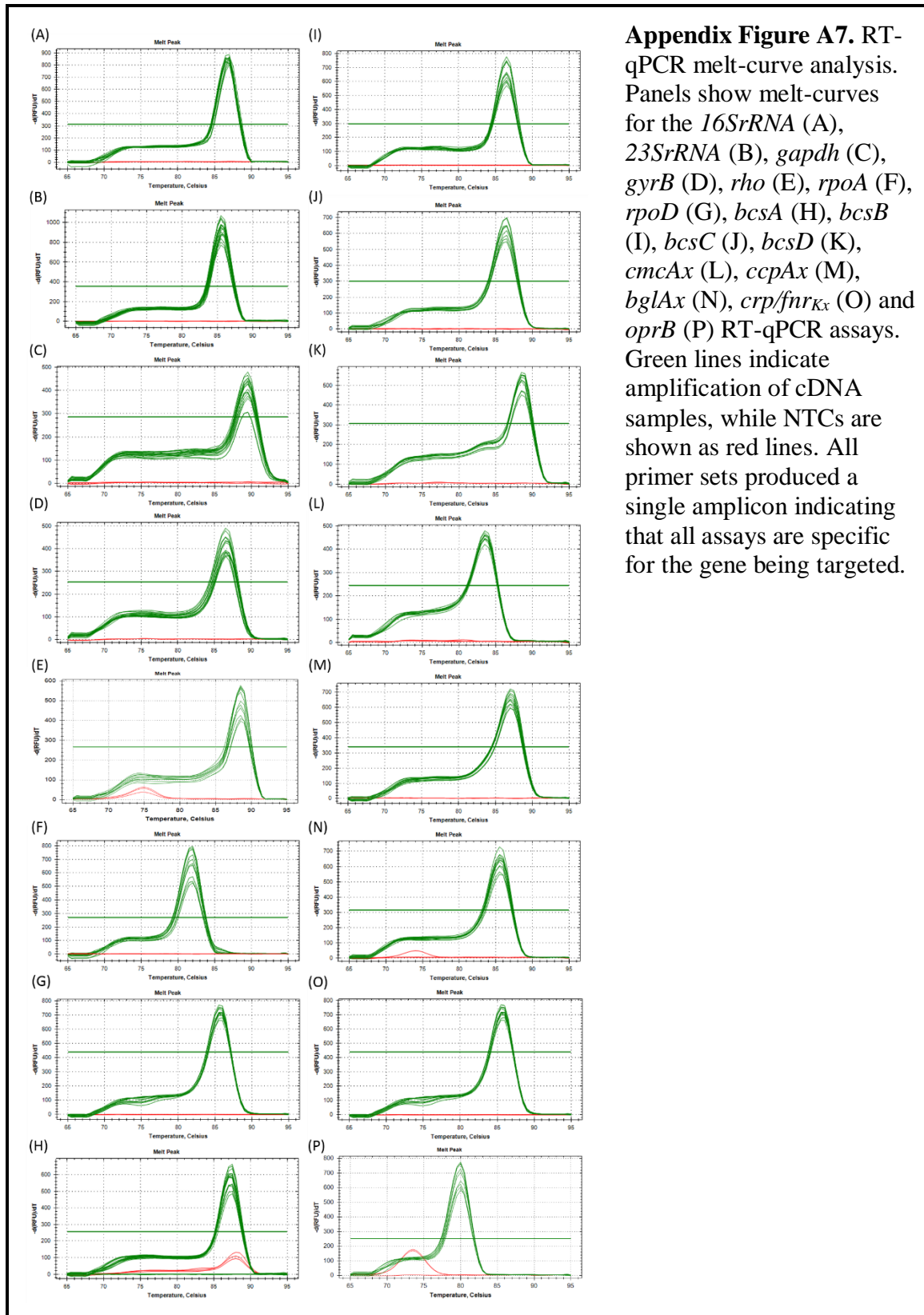


Appendix Figure A5. Pulse experiment RNA. The extracted RNA was electrophoresed on a 2% (w/v) agarose gel in 1X TAE. The gels correspond to RNA samples extracted from *K. xylinus* after 1 hour of growth in the presence of DMSO (untreated) and 10.0 μ M IAA (A), DMSO (untreated) and 10.0 μ M ABA (B), as well as after 24 hours of growth in the presence of acidified (pH 2.5) water (untreated), 10.0 μ M ethephon and 10.0 μ M of phosphate-chloride (C). The two bands that ran at approximately 1000 bp correspond to the 23S (top) and 16S (bottom) rRNA subunits. The band at about 100 bp corresponds to the 5S rRNA subunit and tRNAs. All gels show that the RNA is of extremely high quality. MW of ladder is in base pairs.

Cycling conditions for each RT-qPCR was optimized through the use of annealing temperature gradients, in order to determine the optimal annealing temperature, standard curves, to determine a suitable dilution factor for cDNA samples and to verify the efficiency of each assay, and melt-curves to ensure reaction specificity. Initially, annealing temperature gradients were performed for each primer set. The annealing temperatures that produced the lowest C_t value and a single amplification peak (**Table 6**) were then used for the standard curves. Based on the expression levels of each gene observed during annealing temperature gradients, standard curves utilized particular fold-dilutions (**Table 6**) of pooled cDNA samples. Genes with higher expression levels were subject to a higher fold-dilution and generally had a larger LDR (**Table 6**). For example, the *16SrRNA* and *23SrRNA* genes were expressed significantly higher than any other gene, so a 10X fold-dilution was utilized which produced a large LDR. Highly expressed rRNA genes are expected since they are more highly expressed than mRNA. Lesser expressed genes required a smaller fold-dilution so that the C_t value of the most diluted standard remained under 35 cycles; the generally accepted upper-limit for reliable RT-qPCR data. All primer sets produced an amplification efficiency of 90-110% (**Table 6**) and R^2 values of 0.97-1.0 when the linear dynamic range of template concentrations were analyzed (**Appendix Figure A6**). Each primer set produced a single PCR product as determined by melt-curve analysis, indicating the each RT-qPCR is specific for the target product (**Appendix Figure A7**). The non-pooled cDNA samples were then diluted to within the linear dynamic range of each primer set for the RT-qPCR experiment. The difference in C_t values between the cDNA samples and the no-reverse transcription controls (NRT) was a minimum of 8 C_t indicating the cDNA samples contained insignificant levels gDNA contamination. Furthermore, amplification of the no template controls (NTC) always occurred after 35 cycles indicating the cDNA samples were void of nucleic acid contamination.



Appendix Figure A6. RT-qPCR standard curves. Panels show standard curves for the *16SrRNA* (A), *23SrRNA* (B), *gapdh* (C), *gyrB* (D), *rho* (E), *rpoA* (F), *rpoD* (G), *bcsA* (H), *bcsB* (I), *bcsC* (J), *bcsD* (K), *cmcAx* (L), *ccpAx* (M), *bglAx* (N), *crp/fnr_{Kx}* (O) and *oprB* (P) RT-qPCR assays. All standard curves produced amplification efficiencies (*E*) of 90-110% and *R*² values of over 0.97 using at least four dilutions.



All seven reference genes (**Table 4**) were analyzed in regards to their expression stability at each time point using three different programs; geNorm, NormFinder and RefFinder. These programs employ different algorithms in order to rank reference gene stability. The geNorm algorithm uses a pair-wise comparison approach, NormFinder compares intra- and intergroup variations and RefFinder integrates results from geNorm, NormFinder, BestKeeper and the comparative $\Delta\Delta C_t$ method to provide a comprehensive reference gene stability ranking. The final reference gene selection was decided using the comprehensive stability ranking computed by RefFinder and the number of genes suggested by analysis of geNorm V values. The geNorm M value was also computed for the reference genes selected for data normalization to ensure their M value was below the 0.5 cut-off value suggested for homogenous sample types (Hellemans *et al.*, 2007).

The stability of reference genes was assessed with RT-qPCR using the 3 day time-course cDNA samples. The most stable reference gene as determined by geNorm was *gyrB* (**Appendix Figure A8A**). NormFinder ranked *gapdh* as being most stable reference gene, but ranked *gyrB* as tied for the second most stable (**Appendix Figure A8B**). Both algorithms ranked *rpoD* as the second most stable reference gene. The comprehensive stability value determined by RefFinder ranked *rpoD*, *gyrB* and *gapdh* as the first, second and third most stable genes, respectively (**Appendix Figure A8C**). The least stable genes, in all cases, were *23SrRNA* and *rpoA*. The optimal number of reference genes to use for normalization of the 3 day time-course RT-qPCR data was determined to be two, since the geNorm $V_{2/3}$ value was below 0.15 (**Appendix Figure A8D**). This indicated the inclusion of a third reference gene did not significantly improve data normalization. In all cases, *rpoD* and *gyrB* were ranked in the top three of the most stable genes and were the top two most stable using RefFinder. As such, *rpoD* and *gyrB* were selected to normalize the 3 day time-course RT-qPCR data and had a final geNorm M value of 0.153 (**Appendix Table A2**), which is below the 0.5 cut-off.

Reference gene stability was also assessed for the 4 day time-course RT-qPCR experiment. Both geNorm and NormFinder ranked *gyrB* as the most stably-expressed gene

and classified *rpoD* within the top three most stable genes (**Appendix Figure A9A and Appendix Figure A9B**). Consistently, RefFinder ranked *gyrB* and *rpoD* as the two most stable reference genes (**Appendix Figure A9C**). The least stable genes, in all cases, were *23SrRNA* and *rho*. The geNorm V2/3 value was below 0.15 (**Appendix Figure A9D**), indicating two reference genes were sufficient for effective data normalization. Therefore, *rpoD* and *gyrB* were selected for normalization of the 4 day time-course data and had a final geNorm *M* value of 0.196 (**Appendix Table A2**), which is below the 0.5 cut-off value.

Optimal reference genes were also determined for the 5 day time-course RT-qPCR experiment. Reference gene analysis showed that geNorm (**Appendix Figure A10A**), NormFinder (**Appendix Figure A10B**) and RefFinder (**Appendix Figure A10C**) ranked *gyrB* and *rho* as the most stably-expressed genes and *23SrRNA* as the least stable gene. The geNorm V2/3 was below 0.15 (**Appendix Figure A10D**) so *gyrB* and *rho* were selected to normalize the 5 day time-course RT-qPCR data. This pair of reference genes had a final geNorm *M* value of 0.204 (**Appendix Table A2**), which is below the 0.5 cut-off value.

All three programs ranked *gyrB* and *gapdh* to be the most stable reference genes and *23SrRNA* and *rho* as the least stable genes for the 6 day time-course RT-qPCR experiment (**Appendix Figure A11A, B and C**). The two most stable genes, *gyrB* and *gapdh*, were used to normalize the 6 day RT-qPCR data since the geNorm V2/3 value was below 0.15 (**Appendix Figure A11D**). The final geNorm *M* value for *gyrB* and *gapdh* was calculated to be 0.212 (**Appendix Table A2**) which is below the 0.5 cut-off value.

Reference gene stability was determined for the 7 day time-course RT-qPCR experiment. It was shown that geNorm (**Appendix Figure A12A**), NormFinder (**Appendix Figure A12B**) and RefFinder (**Appendix Figure A12C**) ranked *rpoA*, *gapdh* and *gyrB* as the three most stably-expressed reference genes. All programs ranked *23SrRNA* and *rho* within the three least stable genes. The geNorm V2/3 value was below 0.15 (**Appendix Figure A12D**), so the two most stable genes as determined by RefFinder (*rpoA* and *gapdh*)

were chosen to normalize the 7 day time-course RT-qPCR data. These two genes had a final geNorm M value of 0.249 (**Appendix Table A2**), which is below the 0.5 cut-off value.

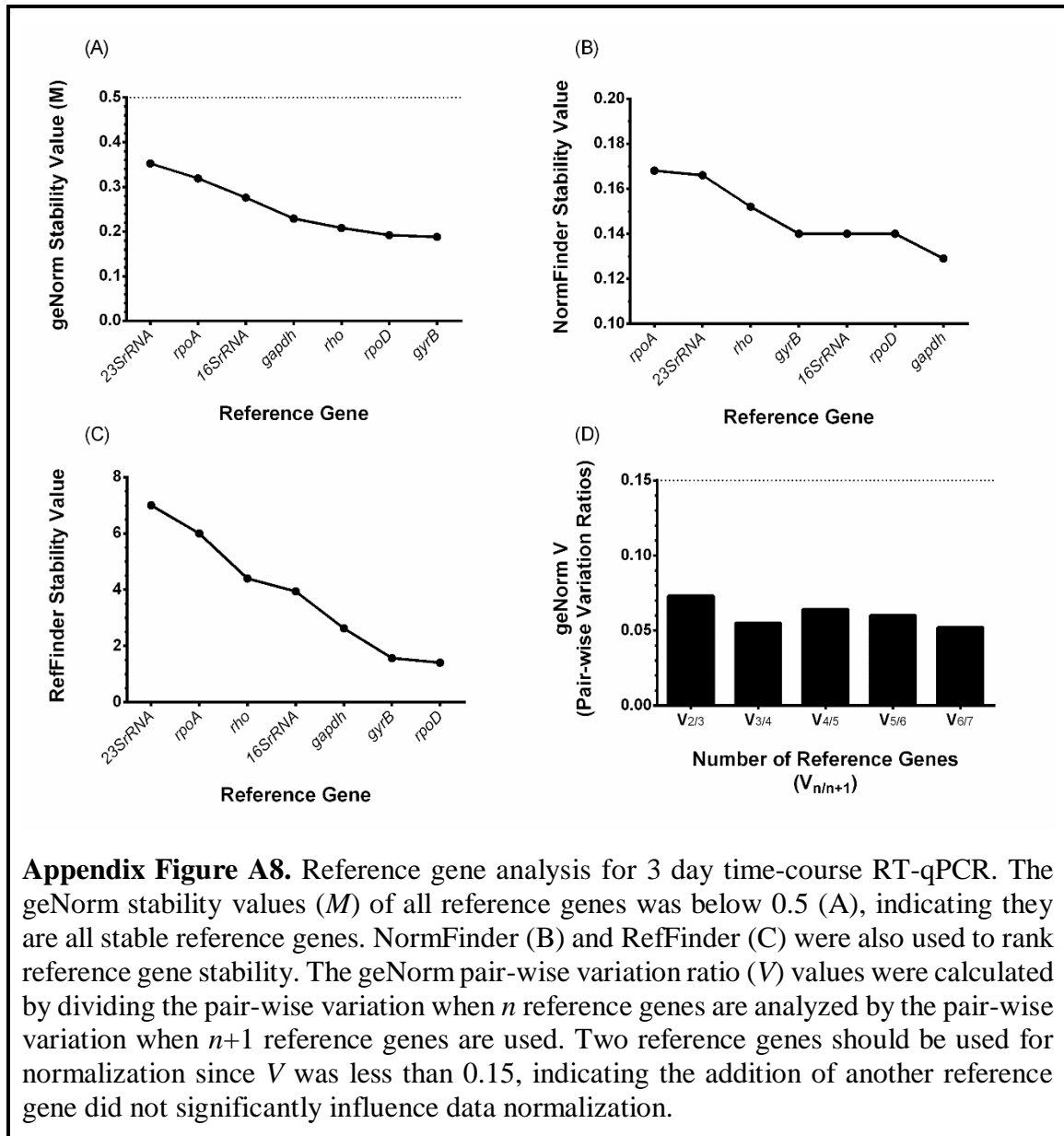
In regards to the IAA pulse experiment, geNorm ranked *16SrRNA* and *23SrRNA* as the two most stable reference genes, but all genes produced stability values well under the 0.5 cut-off (**Appendix Figure A13A**). NormFinder suggested *gyrB* as the most stable gene and *16SrRNA*, *gapdh* and *23SrRNA* as the second most stable genes (**Appendix Figure A13B**). The comprehensive stability ranking as determined by RefFinder indicated *gyrB* was the most stable reference gene, followed by *23SrRNA* (**Appendix Figure A13C**). All programs ranked *rpoD*, *rpoA* and *rho* as the least stable reference genes. The two most stable genes as determined by RefFinder (*gyrB* and *23SrRNA*) were chosen to normalize the IAA pulse RT-qPCR data since the geNorm V2/3 value was below 0.15 (**Appendix Figure A13D**). Reference genes *gyrB* and *23SrRNA* produced a final geNorm M value of 0.099 (**Appendix Table A2**), which is well below the 0.5 cut-off value.

Comparable results were obtained for the ABA pulse RT-qPCR experiment. The geNorm (**Appendix Figure A14A**), NormFinder (**Appendix Figure A14B**) and RefFinder (**Appendix Figure A14C**) algorithms ranked *rpoD*, *gyrB* and *23SrRNA* as the most stable reference genes, although in different orders. All programs ranked *rho*, *16SrRNA* and *rpoA* as the least stable genes. The geNorm V2/3 value was below the 0.15 cut-off value, indicating that only two reference genes were required for effective data normalization (**Appendix Figure A14D**). RefFinder suggested *gyrB* and *23S rRNA* were the most stable genes and were therefore chosen to normalize the ABA pulse RT-qPCR data. These genes produced a final geNorm M value of 0.128, which is below the 0.5 cut-off value.

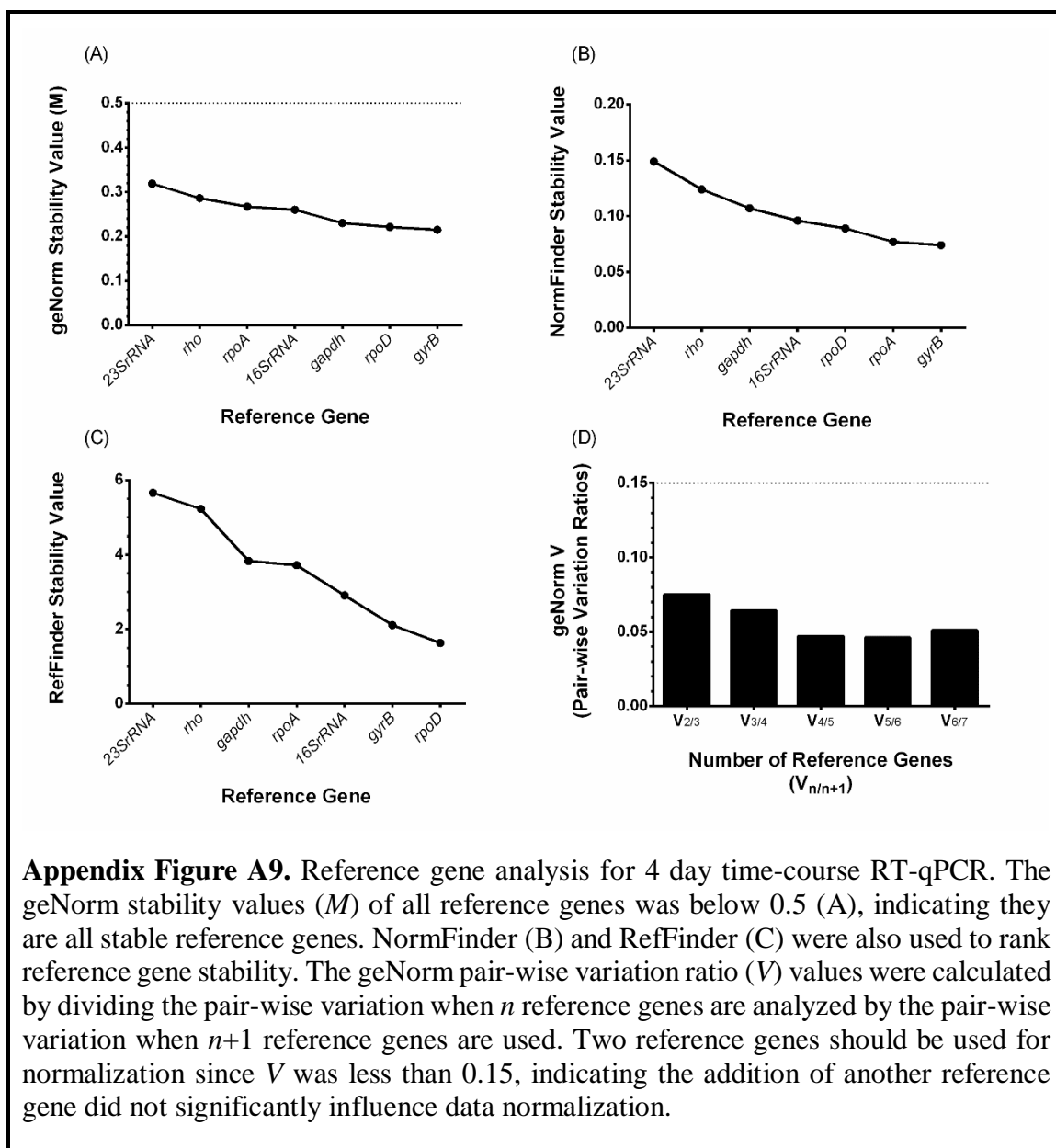
For the ethephon pulse RT-qPCR experiment, all programs ranked *23SrRNA*, *gapdh* and *gyrB* as the most stable reference genes, and *rho* and *16SrRNA* within the three least stable genes (**Appendix Figure A15A, B and C**). The geNorm V2/3 value was below 0.15, indicating the two most stable reference genes should be used for data normalization (**Appendix Figure A15D**). Similar to the IAA and ABA pulse experiment reference gene

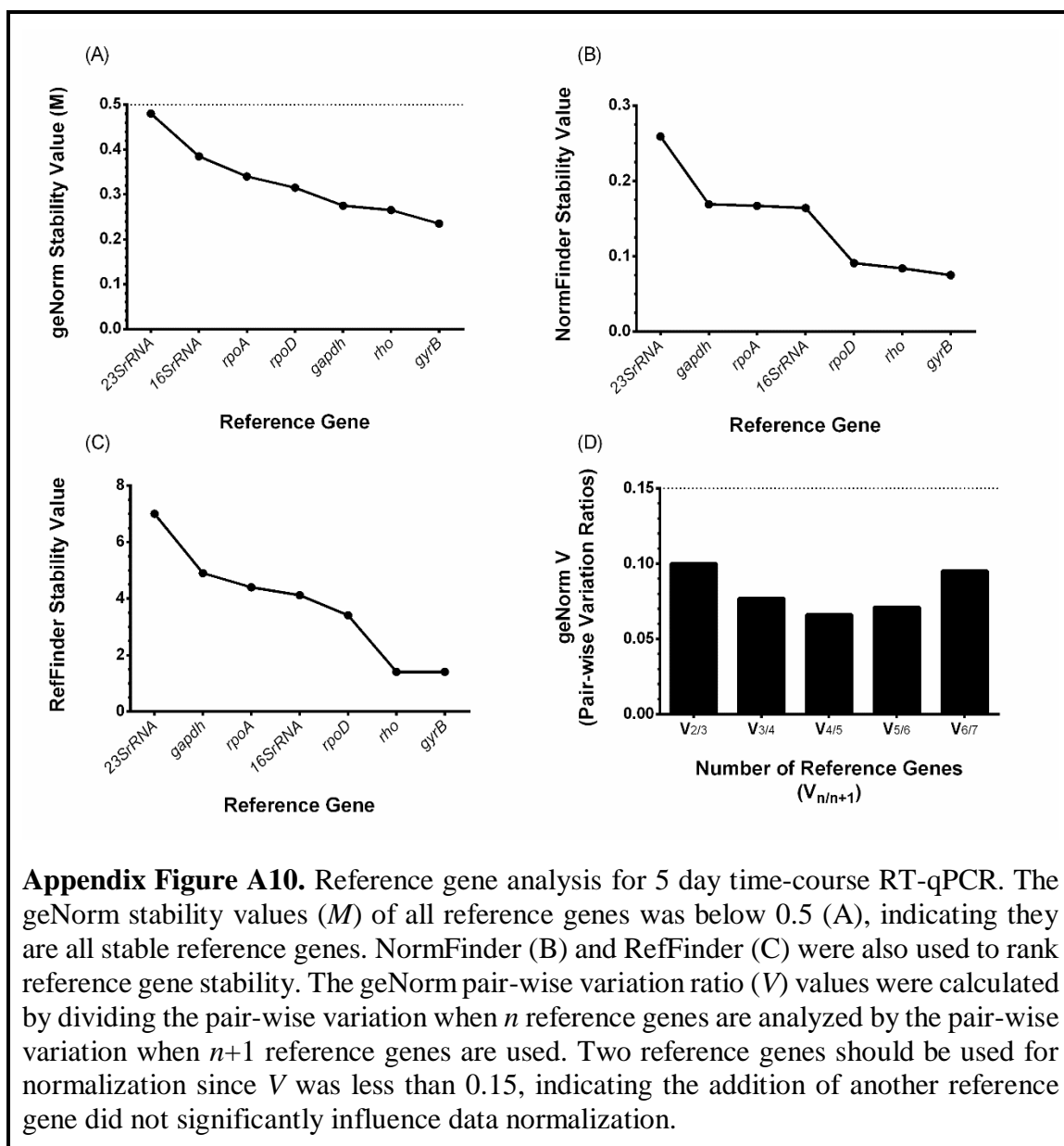
analysis, RefFinder suggested *23SrRNA* and *gyrB* as the two most stable genes. Therefore, *23SrRNA* and *gyrB* were used for normalization of the ethephon pulse RT-qPCR data and produced a final geNorm M value of 0.098, which is well below the 0.5 cut-off value.

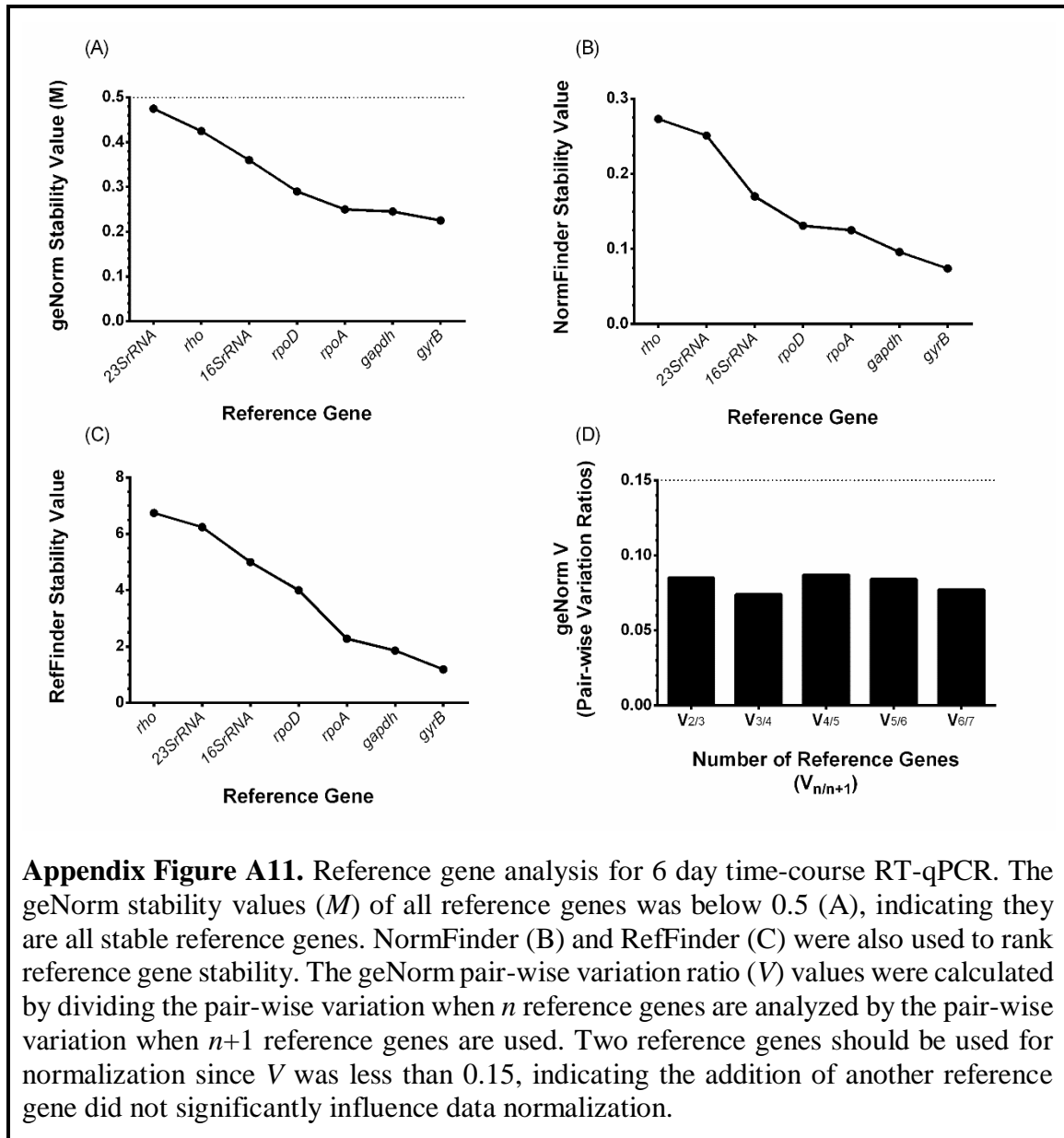
For all experiments, geNorm produced stability values of less than 0.5 for all reference genes, indicating that they were all stable under the tested conditions. Thus, the use of NormFinder and RefFinder allowed for the precise identification of the most stable reference genes using all available algorithms. The overall most stable reference gene was *gyrB* since it was used to normalize 7 out of 8 experiments. Furthermore, *gyrB* was ranked as the third most stable reference gene for the 7 day time-course RT-qPCR; the experiment where it was not used for data normalization.

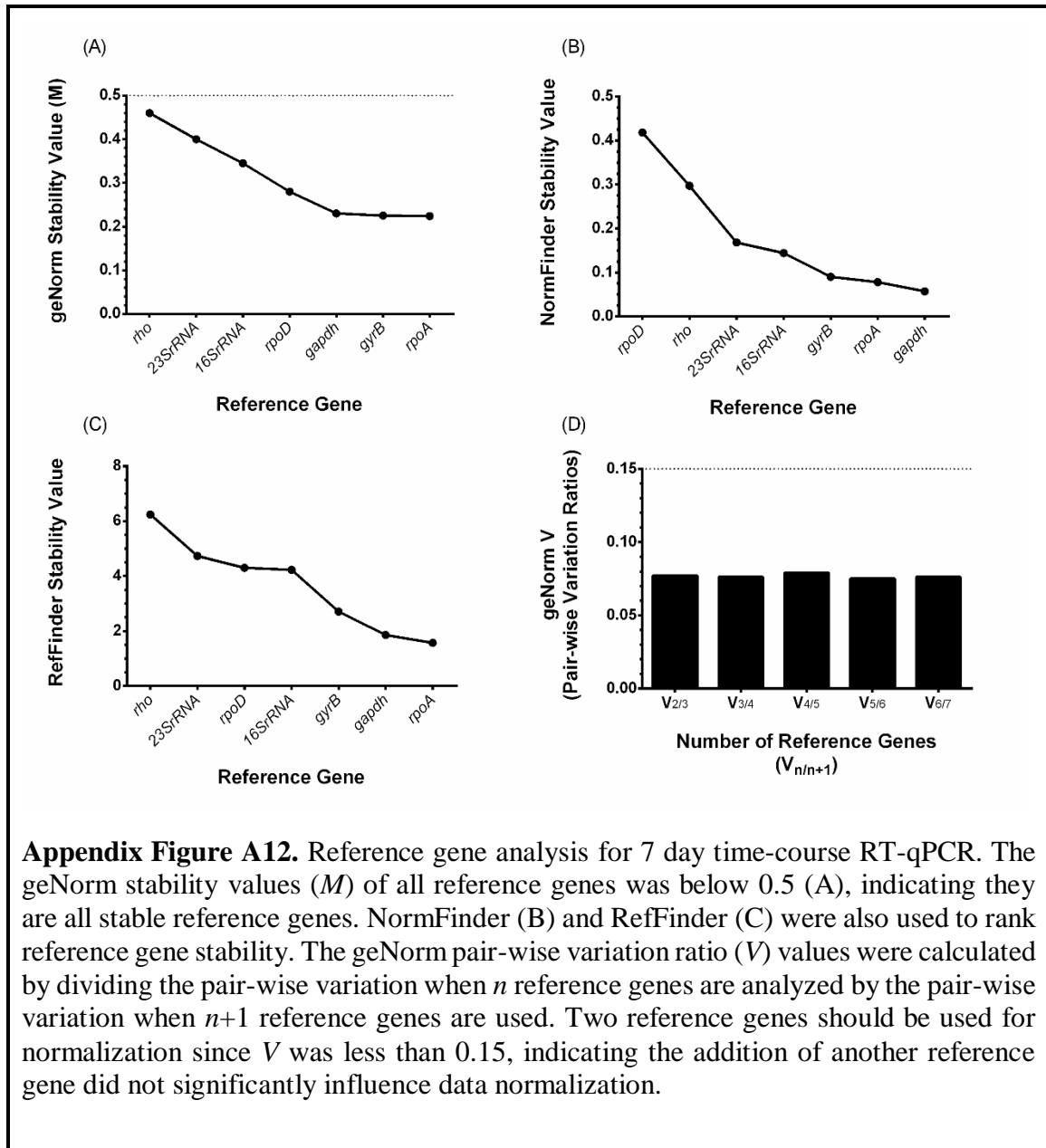


Appendix Figure A8. Reference gene analysis for 3 day time-course RT-qPCR. The geNorm stability values (M) of all reference genes was below 0.5 (A), indicating they are all stable reference genes. NormFinder (B) and RefFinder (C) were also used to rank reference gene stability. The geNorm pair-wise variation ratio (V) values were calculated by dividing the pair-wise variation when n reference genes are analyzed by the pair-wise variation when $n+1$ reference genes are used. Two reference genes should be used for normalization since V was less than 0.15, indicating the addition of another reference gene did not significantly influence data normalization.

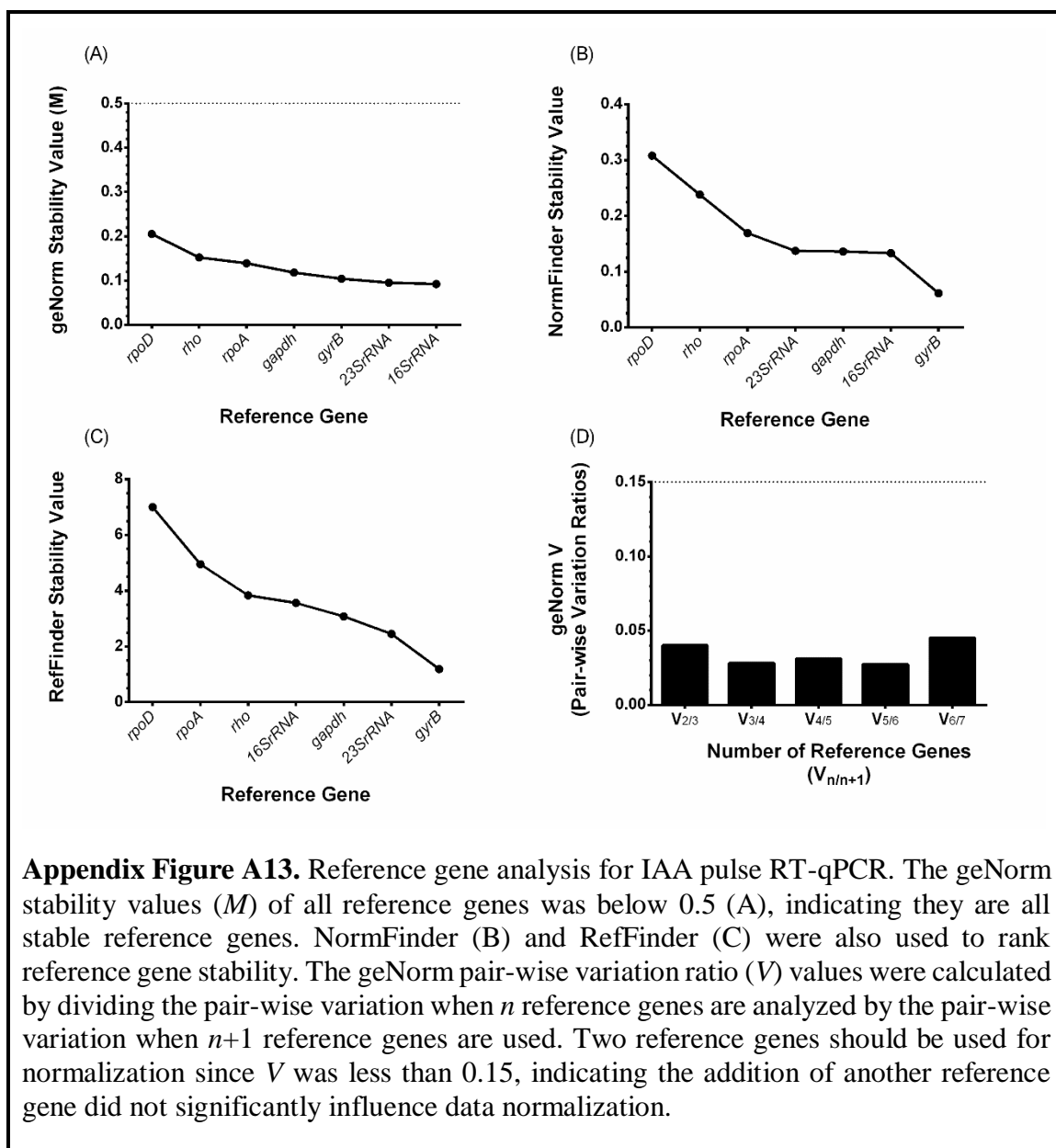


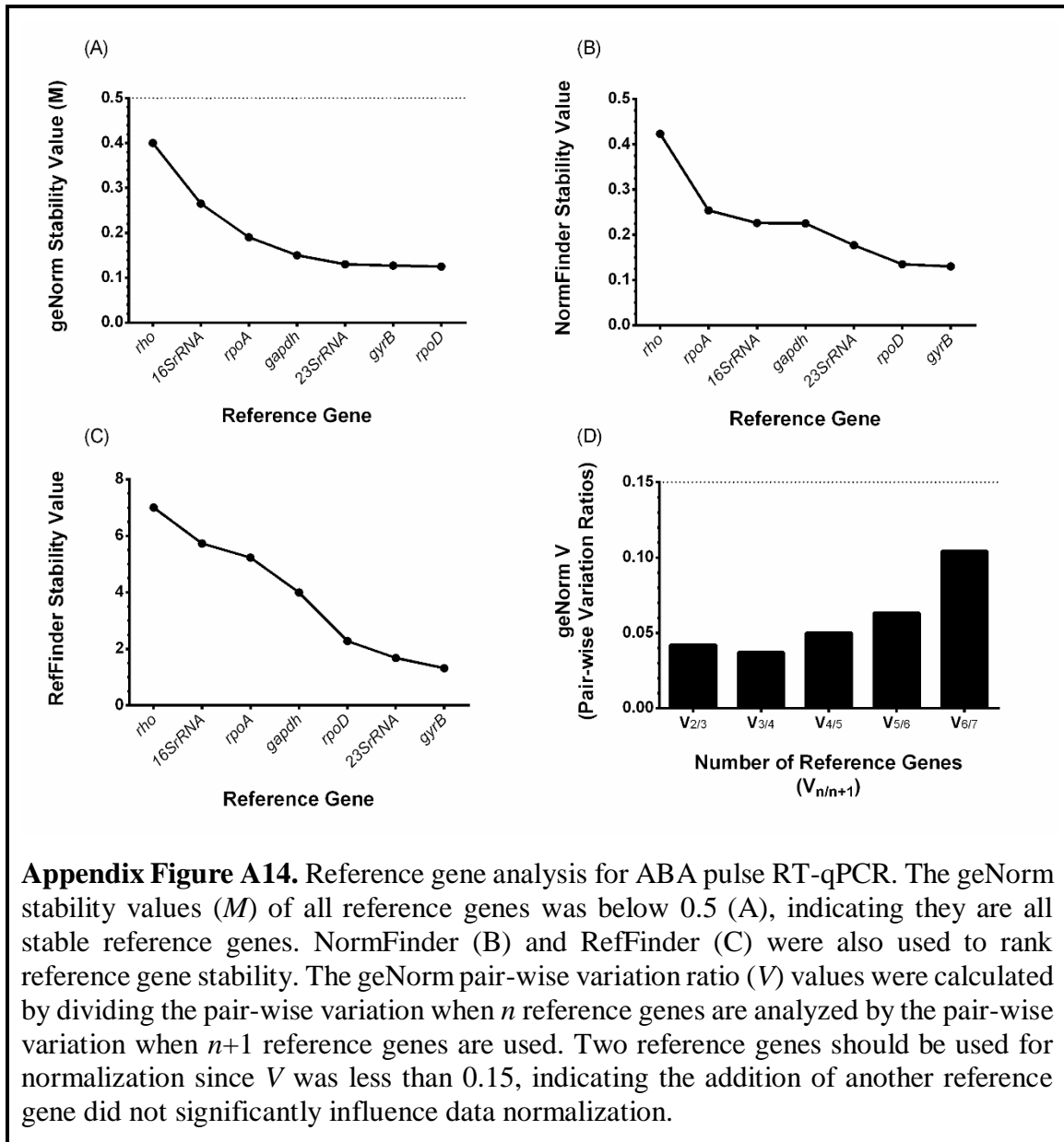


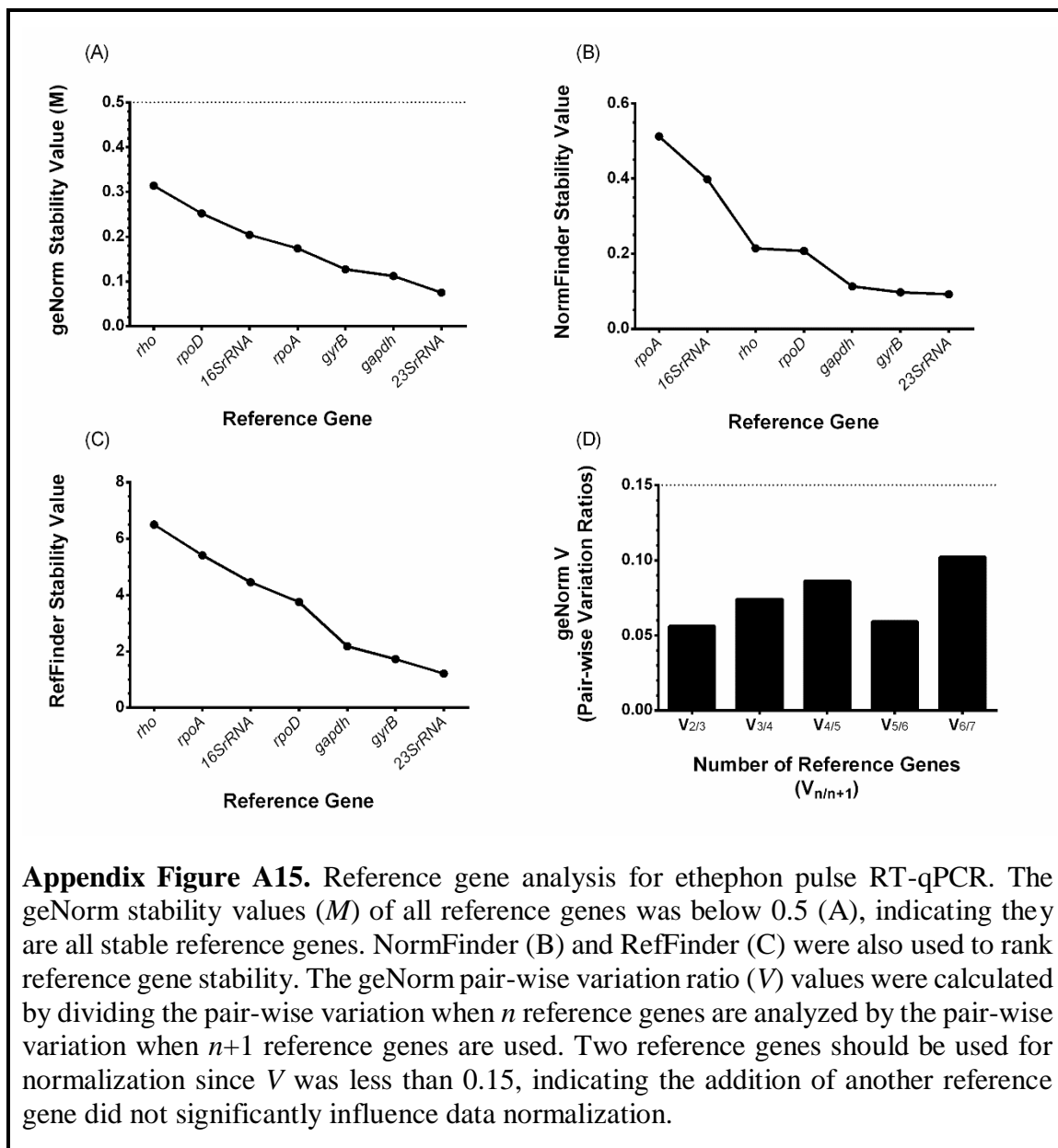




Appendix Figure A12. Reference gene analysis for 7 day time-course RT-qPCR. The geNorm stability values (M) of all reference genes was below 0.5 (A), indicating they are all stable reference genes. NormFinder (B) and RefFinder (C) were also used to rank reference gene stability. The geNorm pair-wise variation ratio (V) values were calculated by dividing the pair-wise variation when n reference genes are analyzed by the pair-wise variation when $n+1$ reference genes are used. Two reference genes should be used for normalization since V was less than 0.15, indicating the addition of another reference gene did not significantly influence data normalization.







Appendix Figure A15. Reference gene analysis for ethephon pulse RT-qPCR. The geNorm stability values (M) of all reference genes was below 0.5 (A), indicating they are all stable reference genes. NormFinder (B) and RefFinder (C) were also used to rank reference gene stability. The geNorm pair-wise variation ratio (V) values were calculated by dividing the pair-wise variation when n reference genes are analyzed by the pair-wise variation when $n+1$ reference genes are used. Two reference genes should be used for normalization since V was less than 0.15, indicating the addition of another reference gene did not significantly influence data normalization.

Appendix Table A2. Summary analysis of reference genes used to normalize RT-qPCR data.

Experiment	Time Point	Number of Reference Genes	Genes Used	Final geNorm <i>M</i>
Time-course	3 day	2	<i>gyrB/rpoD</i>	0.153
	4 day	2	<i>gyrB/rpoD</i>	0.196
	5 day	2	<i>gyrB/rho</i>	0.204
	6 day	2	<i>gyrB/gapdh</i>	0.212
	7 day	2	<i>rpoA/gapdh</i>	0.249
IAA Pulse	1 hour	2	<i>gyrB/23SrRNA</i>	0.099
ABA Pulse	1 hour	2	<i>gyrB/23SrRNA</i>	0.128
Ethephon Pulse	1 hour	2	<i>gyrB/23SrRNA</i>	0.098

